AGRICULTURAL UNIVERSITY OF ATHENS
DEPARTMENT OF NATURAL RESOURCES MANAGEMENT & AGRICULTURAL ENGINEERING
LABORATORY OF FARM MACHINE SYSTEMS

PhD Thesis

Yield Prediction in processing tomato crop, through Precision Agriculture practices

Nicoleta K. Darra

Supervisor:
Spyros Fountas | Professor, Agricultural University of Athens

Three-member committee:
Spyros Fountas | Professor, Agricultural University of Athens
James Arnold Taylor | Research Director, INRAE
Dionissios Kalivas | Professor, Agricultural University of Athens

Athens
2024

AGRICULTURAL UNIVERSITY OF ATHENS
DEPARTMENT OF NATURAL RESOURCES MANAGEMENT & AGRICULTURAL ENGINEERING
LABORATORY OF FARM MACHINE SYSTEMS

PhD Thesis

Yield Prediction in processing tomato crop, through Precision Agriculture practices

Πρόβλεψη παραγωγής σε καλλιέργειες βιομηχανικής τομάτας με χρήση εφαρμογών γεωργίας ακριβείας

Νικολέτα Κ. Δάρρα

Seven-member committee:
Spyros Fountas | Professor, Agricultural University of Athens (supervisor)
James Arnold Taylor | Research Director, INRAE
Dionissios Kalivas | Professor, Agricultural University of Athens
Sotirios Archontoulis | Professor, Iowa State University
Konstantinos Arvanitis| Professor, Agricultural University of Athens
Ilias Travlos | Associate Professor, Agricultural University of Athens
Emmanouil Psomiadis | Assistant Professor, Agricultural University of Athens

Yield Prediction in processing tomato crop, through Precision Agriculture practices

Department of Natural Resources Management & Agricultural Engineering
Laboratory of Farm Machine Systems

Abstract

This research is designed to make a valuable contribution to the field of precision agriculture, by exploring the potential of state-of-the-art technologies and techniques for yield prediction in processing tomato crop. The core aim was to develop and evaluate a robust methodology incorporating cutting-edge technologies, remote sensing data, and sophisticated analytical techniques like machine learning and statistical analysis. The primary objective is to improve the accuracy and dependability of yield predictions at local and regional levels. This was achieved through a progressive approach implemented yearly, utilizing non-invasive methods to track the crop's biological cycle and refine predictive yield models.

Over the course of this study, a progressive methodology was implemented to gather data and refine methodologies. It commenced with a systematic literature review focusing on yield predictions within precision agriculture, to offer an extensive overview of the latest advancements in this domain. Simultaneously, pilot activities were conducted over three years. Ten pilot fields were chosen to integrate proximal, aerial, and satellite measurements with yield assessments in the initial two years, primarily exploring the correlation between crop yield and NDVI (Normalized Difference Vegetation Index), a widely used indicator. This phase aimed to uncover similarities between satellite technology, UAS (Unmanned Aerial System), and proximal sensors concerning crop yield evaluation. Conducting an extensive comparison of satellite, airborne, and proximal technologies, their individual strengths, and limitations were emphasized within the precision agriculture context.

During the second year, alongside the detailed investigation of specific fields using satellite, UAS, and proximal sensors at the field scale, an expanded study involved 108 fields at the regional scale, incorporating satellite data analysis. This phase aimed to assess NDVI and four additional vegetation indices (VIs) in predicting crop yield. Time series data comprising five VIs at a regional scale were deployed to explore the relationship between these indices and the critical phenological stages of the crop. Furthermore, machine learning techniques were applied to VI data collected through satellite images at different growth stages to evaluate their predictive performance for yield in industrial tomato fields. Specifically, AutoML algorithms and statistical analysis were utilized to gauge the correlation between yield and VIs retrieved from satellite datasets. The transformed data was utilized to train and test both statistical and machine learning algorithms, encompassing linear and nonlinear regression models, along with ensemble methods based on decision trees. The analysis encompassed various regression models such as ordinary least squares (OLS), Theil-Sen, and Huber, as well as tree-based methods, support vector machines (SVM), and automatic relevance determination (ARD). This broader scope aimed to deepen the understanding of crop yield estimation based on the findings from the initial systematic review.

During the third year, a more intricate approach was adopted, focusing on the evaluation of spectral bands derived from satellite imagery. Each band's individual performance in predicting crop yield was assessed, allowing for a comprehensive evaluation of their unique contributions to overall yield estimation accuracy. This granular analysis provided deeper insights into the importance and impact of each spectral band in refining the precision of crop yield predictions. The performance of both statistical and machine learning models was assessed to gain profound insights into the most efficient growth stages and VIs for precise yield prediction.

The findings of this study indicated substantial similarity between UAS and Sentinel-2 data, especially in the later stages of the crop's phenological cycle, implying a heightened agreement as

the crop matured. The study identified a moderate correlation between proximal sensor data and UAS/satellite datasets, with discrepancies attributed to variances in measurement wavelengths and the specific focus area of each platform. Regarding the relationship of the VI dynamics in relation to the crop's phenological cycle, the lowest mean values for all VIs were observed shortly after transplanting, marked by limited canopy cover and exposed soil between rows. Notably, as the season progressed, canopy cover percentage gradually increased, particularly at the midpoint of the season when processing tomato crop reached their peak vigor just before reallocating sugars to their fruits.

Regarding yield prediction, the proximal sensor showed higher explanatory power during the initial canopy growth phase, while UAS and Sentinel platforms improved their performance as canopy coverage expanded. The satellite platform demonstrated superior performance during the crucial flowering stage, emphasizing its effectiveness in elucidating yield variability. The study employed basic statistics, notably the Pearson correlation coefficient, highlighting the VIs' optimal performance during specific growth stages. Additionally, machine learning algorithms were integrated to enhance yield prediction accuracy rigorously evaluated through regression analysis and a 5-fold cross-validation procedure. The research identified NDVI, RVI and SAVI as the most effective VIs for yield predictions, achieving high R^2 values and low RMSEs, particularly 90 days after transplanting. Ensembles comprising two regressors emerged as the optimal choice for enhanced predictive accuracy. Remarkably, band combinations of Band 4, Band 8, and Band 12 stood out. The Red Edge/NIR bands displayed notable performance, especially within the 80 to 90 days post-transplanting window, exhibiting the strongest correlation with yield.

Overall, the findings suggest that UAS and satellite sensors demonstrate greater accuracy in predicting crop yield towards the end of the season and offer increased precision during the later stages of development. In contrast, proximal sensors showcase correlations at earlier stages of crop growth. Combining data from multiple sensors and growth stages can enhance prediction accuracy. Using VI and spectral band data in conjunction with machine learning techniques may represent a more effective and economically efficient method for predicting tomato yield.

Scientific area: *Agricultural Engineering*

Keywords: *Precision Agriculture; Remote sensing; Vegetation Indices, NDVI, processing tomatoes, artificial intelligence, AutoML*

Πρόβλεψη παραγωγής σε καλλιέργειες βιομηχανικής τομάτας με χρήση εφαρμογών γεωργίας ακριβείας

Τμήμα Αξιοποίησης Φυσικών Πόρων & Γεωργικής Μηχανικής
Εργαστήριο Γεωργικής Μηχανολογίας

Περίληψη

Αυτή η μελέτη έχει ως στόχο να συμβάλει στον τομέα της Γεωργίας Ακριβείας, εξερευνώντας τις δυνατότητες των προηγμένων τεχνολογιών και μεθόδων στην πρόβλεψη απόδοσης στην καλλιέργεια βιομηχανικής ντομάτας. Το κύριο εγχείρημα ήταν η ανάπτυξη και αξιολόγηση μιας αξιόπιστης μεθοδολογίας που ενσωματώνει προηγμένες τεχνολογίες, δεδομένα τηλεπισκόπησης και προηγμένες αναλυτικές τεχνικές, όπως η μηχανική μάθηση και η στατιστική ανάλυση. Ο κύριος στόχος είναι η βελτίωση της ακρίβειας και της αξιοπιστίας των προβλέψεων απόδοσης σε τοπικό και περιφερειακό επίπεδο. Αυτό επιτεύχθηκε μέσω μιας προοδευτικής προσέγγισης που εφαρμόστηκε ετησίως, χρησιμοποιώντας μη καταστροφικές μεθόδους για την παρακολούθηση του βιολογικού κύκλου της καλλιέργειας και τη βελτίωση των μοντέλων πρόβλεψης παραγωγής.

Κατά τη διάρκεια αυτής της μελέτης, εφαρμόστηκε μια προοδευτική μεθοδολογία για τη συγκέντρωση δεδομένων. Άρχισε με μια συστηματική βιβλιογραφική ανασκόπηση που εστίασε στην πρόβλεψη απόδοσης με μεθόδους Γεωργίας Ακριβείας, για να προσφέρει μια εκτενή επισκόπηση των τελευταίων εξελίξεων σε αυτόν τον τομέα. Ταυτόχρονα, πιλοτικές δραστηριότητες διεξήχθησαν για τρία χρόνια. Τα δύο πρώτα χρόνια επιλέχθηκαν δέκα πιλοτικά αγροτεμάχια για την ενσωμάτωση επίγειων, εναέριων και δορυφορικών δεδομένων και δειγματοληψίες παραγωγής, με κύριο στόχο να εξετάσουν τη συσχέτιση μεταξύ της απόδοσης της καλλιέργειας και του NDVI (Δείκτης Βλάστησης Κανονικοποιημένης Διαφοράς), ενός δείκτη που χρησιμοποιείται ευρέως. Αυτή η φάση είχε ως στόχο να εξερευνήσει τις ομοιότητες μεταξύ των δορυφόρων, των ΣμηΕΑ (Συστήματα μη Επανδρωμένων Αεροσκαφών) και των επίγειων αισθητήρων στην αξιολόγηση της απόδοσης της καλλιέργειας. Με την εκτεταμένη σύγκριση των δορυφόρων, ΣμηΕΑ και επίγειων αισθητήρων, δόθηκε ιδιαίτερη σημασία στα πλεονεκτήματα και περιορισμούς τους στο πλαίσιο της Γεωργίας Ακριβείας (ΓΑ).

Κατά τη δεύτερη χρονική περίοδο, εκτός από τα συγκεκριμένα αγροτεμάχια που υποβλήθηκαν σε λεπτομερή έρευνα με χρήση δορυφορικών, ΣμηΕΑ και επίγειων αισθητήρων, μια διευρυμένη μελέτη πραγματοποιήθηκε που περιλάμβανε 108 αγροτεμάχια σε περιφερειακή κλίμακα, ενσωματώνοντας την ανάλυση δορυφορικών δεδομένων. Αυτή η φάση είχε ως στόχο να αξιολογήσει όχι μόνο τον NDVI, αλλά και τέσσερις επιπλέον δείκτες βλάστησης στην πρόβλεψη της απόδοσης της καλλιέργειας. Χρησιμοποιήθηκαν χρονοσειρές δεδομένων που περιλάμβαναν πέντε δείκτες βλάστησης σε περιφερειακή κλίμακα για να εξετάσουν τη σχέση μεταξύ αυτών των δεικτών και των κρίσιμων φαινολογικών σταδίων της καλλιέργειας. Στο πλαίσιο αυτό πραγματοποιήθηκε η χρήση τεχνικών αυτοματοποιημένης μηχανικής μάθησης (AutoML) σε συνδυασμό με δεδομένα δεικτών βλάστησης που ανακτήθηκαν από δορυφορικά σύνολα δεδομένων για τη συσχέτιση τους με την απόδοση. Τα μετασχηματισμένα δεδομένα στη συνέχεια χρησιμοποιήθηκαν για την εκπαίδευση και τη δοκιμή αλγορίθμων στατιστικής και μηχανικής μάθησης, συμπεριλαμβανομένων μοντέλων γραμμικής και μη γραμμικής παλινδρόμησης και μεθόδων συνόλου που βασίζονται σε δέντρα αποφάσεων Στην ανάλυση χρησιμοποιήθηκαν η μέθοδος ελάχιστου τετραγώνου (OLS), μοντέλα παλινδρόμησης Theil-Sen και Huber και μέθοδοι που βασίζονται σε δέντρα. Συμπεριλήφθηκαν επίσης μηχανές διανυσμάτων υποστήριξης (SVM) και αυτόματος προσδιορισμός συνάφειας (ARD).

Αυτός οι ευρύτερες δραστηριότητες στόχευαν στην εμβάθυνση της κατανόησης στην εκτίμηση της απόδοσης των καλλιεργειών, λαμβάνοντας υπόψη τα ευρήματα από την αρχική συστηματική ανασκόπηση.

Κατά το τρίτο έτος, υιοθετήθηκε μια πιο περίπλοκη προσέγγιση, με επίκεντρο την αξιολόγηση των φασματικών καναλιών από τον δορυφόρο Sentinel 2. Η ατομική απόδοση κάθε καναλιού στην πρόβλεψη της απόδοσης των καλλιεργειών αξιολογήθηκε, επιτρέποντας μια ολοκληρωμένη αξιολόγηση της μοναδικής συνεισφοράς τους στη συνολική ακρίβεια εκτίμησης της απόδοσης. Αυτή η ανάλυση παρείχε βαθύτερες γνώσεις σχετικά με τη σημασία και τον αντίκτυπο της κάθε φασματικής ζώνης στη βελτίωση της ακρίβειας των προβλέψεων απόδοσης των καλλιεργειών. Η αξιολόγηση την απόδοση τόσο των στατιστικών όσο και των μοντέλων μηχανικής μάθησης συνείσφερε στην απόκτηση βαθύτερης κατανόησης σχετικά με τα πιο αποτελεσματικά στάδια ανάπτυξης και τους δείκτες βλάστησης για την ακριβή πρόβλεψη της παραγωγής.

Τα ευρήματα αυτής της μελέτης έδειξαν ουσιαστική ομοιότητα μεταξύ των δεδομένων ΣμηΕΑ και δορυφόρου, ειδικά στα μεταγενέστερα στάδια του φαινολογικού κύκλου της καλλιέργειας, υπονοώντας μια αυξημένη συμφωνία καθώς η καλλιέργεια ωρίμαζε. Η μελέτη εντόπισε μια μέτρια συσχέτιση μεταξύ των δεδομένων εγγύς αισθητήρα και των συνόλων δεδομένων ΣμηΕΑ /δορυφόρου, με αποκλίσεις που αποδίδονται σε διακυμάνσεις στα μήκη κύματος μέτρησης κάθε πλατφόρμας. Όσον αφορά στη σχέση της δυναμικής των δεικτών βλάστησης σε σχέση με τον φαινολογικό κύκλο της καλλιέργειας, οι χαμηλότερες μέσες τιμές για όλους τους δείκτες βλάστησης παρατηρήθηκαν λίγο μετά τη μεταφύτευση, οι οποίες οφείλονται στην περιορισμένη κάλυψη βλάστησης και το εκτεθειμένο έδαφος μεταξύ των σειρών. Ιδιαίτερα καθώς προχωρούσε η καλλιεργητική περίοδος, το ποσοστό φυτικής κάλυψης αυξήθηκε σταδιακά, ιδιαίτερα κατά τη μέση της περιόδου, όταν τα φυτά τομάτας έφτασαν στο μέγιστο της βλάστησης τους λίγο πριν ανακατανείμουν τα σάκχαρα στους καρπούς τους.

Όσον αφορά στην πρόβλεψη απόδοσης, ο επίγειος αισθητήρας έδειξε υψηλότερη επεξηγητική ισχύ κατά την αρχική φάση ανάπτυξης φυλλώματος, ενώ τα δεδομένα από το ΣμηΕΑ και τον δορυφόρο βελτίωσαν την απόδοσή τους καθώς διευρύνθηκε η κάλυψη του φυλλώματος. Η δορυφορική πλατφόρμα επέδειξε ανώτερη απόδοση κατά το κρίσιμο στάδιο της ανθοφορίας, τονίζοντας την αποτελεσματικότητά της στην αποσαφήνιση της μεταβλητότητας της απόδοσης. Η μελέτη χρησιμοποίησε βασικές στατιστικές μεθόδους, ειδικότερα το συντελεστή συσχέτισης Pearson, επισημαίνοντας την βέλτιστη απόδοση των δεικτών βλάστησης σε συγκεκριμένα στάδια ανάπτυξης. Επιπλέον, ενσωματώθηκαν αλγόριθμοι μηχανικής μάθησης για τη βελτίωση της ακρίβειας πρόβλεψης απόδοσης, οι οποίοι αξιολογήθηκαν αυστηρά μέσω ανάλυσης παλινδρόμησης και μιας διαδικασίας διασταυρούμενης επικύρωσης. Η έρευνα ανέδειξε τους δείκτες RVI και SAVI ως τους πιο αποτελεσματικούς για τις προβλέψεις της απόδοσης, επιτυγχάνοντας υψηλές τιμές R^2 και χαμηλά RMSEs, ιδιαίτερα 90 ημέρες μετά τη μεταφύτευση. Οι συνδυασμοί μοντέλων ARD και SVR πέτυχαν σταθερή ικανοποιητική απόδοση, υπογραμμίζοντας την αποτελεσματικότητα του συνδυασμού διαφορετικών μοντέλων. Η χρήση των φασματικών καναλιών 8, 4 και 12 παρείχε αξιόλογα αποτελέσματα. Οι φασματικές ζώνες Red Edge/NIR εμφάνισαν αξιοσημείωτη απόδοση, ειδικά εντός του παραθύρου 80 έως 90 ημερών μετά τη μεταφύτευση, παρουσιάζοντας την ισχυρότερη συσχέτιση με την απόδοση.

Συνολικά, τα ευρήματα υποδηλώνουν ότι οι αισθητήρες ΣμηΕΑ και οι δορυφορικοί αισθητήρες επιδεικνύουν μεγαλύτερη ακρίβεια στην πρόβλεψη της απόδοσης των καλλιεργειών προς το τέλος της σεζόν και προσφέρουν αυξημένη ακρίβεια κατά τα τελευταία στάδια ανάπτυξης. Αντίθετα, οι επίγειοι αισθητήρες παρουσιάζουν συσχετίσεις σε προηγούμενα στάδια ανάπτυξης της καλλιέργειας. Ο συνδυασμός δεδομένων από πολλούς αισθητήρες και στάδια ανάπτυξης μπορεί να βελτιώσει την ακρίβεια πρόβλεψης. Η χρήση δεδομένων δεικτών βλάστησης και φασματικών καναλιών σε συνδυασμό με τεχνικές μηχανικής μάθησης συνιστά μια πιο αποτελεσματική και οικονομικά αποδοτική μέθοδο για την πρόβλεψη της παραγωγής βιομηχανικής ντομάτας.

Επιστημονική περιοχή: *Γεωργική Μηχανική*

Λέξεις κλειδιά: *Γεωργία ακριβείας, Τηλεπισκόπηση, Δείκτες βλάστησης, NDVI, βιομηχανική τομάτα, Τεχνητή νοημοσύνη, AutoML*

Certificate of Originality

I hereby certify that the text of this thesis does not contain any material that has been accepted as part of the requirements for a degree or diploma at any university, nor does it contain any material that has been previously published or written, unless such material is referenced.

In addition, with my permission, this thesis has been checked and verified for validity and originality by the examination board using plagiarism detection software available from the Agricultural University of Athens.

Nicoleta K. Darra

List of publications

International scientific journal publications

1. **Darra, N.,** *Anastasiou, E., Kriezi, O., Lazarou, E., Kalivas, D., & Fountas, S. (2023). Can Yield Prediction Be Fully Digitilized? A Systematic Review. Agronomy, 13(9), 2441.*

2. **Darra, N.,** *Espejo-Garcia, B., Kasimati, A., Kriezi, O., Psomiadis, E., & Fountas, S. (2023). Can Satellites Predict Yield? Ensemble Machine Learning and Statistical Analysis of Sentinel-2 Imagery for Processing Tomato Yield Prediction. Sensors, 23(5), 2586.*

3. **Darra, N.**, *Psomiadis, E., Kasimati, A., Anastasiou, A., Anastasiou, E., & Fountas, S. (2021). Remote and proximal sensing-derived spectral indices and biophysical variables for spatial variation determination in vineyards. Agronomy, 11(4), 741.*

Book chapters

1. **Darra, N.**, *Kasimati, A., Koutsiaras, M., Psiroukis, V., & Fountas, S. (2023). Digital transformation of SMEs in agriculture. SMEs in the Digital Era: Opportunities and Challenges of the Digital Single Market, 65.*

2. *Psiroukis, V., Papadopoulos, G.,* **Darra, N.**, *Koutsiaras, M. G., Lomis, A., Kasimati, A., & Fountas, S. (2023). Unmanned aerial vehicles applications in vegetables and arable crops. In Unmanned Aerial Systems in Agriculture (pp. 71-91). Academic Press.*

2. *Kasimati, A., Lomis, A., Psiroukis, V.,* **Darra, N.**, *Koutsiaras, M. G., Papadopoulos, G., & Fountas, S. (2023). Unmanned aerial systems applications in orchards and vineyards. In Unmanned Aerial Systems in Agriculture (pp. 93-109). Academic Press.*

2. *Fountas, S., Espejo-Garcia, B., Kasimati, A., Mylonas, N., &* **Darra, N.** *(2020). The future of digital agriculture: technologies and opportunities. IT professional, 22(1), 24-28.*

International conference proceedings

1. **Darra, N.,** *Valanides N., Papadopoulos, G., Manganaris G., & Fountas, S. (2023). Pre-Harvest Management and Precision Farming-Integration of Digital Management in Berry Cultivars. 22nd International Conference "Life Sciences for Sustainable Development.", Cluz Napoca, Romania,2023*

2. *Valanides N.,* **Darra, N.**, *Papadopoulos, G., Fountas, S. & Manganaris G., (2023). The employment of remote and proximal sensing technologies to predict the flowering and harvesting periods of three red raspberry cultivars. XIII International Rubus and Ribes Symposium., USA,*

3. *Nikolopoulos D., V. Haghiou, V. Daliani,* **N. Darra**, *M. Liati, E. Mavrogianni, A. Pananastasiou, Th. Porfyraki, V. Psaroudi, C. Fasseas, G. Karabourniotis, G. Liakopoulos Foliar photosynthesis under non-perpendicular illumination: The contribution of leaf optical properties. Photosynthesis for Sustainability in Photosynthesis for Sustainability 2015. In honor of George C. Papageorgiou. International Meeting, Chania, 2015.*

Participation in other publications

International scientific journal publications

1. Kasimati, A., Psiroukis, V., **Darra, N.**, *Kalogrias, A., Kalivas, D., Taylor, J. A., & Fountas, S. (2023). Investigation of the similarities between NDVI maps from different proximal and remote sensing platforms in explaining vineyard variability. Precision Agriculture, 1-21.*

2. Kasimati, A., Espejo-García, B., **Darra, N.**, *& Fountas, S. (2022). Predicting Grape Sugar Content under Quality Attributes Using Normalized Difference Vegetation Index Data and Automated Machine Learning. Sensors, 22(9), 3249.*

3. Psiroukis, V.; **Darra, N.**; *Kasimati, A.; Trojacek, P.; Hasanli, G.; Fountas, S. Development of a Multi-Scale Tomato Yield Prediction Model in Azerbaijan Using Spectral Indices from Sentinel-2 Imagery. Remote Sens. 2022, 14, 4202. https://doi.org/10.3390/rs14174202*

4. Anastasiou, E.; Balafoutis, A.; **Darra, N.;** *Psiroukis, V.; Biniari, A.; Xanthopoulos, G.; Fountas, S. Satellite and Proximal Sensing to Estimate the Yield and Quality of Table Grapes. Agriculture 2018, 8, 94. https://doi.org/10.3390/agriculture8070094*

Long Live Science!

Maxim Gorky (1868–1936)

Acknowledgements

The completion of a substantial research project like this is the result of collective efforts rather than the work of a solitary individual. I am deeply grateful to several individuals who have contributed to this endeavour in various capacities. I extend my heartfelt appreciation to the following individuals in particular.

Foremost, my sincere gratitude goes to Professor Spyros Fountas, my supervisor, whose guidance and inspiration propelled my journey through the PhD program. Spyros' vibrant enthusiasm and unwavering support have allowed me the freedom to explore diverse projects and he supported me whenever I need it. Thank you, Spyros, for your exceptional mentorship! Your guidance has been instrumental in nurturing my research and professional growth, and your counsel on both academic and career matters has been invaluable.

I am also grateful to the other two members of my committee: Professor Dionissios Kalivas, whose expertise, encouragement, and patient guidance significantly enriched my doctoral experience, enabling me to further hone my skills and achieve success in my academic pursuits. Thank you sincerely, Professor Kalivas! Additionally, I'd like to express my gratitude to Dr. James Arnold Taylor, whose consistent advice and support have been invaluable to me. I am truly appreciative of your discreet yet supportive approach in monitoring the progress of my studies, Thank you James for your guidance and encouragement.

Professor Emmanouil Psomiadis for his invaluable experience, feedback and support on this research. It is a pleasure to have you on my PhD committee! Thank you! Additionally, I extend my gratitude to Professors Sotirios Archontoulis, Ilias Travlos, and Konstantinos Arvanitis for graciously accepting the invitation to serve as members of my committee. Your involvement is greatly appreciated.

Furthermore, I would like to thank my friend and mentor Achileas Anastasiou for his unwavering support and continuous guidance. I fondly recall our numerous conversations and his consistent advice. He is a warm-hearted, compassionate individual—one of the kindest personalities I've encountered in recent years.

To my colleagues in the Smart Farming Technology Group. Thank you, Olga Kriezi, for the invaluable support you have given me along the way, both on a professional and personal level. Thank you Dinos Grivakis, Michael G, Koutsiaras, George Papadopoulos, Vasilis Psiroukis, for the support they have given me at all levels of the research project. I am sure we will all remember the eventful data collection in the Thessaly region (and not only there) in the years to come! ;-)

I would like to express my eternal gratitude to Borja Espejo García for his catalytic role in the data analysis. You really helped me to pull this off!

I am also very grateful to Evangelos Anastasiou for their friendly and scientific advice and knowledge, and for many insightful discussions and suggestions. Special thanks to Katerina Kasimati, Hercules Panoutsopoulos, Sofia Mouseti, Giannis Malounas, Erato Lazarou thank you very much for your direct and indirect contribution to fulfilling the requirements of this PhD!

Many sincere thanks to the team of Corteva Agriscience Hellas for allowing me to conduct the data collection and for supporting all relevant activities. I am glad to have built a solid relationship with you and a thank you is not enough for all the time, effort and help you have given me!

I am also very grateful to my friends, who have been very supportive along the way. I would like to express my gratitude to my family, who provided me with a firm foundation upon which to build my life. My heartfelt thanks go to my mother for her unconditional love and for instilling in me kindness and compassion. I extend my deepest gratitude to my father, who taught me resilience and the importance of giving things the value they deserve. I'm also thankful to my sister, who

offered me unlimited help and guidance when I was growing up, teaching me independence and adaptability along the way.

Lastly, I would like to thank myself for believing in me, for putting in all the hard work, continuously striving to do better, and never quitting. I want to thank me for always trying to do more right than wrong, for staying strong, authentic and optimistic in all situations.

Executive Summary

Precision Agriculture (PA) is a management strategy that gathers, processes and analyzes temporal, spatial and individual data and combines it with other information to support management decisions according to estimated variability for improved resource use efficiency, productivity, quality, profitability and sustainability of agricultural production [1].

The initial chapter (Part 1) of this thesis provides an extensive overview on precision agriculture, breaking it down into four main sections: Problem Statement, Precision Agriculture: Past, Present and Future, Remote Sensing in PA, and Processing Tomato Crop. It commences by addressing the challenges prevalent in agriculture and then offers a historical overview of the PA philosophy and principles, emphasizing its benefits. This also encompasses drivers and limitations associated with the adoption of precision agriculture methods. Additionally, it outlines the historical progression of satellite, aerial, and proximal platforms in precision agriculture, before providing detailed insights into processing tomato crops. This involves an examination of the crop's breeding history, its management concerning water and nutrients, and a comprehensive overview of its phenological cycle.

Part 2 provides an overview of the materials and methods with information on the systematic review conducted within the study and the selected study area for field and regional level measurements. A discussion of the platforms used is followed by an overview of data collection, preparation, and analysis. Within this study, data from three different sources (one proximal crop reflectance sensor, a UAS equipped with a multispectral camera, and Sentinel-2 imagery) were analysed over three seasons to assess the similarity of the data and their potential for predicting yield of processing tomato crop at field and regional level. A time-series VI dataset was utilized to meticulously track the phenological cycle of the crop and associate it not only with NDVI but also with four other Vegetation Indices (VIs). At both spatial levels, yield predictions were retrieved using VI and spectral band data from proximal and remote sensing, statistical analysis, and automated machine learning techniques (AutoML). To this end, multiple data processing techniques, alongside statistical and machine learning methods, including linear and nonlinear regression models, ensemble methods, and support vector machines, were employed to analyze the data and forecast crop yield.

Part 3 presents the research findings of this study presenting an overview of recent trends in PA methodologies as documented in literature pertaining to yield prediction. Both descriptive analysis and regression analysis was conducted, seeking to establish correlations among different platforms based on Normalized Difference Vegetation Index (NDVI). Notably, at the field level, the UAS exhibited a robust correlation with satellite NDVI datasets, while the proximal sensor displayed a moderate relationship with them. Furthermore, the study detailed the annual dynamics of VIs for the crop, shedding light on biomass growth patterns across the season. It was also observed that crop yield demonstrated a moderate relationship with VI data, both at the regional and field levels. The accuracy of predictions notably increased during flowering stages, particularly evident in satellite data, showcasing the highest correlations. Leveraging machine learning techniques significantly enhanced prediction accuracy, offering valuable insights into the optimal timing for yield predictions. Lastly, the study explored the use of spectral band information in conjunction with machine learning at a regional level, providing additional insights into yield forecasting.

Part 4 is the discussion and contributions of the whole research including the three research papers produced as part of this PhD thesis: The last two chapters, Part 5 and Part 6, build on each other and draw some conclusions on the above objectives and discuss areas for future research on the implementation of precision agriculture in yield predictions.

Table of Contents

List of Figures

List of Tables

Abbreviations

AI	Artificial Intelligence	**INSEY**	In-Season Estimated Yield
ANN	Artificial Neural Networks	**IOT**	Internet Of Things
ARD	Automatic Relevance Determination	**ISPA**	International Society for Precision Agriculture
APSIM	Agricultural Production Systems Simulator	**IPNI**	International Plant Nutrition Institute
ASTER	Advanced Spaceborne Thermal Emission and Reflection Radiometer	**KOMPSAT**	Korean Multi-Purpose Satellite
AUVSI	Association for Unmanned Vehicle Systems International	**LAI**	Leaf Area Index
AVHRR	Advanced Very High-Resolution Radiometer	**LED**	Light Emitting Diode
CAGR	Compound Annual Growth Rate	**LIDAR**	Light Detection and Ranging
CGIAR	Consortium Of International Agricultural Research Centres	**ML**	Machine Learning
CNN	Convolutional Neural Networks	**MODIS**	Moderate Resolution Imaging Spectroradiometer
DL	Deep Learning	**MSAVI2**	Modified Soil Adjusted Vegetation Index 2
DSS	Decision Support Systems	**MSI**	MultiSpectral Instrument
DSSAT	Decision Support System for Agrotechnology Transfer	**MSS**	Multispectral Scanner System
DVI	Difference Vegetation Index	**NDVI**	Normalized Difference Vegetation Index
EC	Electromagnetic Induction	NASA	National Aeronautics and Space Administration
ECPA	European Conference on Precision Agriculture	**NG**	Normalised Green
ESA	European Space Agency	**NIR**	Near-Infrared
EVI	Enhanced Vegetation Index	**NR**	Normalised Red
FAA	Usa Federal Aviation Administration	**NSI**	Nitrogen Sufficiency Index
FAO	Food And Agriculture Organization	**NUMASS**	Nutrient Management Support System
FIS	Field-Level Geographic Information System	**OSAVI**	Optimised Soil Adjusted Vegetation Index
FMIS	Farm Management Information System	**OLS**	Ordinary Least Squares
GDVI	Green Difference Vegetation Index	**PA**	Precision Agriculture
GIS	Geographic Information Systems	**PLSR**	Partial Least Square Regression
GNDVI	Green Normalized Difference Vegetation Index	**PNSI**	Plant Nitrogen Spectral Index
GNSS	Global Navigation Satellite Systems	**PVI**	Perpendicular Vegetation Index
GOSAVI	Green Optimised Soil Adjusted Vegetation Index	**RGB**	Red, Green, Blue
GPS	Global Positioning System	**RPAS**	Remotely Piloted Aircraft System
GRVI	Green Red Vegetation Index	**RVI**	Ratio Vegetation Index
GSAVI	Green Soil Adjusted Vegetation Index	**SAFY**	Simple Algorithm for Yield

ICT	Information And Communications Technologies	**SAR**	Synthetic Aperture Radar
SAVI	Soil Adjusted Vegetation Index	**USA**	United States of America
SPAD	Soil Plant Analysis Development	**USB**	United Soybean Board
SPOT	Satellite Pour L'observation De La Terre	**USDA**	United States Department of Agriculture
SSC	Soluble Solids Content	**VI**	Vegetation Index
SVM	Support Vector Machine	**VIIRS**	Visible Infrared Imaging Radiometer Suite
UAS	Unmanned Aircraft System	**VRT**	Variable Rate Technology
UAV	Unmanned Aerial Vehicles	**WDVI**	Weighted Difference Vegetation Index

Table 1: Abbreviations

Part 1. Introduction

1.1 Problem Statement

Modern agriculture faces a diverse array of challenges, encompassing the far-reaching impacts of climate change [2], the decreasing availability of essential natural resources [3], transformations in dietary inclinations [4], apprehensions about safety and health [5], and the escalating demands placed on the agricultural sector due to the growing global population. These challenges are not only theoretical but also backed by empirical data. The World Health Organization [6], has estimated that a staggering 820 million people globally still lack sufficient access to food. Moreover, the Food and Agriculture Organization (FAO) anticipates a substantial 70% surge in food demand to cater to the projected global population of 9.1 billion by 2050 [7]. Climate change exacerbates the situation further by unleashing droughts, floods, and heatwaves that further strain food production across various regions [7]. Moreover, conventional agriculture has fallen short in terms of achieving optimal resources efficiency [8], by involving intensive use of agricultural inputs, such as fertilizers and pesticides. Typically, these inputs are applied uniformly across entire farms as a precautionary measure to avert potential nutritional deficiencies or yield losses. However, such practices come at a cost, causing numerous environmental problems including groundwater depletion, eutrophication, diminished surface water flows, excessive nitrogen use, soil erosion and loss of soil organic matter, and excessive pesticide use [9–20]. At the same time, they result in economic losses and heightened environmental impact [21].

In response to these challenges that are placing immense stress on the agricultural sector, there is an urgent need to enhance techniques that can increase crop production through increased efficiency of inputs use and reduced environmental losses [22]. Precision Agriculture is emerging as a sustainable strategy [22], with the ultimate objective of managing crop and soil variability to increase profitability and reduce environmental degradation [23]. Using PA, data are collected to assist farmers in making guided sub-field decisions, including applications of fertilizers and pesticides, distribution densities for seeds, irrigation application rates, and tillage regimes [24]. Decisions that are better than those that would be made with traditional/conventional agricultural practices can boost the efficient use of resources, reduce input costs, minimize environmental degradation, and improve yield and crop quality.

1.2 Precision Agriculture: Past, Present and Future

1.2.1 Definition of Precision Agriculture

Precision agriculture (PA) is a strategic management methodology that leverages information technology to maximize efficiency, enhance productivity and profitability, and mitigate environmental consequences within specific geographical areas. The notion of tailoring agricultural practices to suit specific sites and conditions traces its roots back to Jethro Tull's proposal in 1731. Later in the 1990s, the PA concept emerged with the intention of improving productivity, profitability, and environmental sustainability. The definition of PA was initially surfaced in the USA in the 1997, when the House of Representatives defined it as "an integrated information- and production-based agricultural system designed to increase long-term, site-specific, and whole-farm production efficiency, productivity, and profitability while minimising unintended impacts on wildlife and the environment." This definition underscores the pivotal role of information technology within PA, driving enhancements in production and reducing environmental footprints across the entire agricultural spectrum, encompassing the entirety of the farm-to-fork supply chain.

Since then, multiple definitions provided by researchers, practitioners, and policy makers have contributed to a progressive deepening of understanding concerning the constituent elements of the concept. The Lleida University Research Group in AgroICT and Precision Agriculture lists 27

definitions from the scientific literature and the Internet [25]. Similarly, Trivelli et al. [26] have presented key definitions, as illustrated in the following table (Table 2), which has been updated with more recent terminology.

Table 2: Literature review, definitions and components of precision agriculture. Source: [26]

Year	Definition	Authors	Title and journal
1999	Precision agriculture is the application of technologies and principles to manage spatial and temporal variability associated with all aspects of agricultural production for the purpose of improving crop performance and environmental quality. Precision agriculture is technology enabled	F.J. Pierce, P. Nowak, [27]	Aspects of precision agriculture, Advances in Agronomy, Vol. 67, pp. 1-85
2000	Precision agriculture is a discipline that aims to increase efficiency in the management of agriculture. It is the development of new technologies, modification of old ones and integration of monitoring and computing at farm level	H. Kirchmann, G. Thorvaldsson, [28]	Challenging targets for future agriculture, European Journal of Agronomy, 12, pp. 145–161
2000	Precision agriculture is "information intense" and could not be realized without the enormous advances in networking and computer processing power. precision agriculture, as a crop management concept, can meet much of the increasing environmental, economic, market and public pressures on arable agriculture.	J.V. Stafford, [29]	Implementing precision agriculture in the 21st century, Journal of Agricultural Engineering Research, 76, pp. 267-275
2002	Precision agriculture is conceptualized by a system approach to re-organize the total system of agriculture towards a low-input, high-efficiency, sustainable agriculture	N. Zhang, M. Wang, N. Wang, [30]	Precision agriculture – a worldwide overview, Computer and Electronics in Agriculture, 36, pp. 13-132
2003	Precision Agriculture can be defined as the management of spatial and temporal variability at a sub-field level to improve economic returns and reduce environmental impact	Blackmore, S., Godwin, R., Fountas, S., [31]	The analysis of spatial and temporal trends in yield map data over six years. Biosystems Engineering, 84 (4), 455-466.
2004	Precision agriculture can help in managing crop production inputs in an environmentally friendly way. By using site-specific knowledge, PA can target rates of fertilizer, seed and chemicals for soil and other conditions	R. Bongiovanni, J. Lowenberg-Deboer, [32]	Precision agriculture and sustainability, Precision Agriculture, Vol. 5, pp. 359-387
2005	One generic definition could be "that kind of agriculture that increases the number of (correct) decisions per unit area of land per unit time with associated net benefits"	A. McBratney, B. Whelan, T. Ancev, [33]	Future directions of precision agriculture, Precision Agriculture, 6, pp. 7-23, Springer Science + Business Media
2012	Precision Agriculture is a production system that involves crop management according to field variability and site-specific conditions. Precision agricultural technologies are those technologies which, either used singly or in combination, as the means to realize precision agriculture	Y. S. Tey, M. Brindal, [8]	Factors influencing the adoption of precision agricultural technologies: a review for policy implications, Precision Agriculture, Vol. 13, pp. 713-730

2015	Precision Agriculture can be defined as the management of spatial and temporal variability in the fields using Information and Communications Technologies (ICT).	Fountas, S., Aggelopoulou, K., & Gemtos, T. A [34]	Crop Management for Improved Productivity and Reduced Environmental Impact or Improved Sustainability. Precision Agriculture. In Supply Chain Management for Sustainable Food Networks (pp. 41–65). Chichester, UK: John Wiley & Sons, Ltd. http://doi.org/10.1002/9781118937495.ch2
2021	Precision Agriculture is a management strategy that gathers, processes and analyzes temporal, spatial and individual data and combines it with other information to support management decisions according to estimated variability for improved resource use efficiency, productivity, quality, profitability and sustainability of agricultural production	International Society for Precision Agriculture (ISPA), [1]	This definition was the consensus of 36 PA experts in the Codigital process and the result of 76 generations based on the edits and votes of all participants.

It becomes increasingly evident over time that technology emerges as PA's pivotal and enabling aspect. The Precision Agriculture cycle (Figure 1) could be summarized in the four (4) key stages [25], which include:

i. Visual observations or observations by means of sensors that allow the acquisition of georeferenced data (that is to say, with coordinates that will enable their perfect location on the plot).
ii. Computerized systems for visualizing and processing data (GIS, geographic information systems).
iii. Decision Support Systems for decision making.
iv. Agricultural methodologies or machinery capable of carrying out agricultural operations in a specific way at each point of the plot, what is called VRT (Variable Rate Technology).

The cycle commences with the collection of crop data and environmental information. This involves the use of sensors, visual observations, and traditional sampling methods, all georeferenced using Global Navigation Satellite Systems (GNSS). These data encompass various aspects such as crop geometry, biomass quantity, vigour, soil characteristics, and more. Once the data have been gathered, the next step is to extract valuable insights for farmers and technicians. One crucial piece of information obtained is whether the crop is exhibiting uniform and proper development across the entire field. This information plays a pivotal role in the decision-making phase. During this stage, agronomic management actions are determined, including what operations should be carried out and how they should be executed. The initial decision revolves around whether to maintain uniform field management or if variations in the field recommend differentiated approaches. This decision entails assessing whether specific resources, such as fertilizers, irrigation, plant protection, planting, etc., should be applied differently in various areas of the field, and if so, at what dosage. Currently, this decision-making stage represents one of the primary challenges in PA and requires ongoing research efforts.

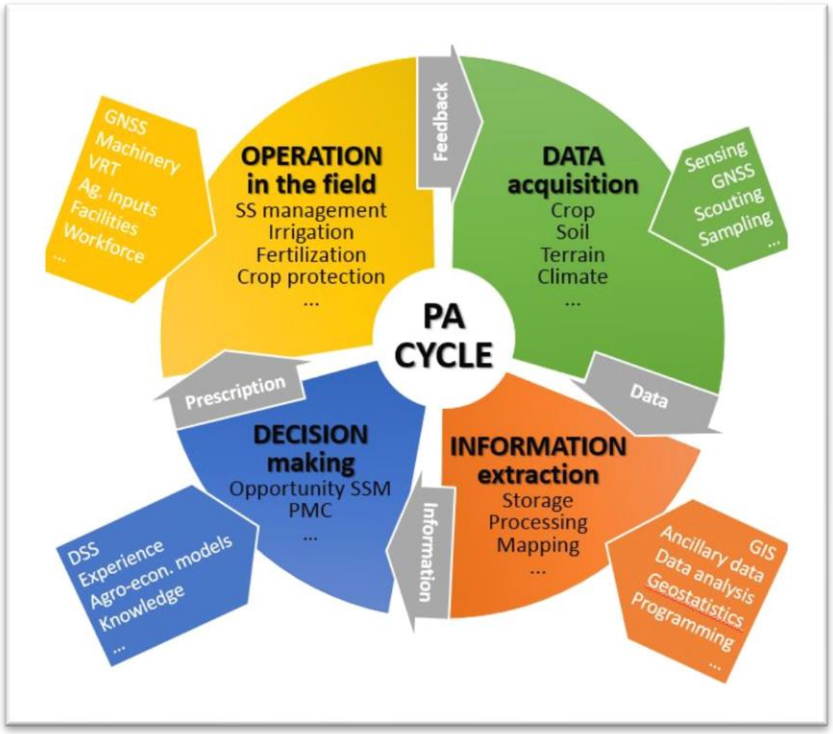

Figure 1. PA cycle. Source: [25]

Finally, action is taken in the field to apply the necessary resources or perform essential operations. In cases where differentiated actions are required, VRT may be employed, allowing machinery to adjust application doses according to the prescriptions developed during the decision-making phase.

In summary, PA consists of performing the right operation in the right place, at the right time, in the appropriate manner and the right amount.

1.2.2 Historical Evolution of Precision Agriculture

The journey of Precision Agriculture (PA) has seen several significant milestones that have revolutionized the way we approach farming and land management (Table 3). The first applications around the world started in the 1980s, when soil scientists and agribusiness researchers in the United States and Europe started to develop equipment and methods for variable rate fertilizer application [35,36]. The first commercially successful grain yield monitors were introduced in 1992. The combination of GNSS-enabled soil sampling, variable rate fertilizer applications, and yield monitoring was the "classic precision agriculture" package in the 1990s and some adoption studies focus on whether that classic package has been adopted. Global Navigation Satellite Systems equipment guidance was commercialized in the late 1990s, first in Australia and shortly after in North America. The introduction of yield sensors and monitors in 1990s laid the foundation for strategies like Variable Rate Application (VRA) and selective harvesting, delivering significant benefits to farmers[37]. Soil sampling has also been also a very important PA application; together with sensing devices, such as Electromagnetic Induction (EC) measuring soil structure and water content and the Hydro-Nitrogen sensor, which senses the chlorophyll and automatically adjust the fertilizer dozes, [38]. Many technological innovations, such as GIS, miniaturized computer components, automatic control, in-field and remote sensing, mobile computing, advanced information processing, and information and communications technologies (ICT), have expanded the application of site-specific approaches while driving a new wave of increased agricultural productivity [39]. In recent years, technologies such as Internet of Things (IoT), Big Data analysis,

and artificial intelligence (AI) are being utilized to optimize agricultural operations and inputs aimed to enhance production and reduce inputs and yield losses[40].

Table 3. Key precision agriculture milestones. Source: [37]

Year	Technology or activity	Company/organization, product name	Reference
1983	Executive order that allowed civilian use of GPS	US government	Brustein, 2014 Rip and Hasik, 2002 [41,42]
1987	Computer-controlled VRT fertilizer	Soil Teq	Mulla and Khosla, 2016, [36]
1988	Handheld GNSS	Magellan	Smithsonian, 2018[43]
1992	First conference dedicated to precision agriculture research	International Conference on Precision Agriculture	Khosla, 2010, [44]
	Impact plate grain yield monitor	Ag Leader, Yield Monitor 2000	Ag Leader, 2018[45]
1995	First conference dedicated to precision agriculture industry	InfoAg	IPNI, 2010
1997	Auto guidance	Beeline	Rural Retailer, 2002
	On-the-go soil EC sensor	Veris	Lund, E., 2018
	Cotton yield monitor	Micro-Trak, Zycom	Vellidis et al., 2003[46]
	First ECPA conference in Europe	John Stafford. and A. Werner	John Stafford and A. Werner [47]
2000	End of GNSS selective availability	US government	Coalition to Save Our GPS, 2012, [48]
2002	Integrated optical sensor and variable rate nitrogen applicator	N-Tech Industries, Greenseeker	Rutto and Arnall, 2017 [49]
2003	On-the-go soil pH sensor	Veris, Soil pH Manager (MSP)	Lowenberg-DeBoer, 2003 [50]
2006	Automated sprayer boom section controllers	Trimble, AgGPS EZ-Boom 2010	Trimble, 2006 [51]
2009	Planter row shutoffs	Ag Leader, Sure Stop	Ag Leader, 2018 [45]
2017	First fully autonomous field crop production	Harper Adams University	Hands Free Hectare, 2018[52]

The history of PA has demonstrated that technological innovations have exerted a more profound influence compared to innovations in information analysis and decision support [36]. Initially, technologies like GNSS and yield monitors were perceived as valuable additions to existing farm equipment. Over time, these technologies became standard features on farm combines, making them equally prevalent among precision and conventional farming practitioners. The integration of GNSS into farm machinery paved the way for significant advancements in precision farming, including autosteer and variable rate fertilizer application (Figure 2).

Conversely, information analysis and decision support systems for tasks like delineating management zones or providing variable rate recommendations have not been widely integrated into routine farm operations. Often, these functions are outsourced to crop retailers, consultants, or agribusiness service providers for a fee. However, there is a noticeable shift towards placing more emphasis on information analysis and decision support systems within PA. Large corporations

and researchers are increasingly focusing on big data challenges, which involve amalgamating spatially and temporally variable data from sources like yield monitors, soil fertility measurements, crop stress assessments, and climate data. This data is collected from numerous farming operations and used to identify and model relationships with soil and landscape characteristics that can inform precision farming decisions.

Figure 2. i) Pierre Robert explaining his computerized farming by soil map database (1985) to Jim Anderson at the University of Minnesota, ii) First commercial unit (1980) of the Geonics EM-38 single dipole electromagnetic induction conductivity meter, iii) Variable rate herbicide applicator developed by Stafford and Miller (1993), iv) Soil organic matter sensor based on NIR reflectance (1991). Source: [36].

Future historians might reflect on the VRT equipment and services introduced in the early 1990s as an essential initial stride, albeit not the optimal solution for spatial management of crop inputs. Over time, we have seen a significant growth in the volume, diversity, and value of databases. Smart robots have been integrated, AI algorithms and simulation models have been refined, while the scale at which management decisions are being visualized and implemented has improved. This continuous progression has been steering us towards an increased dependence on predictive precision farming practices, providing robust solutions characterized by heightened autonomy and precision. The evolution from VRT to these significant advancements will serve as a continuous reminder that future waves of innovation will consistently bring about remarkable transformations in the field of PA.

1.2.3 Why Precision Agriculture?

Farmers are facing multiple challenges related to agricultural production. PA has the potential to offer many benefits, including increased efficiency and productivity, lower input costs and better environmental management, making it an attractive choice for modern farming. Essentially it aims to do more with less resources.

Enhanced Resource Utilization and Site-Specific Management

PA revolutionizes how agricultural resources are managed. It is intrinsically linked to the spatial and temporal variability in yield and quality, recognizing that every field is unique and requires tailored management approaches. By utilizing data from remote sensing and on-site sensors, farmers can identify variations in soil composition, moisture levels, and other factors across their fields. This enables them to divide their fields into management zones, each receiving customized treatments based on its specific needs. This site-specific approach ensures that resources are allocated efficiently, leading to more balanced growth and yield across the entire field. For example, PA can optimise irrigation and fertilisation practises by making site-specific recommendations based on real-time soil moisture and nutrient data, improving water and nutrient use efficiency, and reducing the risk of over-irrigation and nutrient leaching [53]. PA can also improve pest and disease control by providing early warning of infestations and targeted treatments, reducing the use of pesticides and other inputs [54].

Nonetheless, gaining a deep understanding of field variability is of utmost importance. Several critical questions emerge to ascertain whether a uniform or differentiated management strategy is effective in agricultural production: Is the variation significant enough to warrant deviation from uniform management? Is the spatial variation stable over time? Does targeted management make economic and/or ecological sense?

When commercial yield mapping initially emerged, there was an expectation that certain parts of a field would consistently yield well, while others would yield poorly [23,34]. This expectation was based on the assumption that permanent soil characteristics would exhibit consistent behaviour from year to year. However, contrary to these initial expectations, it became apparent that spatial trends in yield could vary significantly in time as well. As a result, numerous researchers dedicated their efforts to developing spatially and temporally trend maps over the years to depict these trends within agricultural fields accurately. Spatial databases have been generated using various GIS systems by integrating maps derived from remote sensing, soil sampling, yield monitoring, and various sensors. Advanced geostatistical methods are used to analyze the spatial and temporal variability [55]. Crop-modeling techniques have been incorporated to develop yield potential maps as a base for fertilizer prescription [56]. Technologies like GNSS, sensors, and data analytics have been deployed, so that farmers can precisely target the application of water, fertilizers, and pesticides.

Furthermore, the level of variability plays a crucial role in determining the efficiency of PA. For instance, variability may be too small or randomly distributed so that spatial control is not feasible. Uniform cropping strategies exhibit optimal efficiency and cost-effectiveness when there is negligible variation between sites, thereby obviating the necessity for PA. VRT technology is not currently capable of dealing with highly variable sites, and the profitability of sites with low variability may not be sufficient to offset the costs of implementing PA. Note that environmental costs can be expressed in monetary terms, which could make low variability sites eligible for PA.

In summary, the performance of PA depends on the significance and stability of variations within a field, and whether site-specific management proves economically and ecologically viable. Taking a strategic approach that entails careful planning and thoughtful implementation when employing PA practices and technologies, is essential for achieving high performance across diverse contexts.

Profitability

The introduction of precision farming marked a significant shift in agriculture, offering the promise of increased efficiency and reduced operational costs. PA aims to minimize operational costs by reducing the excessive use of inputs. With accurate data on soil conditions, nutrient levels, and pest presence, farmers can make precise decisions about the amount and timing of fertilizer and pesticide applications. This not only cuts down on expenses related to inputs but also decreases the environmental impact associated with excess chemical use. However, since the inception of precision farming, scientists, farmers, and practitioners alike have questioned its economic

feasibility [36]. While the concept held great potential, assessing the tangible economic benefits associated with PA technologies has proven to be a complex and challenging task [57], as several factors influence the investment value of PA. These factors include the current farm gross margin, the cost of PA equipment, the area and number of years over which the equipment is used, and the rate at which benefits from its adoption start to materialize[58]. Furthermore, an additional challenge in evaluating the profitability of PA technologies stems from the diverse range of agricultural contexts and practices. Farming operations vary widely in terms of scale, crops grown, environmental conditions, and available resources. Consequently, the economic impact of PA technologies can differ significantly from one farm to another.

So far, some fundamental research studies have contributed valuable insights into the potential cost savings linked to the implementation of PA. For instance, in a review article conducted by Griffin and Lowenberg-DeBoer (2005), it was reported that approximately 68% of the 210 studies examined reported benefits from adopting various PA technologies [59]. Interestingly, about half (52%) of these studies reporting benefits were authored or co-authored by economists, underlining the significance of economic analysis in assessing the advantages of PA. The USDA's (United States Department of Agriculture) October 2016 report highlighted that PA technologies significantly boosted net returns and operational profits [60]. On average, corn farms embracing PA observed operating profits $163 per hectare higher than those not adopting PA, especially on larger farms exceeding 1500 hectares, where computer mapping, guidance, and variable-rate equipment were most commonly adopted [60]. These profit margins could increase further, reaching up to $272 per hectare, depending on the crop.

Heisel et al. (1996) and Timmermann et al. (2002) have demonstrated that making informed decisions about input applications, such as herbicides, could result in substantial cost reductions [61,62]. However, it is important to note that cost savings do not always immediately translate into profitability. In some cases, studies like those by Carr et al. (1991) and Biermachera et al. (2009) have indicated that there may be an insignificant difference in the return on investment between using PA technologies for fertilizer applications and traditional methods [63,64]. Furthermore, other studies [65,66] have suggested that applying soil sampling tests for soil fertility, a common practice in precision farming, may not consistently lead to increased profitability

In conclusion, the economic feasibility and benefits of PA are complex and context dependent. While there is evidence of cost savings and improved resource management, the economic impact of PA technologies can vary widely across different farming scenarios. This underscores the importance of conducting comprehensive economic assessments tailored to specific agricultural contexts to determine the true profitability of precision farming practices.

Innovative Technologies: Agriculture 4.0 and 5.0

Precision Agriculture drives the adoption of cutting-edge technologies in the agricultural sector. Modern technologies such as the Internet of Things, Remote Sensing, Big Data and DSS are expected to leverage this development and introduce more robots and artificial intelligence in farming. The data gathered through these technologies goes beyond immediate decision-making, providing valuable insights into soil, climate, crop growth, and yield interactions. Researchers can use this data to refine farming practices and develop innovative technologies and contribute to the continuous enhancement of agricultural practices. These advancements offer detailed information on soil, crop status, and environmental conditions, facilitating precise phytosanitary product applications. This precision reduces herbicide and pesticide use, enhances water efficiency, and boosts crop yield and quality.

One of the fundamental differences between traditional and modern farming is, apart from the mechanization level, the data collected directly from the crops. In traditional farms where growers judge by visual assessment, decisions are relative and subjective. Traditional farming relies on subjective visual assessments by growers for decision-making, while modern farming relies on quantitative data for making objective decisions. Sensors enable field data collection, but the integration of non-invasive technologies and real-time sensing from mobile platforms has

revolutionized data gathering. Remote sensing, particularly through artificial satellites, has been instrumental in advancing Smart Farming by providing widespread access to field data. Remote sensing technologies mounted on aircraft, drones, or satellites to collect data pertaining to various crop attributes. These include canopy coverage, leaf area index (LAI), and soil moisture, all of which provide precise spatial insights into crop health and performance. This data subsequently informs specific site-oriented management strategies. The core objective is to gather intricate information about Earth's surface characteristics and dynamics. Optical sensors, in particular, play a pivotal role in this process by utilizing the phenomenon of sunlight reflection from terrestrial objects. The functionality and effectiveness of these sensors are underpinned by a range of critical parameters including spatial resolution, radiometric resolution, spectral resolution, and temporal resolution.

However, the complexity of data is also a serious challenge to cope with, as vital information may result in being masked by noise. A common way to manage field data displayed on maps and culminate with a practical solution is through the use of GIS. This suite of computer-based tools or data platforms enables the storage, analysis, manipulation, and mapping of georeferenced information of any kind. For PA applications, a specific GIS system named the Field-level Geographic Information System (FIS) was developed [67], but it was designed for older computer operating systems like Windows 3.1x, 95, 98, or NT [68]. A more updated version known as the Farm Management Information System (FMIS), as outlined by Burlacu et al. [69] is a management information system designed to assist farmers with various tasks, ranging from operational planning, implementation and documentation to the assessment of performed field work.

Beyond remote sensing and GIS, PA entails the utilization of other information technologies. IoT, GNSS, DSS are instrumental in processing and mapping spatial relationships, aiding in management decisions informed by multiple layers of information.

IoT is a fundamental driver behind the emergence of Agriculture 4.0, signifying a substantial transformation in agricultural practices [70]. It encompasses the utilization of sensors and various devices to transform every aspect and action within farming into valuable data. In fact, IoT technologies is one of the reasons why agriculture can generate such a big amount of valuable information, and the agriculture sector is expected to be highly influenced by the advances in these technologies [71]. One of the main advantages of IoT adoption in agriculture is that facilitates increased crop yields and cost reduction. Studies conducted by OnFarm, for instance, reveal that the utilization of IoT on an average farm result in a 1.75% boost in crop yields and substantial energy cost savings ranging from 17 to 32 dollars per hectare, while water use for irrigation falls by 8%[72]. Currently, an estimated 10% to 15% of U.S. farmers have embraced IoT solutions, covering an extensive agricultural expanse of approximately 1.2 billion hectares and spanning 250,000 farms [73]. Projections suggest that, with the adoption of new techniques, IoT could increase agricultural productivity by a staggering 70% by 2050 [74]. This is particularly significant given the world's need to ramp up global food production by 60% by 2050 to accommodate a population expected to exceed nine billion [75].

Furthermore, the escalating expansion of databases in terms of volume, velocity, and variety has given rise to the concepts of " Big Data " and " Big Data analytics." These concepts have the potential to significantly amplify research and development efforts in the pursuit of smarter farming, thereby addressing the substantial challenge of producing higher-quality food on a larger scale and in a more sustainable manner. Even though the concept of Big Data is present in many economic sectors, its integration into agriculture remains a question [70]. Kunisch concluded that Big Data finds application only in certain agricultural scenarios, contingent upon individual farm setups and their technology adoption levels [76]. Nevertheless, it is evident data was being increasingly applied in the agriculture sector. Kamilaris et al. [77] referenced 34 works illustrating the use of Big Data in agricultural applications, while Wolfert et al. [78] conducted a review on Big Data applications in Smart Farming. In line with this trend, the Consortium of International Agricultural Research Centers (CGIAR, Montpellier, France) established a Platform for Big Data in Agriculture, aiming to address agricultural development challenges more swiftly, effectively, and

on a larger scale using big data methodologies [79]. While Big Data's application in precision farming is currently in an early development stage, it can be inferred that Big Data will cause major changes in agricultural domain.

Decision support systems (DSS) have also made significant strides by empowering farmers to make well-informed decisions regarding crucial aspects like planting, irrigation, fertilization, and pest management. They serve as valuable tools for farmers to manage their farms efficiently by collecting, processing, storing, and sharing data related to agricultural activities. These systems often utilize agronomic models and field data to foster effective long-term planning by identifying trends and patterns in field performance, thereby enabling farmers to make more informed decisions for the future. To be effective, agricultural DSS should meet criteria such as profitability, user-friendliness, credibility, adaptability, maintenance, and updates. Some level of user knowledge is also necessary for their utilization. These systems gather data from various sources, including weather stations, field sensors, image capture systems, and information technology tools like smartphones and provide information related to various agricultural tasks.

Navarro-Hellín et al developed a DSS for citrus orchards that estimates weekly irrigation needs by considering climate and soil variables [80]. Lindsay Corporation, based in Omaha, Nebraska, USA, developed and received recognition for FieldNET Advisor™ [81,82] a DSS that offers irrigation management guidance to growers. Similarly, HydroLOGIC, designed for individual fields in Australia, integrates knowledge of crop physiology, agronomy, available water resources, soil properties, and climate to optimize cotton yield and water utilization[83]. In addition, web-based pest forecasting models and DSS are gaining popularity as well, with expectations of increased demand in the future. Damos and Karabatakis (2013) developed a web-based DSS that predicts pest population phenology during the growing season by considering region-specific average temperatures and climatic factors [84].

For efficient fertilization management, DSS based on agricultural models have been developed. These systems calculate optimal fertilization rates and dosages based on extensive crop fertilization experiments, considering multiple factors influencing fertilizer decision-making[85]. For instance, the Nutrient Management Support System (NuMaSS) software evaluates soil characteristics related to organic matter, including carbon, nitrogen, phosphorus, moisture content, clay, and CaCO3, among others [86]. AgriSupport aids farmers in optimizing resource allocation according to their business prospects while effectively managing production risks, as detailed by Recio et al. in 2003[87]. PCYield, developed in collaboration with the United Soybean Board (USB), Weather Services International (WSI Corp.), and a network of agricultural providers, offers support for soybean cultivation decisions [88].

Automation also has brought about significant enhancements in the productivity of agricultural machinery by improving efficiency, reliability, and precision while reducing the reliance on human intervention [89]. The concept Agriculture 5.0 implies that farms are following PA principles and using equipment that involves unmanned operations and autonomous decision support systems, including the use of robots and some forms of AI [90]. AI systems are increasingly employed to assist in identifying diseases in plants, recognizing pests, and diagnosing issues related to poor plant nutrition on farms. AI sensors can detect and pinpoint weeds, subsequently determining the appropriate herbicides to apply within the correct buffer zone. This approach helps mitigate the risk of over-applying herbicides, which can lead to an excess of toxins in our food supply. Furthermore, the automation of agricultural robots is now considered essential for improving work efficiency and should include the potential for enhancing the quality of fresh produce, lowering production costs and reducing the drudgery of manual labour [91]. According to the Verified Market Intelligence report, agricultural robots will be capable of completing field tasks with greater efficiency as compared to the farmers [92]. A Forbes study [93] further highlights how farm robots contribute to the human labor force, enabling the harvesting of crops at a higher volume and a faster pace compared to human laborers. While there are instances where robots are not as fast as humans, the agricultural industry is actively developing robotic systems to assist farmers with repetitive tasks [94–96], driving the evolution of agriculture towards the emerging concept of Agriculture 5.0. As noted by Reddy et al. [97], the advent of robots in agriculture drastically

increased the productivity in several countries and reduced the farm operating costs. It is evident that the field of robotic innovations is experiencing exponential growth [98], which is bolstering the global agriculture and crop production market. Startups that leverage robotics and machine learning to address agricultural challenges gained momentum in 2014, aligning with the increasing interest in AI [99]. In fact, venture capital funding in AI has surged by 450% over the past five years [100]. Nonetheless, these technologies remain prohibitively expensive for many farmers, particularly those with smaller farm [101], as economies of scale make larger farms more profitable [102]. However, as technology costs continue to decrease over time, agricultural robots are poised to become a viable option in the future, serving as an alternative to achieve higher production levels [103,104].

In summary, PA not only improves productivity and efficiency but also encourages innovation, by presenting a wide-ranging suite of technologies that, when combined, significantly elevate agricultural practices, bolster economic viability, and reinforce environmental sustainability. The amalgamation of technologies such as GPS, remote sensing, IoT, GIS, AI, automation, and DSS within farming practices sets the stage for ongoing technological progress that not only benefits farmers but also enhances the agricultural industry as a whole. By focusing on precise resource management, effective data utilization, and ongoing innovation, PA stands as a transformative approach that empowers farmers to address the challenges posed by our rapidly evolving world.

Improved Environmental Sustainability

The agricultural sector plays a substantial role in climate change, accounting for approximately 13.5% of the total global anthropogenic greenhouse gas (GHG) emissions [105]. PA offers substantial environmental benefits due to its targeted and resource-efficient approach. This method minimizes the usage of water, fertilizers, and pesticides, thereby reducing the potential for contamination of water bodies. Furthermore, PA practices aid in the mitigation of soil erosion and promote soil health. These sustainable land management practices contribute to the well-being of ecosystems and bolster long-term environmental sustainability.

The alignment between PA and sustainable farming practices is a noteworthy aspect. Farmers actively engage in preserving ecosystems and ensuring the long-term sustainability of agricultural activities by optimizing the use of resources, reducing waste, and conserving natural resources. This approach ensures that agriculture can continue to meet the needs of future generations.

Precision farming to reduce the risks of pesticide leaching to groundwater in sandy soils was first studied by Mulla et al. (1996) at a field site in Washington State [36]. Measured concentrations in carbofuran applied at 8.1 kg ha−1 i.e. were measured to a depth of 1.8 m at 57 locations throughout the field and this data wad used to calibrate the convective-dispersive equation for pore water velocity, dispersion coefficient, and retardation factor [106]. To date, numerous studies have highlighted the potential of PA technologies to reduce the environmental impacts associated with agriculture [107–110] PA technologies excel in precisely matching farm inputs with crop requirements, thereby avoiding over-application [111]. For instance, applying just the right amount of nitrogen to achieve maximum crop yield has the potential to decrease nitrate contamination in groundwater and the pollution of downstream water sources [63]. This is particularly critical as agricultural non-point source pollution significantly contributes to the contamination of numerous global waterways.

In a study conducted [112], it was observed that among the 14 environmental aspects considered, agricultural inputs were the most influenced in all categories, while gaseous emissions of all types (with CO2 being the most affected) were the least affected aspects. An increase in soil biodiversity was also noted, likely because the rational use of inputs derived from the application of PA technologies reduces the impact on fauna and flora, thus contributing to biodiversity preservation.

It is evident that PA significantly mitigates the environmental impact of agriculture, addressing concerns such as greenhouse gas emissions, water contamination, and soil health. Research highlights PA's potential to reduce pollution risks, especially in pesticide management and

groundwater protection, while promoting precise resource use. This approach benefits ecosystems and preserves biodiversity, reinforcing its role in sustainable farming and environmental stewardship.

1.2.1 Precision Agriculture adoption: Key Factors

The applicability of PA extends to diverse agricultural domains, ranging from crop cultivation and livestock management to fisheries and forestry. The adoption of PA has been steadily increasing in recent years, as demonstrated by a study conducted by Maloku et. al. [113].Their research revealed a consistent and notable increase in the number of scientific articles dedicated to PA between 1996 and 2018. By 2018, the total count of scientific articles in the field of precision agriculture had reached an impressive 272. Interestingly, the study also highlighted that Chinese and USA-based organizations exhibited a higher level of interest in publishing articles related to PA compared to organizations in other countries. However, the assimilation of PA practices in agriculture often faces a number of challenges contingent on the local context.

The exploration of factors influencing the adoption of PA has yielded a substantial body of literature. Over the years, several studies have tried to provide a world-wide overview of PA adoption [30,59,114]. Zhang et al. (2002) focused mainly on the technical issues associated with PA adoption and cited several adoption studies from the United States, United Kingdom, and Australia [30]. They identified the following constraints to adoption: (i) the quantity of PA data exceeds the ability of farmers to analyze and use it for management, (ii) lack of scientifically validated procedures determining variable rate application of inputs, (iii) absence of evidence for the benefits of PA, (iv) labor intensive and costly data collection, and (v) need for improved technology transfer. Furthermore, Griffin and Lowenberg-DeBoer (2005) summarized the worldwide data on PA adoption, reviewed the studies of PA economics, and drew implications for Brazil[59]. They reported detailed US PA survey information and worldwide PA adoption in terms of the number of combine yield monitors used in the United States, Australia, South Africa, several Latin American countries, and nine western European countries. Likewise, several other studies have examined broad aggregate factors such as farmer age, farm size, subsidy payments, the cost and complexity of technology [115], level of farmer education and access to crop consultants [116] and their influence and relationship with the adoption rate of PA technologies.,

Tey and Brindal ,(2012) found that the adoption of PA technologies is a result of multi-dimensional considerations and is positively associated with (i) socio-economic factors (farmers who are older and have higher education level), (ii) agro-ecological factors(farmers whose farm has better soil quality, is self-owned, and is large), (iii) institutional factors (farmers who face greater pressure for sustainability), (iv) informational factors(farmers who have hired consultants and agreed on the usefulness of extension services),(v) farmer perception (farmers who perceived that PA technologies would bring profitability), and (vi)technological factors (farmers who have used computers) [8]. Operator age has been identified as a significant explanatory factor, showing a negative correlation with the adoption of high-technological practices, such as computers [117]. This negative relationship is often attributed to older farmers having shorter planning horizons, reduced incentives for change, and limited exposure to Precision Agriculture technologies [118]. Conversely, younger farmers tend to have longer career horizons and a greater inclination toward technology adoption [119]. They may be more motivated to explore PA technologies compared to their older counterparts. Farming experience, on the other hand, quantifies the duration for which farmers have been engaged in agricultural production activities. Greater experience can lead to a better understanding of spatial variability in the field [120], and potentially enhance operational efficiency through experiential learning [121]. However, more experienced farmers may perceive a reduced need for the additional information provided by PA technologies and, therefore, opt not to adopt them [122]. Since the implementation of PA technologies demands substantial technological literacy, analytical skills, and knowledge-based interpretation, farmers with higher levels of formal education are more likely to possess the necessary human capital [119].

Furthermore, the utilization of precision agriculture technologies raises concerns regarding potential adverse environmental impacts and effects on the livelihoods of small-scale farmers.

Moreover the adoption of Precision Agriculture technologies tends to be more prevalent on large farms [8]. This pattern emerges because larger farms possess a greater capacity to absorb the associated costs and risks, while simultaneously being able to spread these factors over a larger productive area. Additionally, as arable land becomes increasingly scarce due to development, the pressure to transition to more productive agricultural practices intensifies. Under such circumstances, farmers who face this pressure are more inclined to adopt PA. Furthermore, the information required for implementing PA technologies is typically sourced from extension services or agricultural consultants. However, these public services are designed for mass consumption, which can limit the officials' focus and availability to provide tailored assistance to specific farms. Given the technical complexity of PATs, many farmers opt to hire the services of third parties, such as cropping consultants, to set up and utilize these technologies effectively. This tendency has been substantiated by the research conducted by Robertson et al. (2012) and Larson et al. (2008)[116,119]. Furthermore, computer technology plays an indispensable role in Precision Agriculture [118]. Consequently, the utilization of computers is often identified as a key indicator of the propensity to adopt PA technologies, as observed in several studies [24,122,123].

It is evident that extensive research has been conducted to identify factors influencing the adoption of PA by individual farmers [8,24,39,39,111,116,118–120,122–135].These studies have highlighted various statistically significant factors, including the age of the farm operator, education, years of farming experience, farm specialization, land tenure, farm size, full or part-time farming, debt-to-asset ratio, use of a crop consultant, perceived profitability of PA, computer usage, and irrigation. It's important to note that most of these studies have been conducted in developed countries, with limited research focusing on PA adoption in the developing world. Mondal and Basu (2009) outlined the theoretical reasons why PA should be adopted by farmers in developing countries [136]. Say et al. (2018) added to the literature by documenting the beginnings of PA adoption in middle- and lower-income countries [137]. They confirm that guidance is the most commonly adopted PA technology in developing countries.

PA is called to be the agriculture of the 21st century. Although the assimilation of precision agriculture technologies has progressed, its adoption is influenced by social, economic, and environmental implications. Therefore, it's crucial to acknowledge that significant transformations require time for widespread acceptance. Just as the adoption of tractors in agriculture took time to become the norm, the complete embrace of PA necessitates a gradual approach to realize its full potential throughout the agricultural sector.

1.3 Remote Sensing in PA

Remote sensing applications in agriculture rely on the interaction between electromagnetic radiation and soil or plant materials, with a focus on measuring reflected radiation rather than transmitted or absorbed radiation. These applications are often categorized based on the type of platform used for the sensors, which can be satellite-based, aerial, or ground-based.

Various remote sensing platforms possess distinct advantages and limitations concerning factors like spatial and temporal resolutions, spectral characteristics, coverage area, revisit frequency, data availability, cost, and processing needs. Consequently, choosing the optimal remote sensing platform for a particular crop yield prediction task relies on multiple considerations including crop type, analysis scale, forecasting objectives, available resources, and user preferences.

1.3.1 Satellite remote sensing

Satellites serve as versatile tools with applications in diverse domains, ranging from geology and agriculture to climate and emergency response (Figure 3). For over four decades, satellites have also played a pivotal role in advancing PA applications.

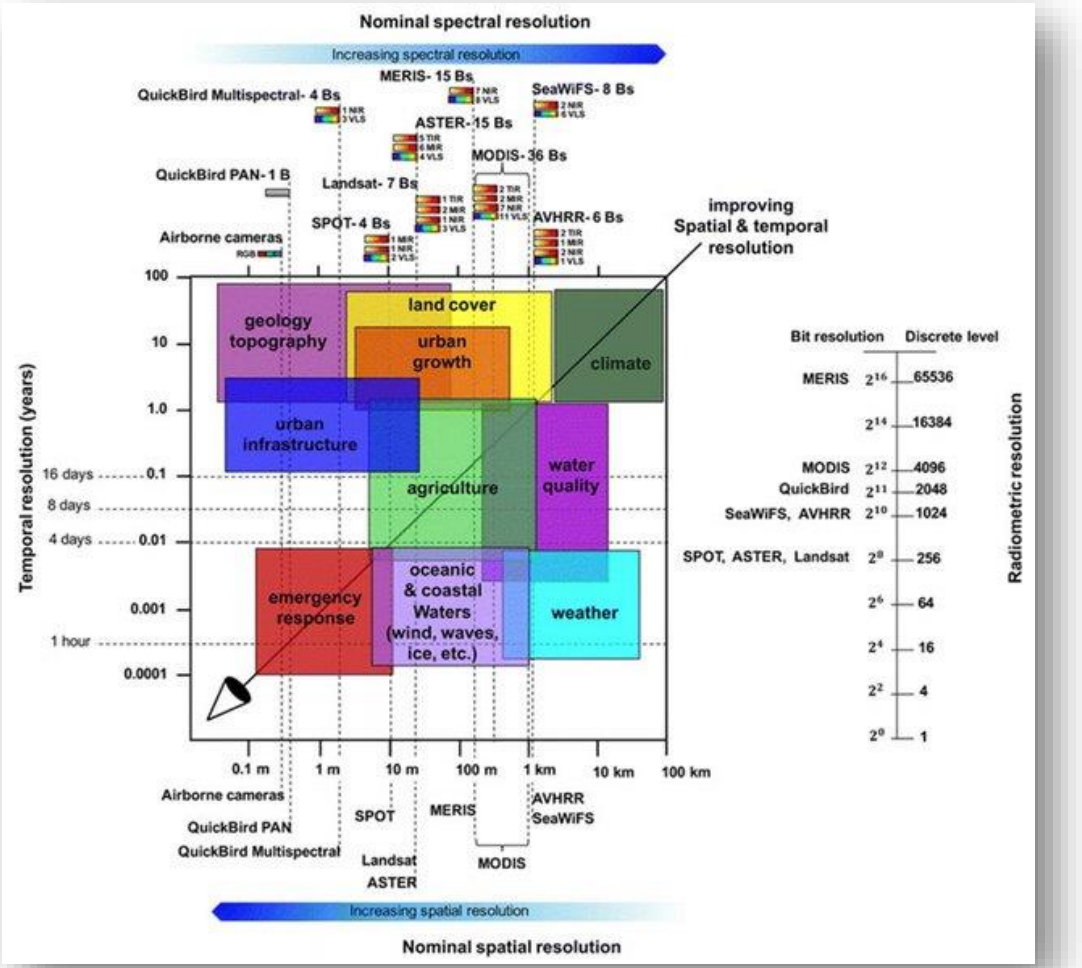

Figure 3. An overview of spectral, spatial, temporal, and radiometric resolution of different optical satellite system. Source: [138]

The evolution of satellite technology has been remarkable, with three generations of instruments shaping this progress. The first generation offered relatively low spatial resolutions, ranging from 1 km to 100 m. In the second generation, this improved to 30–10 m, while the third generation reached new heights with very high spatial resolutions of 5–0.5 m and less, leading to more accurate feature recognition [138]. This journey commenced for agriculture with the launch of Landsat 1 in 1972 (Figure 4) by the National Aeronautics and Space Administration (NASA). This was equipped with a multispectral sensor and possessing a spatial resolution of 80 meters per pixel, observed at 18-day intervals. After Landsat 1, a series of Landsat satellites (Landsat 2–9) were launched to provide high quality images to researchers, land managers, and policy makers to help in the management of natural resources globally. Later, in 1984, the Landsat 5 Thematic Mapper was launched to collect higher resolution (30 m) images in more bands in visible and NIR region.

Landsat imagery was investigated for diagnosis of agricultural problems by Robert (1982), but difficulties in processing satellite remote sensing data at that time prevented meaningful results [139]. Zheng and Schreier (1988) and Bhatti et al. (1991) were the first to use aerial and satellite imagery, respectively, for the specific purpose of estimating spatial patterns in soil fertility that could be used to guide variable rate fertilizer applications [140,141]. Zheng and Schreier (1988) found that potassium fertilizer recommendations for a bare field in British Columbia could be

reduced relative to uniform applications if rates were varied according to spatial patterns in soil organic matter content identified using color aerial photographs. Bhatti et al. (1991) found that spatial patterns in soil organic matter from Landsat satellite imagery for bare soil on a commercial farm in Washington State were strongly related to patterns in soil phosphorus and wheat yield. They proposed that areas with low organic matter content and low crop productivity "could be managed with customized fertilizer and tillage practices" for environmental protection.

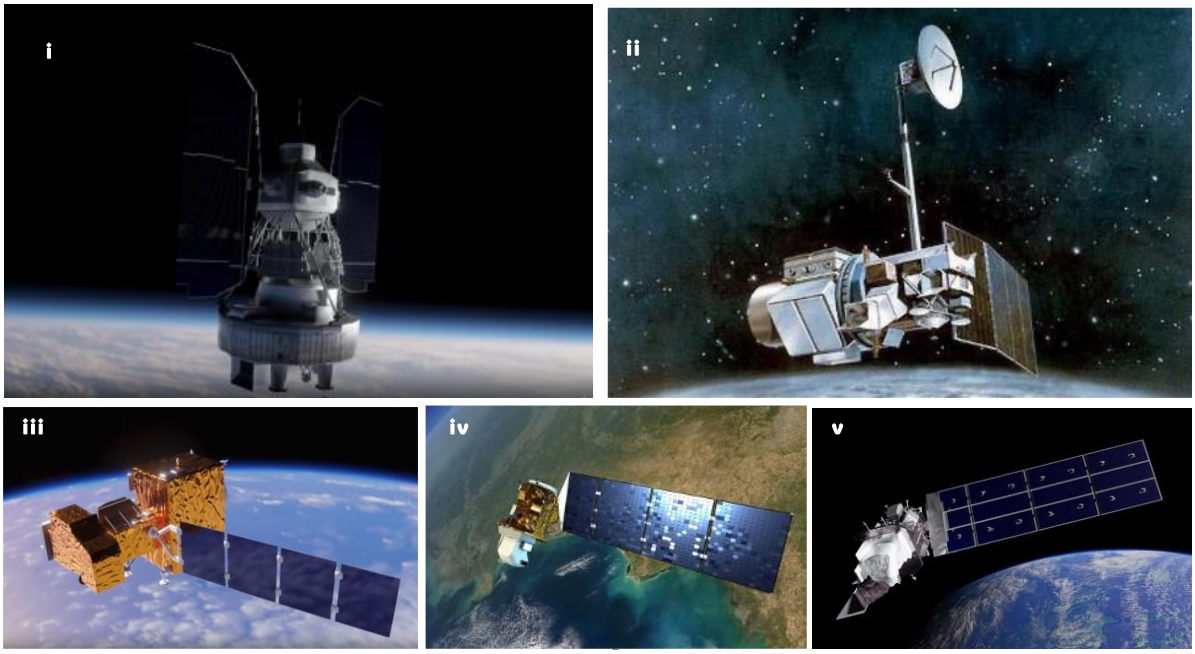

Figure 4. Visual presentation of i) Landsat 1-3, ii) Landsat 4-5, iii) Landsat 7, iv) Landsat 8, v) Landsat 9, Source: NASA. Source: [142]

Until launch of the commercial IKONOS satellite in 1999, there were few instances where satellite remote sensing was used for precision farming applications [143]. IKONOS, collected imageries at 1-m resolution in panchromatic image and 4-m spatial resolution in visible and NIR bands with a revisit period of up to five days [143]. Imageries collected from IKONOS have been used for multiple purposes in PA, including soil mapping, crop growth and yield prediction, nutrient management, and ET estimation [144,144–146]. In 2001, DigitalGlobe, Longmont, CO, USA launched a satellite named QuickBird with capabilities similar to IKONOS and a revisit frequency of 1–3 days.

After remote sensing applications started to have a wide research impact, efforts were made to design satellite imaging systems with higher spatial resolution and quicker revisit cycles. For instance, GeoEye-1 (2008), Pleiades-1A (2011), Worldview-3 (2014), SkySat-2 (2014), and Superview-1 (2018), were launched and collected multispectral images at a high spatial resolution of ≤2 m with a daily or sub-daily revisit period. A significant milestone in this progression was the introduction of WorldView 3 in 2014. This sophisticated satellite boasts an exceptional resolution of merely 0.31 metre panchromatic and 1.24 metre in the eight VNIR bands, 3.7m in the eight SWIR bands and a 30 m resolution in the CAVIS (Clouds, Aerosols, Vapours, Ice and Snow) bands. Moreover, it operates at an impressively swift update rate ranging from 1 to 4 days. In the same year the Copernicus Programme, led by the European Space Agency [147], marked a new era in open access Earth observation by launching the first Sentinel satellite, Sentinel-1A. Subsequently, the Copernicus Programme has successfully launched several satellite missions, including open-source satellites Sentinels-1, 2, 3, and 5. One significant contribution of the Copernicus Programme was the launch of the multispectral instruments aboard the Sentinel-2 satellites. The Sentinel-2 constellation consists of twin satellites, Sentinel-2A and Sentinel-2B, each making distinctive contributions to Earth observation [148]. Sentinel-2A was launched on June 23, 2015, with the first images received a few days later, marking a significant milestone in the

Copernicus Programme's ongoing mission to enhance our understanding of Earth's dynamics. It has multiple multispectral bands with a spatial resolution of 10 to 60 metres per pixel.

Each satellite is equipped with optical sensors designed to measure features on the Earth's surface by detecting and recording sunlight reflected from objects (Figure 6). The effectiveness of these sensors is determined by several critical factors, including their spatial, radiometric, spectral, and temporal resolution[149].

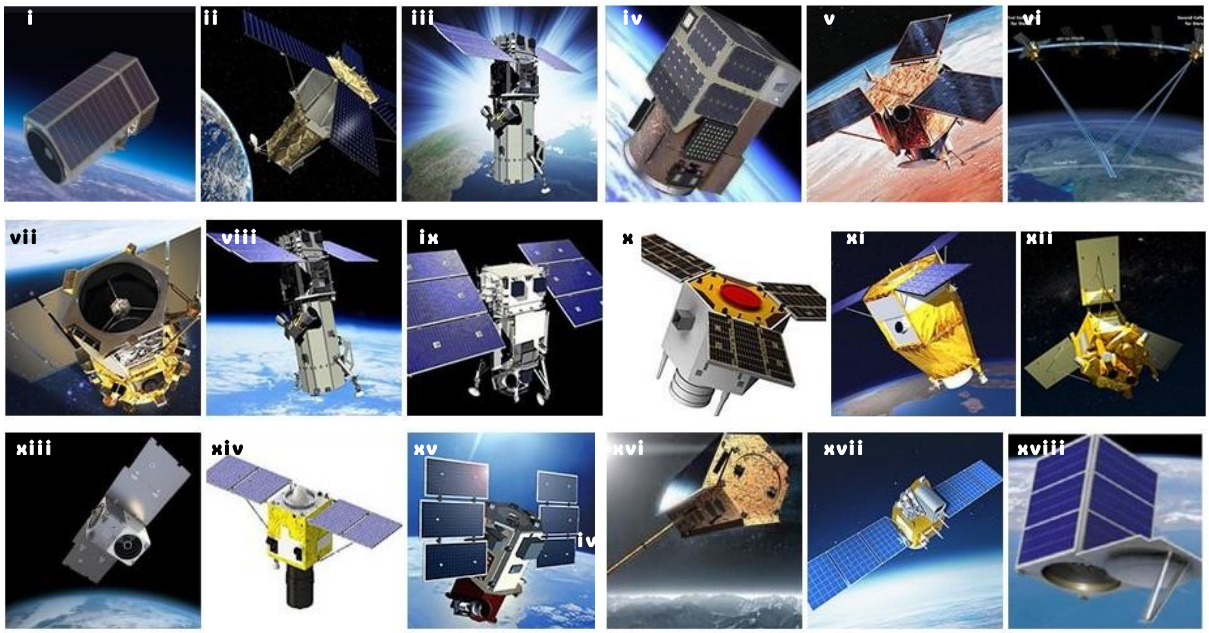

Figure 5. Visual presentation of i)Albedo (10cm), ii) WorldView-4 (30cm), iii) Worldview-3, iv) Satellogic (0.7m), v)IKONOS (0.82m), vi) Stereo Satellite, vii) GeoEye-1 (0.41m), viii) WorldView-2 (0.46m), ix) WorldView-1 (0.46m), x) Jilin-1 (1m), xi) SPOT-7 (1.5m), xii) SPOT-6 (1.5m), xiii) Pelican, xiv) SuperView-1 (0.5m), xv) QuickBird (0.61m), xvi)TerraSAR-X, xvii) TH-01 (2m), xviii) SkySat (50cm). Source: NASA, [150]

Spatial resolution, a fundamental aspect of remote sensing, refers to the inherent capacity of a sensor to discern the smallest detectable ground object. This resolution is inextricably linked to pixel size and image coverage, both of which are influenced by the number of pixels within the sensor and its proximity to the Earth's surface. This interplay is exemplified by sensors like Landsat, characterized by 30-meter pixels, which encompass an expansive image area of 185 km × 185 km. Similarly, the SPOT sensor boasts 20-meter pixels and is capable of generating comprehensive images spanning 60 km × 60 km. Meanwhile, the deployment of UAS sensors at altitudes of up to 3 km yields resolutions as impressive as 1-2 meters and image coverage that extends across approximately 100 hectares. Pleiades-1A and Worldview-3 have been used for many PA applications requiring high spatial resolution imagery, including disease and crop water stress detection [151–153].

Radiometric resolution, another indispensable facet, quantifies the sensor's ability to capture the intensity of radiation emitted by a target within a specific waveband. This resolution translates into the number of discrete radiometric levels available for individual pixels to record this intensity. For instance, sensors with an 8-bit radiometric resolution offer 256 distinguishable intensity levels, rendering a gradation from the darkest (0) to the brightest (256). Conversely, sensors with a 10-bit radiometric resolution extend this capacity to an impressive 1024 levels per image pixel, enabling finer distinctions in recorded intensities.

Spectral resolution, an intricate dimension of remote sensing, dictates the number of distinct wavebands of data that a sensor can simultaneously capture at each pixel. This resolution is profoundly significant due to its connection with the reflectance profiles of objects under study. For instance, as a prime example, vegetation exhibits distinct reflectance behaviours in response to

different wavebands. Photosynthesizing plants, including a range of flora such as groundcovers and vines, exhibit reduced reflectance in blue and red wavelengths. This can be attributed to the absorption of incident energy by chlorophyll and related pigments for photosynthesis. Conversely, these plants reflect a notably higher proportion of light within green wavelengths, thereby manifesting their characteristic green appearance to the human eye. Interestingly, in the near-infrared range (wavelengths exceeding 700 nm), photosynthetic plants display a substantial increase in reflected sunlight—over 65%—which, while unperceivable to the human eye, can be effectively detected using specialized instruments. This pronounced reflectance in the near-infrared range is intrinsically tied to leaf cell structure and moisture content, which profoundly influence this reflective behaviour.

Temporal resolution, the final cornerstone, encapsulates the frequency with which a sensor can amass data over time. This temporal dimension holds particular significance in capturing dynamic and evolving phenomena. For instance, the progression of vegetation growth or the onset and progression of stress conditions in crops can be accurately tracked and monitored through sensors with varying temporal resolutions.

Spatial and temporal resolution requirements vary widely for monitoring terrestrial, oceanic, and atmospheric features and processes (Table 4). Each application of remote sensing sensors has its own unique resolution requirements and, thus, there are trade-offs between spatial resolution and coverage, spectral bands and signal-to-noise ratios. For a comprehensive overview,

Table 4. Spatiotemporal resolutions of the satellite sensors used for PA applications.Source: [154]

Satellite	Years Active	Sensor (Spatial Resolution)	Temporal Resolution	Application in PA
Landsat 1	1972–1978	MS (80 m)	18 days	Crop growth [155]
AVHRR	1979-present	MS (1.1 km)	1 day	Nutrient management [146]
Landsat 5	1984–2013	MS and Thermal (30 - 120 m)	16 days	Biomass [156]; crop yield [157]; crop growth [158]
Landsat 7	1999-2022	MS and Thermal (30 - 60 m)		
Landsat 8	2013-present	MS and Thermal (30 - 100 m)		
SPOT 1	1986–1990	MS (20 m)	2–6 days	Water management [159]
SPOT-2	1990–2009			
IRS 1A	1988–1996	MS (72 m)	22 days	Water management, nutrient management [136]
LiDAR	1995	VIS (10 cm)	1 N/A	Topography, nutrient management [160]
RadarSAT	1995–2013	C-band SAR (30 m)	1–6 days	Crop growth [161]
IKONOS	1999–2015	MS (1 to 4 m)	3 days	Crop [162]; soil properties [163]; nutrient management[146]; ET estimation [144]
EO-1 Hyperion	2000–2017	HS (30 m)	16 days	Disease[164,165]
Terra MODIS	1999-present,		1–2 days	

Aqua MODIS	2002-present	MS (Spectroradiometer; 250–1000 m)		Crop yield [166]; crop growth [167]
Terra-ASTER	2000-present	MS and Thermal (15 m–V, NIR, 30 m–SWIR, 90 m–TIR)	16 days	Water management [168]
QuickBird	2001–2014	MS (2.44 m)	1–3.5 days	Disease [169]
AQUA AMSR-E	2002–2016	MS (Microwave Radiometer; 5.4 km–56 km)	1–2 days	Water management [170]
Spot-5	2002–2015	MS (V, NIR–10 m, SWIR–20 m)	2–3 days	Crop yield [][171]
ResourceSat-1	2003–2013	MS (5.6m–V, 23.5 m–SWIR)	5 days	Nutrient management [172]
KOMPSAT-2	2006-present	MS (4 m)	5.5 days	Crop yield [173]
Radarsat-2		C-band SAR (1–100 m)	3 days	LAI and biomass [174]
RapidEye	2008-present	MS (6.5 m)	1–5.5 days	Water management [175]; crop yield [176]; crop growth and chlorophyll [177]
GeoEye-1	2008-present	MS (1.65 m)	2.1–8.3 days	Nutrient management [178]
WorldView-2	2009-present	MS (1.4 m)	1.1 days	Crop growth [[179]
Pleiades-1A		MS (2 m)	1 day	Crop growth [180,181]
Pleiades-1B	2012-present			
VIIRS Suomi-NPP	2011-present	MS (IR Radiometer, 375 m and 750 m)	16 days	Crop management (NDVI[182])
VIIRS-JPSS-1	2017-present			
KOMPSAT-3	2012-present	MS (2.8 m)	1.4 days	Crop growth[183]
Spot-6	2012-present	MS (2.5 - 20 m)	1-day	Disease[184]
Spot-7	2014-2023			
SkySat-1	2013-present	MS (1 m)	sub-daily	Crop growth [185]
SkySat-2	2014-present			
Worldview-3	2014-present	SS (1.24 m)	<1 day	Crop growth[186]; weed management [102]
Sentinel-1	2014-present	C-band SAR (5–40 m)	1–3 days	Crop growth[187]
Sentinel-2	2015-present	MS (10 m–V and NIR, 20 m–Red edge and SWIR, 60 m–2 NIR)	2–5 days	Yield [188]; N management [189]
KOMPSAT-3A	2015-present	MS (V NIR–2.2 m, SWIR–5.5 m)	1.4 days	Disease [190]
SMAP	2015-present	L-band SAR (1–3 km) and radiometer (40 km)	2–3 days	Crop yield [191]; water management [192]

TripleSat	2015-present	MS (3.2 m)	1 day	Soil properties[193]
ECOSTRESS-PHyTIR	2018-present	Thermal (38 × 69 m)	1–5 days	ET [194]
Landsat 9	2021-present	OLI-2(30 m)	16 days	Water quality monitoring, crop status

Several trends are apparent in satellite based remote sensing (Table 4). Firstly, the spatial resolution of imaging systems has improved from 80 m with Landsat to sub-metre resolution with GeoEye and WorldView. Secondly, the return visit frequency has improved from 18 days with Landsat to subdaily with SkySat. Thirdly, the number of spectral bands available for analysis has improved from four bands (bandwidths greater than 60 nm) with Landsat to eight or more bands (bandwidths greater than 40 nm) with WorldView. Hyperspectral imaging systems such as Hyperion on the National Aeronautics and Space Administration (NASA) earth observing 1 (EO 1) satellite provided even greater spectral resolution, with imaging from 400 to 2500 nm in 10 nm increments.

While these advancements in satellite systems mark substantial leaps forward, they have certain limitations, particularly concerning crop monitoring. Moran et al. in 1997 and Yao et al. in 2010 succinctly outlined the primary hurdles associated with the utilization of satellite remote sensing in PA [195,196]. One of the significant limitations lies in the reliance on satellite imagery captured in the visible and near-infrared (NIR) bands, which are contingent upon cloud-free conditions for optimal functionality. These bands perform best when solar irradiance remains relatively consistent over time. In contrast, radar imagery obtained via satellites or aircraft remains unaffected by cloud cover, offering a more reliable alternative. Additional challenges entail the need to calibrate raw digital numbers to accurately represent surface reflectance, the correction of imagery to eliminate atmospheric interferences and accommodate off-nadir view angles, and the geo-rectification of pixels through the utilization of GPS-based ground control locations [143]. These intricacies underscore the complexities involved in harnessing satellite remote sensing for PA.

On the other hand, satellite platforms enable the assessment of crop growth and yield potential on a large scale, providing valuable insights for agricultural management and planning. The ability to monitor crop health and productivity remotely allows for identifying regions with potential yield losses and implementing targeted interventions to mitigate risks. Secondly, satellite-based yield prediction offers a non-destructive and cost-effective approach that reduces the reliance on labour-intensive field surveys, thereby increasing efficiency and reducing costs. Compared to the rest of the platforms, satellites can offer broad coverage, high temporal resolution, while being cost effective [197]. They can also be used in multisource data integration, such as the integration of optical and SAR remote sensing[154]. Additionally, satellite-based yield prediction has the potential to provide timely and up-to-date information, allowing for better decision-making and response to climate variability and extreme events. These advantages can explain why the majority of the studies incorporated satellite remote sensing approaches.

In summation, the convergence of satellite-based observations, remote sensing technologies, and data-driven analytics has opened up new avenues for monitoring and managing agricultural landscapes at unprecedented levels of granularity. By harnessing the power of satellite data, researchers and practitioners can obtain real-time insights into various aspects of crop health, soil moisture, nutrient distribution, and environmental conditions. These insights, when coupled with advanced yield prediction models, enable farmers and stakeholders to make informed decisions that optimize resource allocation, minimize risks, and maximize overall crop yield. Moreover, VIs derived from satellite imagery have shown promise in capturing the spatiotemporal variations of crop health and productivity.

1.3.2 UAS Platforms

As technology continues to advance, the utilization of unmanned aerial systems (UAS), commonly known as drones or unmanned aerial vehicles (UAVs), has gained remarkable traction for data collection and various applications in agriculture [198]. These versatile aerial platforms, encompassing both fixed-wing and rotary-wing aircraft, are equipped with a wide array of sensors for comprehensive monitoring and can operate autonomously or be controlled remotely.

The history of unmanned aerial systems (UASs) has seen significant milestones. Formally, the drones' chronicle starts in 1783 in France, where Montgolfier brothers made a public demonstration flight of a globe shaped balloon filled with smoke [198]. However, the forerunner of modern remote-controlled drones is considered the first radio-operated boat; a technological masterpiece shown by Nikola Tesla in Madison SquareGarden in 1898. The earliest unmanned radio-controlled aircraft made its appearance during World War I, known as the Curtiss N-9, which was invented by Cooper and Sperry in 1917. Around this time, Kettering conceptualized the "Kettering Bug," regarded as a predecessor to the modern cruise missile (Figure 7). The significant development of drones continued during World War II with the creation of the Radioplane OQ-2 in 1940, marking the first mass-produced drone in the United States. Subsequently, in 1945, an adapted version known as the OQ-3 was utilized for reconnaissance missions. Post-World War II, the United States introduced the Ryan Firebee, a series of target drones, which were noteworthy for being the first jet-propelled drones, primarily used for air-to-air combat training. In the mid-1950s, the Convertawings Quadrotor, the first four-rotor helicopter, was introduced, featuring an "H" configuration for its four rotors. Another pioneering moment in UAS history was the Mastiff, the first Israeli Military UAS equipped with live-streaming capabilities in 1973. Initially transmitting black-and-white video, it was later upgraded to a colored camera, ushering in a new era of drone applications, particularly for tracking humans or vehicles. In 1986, the RQ2 Pioneer UAS was employed by the US Navy to provide real-time battlefield imagery and perform various tasks, including reconnaissance and surveillance. The 1990s saw the recognition of the significance of UAS in warfare, leading to advancements in lightweight materials and communication technology. One standout development during this period was the remotely piloted aircraft RQ-1 Predator, initially equipped with a reconnaissance camera. In 2002, it was renamed "MQ-1," with "R" representing "Reconnaissance" and "M" indicating "Multi-role." These historical milestones demonstrate the evolution of UASs from early experimental designs to crucial tools in modern military operations. Yamaha developed probably the first UAS applied to agriculture in 1997 by using a rotary wing aircraft [199]. Using helicopters showed big advantages in field spraying due to their high maneuverability, reduced speed and velocity and the positive impact of the airflow from the rotor in spraying tasks. Nevertheless, in the 1990s, multiple countries limited or even banned aerial application of products such as pesticides or fertilizers. Moreover, in 2009 the European Union mostly prohibited aerial spraying of pesticides, which effectively ruined most commercial services of aerial application in all member states and overseas territories.

Figure 6. i)Prototype Kettering Bug (circa 1918); ii)OQ-2 on display at the Aviation Unmanned Vehicle Museum, iii)BQM-34F Firebee II RATO launch, Tyndall AFB 1982 Source: Wikipedia

The technological progress of drones in recent years is undeniable. Initially designed primarily for military applications, these UASs have evolved significantly. As the landscape shifted towards commercial utilization, government agencies and private entities began testing and deploying drones for a wide array of purposes such as. environmental monitoring, response to humanitarian disasters, surveying and mapping, as well as engineering and construction

In agriculture, drones provide crucial data for precision farming practices, optimizing crop yields and resource usage. A recent analysis and forecast report [200]conducted in the USA, using data spanning from 2014 to 2017, highlights the PA among primary application areas for unmanned aerial vehicles (UAVs). The PA application is expected to record a considerable Compound Annual Growth Rate (CAGR) of over 15% from 2023 to 2030 as drones are becoming one of the essential aspects of farm management [201]. Furthermore, the USA Federal Aviation Administration (FAA) forecast for the period 2019–2038, as provided by Association for Unmanned Vehicle Systems International (AUVSI), ranks agriculture as the sixth most prominent sector in terms of the number of missions, accounting for 7% [202].The last decade UASs increasingly playing an active role in the field of agriculture (Figure 7).

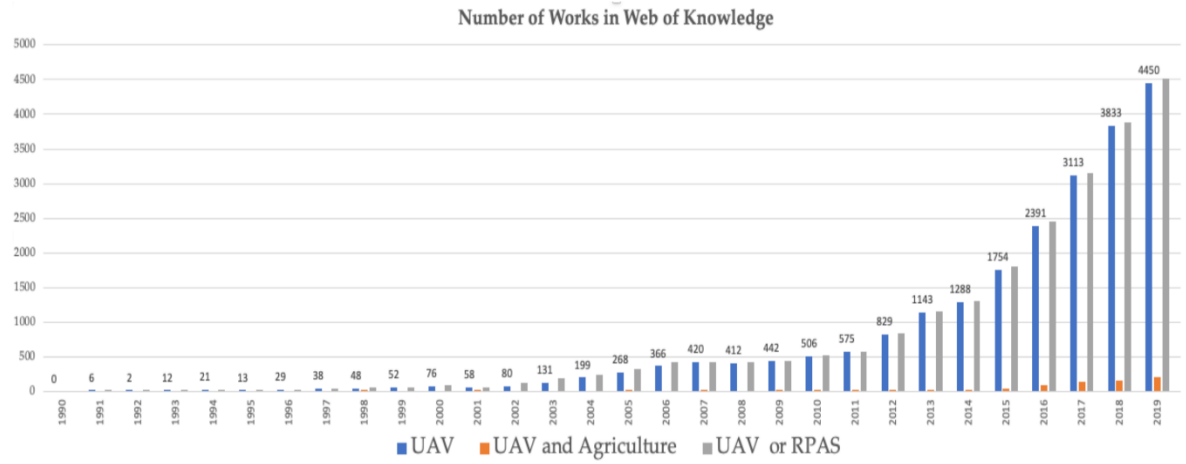

Figure 7: The number of studies in Web of Science on UAS/UAV applications in agriculture. Source: [193]

Their area of application is wide (Figure 8) including nutrients evaluation and health assessment, water stress analysis, yield and biomass estimate [203], soil monitoring, weeds detection[204–207], environmental monitoring, aerial spraying [208], mapping, greenhouses [209–212]. These devices offer valuable assistance to farmers in a wide range of tasks, such as crop planning, analysis, and field monitoring to assess crop growth and health [213].

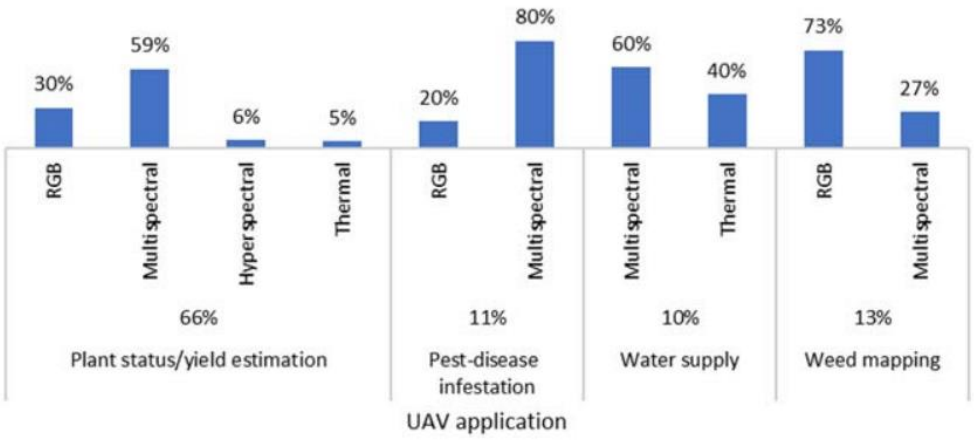

Figure 8: Share of UAS in specific tasks in agriculture and remote sensing platforms utilised in various aspects. Source: [198].

Their distinguishing attributes of UAS encompass high spatial ground resolution [214], ranging from 0.1 to 0.5 meters per pixel in lighter models, with some models achieving ultra-high resolutions as fine as 0.01 meters per pixel. Moreover, these autonomous platforms, whether under remote human control or autonomously operated, provide flexible and timely surveillance. These qualities make them particularly well-suited for medium to small crops, which typically span from 1 to 20 hectares, especially in areas characterized by substantial heterogeneity [215]

Nonetheless, it is imperative to underscore that UASs face certain limitations that warrant consideration. The effectiveness of UAS data collection hinges on the sensor technologies they employ. While UASs can capture ultra-high-resolution images nearly in real-time, they must adhere to flight permits and regulations, which can introduce inflexibility in flight scheduling and lead to higher operating costs. To operate aircraft, obtaining operational clearances from civil aviation authorities and ensuring the presence of qualified pilots are mandatory prerequisites. Furthermore, certain areas, including prisons, military installations, airports, and restricted or hazardous zones, are off-limits for UAS operations. Regulatory authorities offer pilots guidance through maps and lists to facilitate aerial activities within designated surveillance zones. Discussions and deliberations concerning UAS regulation have been actively conducted within organizations such as the European RPAS (Remotely Piloted Aerial System) Steering Group and the Federal Aviation Administration. Additional constraints are associated with payload weight, which encompasses the equipment required for specific tasks, and limited flight duration, typically falling under one hour due to battery capacity.

The landscape of UASs encompasses a wide range of types varying in size, shape, configuration, and flight characteristics, adding complexity to their operation. The deployment of UASs on a commercial scale, including expenses related to equipment, data processing, and software, can be a substantial investment for small-scale farmers [216,217]. UAS surveys entail handling large data volumes and preprocessing, with generated datasets restricted to the user's collected information [218]. Consequently, deploying UASs on a commercial scale involves significant expenses, encompassing equipment, data processing, and software costs, which can be a substantial investment for small-scale farmers [216,217]. In addition, UASs are subject to certain constraints related to weather conditions. These constraints imply that UAS operations can be influenced or restricted by various atmospheric factors, such as wind, precipitation, and clouds (Figure 9). Despite these challenges, continuous advancements in low-cost sensor technologies and the potential for cost savings and benefits are anticipated to outweigh these initial costs in the future.

Figure 9: An example of a partly cloudy day that is unfavorable for UAS flights. Source: Personal Archive

In summary, the growth in the development and utilization of UASs has facilitated the acquisition of high spatial, spectral, and temporal resolution data, essential for PA management at the field or farm level. Moreover, multispectral, high spatial resolution data collected through UASs can be integrated with existing satellite data, extending their applications to larger agricultural areas [219]. However, UASs grapple with limitations such as abbreviated flight times—typically less than 30 minutes for rotorcraft and 60 minutes for fixed-wing aircraft—and the requirement for pilots to be duly licensed and adhere to guidelines delineated by national civil aviation authorities [220]. Privacy and data security concerns are additional considerations entwined with UAS use in agriculture. Despite these constraints, the growing utilization of UASs in agriculture remains inevitable due to their cost-effective data collection capabilities and efficient monitoring potential [221].

1.3.3 Proximal platforms

Ground-based remote sensors have been in use for nearly three decades (Table 5). The shift from remote sensing to proximal sensing for crop status assessment was pioneered by Schepers, Francis, Vigil, and Below in 1992 [222]. They utilized a Minolta Soil Plant Analysis Development (SPAD) meter to measure leaf greenness (chlorophyll) in maize crops during the silking stage, varying the applied nitrogen (N) fertilizer rates. Their study revealed that SPAD meter readings of leaf reflectance at 650 and 940 nm correlated with the amount of applied N fertilizer and independent measurements of leaf N concentration.

Table 5: Innovations in remote and proximal leaf sensing in precision agriculture. Source: [143]

Year	Innovation	Reference
1992	SPAD meter (650, 940 nm) used to detect N deficiency in corn	Schepers et al., 1992; [222]
1995	Nitrogen sufficiency indices	Blackmer & Schepers, 1995; [223]
1996	Optical sensor (671, 780 nm) used for on-the-go detection of variability in plant nitrogen stress	Stone et al., 1996; [224]
2002	Yara N sensor	Link et al., 2002, TopCon industries; [225]
	GreenSeeker (650, 770 nm)	Raun et al., 2002, NTech industries
	CASI hyperspectral sensor-based index measurements of chlorophyll	Haboudane et al., 2002, 2004; [226,227]
	MSS remote sensing of ag fields with UAS	Herwitz et al., 2004; [228]
2003	Fluorescence sensing for N deficiencies	Apostol et al., 2003; [229]
2004	Crop Circle (590, 880 nm or 670, 730, 780 nm)	Holland et al., 2004, Holland scientific; [230]

Blackmer and Schepers (1995) introduced the concept of a nitrogen sufficiency index (NSI) to assess the degree of N stress in maize [223]. The NSI was defined as the ratio of SPAD meter greenness readings for crops in a given field location relative to SPAD readings for the same crop in a well-fertilised reference strip with no N deficiencies. NSI values less than 0.95 were used to indicate areas with N stress that required additional N fertiliser. Varvel, Schepers, and Francis (1997) showed that SPAD meters and NSI values could be used for in-season correction of N deficiency in maize [231]. Bausch and Duke (1996) showed that the SPAD meter could be replaced with a boom-mounted radiometer to estimate spatial patterns in NIR/G ratio and NSI across an irrigated maize field based on comparisons with a well-fertilised reference strip [232]. They observed that this approach could detect N deficiencies in the V6 growth, but results were confounded by interference with reflectance patterns from bare soil[233].

Stone et al. (1996) measured spectral radiance in the red (671 nm) and NIR (780 nm) bands in wheat with a sensor mounted on a mobile lawn tractor [224]. They used these data to estimate a spectral index known as the plant nitrogen spectral index (PNSI), which was the absolute value of the inverse of NDVI. Results showed that PNSI was strongly correlated with crop N uptake. Sensor readings were used to vary N fertiliser rates using an algorithm that increased exponentially with PNSI values[234] . This was the beginning of technology to variably apply N fertiliser "on-the-go" in response to proximal crop sensing and was the basis for commercial development of the GreenSeeker NDVI active sensor marketed by NTech Industries, Ukiah, CA, USA in 2001. Raun et al. (2002) subsequently developed a seven-step response index (RI)-based algorithm to estimate crop N fertiliser needs for maize and wheat based on in-season sensing of crop reflectance relative to check plots with no added fertiliser and reference plots with sufficient fertiliser[235]. This algorithm accounted for both season-to-season temporal variability in crop growth using the concept of in-season estimated yield (INSEY) as well as within-field spatial variability in N supply. Algorithms for estimating potential crop yield and N uptake are available for many crops and locations around the world [236]. The RI is estimated as the ratio of NDVI values in the crop relative to those in a reference strip with sufficient fertiliser.

Link, Panitzki, and Reusch (2002) and Reusch, Link, and Lammel (2002) created a passive sensor mounted on a tractor to assess crop nitrogen (N) status based on NDVI [225,237]. Initially called the Hydro-N sensor, it has since been rebranded as the Yara-N sensor by Yara in Oslo, Norway. Another version of the Yara-N sensor is available, incorporating active sensors, as developed by Link and Reusch (2006) [238]. These active sensors mitigate errors caused by varying cloud cover and enable tractor operators to work at night.

Holland et al. (2004) introduced the Crop Circle sensor, which initially used green and near-infrared (NIR) reflectance to estimate crop nitrogen (N) deficiencies [230]. They chose green reflectance over red based on research showing that, with a crop leaf area index (LAI) above 2.0, green NDVI becomes more sensitive to chlorophyll changes and potential yield, as demonstrated in prior studies [239–241]. This addressed limitations of the GreenSeeker sensor in advanced crop growth stages. Solari et al. (2008) found that N deficiencies could be more accurately predicted with a green chlorophyll index ((NIR880/VIS590) – 1) compared to green NDVI, using the Crop Circle sensor [242] . Sripada et al. (2008) showed that spectral index performance improved when using ratios with corresponding values from reference strips receiving sufficient N fertilizer [243]. Kitchen et al. (2010) and Scharf et al. (2011) demonstrated that Crop Circle sensor use allowed farmers to reduce N fertilizer, boosting crop yields and farm profitability [244,245].

One limitation of the chlorophyll meter, GreenSeeker, Yara N and Crop Circle sensors, however, is that they cannot directly estimate the amount of N fertiliser needed to overcome crop N stress [246]. To overcome this, scientists have conducted comparisons of sensor readings with readings in reference strips receiving sufficient N fertiliser [223,235,243,244]. They have used these data to develop N fertiliser response functions that relate sensor readings to the amount of N fertiliser needed to overcome crop N stress [245]. Even with this approach, reference strips with adequate fertiliser have to be strategically placed in representative soils and landscapes because yield response to N fertiliser exhibits significant spatial variability across production fields [247].

Ground-based sensors encompass various instruments grouped by their functionalities and applications. These instruments include weather data recording through local meteorological stations and soil sensing. Soil sensing involves continuous real-time monitoring of spatial variations in soil properties using sensors mounted on tractors. The first application of this approach was for soil organic matter sensing based on reflectance from multiple light emitting diode (LED) sensors emitting radiation at 660 nm [143]. A major breakthrough in PA occurred when Carter, Rhoades, and Chesson (1993) introduced continuous real-time, non-contact proximal sensing of soil apparent electrical conductivity using non-invasive electromagnetic induction with the Geonics EM-38 (Geonics Ltd., Mississauga, Ontario, Canada)[248].

Although ground-based sensors do provide some capabilities unavailable from other remote sensing platforms, there are some drawbacks to these types of sensors. Gathering data using

handheld sensors can be tedious and time consuming. Even if the sensors are mounted to vehicles, the data collection process is highly inefficient when used on larger fields. Some of these sensors are inflexible regarding the type of spectral data that can be collected.

In contrast to the predominantly passive sensors carried by satellite or UAS, most ground-based sensors are active and are generally either handheld or mounted on various equipment. Active sensors produce their own light signal and measure the resulting reflectance while passive sensors only capture the reflectance from ambient sunlight [249]. These active ground-based sensors have some benefits unmatched by the other systems. In comparison to collecting data using other platforms, ground-based sensors tend to be less expensive, and since most of these sensors are active, they are not as restricted by weather conditions. Cloud cover does not affect the data since the sensors produce their own light [249]. Due to the close proximity at which the data are collected, there is less atmospheric interference leading to more accurate data as well as high spatial resolution. These ground-based sensors are also more suitable for some applications, particularly those using smaller fields.

In summary, proximal sensors present distinct advantages in terms of precision and cost-effectiveness in agriculture. Since most of these sensors are active, they are not as restricted by weather conditions Collecting data in close proximity minimizes atmospheric interference, resulting in highly accurate data with superior spatial resolution [249]. Nevertheless, r, they do have limitations related to coverage, data interpretation, maintenance requirements, and initial costs. Hence, careful assessment of individual needs and available resources is crucial when considering the implementation of remote sensor technology.

1.3.4 Vegetation Indices

Remote sensing refers to non-contact measurements of radiation reflected or emitted from agricultural fields. Canopy reflectance is used to identify biophysical and biochemical properties of the canopy. The spectral response of the vegetation is unique, as it reflects the plant's health and nutritional status, and is highly dependent on solar radiation, soil properties, and available nutrients. VIs and soil properties can be calculated using optical sensors mounted on a UASs, satellites or ground vehicles. They are a numerical depiction of the relationship between various wavelengths of light reflected from the plant surface. More than one hundred VIs have been derived from multispectral imagery to simplify the monitoring method [250]. Because of the significant correlation between N and absorption of chlorophyll in the visible and near infrared region, most of the VIs were calculated from bands in the visible and near infrared range [251,252].

The most renowned and applied VI is the Normalized Difference Vegetation Index (NDVI), computed as the normalized difference between NIR and red reflectance, and generally used to assess vegetation greenness in space and time [253]. NDVI has been used to detect crop nutrient deficiencies, patterns in crop yield, insect and weed infestations, and crop diseases [36]. However, NDVI has several limitations, however, including potential interference from soil reflectance at low canopy densities and insensitivity to changes in leaf chlorophyll content in mature canopies with leaf area index values that exceed 2 or 3 [254] As a result, there has been significant research effort devoted to finding broadband multispectral indices that can be used as an alternative to NDVI [241]. In general, there are three classes of broadband multispectral indices used in precision farming. These include soil-adjusted VIs, ratios of green and near-infrared reflectance bands, and ratios of red and near-infrared reflectance bands [255]. Soil-adjusted vegetation indices reduce reflectance from bare soil that interferes with the interpretation of reflectance from a growing crop before canopy closure. Red ratio indices typically are sensitive to absorption of radiation by leaf chlorophyll, while green ratio indices are sensitive to leaf pigments other than chlorophyll. In commonly used red and green ratio indices, either the red or green or the near-infrared reflectance can appear in the numerator of the ratio.

Many broadband spectral indices (Table 6) other than NDVI are available for use in PA [243,256,257]. These indices reflect two historical trends in remote sensing for crop characteristics:

the prediction of reflectance ratios in the Red (R) and NIR bands versus ratios in the green (G) and NIR bands. The Normalised Red (NR) index focuses on the portion of the spectrum where chlorophyll strongly absorbs radiation. In contrast, the Normalised Green (NG) index focuses on the portion of the spectrum where pigments other than chlorophyll (carotenoids, anthocyanins, xanthophylls) absorb radiation. Similarly, there are two forms of the Ratio Vegetation Index (RVI), one that consists of the ratio of NIR to R reflectance, the other Green Ratio Vegetation Index (GRVI) that consists of the ratio of NIR to G reflectance. Two forms of the NDVI exist, one that involves NIR and R reflectance, the other Green Normalized Difference Vegetation Index (GNDVI) involves NIR and G reflectance. The Difference Vegetative Index (DVI) was developed using the difference between reflectance in the NIR and R bands to compensate for effects of soil reflectance (Tucker, 1979). Sripada et al. (2006) found that economically optimum N rate in corn was better correlated with green difference vegetation index (GDVI) (NIR – G) than DVI (NIR – R), and these indices that compensated for soil effects performed better than NIR and R ratio indices such as NDVI and RVI that did not compensate for soil effects. A wide range of other indices have been developed to compensate for soil effects, including Soil Adjusted Vegetation Index (SAVI), Green Soil Adjusted Vegetation Index (GSAVI), Optimised Soil Adjusted Vegetation Index (OSAVI), Green Optimised Soil Adjusted Vegetation Index (GOSAVI) and Modified Soil Adjusted Vegetation Index (MSAVI).

Table 6. Multi-spectral VIs available for use in precision agriculture. Source: [143]

Index	Definition	Reference
NG	G/ (NIR + R + G)	Sripada et al., 2006[241]
NR	R/ (NIR + R + G)	Sripada et al., 2006, [241]
RVI	NIR/R	Jordan, 1969 [258]
GRVI	NIR/G	Sripada et al., 2006, [241]
DVI	NIR - R	Tucker, 1979[259]
GDVI	NIR - G	Tucker, 1979, [259]
NDVI	(NIR - R)/ (NIR + R)	Rouse et al., 1973 [260]
GNDVI	(NIR - G)/ (NIR + G)	Gitelson et al., 1996, [239]
SAVI	1.5*[(NIR - R)/ (NIR + R + 0.5)]	Huete, 1988[261]
GSAVI	1.5*[(NIR- G)/ (NIR + G + 0.5)]	Sripada et al., 2006, [241]
OSAVI	(NIR - R)/ (NIR + R + 0.16)	Rondeaux, Steven, & Baret, 1996[262]
GOSAVI	(NIR G)/ (NIR + G + 0.16)	Sripada et al., 2006, [241]
MSAVI2	0.5*[2*(NIR + 1) -SQRT ((2*NIR + 1) ^2 8*(NIR - R))]	Qi, Chehbouni, Huete, Keer, & Sorooshian, 1994

So far, a wide number of studies have demonstrated that spectral indices are effective in identifying spatial patterns of crop parameters, making them valuable tools for precision agriculture and crop management. These indices, with their unique focus on specific aspects of plant health and soil correction, play a pivotal role in PA for optimizing agricultural practices and decision-making.

1.4 Processing Tomato Crop

The tomato, scientifically classified as Solanum lycopersicum L., belongs to the Solanum genus within the broader Solanaceae family. Although it is customarily considered a vegetable it is actually a fruit and more specifically a berry based on its plant parts. This misunderstanding was a question of debates during the 19th century in USA, with the special case of Nix vs. Hedden – 149 U.S. 304 (1893). In 1887, Nix contested the decision of the tax collector of the port of New York to recover taxes on tomatoes imported from the West Indies in the spring of 1886, which the collector assessed as a vegetable. The court opined: "Botanically speaking, tomatoes are the fruit of a vine, just as are cucumbers, squashes, beans, and peas. But in the common language of the people, [...] all these are vegetables which are grown in kitchen gardens, and which, whether eaten cooked or raw, are, like potatoes, carrots, parsnips, turnips, beets, cauliflower, cabbage, celery, and lettuce, usually served at dinner in, with, or after the soup, fish, or meats which constitute the principal part of the repast, and not, like fruits generally, as dessert" [263]. The name Lycopersicon, bestowed by Miller in 1788, is universally recognized and adopted by researchers studying tomatoes.

1.4.1 History

The history of tomato dates back to 700 A.D., in the tropical regions of South America (Peru, Bolivia, Ecuador) or Mexico, where wild plants can be still found. The word "tomato" itself is believed to have been derived from the Aztec Nahuatl word "tomatl" [264] that gave rise to the Spanish word "tomate". It was first introduced in Europe from Spanish explorers in the early 16th century, and was cultivated in various European countries, including Portugal, Spain, Italy, France, England, and Belgium. It was initially used as a food by the Italians. Italy holds the distinction of providing the first recorded description of the tomato in 1554, affectionately referring to its fruit as "golden apples" (pomi d' oro), possibly because one variety of the plant bore fruits with a striking yellow hue. In the northern Europe, tomato was originally cultivated as an ornamental plant and was considered poisonous. However, this is partly true, since all the green parts of the plant contain the neurotoxin solanine. It's cultivation in the USA began two centuries later.

Tomatoes are divided in two categories, based on the direction of the production; the first is the fresh consumption and the second is the processed tomato, where the production is processed into other products. A pivotal moment in the history of tomato processing occurred in the early 1800s in the United States with the emergence of canning tomatoes as one of the earliest forms of tomato processing. However, a significant breakthrough came about in 1893, when John W. Gates, an innovative entrepreneur and inventor, introduced the pneumatic tomato-paste process. This groundbreaking innovation revolutionized the production of tomato paste, transforming it into a fundamental ingredient for various food products.

The early 20th century witnessed a remarkable expansion in tomato cultivation, predominantly driven by the burgeoning canning industry's demand for tomato paste, as elaborated by Gould in 2013 [265]. In Greece it was originally cultivated in the Dodecanese. In 1915, the production of tomato paste in a small pre-industrial technology plant in the village of Messaria in Santorini [266]. In just seven years, one of the first tomato canning factories in the Balkans was built, that was a state-of-the-art technology factory at that time. After 1945, there was a significant expansion in the tomato processing industry. Modern industrial processing units were created, and they had a daily processing capacity of 3,500 baskets of tomatoes, indicating the growing importance of tomato processing in the region.

With the growth of the food industry and an increasing demand for convenient food products, tomato processing continued to evolve. This suggests that the tomato processing industry adapted to changing consumer preferences and technological advancements to meet the growing demand for tomato-based products.

1.4.2 Breeding

Tomatoes intended for processing are primarily grown in fields, while fresh tomatoes can be cultivated either in fields or greenhouses, with or without temperature control. Over time, breeding objectives for tomatoes have evolved, with cultivars released and growing systems modified. Although three main objectives persist—adaptability to the environment, resistance to pests and diseases, and fruit yield and quality—tomato breeding has gone through four distinct phases: breeding for yield in the 1970s, for shelf-life in the 1980s, for taste in the 1990s, and more recently, for nutritional value [267–271].

Figure 10. Processing tomatoes grown in open fields. Source: Personal Archive

Breeding efforts in tomato started more than 200 years ago [267]. Until the 1950s, tomato breeding developed multipurpose cultivars to meet several needs. Some interesting traits were introduced such as tolerances to abiotic stresses, broad adaptability to different environments and early fruit maturity. Subsequently, breeding objectives depended upon the method of production: open field ***vs*** greenhouse production, and whether the fruits are used fresh or processed [272,273]. Processing tomato needed the introduction of specific morphological and phenological traits such as: determinate growth habit, concentrated flowering and fruit set, canopy suitable for once-over machine harvest, easy separation of fruit from the vine (jointless characteristic) [272,274]. More specifically, varieties intended for processing should possess the following specific attributes [271]:

- Concentrated Flowering and Fruiting: These varieties should exhibit a concentrated pattern of flowering and fruiting, which means that a significant number of flowers should develop into fruits in a relatively short time frame. This characteristic ensures efficient machine harvesting.

- Determinate Growth Controlled by the sp. Gene: The plants should have a determinate growth habit controlled by the "spontaneous self-pruning" (sp.) gene. This genetic trait helps control the size and structure of the plant, making it more conducive to mechanical harvesting. The "spontaneous self-pruning" mutation (sp.), which emerged in 1914, allowed the development of bushy growth habit cultivars. This mutation also concentrated flowers and, consequently, fruits, contributing to fruit firmness and resistance to over-ripening. Cultivars with this mutation became the preferred choice for mechanical harvest. The "jointless" mutations (j and j2) are characterized by the absence of an abscission zone in the fruit pedicel, enabling harvest without calyx and pedicel, resulting in fruit free from any "green" parts [271]. The presence of a jointless pedicel, which means that there is no natural separation point between the fruit and the stem, is desirable for machine harvesting. This feature allows the fruit to be cleanly detached from the plant without leaving any "green" parts behind.

- Elongated Fruit Shape: In general, varieties with elongated fruit shapes tend to suffer less damage during machine harvesting compared to round or irregularly shaped fruits. This attribute contributes to higher yield retention.

- Resistance to Cracking, Crushing and Puncture: Varieties should be resistant to fruit cracking, which can occur due to environmental factors or uneven ripening Processed tomatoes should also have fruits that are resistant to crushing and puncture. This ensures that the fruits remain intact during the mechanical harvesting process and maintain their quality for processing.

- Uniform Fruit Set and Synchronous Maturity: Uniformity in fruit set and ripening is crucial for mechanical harvesting systems. Synchronous maturity, where fruits on the same plant ripen at the same time, is often a dominant or overdominant trait that is polygenically inherited. This trait is highly desirable for efficient machine harvesting because it minimizes the need for multiple passes through the field and ensures that the machine can efficiently collect fruits at the right stage of maturity.

Moreover, also specific fruit quality traits are required, such as: low pH, high soluble solids, total solids and viscosity [265,267,275].

A significant milestone in tomato cultivation has been the breeding of cultivars specifically designed for mechanical harvesting. The creation of VF 145, which was the first cultivar intended for mechanical harvesting and subsequently became a major player in the California processing tomato industry for over a decade, is a fascinating story (G. C. Hanna, unpublished) [272]. In the early stages, the concept of tomato harvesters didn't even exist, and there was no clear idea of how they might function. However, two critical needs were identified: the fruit needed greater firmness to withstand machine handling, and the plant had to have a very short fruit-set period to ensure a high percentage of ripe fruits at the same time. Hanna's vision for a machine-harvestable cultivar began to take shape in 1947 when he released a small determinate strain resulting from a cross between 'Gem' and 'San Marzano,' known as 'Red Top.' By using 'Gem' as a parent, he developed multiple small determinate strains. Unfortunately, these strains were more susceptible to verticillium wilt at the beginning of fruit ripening, leading to small clusters of sunburned fruit. The heavy concentration of fruit on these small plants created stress and increased their vulnerability to disease. To address this issue, a verticillium-resistant strain known as VR 11, developed at the USDA, was introduced to incorporate disease resistance.

Efforts to develop tomato varieties specifically suited for machine harvesting have been extensively reviewed by Lukyanenko [276], indicating the importance of ongoing research and breeding to meet the demands of modern agricultural practices and processing industries. These efforts aim to optimize tomato varieties for efficient and cost-effective mechanical harvesting, ultimately benefiting both growers and consumers.

1.4.3 Water and Nutrient management

Irrigation and the absorption of essential nutrients are pivotal factors in the development of field crops, with processing tomatoes being a notable example.

The way in which field crops like tomatoes absorb nitrogen and potassium undergoes a specific pattern throughout their growth cycle (Figure 11). Initially, the uptake of these two essential nutrients is relatively slow. However, as the plants progress through the flowering stages, their demand for nitrogen and potassium rapidly increases. This surge in nutrient uptake is particularly crucial during the flowering period, as it sets the stage for the development of healthy and productive tomato plants.

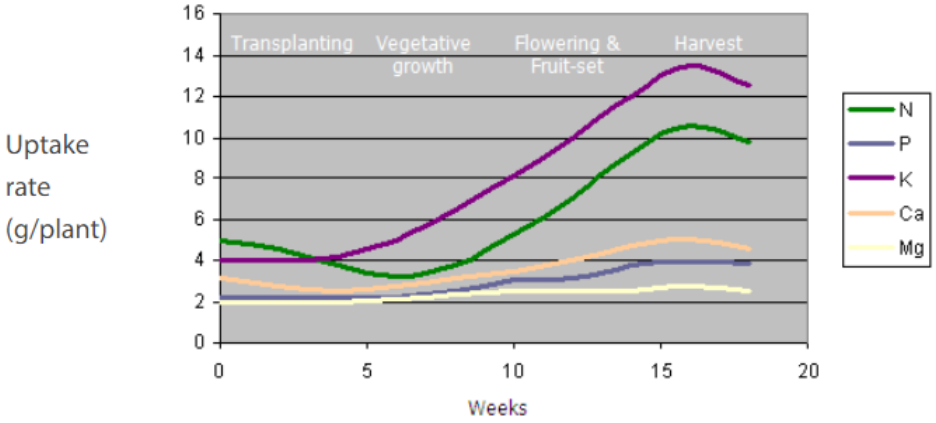

Figure 11. The uptake dynamics of the macro- and the secondary nutrients by a tomato plant. Source: [277]

When it comes to potassium, its demand and absorption reach their peak during the phase when the fruits are forming and maturing (Figure 12). This nutrient plays a pivotal role in fruit development, contributing to the overall quality and yield of the crop.

On the other hand, nitrogen uptake predominantly occurs after the formation of the first fruit. This timing is significant because it aligns with the period when the plant diverts its energy and resources towards producing and ripening the fruit, making nitrogen crucial for this phase of growth.

In addition to nitrogen and potassium, other essential nutrients like phosphorus (P), calcium (Ca), and magnesium (Mg) are also vital for the overall health and productivity of the tomato plant. These nutrients are needed at a relatively consistent rate throughout the entire lifespan of the plant. Phosphorus is essential for root development and overall plant vitality, while calcium and magnesium are important for various physiological processes, such as cell structure and photosynthesis. Ensuring that these nutrients are supplied in adequate quantities and at the right times is crucial for optimizing the growth and yield of processing tomatoes.

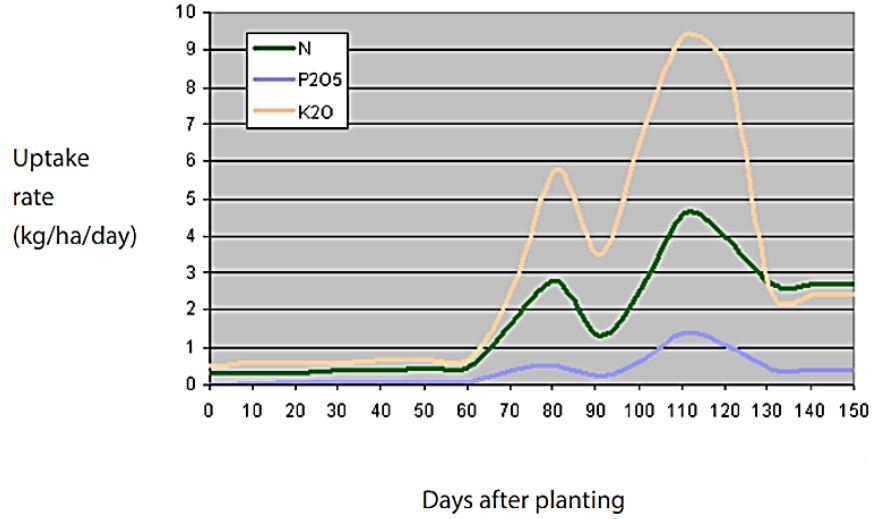

Figure 12. Daily uptake rates of plant nutrients by processing tomatoes yielding 127 ton/ha. Source: [278]

A number of studies [279–284] provide further details and insights into the specific practices and strategies used in managing nutrient uptake in the context of this crop.

When it comes to processing tomatoes, one distinctive characteristic is their substantial demand for water [285]. The reproductive phase of the plant, especially the critical flowering stage, is exceptionally sensitive to any form of water stress [286].

The quantity of water required by the crop is contingent on several factors, including the plant's developmental stage, prevailing temperatures, the rate of evapotranspiration (Figure 13), soil type, and the quality of the water [287]. Interestingly, the irrigation schedule preceding the flowering and maturation of the initial fruits seems to have minimal influence on the crop's performance, as long as the soil moisture level at the time of planting is close to field capacity [288]. At this early stage of its growth, the plant's water demand remains relatively low due to its limited surface area for evaporation and its underdeveloped root system. Consequently, in most cases, the natural moisture content in the soil is sufficient to prevent any water-related stress that could adversely affect the crop.

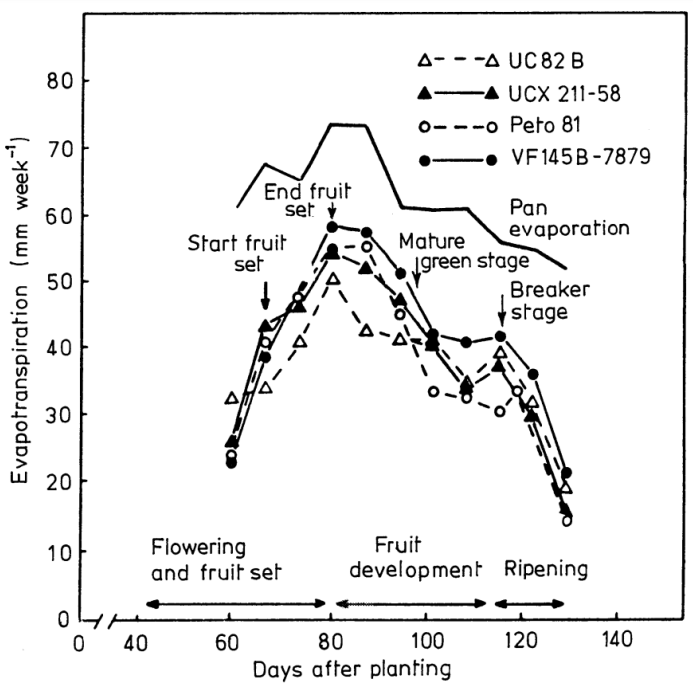

Figure 13. Evapotranspiration from four cultivars of bush tomato grown in the open field in California. Source: [289]

During the initial stages of growth, processing tomato plants have relatively lower water requirements. Irrigation is typically managed to ensure that the soil remains consistently moist but not waterlogged. This helps establish a strong root system and promote healthy vegetative growth. As the tomato plants transition into the flowering and fruit-setting stage, their water needs begin to increase. This is a critical phase where adequate water availability is essential for successful pollination, fruit formation, and early fruit development. Evapotranspiration rates are relatively higher during this period. The fruit development stage is when processing tomatoes require the most water. As the fruit expands and matures, the water demand peaks. Proper and consistent irrigation is crucial to support fruit growth and prevent issues like blossom-end rot or fruit cracking. Towards the end of the growth cycle, as the fruit begins to ripen and mature, the water requirements start to decrease. It's important to gradually reduce irrigation to avoid over-watering, which can negatively impact fruit quality. Several studies [290–292] offer comprehensive insights and detailed information regarding the specific practices and strategies employed for managing nutrient uptake in the context of processing tomato cultivation.

It's worth noting that land-levelling is also necessary for an even water distribution from either rain or irrigation water and diminishes the danger of waterlogging (Figure 14). When soil becomes waterlogged, it quickly and significantly transforms both the physical and biological conditions of the root environment for processing tomato plants. In reaction to this waterlogging, various physiological changes take place within the plant, profoundly influencing its growth and development. The primary consequence of soil flooding is a significant restriction in the diffusion of oxygen to the root zone, which has a pervasive impact on the plant's overall well-being. Additionally, it's important to highlight that drought conditions can also result in decreased crop

yields [293]. Drought-induced water scarcity can significantly impact the growth and productivity of the crops (Figure 14).

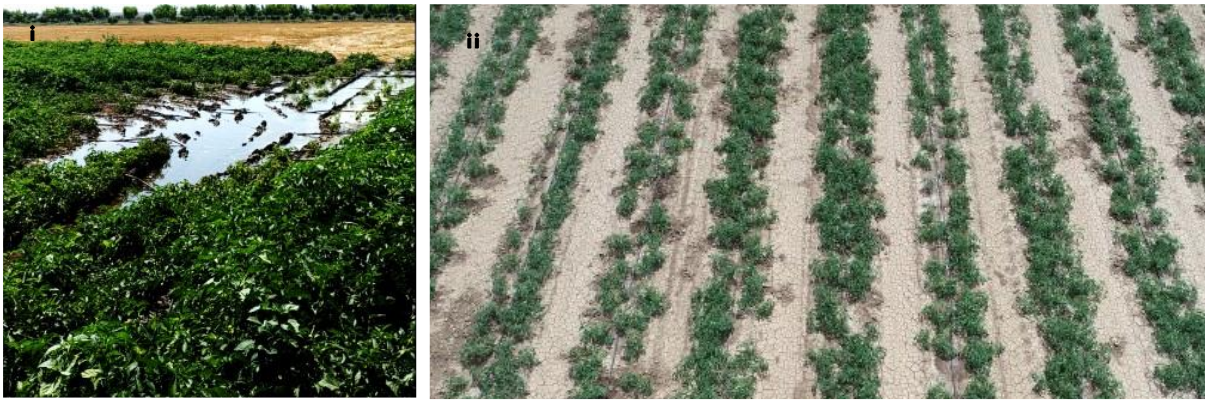

Figure 14. i) Waterlogging and ii) Drought Events on Processing Tomato Crops. Source: Personal Archive

In summary, achieving successful processing tomato cultivation necessitates precise nutrient and water management. The intricate relationship between nutrient absorption and plant development is closely tied to effective water management, especially during the sensitive flowering phase.

1.4.4 Phenological cycle

The phenological cycle of processing tomato is the sequence of developmental stages that the tomato plant goes through from seed to harvest. The phenological cycle can be divided into four main phases: germination, vegetative growth, reproductive growth, and ripening Figure 17.

Germination

Germination is the fundamental process of a seed sprouting and the subsequent emergence of a seedling. The successful germination of a seed is contingent on several factors, including temperature, moisture levels, and the availability of oxygen in the soil [294].

Under ideal conditions, germination typically occurs within a span of 5 to 10 days. To further enhance the germination process, biostimulants like chitosan can be employed. These substances have the capacity to augment the overall seed vigor, accelerate the germination rate, and improve the quality of tomato seedlings. Tomato transplants for open-field production could be raised in a greenhouse or in tunnels if they are to be grown in a season when climatic conditions outside would not be favourable for growth. If they are to be produced when climatic conditions are suitable transplants could be grown outside in soil on raised, well-prepared beds. In a nursery sown in the ground in open field or tunnels, the row distances should be 8-12 cm.

In recent years production of transplants has been more and more the province of specialized commercial nurseries. This is because hybrid varieties are now used extensively with fresh market tomatoes and also with processing tomatoes to a lesser extent. Many growers find it more convenient, safe and profitable to buy the ready plants from a specialist nursery (Figure 15). The principal advantage of the current hybrid cultivars has been more consistent performance, so that growers can get satisfactory yields when weather and cultural conditions are poor. There is evidence that the bigger the transplant the earlier the yield, but the more expensive the plants will be and more labour and skill needed to handle the plant [295]. Increasing the age of the transplant had an unfavourable effect on the subsequent yield.

Figure 15. Photographs depicting the transplanting of processing tomato hybrids in a pilot field. Source: Personal Archive

Following germination and transplanting, vegetative growth proceeds at first alone and then coincident with reproductive growth.

Vegetative development

The vegetative growth phase represents a period of rapid development and expansion of plant organs, including roots, stems, leaves, and branches. In the context of tomato plants, vegetative development can also be associated with the rate of leaf appearance, which is closely linked to the appearance of trusses, given the species' sympodic nature, typically producing one inflorescence every three leaves [296].

This growth phase typically extends for a duration of 40 to 60 days following germination [297]. The development of the first flower-trusses and fruit-set can be anticipated roughly 4-7 weeks after seeding or 2-3 weeks after transplanting in processing tomatoes, although the exact timing depends on the specific growing habits of the varieties. Indeterminate tomato types often initiate the first flower-truss after 7-11 leaves, while most determinate varieties tend to do so after 5-7 leaves [298].

Numerous factors influence this stage, including light, temperature, water availability, nutrient supply, and plant density. Research conducted by Van der Ploeg and Heuvelink in 2005, the optimal temperature for the early vegetative growth of tomato plants is around 25°C [299]. De Koning's work in 1993 further highlighted the impact of temperature, indicating that the number of trusses per week increases by approximately 0.05 trusses per week for each degree Celsius rise in temperature [300]. His research also demonstrated a linear correlation between the leaf appearance rate and the average air temperature. This rate increased from 0.2 leaves per day at 12°C, peaking at 0.5 leaves per day at 28°C, and then declining to zero at 48°C [301].

Additionally, the work of Adams et al. in 2001 revealed that the optimal temperature range for vegetative development in tomatoes falls within 22°C to 26°C [302]. Similar temperature values were also observed for the early reproductive phase (progression to anthesis). Furthermore, the research indicated that the rate of truss appearance exhibited a linear increase from 0.11 to 0.17 trusses per day as the average temperature rose from 17°C to 23°C. Simultaneously, there was a strong correlation between weekly "above-ground" fresh weight growth and the light received by

the crop each week[301]. However, the efficiency of light utilization (weight increase per unit of light) was notably higher during the initial phase of growth.

It's interesting to note that many plants exhibit an optimal temperature for photosynthesis that closely aligns with their typical growth temperature, as suggested by Lambers et al. in 1998 [303]. For tomatoes, which thrive in temperatures between 22 and 30 °C, single-leaf photosynthesis operates optimally between 20 and 30 °C under normal CO2 levels; this range shifts to 25-30 °C under elevated CO^2 [303–305]. In an experiment by Xu et al. in 1999, net photosynthesis increased from 18 to 23 °C but declined beyond 23 °C, with dark respiration increasing exponentially [306]. Ogweno et al.'s 2009 study exposed detached tomato leaves to temperatures of 15, 25, and 35 °C for 5 days, showing similar photosynthetic rates at 15 °C and 25 °C, with significantly lower rates at 35 °C [305]. Hu et al. (2006) found that decreased photosynthesis at 35 °C was due to impaired photosynthetic apparatus, not stomatal function [307]. The optimal temperature for photosynthesis in tomatoes at 350 ppm CO2 is reported to be between 22 °C and 30 °C, whereas low temperatures of 4-6 °C dramatically reduce photosynthesis, with photosynthesis ceasing at 1 °C [308,309].

Vegetative growth can be enhanced by using biostimulants, which can increase the plant height, stem thickness, chlorophyll content, and water use efficiency of tomato plant [297]. The duration of the vegetative phase may be prolonged by deficiencies of inorganic nutrients in the rooting medium.

It's essential to recognize that the majority of our knowledge concerning the vegetative growth of tomatoes is derived from studies involving greenhouse cultivars grown under controlled environmental conditions [298]. Consequently, the existing literature primarily pertains to tomatoes cultivated in greenhouses, and there is relatively less information available regarding tomatoes grown in open fields. Nonetheless, when summarizing these studies, we can distil that this phase is characterized by the rapid development of roots, stems, leaves, and branches, typically spanning a 40 to 60-day period post-germination. A multitude of factors, including light, temperature, water availability, nutrient supply, and plant density, come into play during this growth phase, with temperature emerging as a significant influencer. An optimal temperature range of 22-26°C is observed, affecting various facets of growth. Notably, photosynthesis is also temperature-sensitive, with an ideal range of 20-30°C under normal CO2 levels.

Reproductive growth

Reproductive growth marks the phase of a plant's life cycle that involves essential processes such as flower initiation, pollination, fertilization, and the fruit set. Various factors, including temperature, day length, light intensity, water availability, and the influence of plant hormones strongly influence this stage. Typically, the reproductive growth phase extends over a period of 20 to 40 days [310].

The formation of flowers (Figure 16) is a prerequisite for the formation of fruits, and flowering delays can lead to fruit production delays. Flowering typically begins around 55 days after transplanting and continues until approximately 88 days after transplanting [311], depending on environmental conditions and cultivars. Variations in the rate of flower formation can have significant implications for fruit production at different stages of a crop's growth. Short-term spikes in yield may be linked to the emergence of an unusually high number of flowers within a single inflorescence, as noted by Hurd and Cooper in 1967 [312]. Alternatively, a rapid initiation of successive inflorescences can also contribute to increased yield. This phenomenon becomes particularly crucial when there's a demand for high yields early in a crop's lifecycle. However, it's essential to note that such abrupt increases in fruit production might trigger growth restrictions later on due to the competing demands of developing fruits, as discussed by Fisher in 1977 [313] and further elaborated on by Slack and Calvert in 1977 [314].

Figure 16. Formation of the first flowers in processing tomato crop. Source: Personal Archive

In both indeterminate and determinate tomato cultivars, the production of fruits can face limitations when flowers fail to develop into viable fruits. In some cases, flowers may cease their growth and wither prematurely before they even have a chance to open. In harsh environmental conditions, characterized by high temperatures and low levels of sunlight, it's possible for all the flowers on an inflorescence to be lost. When this occurs during the early stages of floral development, the inflorescence remains underdeveloped and appears as little more than a bulging piece of tissue emerging from the stem[315].

Heuvelink (2005) reported that flower fertilization in tomatoes is greatly reduced at temperatures outside the 5 to 37 °C range and that pollen tube growth rate is adequate within this temperature range[304]. A linear relation between flowering and air temperature has also been observed by Abreu et al. [316].

In addition to temperature, irrigation another principal component of this stage. Studies have shown that the irrigation regimen significantly influences the number of flowers and fruit production [311]. A study conducted by Takahashi, Eguchi, and Yoneda in 1973 demonstrated that flower initiation was notably delayed when there were deficiencies in essential nutrients such as nitrogen, phosphorus, and potassium. Importantly, these delays in flower initiation due to nutrient shortages might indicate a broader deceleration in the overall growth and development of the entire plant, rather than having isolated effects specific to the flowering process [317].

Moving on to the fruit set stage, the first fruit buds become visible approximately 50 days after transplanting. In the process of pollination and fruit setting temperature plays a pivotal role, as highlighted in various scientific studies. The temperature range for fruit setting in tomatoes is narrow, with particular sensitivity to nighttime temperatures. A noteworthy study [281] demonstrated that the most critical stage for successful pollination appears to be meiosis, a process occurring approximately 9 days before the flowering stage. According to these authors, the optimal temperature range for effective pollination typically falls between 17 and 24 °C. High-temperature conditions may result in cone splitting, stigma exertion, and pollen sterility, with maximal daytime temperatures exceeding 32 °C and minimal nighttime temperatures above 21 °C significantly reducing fruit set [318,319]. Similarly, the research by Atherton and Harris (1986) suggests that

fruit pollination faces the risk of failure when temperatures exceed 40 °C [281]. However, differences may occur between heat-sensitive and heat-tolerant tomato cultivars. This underscores the crucial role of temperature in the pollination and fruit-setting process.

Fruit growth and progression to maturity

The fruit yield of a tomato plant depends on both the quantity and weight of individual fruits, making proper fruit set and development crucial for achieving high tomato yields. However, the market value of the fruits is determined by factors like fruit quality (such as size, shape, firmness, color, taste, and solids content) and market demand, which can vary with the season, especially for fresh market tomatoes. In practice, both the quantity and quality of fruit yield have been enhanced by manipulating the processes involved in fruit development, from pollination to maturity. While fruit quality has seen improvements through plant breeding, the quantity of fruit has been increased, particularly in greenhouses, by carefully controlling the growing environment to optimize growth processes.

To attain fruit maturity, it's essential to accumulate a critical temperature sum during an individual fruit's growth period [296]. In the case of indeterminate greenhouse tomato varieties, the duration of fruit growth represents the time it takes for an individual fruit to progress from anthesis (the flowering stage) to optimal ripeness for hand harvesting within the same cohort. For indeterminate greenhouse cultivars, flower cluster formation and ripening continue over several months, even as the first fruits are being harvested. In contrast, semi determinate field-grown tomato varieties, typically harvested over 1 to 2 weeks, exhibit a distinct pattern where the time for an individual fruit to develop from anthesis to maturity (green-breaker stage) for the initial larger fruits closely aligns with the entire crop's duration from the first fruit setting to full crop maturation, usually taking only a few days [320].

Temperature is a pivotal factor influencing the duration of the tomato fruit growth period, as highlighted by De Koning's research [321]. His results showed this period to be 73 days at 17 °C and 42 days at 26 °C. Similar results were observed by Rylsky in 1979 [322]. and Verkerk in 1955 found that the time interval from anthesis to harvest was 90 days at 13 °C, 53 days at 19 °C, and 40 days at 26 °C. [315]. For this later phase, Adams et al. [302] dentified an optimal temperature of 22°C, while De Koning [301] suggested approximately 21°C as the optimum.

Adams et al. (2001) and Adams and Valdez (2002) found that as tomato plants were grown at different temperatures (14, 18, 22, and 26 °C), the time required for fruit ripening varied: 95, 65, 46, and 42 days, respectively[302,323]. Notably, elevated temperatures affected the later stages of fruit maturation more. Increasing temperatures from 18 to 25 °C for three weeks reduced the time to harvest by 8.7 to 11.2 days. Aikman (1996) proposed that the time from anthesis to maturity for tomato is 806 degree-days [324]. Using the 4 °C of De Koning (1994), this time translates to 940 degree-days, whereas Scholberg et al. (1997) calculated 722 degree-days using a base temperature equal to 10 °C [301,325]. Beyond these differences in computing thermal units, it is also likely the cultivars may differ in the duration from anthesis to harvest maturity.

The influence of the irrigation regimen appears to be less significant when compared to the choice of tomato variety [326]. In general, intensive irrigation applied during the fruit development and maturation phase is shown to have an unfavorable impact on several quality indicators, as reported in previous studies [288,327,328]. More recent research studies have focused on assessing the effects of deficit irrigation on various aspects, including plant growth, physiological traits, yield, and water productivity, in the context of processing tomato cultivation [286,311,311,329,330].

Varieties with concentrated fruit set, especially processing tomatoes, can be artificially ripened by spraying the entire field with commercial ethephon. The amount of ethephon to be applied depends very much on temperatures prevailing at the time of application and during the following three days. This technique allows for the synchronized ripening of fruits, which can be advantageous for large-scale harvest and processing operations.

Summarising the results, optimal temperatures for this later fruit growth phase are around 21-22°C, as observed in different studies, with temperature playing a critical role in determining the duration of the fruit growth period [321]. The warmer the temperature, the shorter the time it takes for tomatoes to reach maturity, while cooler temperatures prolong this period [322]. Variations in temperature can significantly impact the time required for fruit ripening, with elevated temperatures accelerating the process. An estimate of 806 degree-days was suggested for tomatoes to mature, based on a specific temperature threshold [324]. Some studies calculated a different value of 722 degree-days, accounting for variances among tomato cultivars [301,325].

Figure 17. Phenological stages of the processing tomato: i) Vegetative development, ii) Reproductive growth, iii) Fruit growth and progression to maturity. Source: Personal Archive

Harvest

Deciding when to terminate irrigation in processing tomatoes requires careful consideration. It involves assessing its potential impact on fruit quality, particularly the TSS content, as well as the risk of fruit rot. In cases where mechanical harvesters are used (Figure 18), the soil surface needs to be sufficiently dry for the harvester to function effectively. The period between the last sprinkler irrigation and harvest can range from 25 to 30 days in medium and heavy soils, depending on soil and climatic conditions. In very warm regions, irrigation may be extended up to 10-12 days before harvest.

Under optimal climatic conditions, provided that plant diseases and pests have not significantly damaged the foliage, the ideal time to commence harvesting a tomato field is when approximately 90% of the fruit has reached a red or pink coloration [295]. In most countries where processing tomatoes are grown, a single, comprehensive harvest is conducted. This process involves cutting the entire plant at ground level or manually uprooting it and shaking it to release the fruit. Subsequently, the fruit suitable for processing is collected either by hand or mechanically and placed into bins, gondolas, or tandem truck trailers for transportation to the processing facility. Modern tomato varieties intended for processing are well-suited for this method due to their highly concentrated fruit set and their capacity to retain ripe fruit on the vine without deterioration. These fruits can maintain their quality for 25-35 days after reaching full ripeness, making it possible to utilize 90-95% of the fruit harvested at once for processing. Furthermore, the fruit's consistency enables mechanical harvesting and bulk transportation with a load height of 1.0-1.5 meters without causing damage that would lead to rejection by the industry. Handpicking would require 3-5 labor hours per metric ton, while machine harvesting can be accomplished by a team of 6-15 individuals operating the harvester, with the capacity to harvest 20-30 tons per hour.

Figure 18. Mechanical harvesting and processing of tomato. Source: Personal Archive

Fruit soluble solids content is also of tremendous importance to the processing tomato industry. Soluble solids encompass sugars and organic acids, and their ratio, combined with volatile aroma composition, defines the fruit's flavor. Organic acids also determine the pH of the final product. A pH above 4.5 can lead to the growth of microorganisms, spoiling the product. To address this issue, higher temperatures and extended processing times are necessary but also increase processing costs. Insoluble solids, consisting of cell wall components and proteins, influence fruit firmness and the viscosity of final products like tomato juice, ketchup, soups, and paste.

The quality of the fruit delivered to the processing plant is usually outlined in the contractual agreement between the grower and the processor. Quality standards may encompass factors such as color, the percentage of green and pink fruit, the presence of dry or wet wounds, mold, foreign materials other than tomatoes, the presence of calyx on the fruit, over-ripeness, the presence of worms or worm-related damage, peelability, and TSS measurement in Brix (Figure 19).

Figure 19. Quality standards measurements in processing tomato. Source: Personal Archive

When cultivated under stressful conditions, Tomatoes tend to exhibit enhanced flavor, and their shelf life may show a slight improvement for the same underlying reasons. The more water is supplied to these plants, the higher the yield they typically produce, but this can come at the cost of a decrease in Total Soluble Solids (TSS).

1.4.5 Significance of Processing Tomato

The tomato ranks as one of the most widely consumed vegetables globally, second only to potatoes and ahead of onions and considered among the most favored garden crops [331]. From 1961 until nowadays the European tomato yield increased by ~ 250% (FAOSTAT, 2018)[332]. It is estimated that on average about half of the increase in crop productivity was due to cultivar improvement through breeding[333]. While tomatoes are grown in over 100 countries, more than 80% of the production is concentrated in the United States, China, Italy, Iran, Turkey, Spain, Brazil, Portugal, Greece, and Chile [334]. The majority of tomato production, about 90%, takes place in the northern hemisphere, primarily in regions like the Mediterranean, California, and China[334]. Interestingly, while Europe and the America were the dominant producers two decades ago, the landscape has shifted significantly, with Asia now taking the lead in the global tomato market. China holds the top spot, followed by India, the USA, Turkey, Egypt, Iran, Italy, Brazil, Spain, and Uzbekistan, in that order [331]. In Europe, countries with the highest tomato yields are often found in northern Europe, where the climate isn't particularly favorable for tomato cultivation, and the dedicated cultivation areas are relatively small [331]. These nations heavily rely on controlled greenhouse conditions for tomato production. When it comes to tomato consumption, three countries stand out as the leaders: Libya, Egypt, and Greece, with each exceeding 100 kg per capita per year[331]. Broadly speaking, the Mediterranean and Arabian countries exhibit the highest tomato consumption levels, with average figures ranging from 40 to 100 kg per capita per year[331].

In 2011, the world experienced a remarkable global production of nearly 160 million tons of tomatoes, ranking it as the seventh most significant crop species, trailing behind maize, rice, wheat, potatoes, soybeans, and cassava[331]. Out of 160 million tons total tomato production, about 40 million tons are processed tomato production [335].

Tomato processing encompasses a wide range of methods, including canning, making tomato paste, producing tomato sauce and puree, drying tomatoes, and creating various tomato-based products. The processed tomato industry plays a vital role in providing consumers with year-round access to tomato products and contributes significantly to the global food supply chain. Being rich in antioxidants such as lycopene and carotenoids [336,337], the processing tomato fruit is a raw material in the production of ketchup, dried tomato fruits, and lycopene products[311]. In general, the quality of the tomato fruit can affect the quality of the final products. The quality of fruits is highly related to its maturity degree. For example, soluble solids content (SSC) is a key quality attribute that has an impact on the flavor, consistency, and taste of processed products. The level of titratable acid and lycopene can affect the acidity and color of processed products. Therefore, these are key indicators for assessing the quality of processing tomato[338]. Traditional testing methods to measure quality attributes such as SSC, titratable acid and lycopene require a destructive sampling procedure and a series of complex and time-consuming experimental operations, which makes it difficult in achieving a large-scale of fruit testing due to the high cost of labor-work and chemical usage [339]. Therefore, there is an increasing demand in the fruit industry to seek rapid and non-destructive testing solutions for nutritional quality determination and fruit maturity stage classification.

Greece, despite its minor role in global tomato product production (1.2%), stands out as a remarkable exporter with a wide reach [340]. The tomato products are shipped to over 40 countries, including Europe, the Middle East, the Far East, and the USA. In 2017, Greece achieved notable rankings globally, ranking 10th in paste exports, 4th in canned tomato exports, and 35th in sauce exports [340]. Their revenue from exports reached 13th place worldwide, with a turnover of USD 76 million (approximately EUR 62 million on average over the past five marketing years). This success underscores Greece's ability to effectively penetrate international markets, despite its relatively small share of global tomato product production [340].

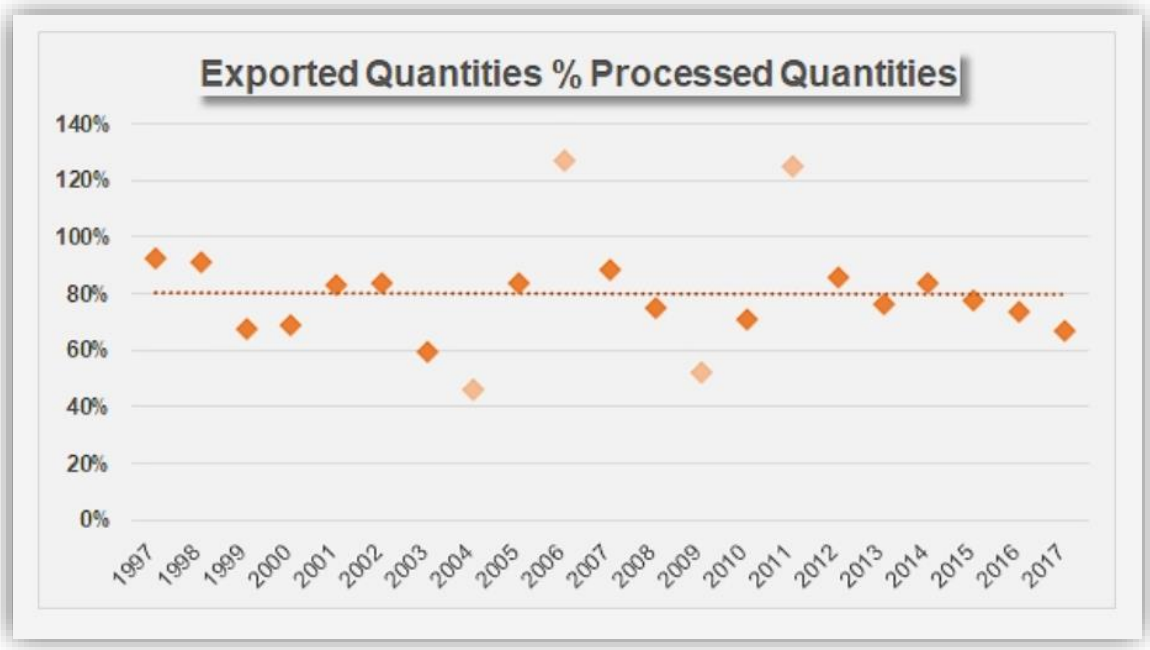

Figure 20. The exported quantities of Greek processing tomatoes on international markets over the past two decades. Source: [340]

The Greek tomato industry primarily focuses on exporting tomato pastes and canned tomatoes, while the export quantities of sauces and ketchup remain relatively small (Figure 21). In 2022, revenue generated from the external sales of tomato pastes amounted to approximately EUR 41 million[341]. Additionally, the financial significance of canned tomato exports in Greece's foreign trade results has seen a substantial increase, rising from 28% in 2013 to over 44% in 2022, with an income of about EUR 37 million in 2022. In contrast, exports of sauces have shown little variation over the past decade, consistently contributing around 6% to the total income, resulting in an average annual turnover of approximately EUR 4.6 million over the past five years.

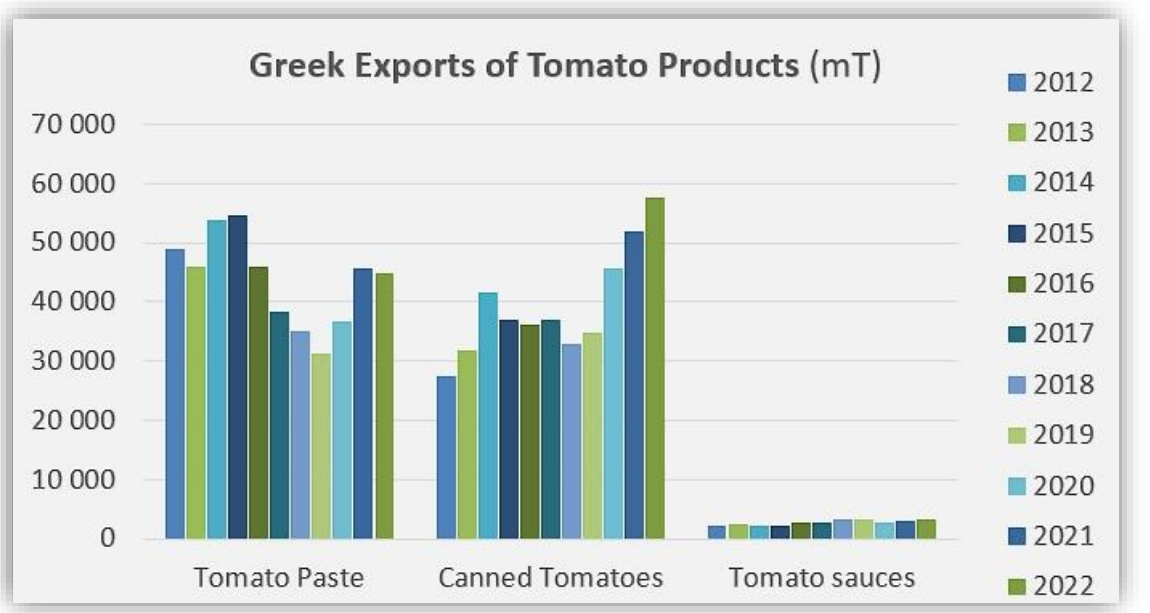

Figure 21. The quantities of Greek tomato sauce, pastes, and canned tomatoes have been exported over the past decade. Source [341]

Overall, Greek exports of tomato products, which have increased significantly in quantity and value in recent years, generated an overall turnover of about EUR 83 million in 2022, of which 57% on European Union markets and 95% on the European continent as a whole (Figure 22).

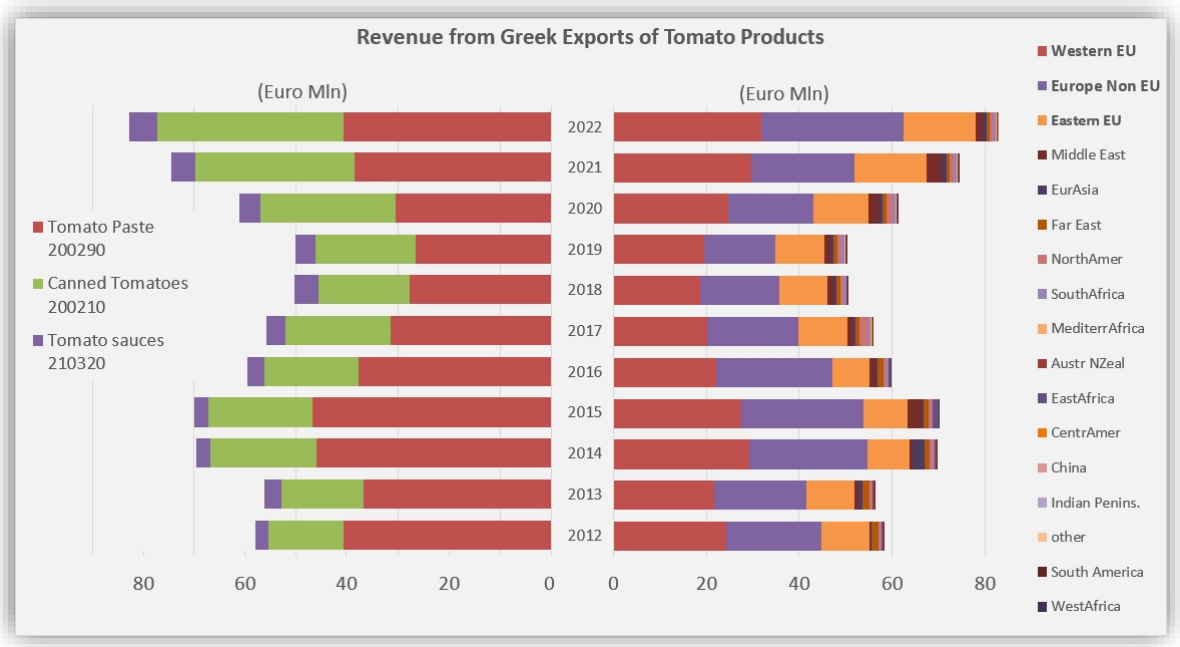

Figure 22. Revenue of Greek exports of tomato products over the past decade, according to category and region of destination. Source [341]

According to the Figure 22, the export dynamics show a slight decline during the pre-pandemic period (2017-2019), but there was noticeable progress in the subsequent years.

Overall, since its discovery in the 16th century and its initial steps into domestication and breeding, the tomato has evolved into one of the most, if not the most, crucial vegetable crops on a global scale [331]. The tomato isn't just a staple in the fresh produce market; it also plays a pivotal role in the processing industry, serving as the foundation for soups, paste, concentrate, juice, and ketchup. The profound significance of this fruit arises from its exceptional quality attributes, unmatched versatility, and far-reaching impact on the food industry and international trade. The tomato is a culinary cornerstone that has left an indelible mark on the global food industry.

Aim and Objectives

This research is designed to make a valuable contribution to the field of precision agriculture, by exploring the potential of state-of-the-art technologies and techniques for yield prediction. The primary objective was to formulate and assess a comprehensive methodology that seamlessly integrates cutting-edge technologies, remote sensing data, and advanced analytical techniques, such as machine learning and statistical analysis, with the principal goal of enhancing the precision and reliability of yield predictions at both local and regional scales. To achieve this, a dynamic approach was adopted, progressing each year, which involved the utilization of non-destructive methods to monitor crop biological cycle and to refine the predictive models for yield estimations.

The specific objectives of this study are as follows:

1. To offer valuable insights into the deployment and integration of state-of-the-art precision agriculture methods and technologies, with a particular focus on their application in the field of crop yield prediction. This is accomplished through a systematic review of the existing literature, offering a comprehensive overview on the latest advancements in this field.

2. To thoroughly compare satellite, UAS, and proximal technologies, placing specific emphasis on their unique strengths and limitations when applied in the context of precision agriculture. This is realized through field-scale measurements using these three platforms.

3. To investigate the relationship between vegetation indices, the critical phenological stages of the crop. This involves deploying time series of five VIs at a regional scale.

4. To evaluate the performance of both statistical and machine learning models, generating clear insights into the most effective growth stages and vegetation indices for accurate yield prediction. To this end, all platforms were deployed, along with yield measurements at both field and regional scales.

The outcomes of this research yield benefits that extend beyond the academic community, offering valuable support to various audiences, including policymakers, researchers, agricultural practitioners, and those involved in decision-making related to resource allocation, food security, and sustainable agricultural development.

Part 2. Materials and Methods

2.1 Workflow Overview

This study followed a progressive trajectory in data collection and methodology (Figure 23). The research initiation involved a systematic literature review to explore the landscape of yield predictions within the framework of precision agriculture applications. Simultaneously, eight fields were selected for detailed investigation through pilot activities that incorporated proximal, aerial, and satellite measurements together with yield sampling. The primary focus of this phase was to examine the relationship between crop yield and NDVI (Normalized Difference Vegetation Index), a commonly used index. The investigation also aimed to identify similarities between satellite technology, UASs, and proximal sensors in the context of crop yield assessment.

Moving into the second year, two distinct fields were individually investigated using satellite, UAS, and proximal sensors at the field level scale. Additionally, a total of 108 fields were included at the regional scale, incorporating satellite data for analysis and thus expanding the experiment's scope. This phase aimed to evaluate the effectiveness of not only NDVI but also four additional VIs in predicting crop yield. Furthermore, AutoML algorithms were deployed along with statistics to assess the correlation between yield and the retrieved VIs from the satellite dataset. The broadening of this study in terms of spatial scale, VIs and research methods, was intended to provide a more thorough understanding of crop yield estimation on the basis of the systematic review results.

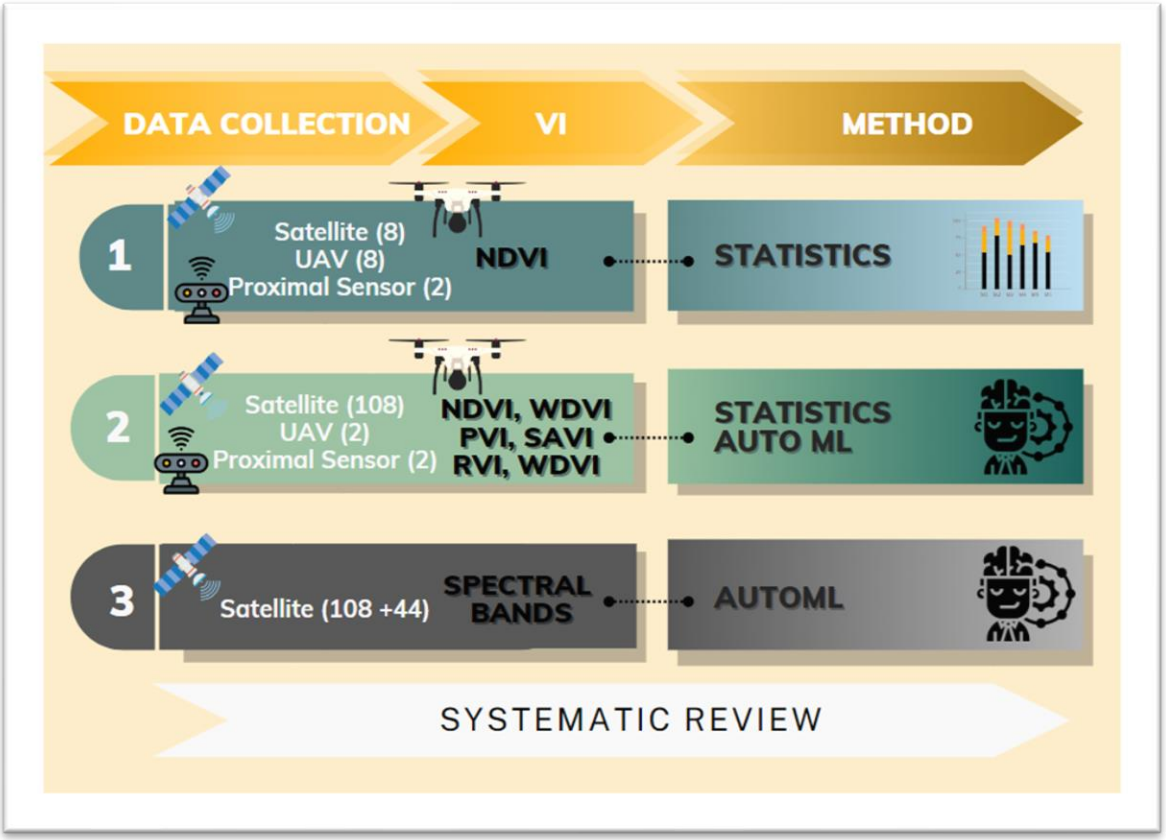

Figure 23. Workflow for assessing the effectiveness of Vis spectral bands to predict processing tomato through proximal aerial and satellite remote sensing. Source: Created by N. K. Darra

During the third year of the study, a more intricate and detailed approach was adopted. Spectral bands derived from satellite imagery played a central role as they were individually assessed to determine their performance in predicting crop yield. This step enabled a comprehensive

evaluation of the unique contribution of each spectral band to the overall accuracy of crop yield estimation. This approach yielded a deeper understanding of the significance and influence of each individual spectral band in enhancing the precision of crop yield predictions.

2.2 Systematic Review

In this study, a systematic review of peer-reviewed articles on PA technology's application in yield prediction was conducted to identify the most common approaches used in yield prediction. A comprehensive search strategy was developed by utilizing Scopus " www.scopus.com" and Web of Science (WoS) " www.webofscience.com" search engines following the Preferred Reporting Items for Systematic Reviews and Meta-Analyses (PRISMA) framework [342]. Specifically, the PRISMA Statement consists of a 27-item checklist and a four-phase flow diagram, aiming at helping authors improve the reporting of systematic reviews and meta-analyses [342]. To ensure the selection of pertinent research articles, the study's approach was designed based on specific research questions and the review's objectives. Recognizing that a simple search using "yield prediction" would yield numerous articles from various fields unrelated to the review's aim, a more focused approach was taken. Therefore, the research words [343–345] were also considered to narrow the focus from a main concept to the central idea. Specifically, the query used for encompassing all the works related to the topic without risking excluding any item is presented in (Table 7).

Table 7. Search engines and queries that were used for the scope of this study.

Search Engine	Query
Scopus	TITLE-ABS-KEY ("yield forecasting" OR "yield prediction" OR "yield estimation" OR "crop modeling") AND TITLE-ABS-KEY ("satellite" OR "UAV" OR "proximal" OR "remote sensing" OR "proximal sensing" OR "aerial")
WoS	TS = ("yield forecasting" OR "yield prediction" OR "yield estimation" OR "crop modeling") AND TS = ("satellite" OR "UAV" OR "proximal" OR "remote sensing" OR "proximal sensing" OR "aerial")

A filtering process was then implemented by utilizing exclusion criteria provided within the Scopus and WoS search engines, specifically focusing on document type, language, and publication year. Only open-access articles published in the English language were included, while review articles and conference papers were excluded. This selection was based on the belief that open-access publishing aligns with the principles of open science, promoting transparency and ensuring that research is readily accessible for comprehensive scrutiny, thus upholding the core principles of scientific integrity. Additionally, the study's timeframe gathered the entire literature for the period 2002 to 2022.

The initial search query yielded 725 records from Scopus and 704 from WoS, with publication details categorized into sections such as "Author, Title, Source," "Abstract, Keyword, Addresses," and "Cited, References, and Use." Furthermore, after eliminating duplicate and review articles from the two chosen databases, 864 articles were subjected to screening based on their titles and abstracts.

2.2.1 Article Selection Criteria

The articles initially retrieved were selected according to particular criteria, such as the remote sensing technology utilized and the method employed for yield prediction. Examining the abstracts

of these articles helped to identify pertinent keywords and facilitated the selection process. To maintain the review's relevance and focus, specific exclusion criteria were utilized.:

- Records not pertinent to the research objective (e.g., satellite RNA in plant pathology) were excluded;
- Articles falling within the agricultural sector but not directly related to crop yield prediction were also removed from consideration;
- Publications that did not incorporate the use of satellites, airborne/UAS, or ground-based sensors for crop yield prediction were excluded;
- Literature search for articles that are published between 1 January 2002 to 31 December 2022;

Articles were considered for inclusion only if they involved crop yield prediction, whether in absolute or relative terms, and provided performance metrics for assessment. To ensure uniformity and comparability, special emphasis was placed on the presence of evaluation metrics like the Coefficient of Determination (R^2) and error metrics such as the Root Mean Square Error (RMSE). Studies lacking performance metrics were excluded to standardize the evaluation process.

After applying all the exclusion criteria, a total of 456 full-text articles were examined for eligibility. Figure 24 illustrates the article selection and rejection process from the databases, following the PRISMA framework.

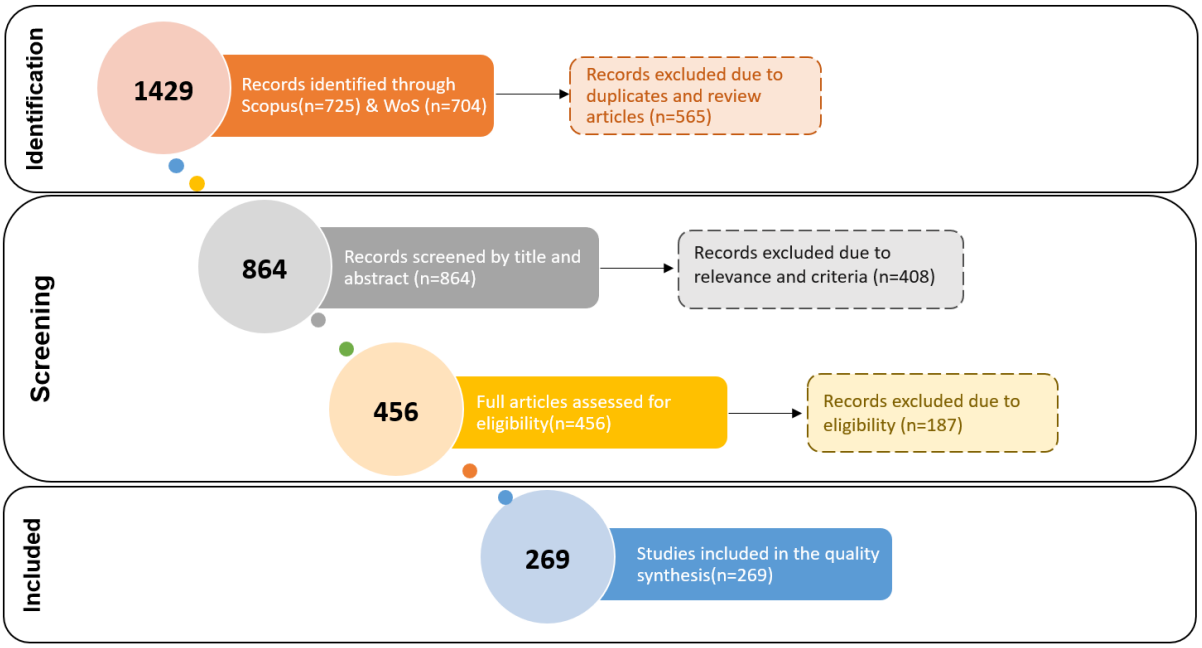

Figure 24. Systematic review procedure for article selection.

The eligibility process involved thoroughly analyzing the full articles to ensure that only the studies that met the necessary aforementioned criteria were included. As a result, a total of 269 studies were deemed suitable and incorporated into this comprehensive review.

2.2.2 Scientific Studies Classification & Statistical Analysis

The selected papers were tabulated and standardized to enable comparison and systematic evaluation by extracting the following variables from each study:

- Study data: lead author, year, title, citations;
- Experiment setup: study region, type of crop;

- Platform type: Satellite, Airborne/UAS measurements (Unmanned Aerial Systems—UAS or Manned Flight), Ground based measurements;
- Method type: machine learning, statistical analysis, model-based approach, VIs;
- Evaluation: performance measures (e.g., R2, RMSE, MAE).

Subsequently, the actual data collected from the papers were subjected to statistical analysis using XLSTAT software version 2016 from Addinsoft (www.xlstat.com). This analysis involved determining the number of research articles produced annually and by type. Additionally, further analyses were conducted based on crop type, platform type, sensor type, and the method's focus area for each year over the past two decades.

2.3 Description of the study area

The pilot research was conducted within the broader region of Thessaly and Central Greece, spanning from E:22°13'20" N:39°42'40" to E:24°6'40" N:38°10'40". Within this area, a total of 504.14 hectares of processing tomato fields were chosen as the pilot fields for the study

Table 8. the boundaries of the pilot fields were digitally captured using georeferenced layers in KML format. An illustrative example of these vector layers, showing the field locations is demonstrated in Figure 25.

Figure 25 The pilot fields' position at the national level and a close-up at regional level. Created by N. K. Darra (ArcGIS, 2023).

These pilot fields encompassed three distinct hybrid varieties: Dexter, Faber, and Foster. Their sizes ranged from 1 to 14 hectares, with double rows planted at an average spacing of 0.4 to 0.6 meters, reflecting the prevalent extensive farming practices in the region. Planting dates for these pilot fields varied, occurring between mid-April and mid-May of each season, with harvesting completed across all fields by late August.

The study's framework, as summarized in

Table 8, outlined the research activities over a span of three years. The first year, the study utilized satellite, UAS, and proximal sensor technology to extract the NDVI. A total of 8 fields, covering 21 hectares, were assessed to evaluate the use of satellite and UAS data for yield prediction. In 2021, a similar approach was applied, focusing on only 2 fields covering 6 hectares. During the same year, the research focus shifted primarily to satellite technology, with 108 fields totalling 410 hectares being considered for the evaluation of NDVI and other four VIs.

In the final year (2022), the study further broadened its scope to include an assessment of all spectral bands to refine yield prediction capabilities. The research concentrated on satellite data, incorporating thirteen spectral bands. A comprehensive evaluation was conducted, encompassing 108 fields for the 2021 season and 44 fields for the 2022 season, all included in this evaluation to investigate the efficacy of these spectral bands for yield prediction.

Table 8. Study's framework

Year	Scale	Technology or activity	Vegetation Indices	Number of Fields	Total Area (ha)
2020	Field level	Satellite UAS Proximal Sensor	NDVI	8	21
2021	Field level	Satellite UAS Proximal Sensor	NDVI	2	6.9
	Regional Level	Satellite	NDVI, RVI, WDVI, PVI, SAVI	108	410
2022	Regional Level	Satellite	NDVI, RVI Bands	44	22,24

The sequential progression of the study's framework, was strategically designed to explore, refine and upscale yield prediction capabilities over a three-year span.

2.4 Data collection and Preprocessing

Data collection and preprocessing procedures involved the acquisition of satellite imagery data at 5-day intervals. However, it's important to note that the sample size was not consistently uniform throughout the data collection process. This variability in sample size is attributed to the presence of total cloud cover, which occasionally hindered data collection efforts, as summarized in

Table 9.

Table 9. Acquisition dates of satellite data for the 2020 to 2023 growing season.

MONTH	ACQUISITION DATES					
	2020					
MAY	03/05/20	13/05/20	18/05/20	23/05/20 *Cloud Cover*	28/05/20 *Cloud Cover*	
JUNE	02/06/20*	07/06/20	12/06/20	17/06/20*	22/06/20 *Cloud Cover*	27/06/20
JULY	02/07/20*	07/07/20 *Cloud Cover*	12/07/20	17/07/20*	22/07/20	27/07/20

AUGUST	**01/08/2020***	06/08/20 *Cloud Cover*	**11/08/20***	16/08/20	21/08/20 *Partial cloud cover*	26/08/20
2021						
APRIL	*Cloud Cover*					
MAY	03/05/21 *Cloud Cover*	08/05/2021 *Cloud Cover*	13/05/21	18/05/21	23/05/21	28/05/21
JUNE	02/06/21	**07/06/21****	12/06/21	17/06/21	**22/06/21***	27/06/21
JULY	02/07/21	**07/07/21***	12/07/21	17/07/21	**22/07/21***	27/07/21
AUGUST	01/08/2021	**06/08/21***	11/08/21	16/08/21	**21/08/21***	26/08/21
2022						
APRIL	03/04/22	08/04/22	13/04/22	18/04/22	23/04/22	28/04/22
MAY	03/05/22 *Cloud Cover*	08/05/22 *Partial cloud cover*	13/05/22	18/05/22	23/05/22	28/05/22
JUNE	02/06/22	07/06/22	12/06/22	17/06/22	22/06/22	Cloud Cover
JULY	02/07/22	07/07/22	12/07/22	17/07/22	22/07/22	Cloud Cover
AUGUST	*Cloud Cover*	06/08/22	11/08/22	16/08/22 *Partial cloud cover*	21/08/22 *Cloud Cover*	26/08/22 *Partial cloud cover*

***UAS and proximal measurements**
**** Due to weather conditions (increased wind) the UAS flight was not feasible**

The next phase of the data processing pipeline involved the establishment of a geodatabase structured at a 10x10 grid cell level, corresponding to the geometry of the satellite imagery for the 2020 and 2021 pilot measurements. The satellite image grid (10x10) was extracted and used as a reference grid for all measurements to ensure that the vegetation indices are consistent and comparable across different satellite images and acquisitions. The grid (.shp) stored the average values of the VIs or NDVI for each sensor's observations within a particular cell, recorded for specific dates.

2.4.1 UAS measurements

For the years 2020 and 2021 remote assessments of processing tomato vigour were made using Phantom 4 Pro UAS (SZ DJI Technology Co., Ltd., Shenzhen, Guangdong, China) equipped with a Parrot Sequoia+ multispectral camera (Parrot SA, Paris, France) and associated 3-axis georeferencing metadata using the cameras integrated positioning system (Figure 26). The UAS used in this context incorporates a gimbal, which adjusts the camera's position relative to the vehicle to maintain the selected shooting angles during movement. It is equipped with a multispectral camera, GPS, and a barometric sensor for measuring altitude differences. Its telemetry system enables communication between the UAS and the operator via a specialized console, with a range of several kilometres. The multispectral camera is specifically designed for agricultural applications, capturing high-resolution images of reflected solar radiation in four wavelength bands (Red, Red Edge, Green, and NIR). This makes it suitable for studies related to plant resilience and other precision agriculture applications. The aerial UAS imagery was acquired around midday with nadir flights at 30 m above the ground The acquisition interval of the multispectral camera was set at 2 s, and the flight plan overlap, and side lap were 80% and 70%, respectively.

Figure 26. i) a Phantom 4 Pro UAS used to collect imagery, ii) Parrot Sequoia+ multispectral camera of the UAS, iii) On site data collection

The multispectral images captured by the UAS were mosaicked using Pix4D software (Pix4D S.A., Prilly, Switzerland) through the 'Ag Multispectral' photogrammetric model pipeline. Radiometric calibration was applied to the generated orthomosaic using the reference images of a radiometric calibration target (Airinov Aircalib) acquired after each flight. Finally, the generated NDVI orthomosaic was masked to the boundaries of the fields and then scaled up to the same 10 x10 reference (satellite) geometry grid, using a mean aggregation approach.

2.4.1 Proximal sensing measurements

The GreenSeeker hand-held optical sensor (N-Tech Industries, Ukiah, CA), was employed for instantaneous measurement of the NDVI. This sensor utilizes a self-illumination system in both red (656 nm) and near-infrared (774 nm) wavelengths. It includes a datalogger that records the geographic coordinates of the acquired values and generates a shapefile (shp). Proximal measurements were conducted three times throughout the growing season for two fields in both the 2020 and 2021 seasons (Figure 27).

Figure 27 : GreenSeeker hand-held optical sensor. Source: Personal Archive

To standardize the data, the geographic coordinates of all proximally acquired canopy reflectance data collected throughout the season were initially converted to projected coordinates (UTM Zone

34N). Subsequently, preprocessing steps involved cleaning and removing data points falling outside the field boundaries and eliminating outliers (values > ±2.5σ) following the methodology outlined by Taylor et al. in 2007 [346].

The point data were then interpolated to a common grid file corresponding to the field boundaries using a 1-m grid with block kriging on a 10x10-m block size and a local variogram, utilizing the Vesper software [347]. The resulting grids were converted to .tiff format in ArcMap v10.3 (ESRI, Redlands, CA, USA) and scaled up to 10 m x 10 m plots using the satellite geometry grid. This process ultimately generated a time series of NDVI maps with a spatial resolution of 10 m x 10 m, precisely aligned with the corresponding satellite imagery.

2.4.2 Satellite imagery acquisition

Remote assessments of field vigour were made using Sentinel-2 satellite imagery, that is a satellite mission developed by the ESA as part of the Copernicus program. Sentinel-2 comprises two identical satellites, Sentinel-2A and Sentinel-2B, equipped with multispectral imaging sensors capable of capturing high-resolution Earth surface imagery. These satellites follow sun-synchronous orbits, providing global coverage and revisiting the same area every five days. The MultiSpectral Instrument (MSI) on board captures data across 13 spectral bands, encompassing the visible to shortwave infrared region. These bands include red, green, blue, near-infrared, and others sensitive to various land features, including vegetation and water bodies. Spatial resolution ranges from 10 meters for visible and near-infrared bands to 20 meters for red-edge and shortwave infrared bands. To maintain consistent resolution, a resampling approach using SNAP software (Sentinel Application Platform—ESA Sentinels Application Platform v6.0.4), was applied, resulting in a uniform 10-meter resolution for all bands in this study. For in-depth technical specifications on Sentinel-2 bands, reference can be made to the European Space Agency's documentation [European Space Agency, 2010].

For each observation date, 3 to 5 satellite images, depending on the fields' locations, were acquired to cover the entire study area. The second step of data preprocessing involved mosaicking each survey date's images into a single raster dataset of the whole study area using ArcGIS software (Environmental Systems Research Institute, Redlands, CA, USA).

In this study, Sentinel-2A&B imagery, obtained from the Copernicus Open Access Hub, was level 2A imagery, indicating processing by suppliers using the Sen2Cor processor. This processing encompassed geometric, radiometric, and atmospheric corrections, rendering the imagery immediately usable. Atmospheric correction, a critical step, mitigates atmospheric effects and restores surface reflectance values. These corrections employ atmospheric models and ancillary data, such as meteorological information and aerosol optical thickness, to estimate and compensate for atmospheric influences on satellite measurements.

Furthermore, the satellite image grid (10x10) was extracted and used as a reference grid for all measurements to ensure that the vegetation indices are consistent and comparable across different satellite images and acquisitions.

In the final phase of the study, raw digital number values for each spectral band were extracted utilizing the Google Earth Engine (GEE) platform. This extraction process aimed to investigate potential correlations between these spectral bands and crop yield for the years 2021 and 2022. A total of thirteen distinct spectral bands were acquired as covariates for each observation date. The inclusion of these covariates was driven by the anticipation that they would contribute to enhancing the predictive capabilities of the study. By incorporating a broader range of spectral information, the research sought to gain a more comprehensive understanding of the relationships between the spectral characteristics of the crop fields and the resulting crop yield. This analysis allowed for a deeper exploration of the factors influencing agricultural productivity and provided valuable insights for the study's conclusion.

2.4.1 Yield measurements

The yield quantity and quality were sampled manually before harvest for the 8 fields of 2020 and the two of 2021 growing season. A regular 10x10 reference -cell grid covering the entire area was laid out, using ArcMap v10.3 (ESRI, Redlands, CAUSA). To carry out the yield mapping, an NDVI map was generated for each field using UAS measurement data taken before the harvest. This NDVI map was then classified using the quantile method, which allowed for the visualization of low, medium, and high NDVI values within each field. This classification helped identify different levels of vegetation health and productivity across the fields.

Using these classified NDVI maps as a reference, random points were selected for each of the three designated zones (Figure 28):

a) **Low Zone (L1, L2)**: Representing areas with lower NDVI values, indicating lower crop productivity.

b) **Medium Zone (M1, M2)**: Corresponding to areas with moderate NDVI values, suggesting intermediate crop productivity.

c) **High Zone (H1, H2)**: Encompassing areas with high NDVI values, indicating higher crop productivity.

At each of these selected sampling points, a specific group of plants included two and a half meters along the planting lines was harvested. This group typically comprised four to six plants.

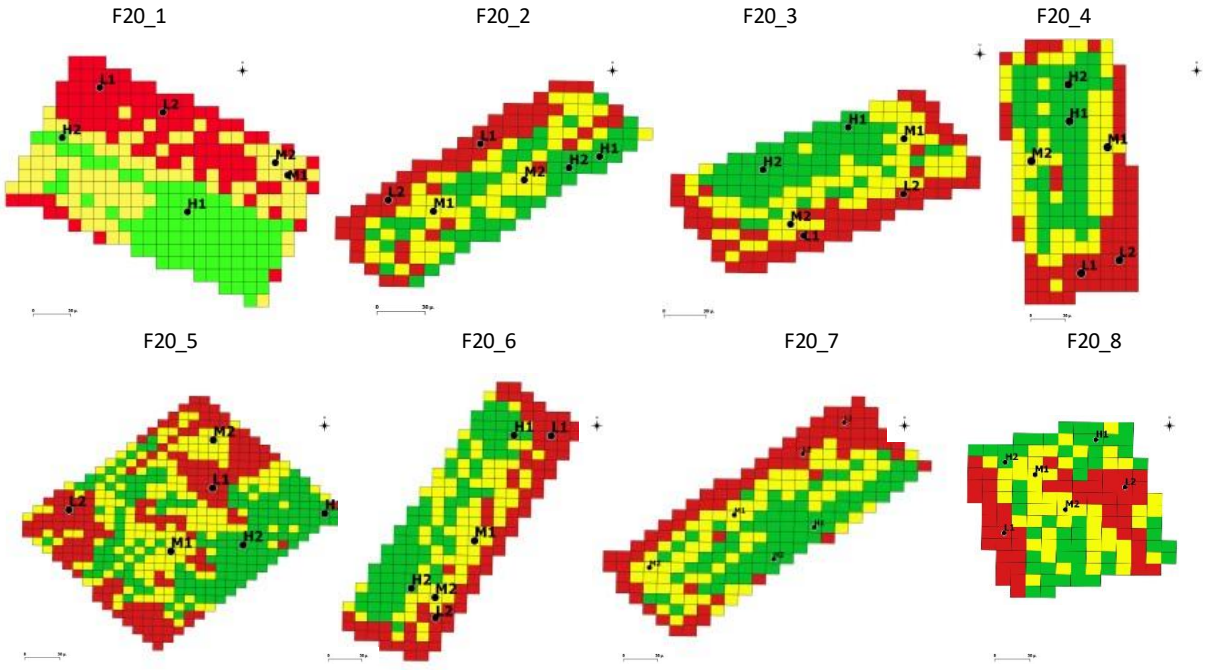

Figure 28 Yield sampling points (L1, L2, M1, M2, H1, H2) for 2020 growing season.

To ensure precise location accuracy in the field, a GPS device was employed. These type of devices allowed for the exact identification of the sampling points within the designated zones. Once the sampling points were accurately pinpointed, the next step involved the collection of tomato samples from the selected location points. This collection process was facilitated by using plastic bags to gather the harvested tomatoes.

An electronic scale was used to weigh the gathered tomatoes after the collection. The process involved considering the green and red tomatoes separately and determining the total weight. This step was essential to accurately measure the yield of tomatoes obtained from each of the sampling

points. The recorded weights provided valuable data for assessing the crop yield in the various zones, allowing for an in-depth analysis of crop productivity across the field. The images below (Figure 29) show the manual collection of tomato samples.

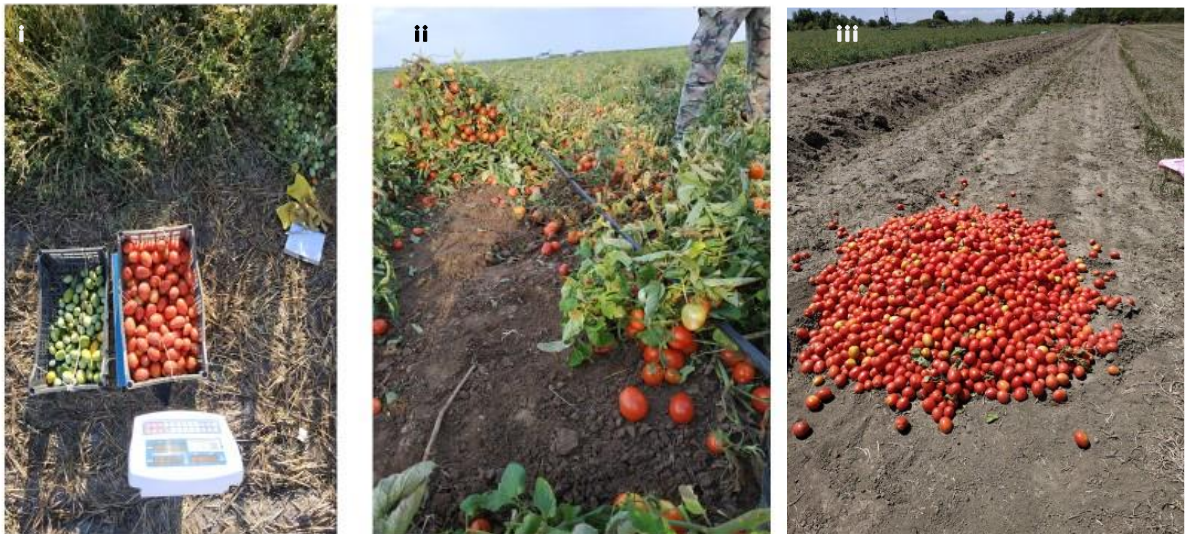

Figure 29. Yield sampling of processing tomatoes, i) separation and weighing of ripe and unripe tomatoes, ii) yield sampling along a length of 2,5 m, iii) the collected of the yield samples per pilot area.

In the final step of the process, the number of plants per hectare was taken into account. This information served as a crucial factor for extrapolation, which involved making estimations and predictions based on the data collected from the sampling points. By upscaling the sampling measurements, the study aimed to assess the reliability and accuracy of the projected production across the entire field. This extrapolation allowed for making informed predictions about the overall crop yield, per pilot field. It provided insights into how the observed data from the sampled points could be scaled up to represent the entire hectare, thus helping in evaluating the reliability and robustness of the yield projections. It's noteworthy that in the case of 2022, each of the two fields included three different varieties. Consequently, six samples were gathered for each variety, resulting in a total of 18 samples per field. Finally, for the years 2021 and 2022 the actual yield of each pilot field within the satellite framework was recorded directly by the farmers under the supervision of agronomists, and the respective total yield values were included in the dataset (Table 10).

Table 10. Summary of yield sampling strategy over the three years

Year	Technology or activity	Vegetation Indices	Number of Fields	Total Area (ha)	Yield Sampling
2020	Satellite UAS Proximal Sensor	NDVI	8	21	6 Yield samples per field
2021	Satellite UAS Proximal Sensor	NDVI	2	6.9	18 samples per field
	Satellite	NDVI, RVI, WDVI, PVI, SAVI	108	410	Total yield per field
2022	Satellite	RVI, NDVI, All Bands	44	22,24	Total yield per field

2.5 Vegetation indices and spectral bands

To evaluate the satellite systems and their relationship to yield, five VIs, namely the NDVI, Weighted Difference Vegetation Index (WDVI), SAVI, RVI, and Perpendicular Vegetation Index (PVI), were calculated for each date via SNAP software (Sentinel Application Platform—ESA Sentinels Application Platform v6.0.4), which is provided free of charge and accessible to everyone as part of the European Copernicus project. Each index captures different aspects of plant vitality and environmental conditions, providing a comprehensive understanding of crop performance. These five VIs were chosen based on their well-established utility and effectiveness in assessing vegetation health and predicting crop yield. Particularly, WDVI and PVI, indices that correct for soil reflectance, show a more linear and less-scattered relation than NDVI and RVI [348]. The research findings [349] also highlight the sensitivity of different VIs to variations in green cover and their associated noise levels. Specifically, at a 40% green cover, the noise level of the NDVI is observed to be four times that of the WDVI and nearly ten times that of the SAVI. These noise levels correspond to vegetation estimation errors of approximately +/- 23% for NDVI, +/- 7% for WDVI, and +/- 2.5% for SAVI. Furthermore, the NDVI and WDVI were found to be significantly crucial for predicting tomato weight, while VIs one month prior to harvest were significant in predicting fruit quantity [350]. These indices have also been found, through the systematic review that generate high correlations with yield [351,352]

As a result, VI raster datasets (10x10m) of the whole area were created by iterating the VI formulas over all satellite image pixels. Once the total number of images was determined, an additional manual filtering step was performed to ensure that each generated mosaic consisted solely of high-quality and cloud-free data from the pilot fields. Given the small size of the fields, pixels outside the pilot farm boundaries were also selected and masked. For each date, a mean VI value was extracted from each field using the zonal statistics tool of the ArcGIS software.

For the VIs calculation, Bands 4 (B4) and 8 (B8) of Sentinel-2 were used, which correspond to the RED and NIR spectrum, respectively. The equations used for the estimation VIs are presented below (Table 11):

Table 11 The selected VIs used in this study and their respective spectral equations.

Index	Equation	Reference
NDVI	$\frac{(NIR - RED)}{(NIR + RED)}$	Rouse et al., [253]
WDVI	NIR– S*RED *where S is the slope of the soil line from a plot of red versus near-infrared.*	Clevers, [353,354]
PVI	$\frac{(NIR - a * RED - b)}{\sqrt{(a\text{^}2 + 1)}}$ *where a is the slope of the ground line, and b is the ground line's gradient.*	Richardson & Wiegand, [355]
RVI	NIR/RED	Pearson & Miller, [356]
SAVI	$\frac{(NIR - RED)}{(NIR + RED + L)}) * (1 + L)$ *where L is a soil adjustment factor*	Huete [261]

NDVI is the most commonly used vegetation index and has found various applications. The result of NDVI calculation is an image with a continuum of pixel values ranging from – 1 to 1. The NDVI varies from a minimum at bare soil reflectance to a maximum for a fully developed canopy with a value slightly less than one [30]. Healthy photosynthetic vegetation is related to higher positive values; on the other hand, stressed vegetation or even bare soil is related to lower values, especially <0.2 [357,358]. In the processing tomato crop, NDVI values are reported to have good correlation with several vegetation parameters, including the ability to predict yield [359].

The same spectral bands were used for RVI (Ratio Vegetation Index or Simple Ratio vegetation index), which is recorded to improve both saturation in high vegetation and sensitivity to the soil in low vegetation compared with NDVI [360]. It was introduced by Pearson and Miller [356] and is based on the contrast between the visible red and far-infrared bands of electromagnetic radiation for the pixels corresponding to vegetation [356]. High values of the index are mainly attributed to healthy vegetation and result from the combination of its low reflectance value for the red and the high reflectance it presents in the near-infrared band. Its value range is from 0 to more than 30, with healthy vegetation usually presenting values of 2 to 8.

Richardson and Wiegand [355] approached the problem of variable soil brightness by developing the PVI, which attempts to eliminate differences in soil background [355]. It can be computed as a spectral indicator of plant development or biomass accumulation and cannot be considered to be independent of soil brightness. While it is effective in removing soil brightness effects for bare soil, it quickly becomes more sensitive as the canopy develops. A PVI value of 0 indicates bare soil, whereas negative values indicate water and positive values indicate vegetation. It is less sensitive to the atmosphere but is considered sensitive to the reflectivity and brightness of the ground, especially in cases with low vegetation cover.

The weakness PVI presents regarding the assumption that there will be only one soil type under vegetation is addressed by the SAVI proposed by Huete [261] and is a hybrid of NDVI and PVI. The originality of this index lies in establishing a simple model that permits an adequate description of the soil–vegetation system [361]. SAVI also attempts to eliminate soil background effects; however, it is much less sensitive to changes in the background caused by soil color or surface soil moisture content than the RVI [362]. Qi et al. [363] shoed that the adjustment factor (L) is not a constant but a function that varies inversely with the amount of vegetation present. Generally, it is best applied to soils with sparse vegetation, and its range of desired values is the same as that of NDVI [364].

The WDVI was introduced by Clevers et al. [353] in 1989. WDVI has been used to overcome high PVI values due to a bright soil background. This index is also based on distance, and it assumes that the ratio between NIR and the red reflectance of bare soil is constant [365]. The WDVI concept was developed in order to correct the influence of soil background, but it is quite sensitive to atmospheric conditions. It is mathematically simpler than the rest of the indicators but with an infinite range of desired values [354].

To conclude the study, raw digital number values for each band were extracted using the Google Earth Engine (GEE) to explore potential correlations with crop yield for the years 2021 and 2022. The Sentinel-2 imagery consists of a total of 13 spectral bands, encompassing a range from visible and near infrared (vis-NIR) to short-wave infrared (SWIR). Among these bands, there were four bands with a spatial resolution of 10 meters, namely B2 (490 nm), B3 (560 nm), B4 (665 nm), and B8 (842 nm). Additionally, there were six bands with a spatial resolution of 20 meters, including B5 (705 nm), B6 (740 nm), B7 (775 nm), and B8A (865 nm). The remaining bands consisted of two SWIR large bands, B11 (1610 nm) and B12 (2190 nm), as well as three bands with a resolution of 60 meters, namely B1 (443 nm), B9 (940 nm), and B10 (1380 nm). These spectral bands were extracted as covariates for each observation date, with the expectation that these would enhance the predictive capacity of the study at multi temporal level.

All the results were recorded in Excel spreadsheets with VIs and spectral band values for all the measurement dates acquired.

2.6 Data Analysis

Data analysis was carried out to assess the strength and significance of these relationships to determine the predictive capabilities of the proximal, UAS and satellite-based indices for processing tomato yield estimation.

2.6.1 Statistical analysis

Pearson's correlation coefficient (r) and regression analyses, facilitated by the XLstat software (R Core Team, 2022), were conducted to explore the relationships between yield and Vegetation Index (VI) data obtained from all three sensors. The objective was to assess the efficiency of VIs predicting yield, and whether they demonstrated a consistent trend. In this analysis, correlation r-values exceeding 0.50 were considered indicative of a moderate to strong relationship.

Descriptive statistics, including mean and standard deviation, were computed for the NDVI data to provide a comprehensive overview of crop production.

2.6.2 Regression Methods and AutoML Set Up

Machine learning techniques have the potential to enhance the modeling capabilities of traditional statistical methods. Nevertheless, the vast array of machine learning algorithms available presents a substantial challenge when it comes to selecting the most suitable one. Furthermore, each of these algorithms involves various hyperparameters that require fine-tuning through trial and error. Consequently, there is no inherent knowledge regarding the optimal configuration, and these hyperparameters are not automatically optimized during the training process. For instance, hyperparameters include the number of trees in methods like Random Forests and AdaBoost, the choice of splitting criteria (e.g., Gini, entropy) for tree-based algorithms, and the handling of outliers in robust linear regression methods like Theil-Sen or Huber.

AutoML is a field of research that has become increasingly popular over the last few years [366]. Different domains, such as image recognition [367] and time series processing [368], take advantage of this technique. Moreover, some specific subfields of AutoML, such as neural architecture search (NAS), have arisen to optimize the search for some specific hyperparameters in the design of neural architectures (e.g., number of layers, activation function, etc.). However, there are still some open concerns [369] because (i) finding the best hyperparameters can still be too computationally expensive and (ii) AutoML adds a new layer of complexity/abstraction that can make the interpretability of the model decisions harder. On the other hand, more studies are arising around this topic; therefore, agriculture, specifically yield prediction, should be used to evaluate the current state of the technologies implementing AutoML techniques.

To improve the predictive power of our model, this study also evaluated several ensemble methods based on decision trees, such as AdaBoosting, Random Forests, and Extra Trees. These combine the predictions of multiple machine learning algorithms to make more accurate predictions than the individual models. All of these ensemble methods start with a decision tree and then use boosting or bootstrap aggregation to reduce its variance and bias (bagging). Ensemble models aim to improve the performance of machine learning models by combining several of them [370]. In the case of regression, the mean of the predictions of the models with the best performance is used as the final prediction (Figure 30). An ensemble can be composed of endless models, however the larger the amount, the higher the computational requirements. Therefore, in this study, ensembles of up to 3 regressors were evaluated.

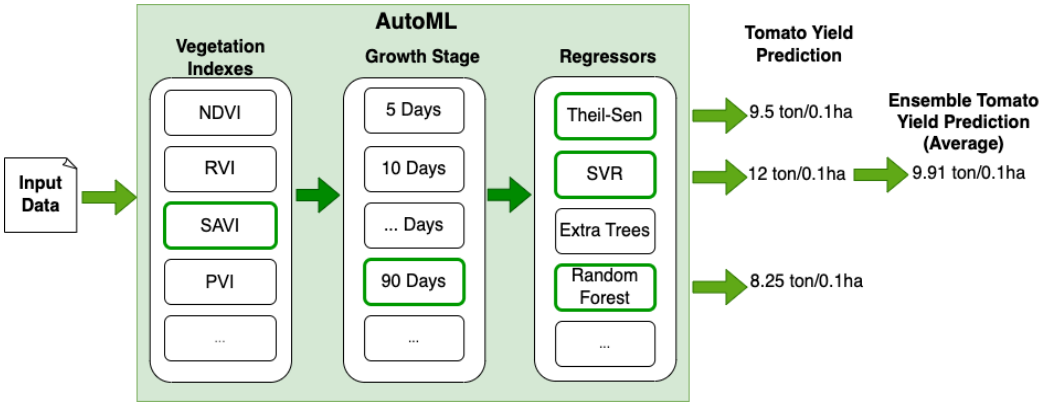

Figure 30. The use of AutoML for selection of the best combination of inputs (vegetation index and growth stage) and creating an ensemble of regression models is proposed as the methodology.

AutoML was studied in this study using linear and nonlinear regression algorithms, including ordinary least square, automatic relevance determination regression, Theil-Sen, and Huber regression models, as well as decision-tree-based algorithms:

- Ordinary least squares (OLS): the most common estimation method for computing linear regression models, which can be found in related work, e.g., Prasetyo et al. [371];
- Automatic relevance determination (ARD) regression: compared to the OLS estimator, the coefficient weights are shifted slightly toward zeros, which stabilizes them [372];
- Theil-Sen estimator method: the most popular non-parametric technique for estimating a linear trend, making no assumptions about the underlying distribution of the input data [373];
- Huber regression: this model is aware of the possibility of outliers in a dataset and assigns them less weight than other samples, in contrast to Theil-Sen, which ignores them [374];
- Decision trees: this method uses a non-parametric learning approach. Its main advantage is that it can be visualized to better understand why the classifier made a particular decision.

To improve the predictive power of the model, in this study, we also evaluated several ensemble methods based on decision trees, such as AdaBoost, Random Forests, and extra trees. These methods combine the predictions of multiple tree-based models to make more accurate predictions than the individual models. Specifically, these ensemble methods start with a decision tree and then use boosting or bootstrap aggregation to reduce its variance and bias (bagging). It is important to remark that these tree ensembles are different from the ensemble of models that are built on top of the system. This means that the final ensemble used to compute the regression can be composed of three tree ensembles (e.g., two random forests and one AdaBoost).

- AdaBoost: The AdaBoost algorithm (adaptive boosting) uses an ensemble learning technique known as boosting, whereby a decision tree is retrained several times, with greater consideration given to data samples for which the regression is imprecise [375];
- Random Forest: A supervised learning approach using the ensemble learning method for regression. In this approach, numerous decision tree regressors are combined into a single

model trained for many data samples collected on the input characteristic (in this case, NDVI) using the bootstrap sampling method [376];

- **Extremely Randomized Trees:** Extra trees is similar to random forest in that it combines predictions from many decision trees, but instead of bootstrap sampling, it uses the entire original input sample [377].

The auto-sklearn framework [378] was used to implement the AutoML pipeline. This means that three main techniques were used. First, Bayesian optimization was used as the global optimization algorithm. Since finding the best regressor and its hyperparameters is a non-convex, computationally expensive problem, the Bayes theorem can be used to direct an efficient and effective search of an optimal hyperparameter configuration [379]. Secondly, a metalearning step was used to warm start the Bayesian optimization procedure, which resulted in a considerable boost in efficiency. In the case of auto-sklearn, the metalearning approach used an offline phase to learn the best initialization configurations along 140 datasets from the OpenML [380] repository. Thirdly, auto-sklearn implements an ensemble building technique whereby the most suitable models are combined to boost the prediction performance.

2.6.3 Evaluation methodology

The assessment involves evaluating the performance and accuracy of satellite-derived indices for predicting processing tomato yield. This evaluation is achieved by comparing the satellite-derived data with ground truth information collected during field surveys. The analysis takes into account factors such as spatial resolution, spectral characteristics, and temporal variability, allowing for a comprehensive examination of the agreement and discrepancies between and satellite data.

To measure the prediction accuracy, two key metrics are employed: the R^2 and the RMSE. R^2 provides insights into the degree of correlation between predicted and observed values, while RMSE quantifies the error between them. Additionally, a 5-fold cross-validation procedure is implemented for each regression model to assess their generalization ability and ensure their robustness. To further enhance the precision of the final performance assessments, the experiments are conducted 20 times with different data splits.

This approach ensures a comprehensive evaluation of the satellite-derived indices, their predictive accuracy, and their robustness, providing a well-rounded assessment of their suitability for processing tomato yield prediction.

Part. 3 Results

3.1 Yield Estimation using Precision Agriculture – Systematic Review

One of the key findings in the systematic review pertains to the annual publication count spanning from 2002 to 2022. Figure 31 provides insight into the changing patterns of research output in the field of yield prediction over this two-decade period. The findings of the study [381] indicating that during 2002 to 2012, the publication rate was low, with an average of roughly one paper per year. However, between 2013 from 2019 onwards, a rapid increase in publications is evident, confirming the growing interest among researchers, which also reflects the yield prediction used in the literature. This also aligns with similar systematic review for machine learning [382], that mark 2019 as a year of with high research activity.

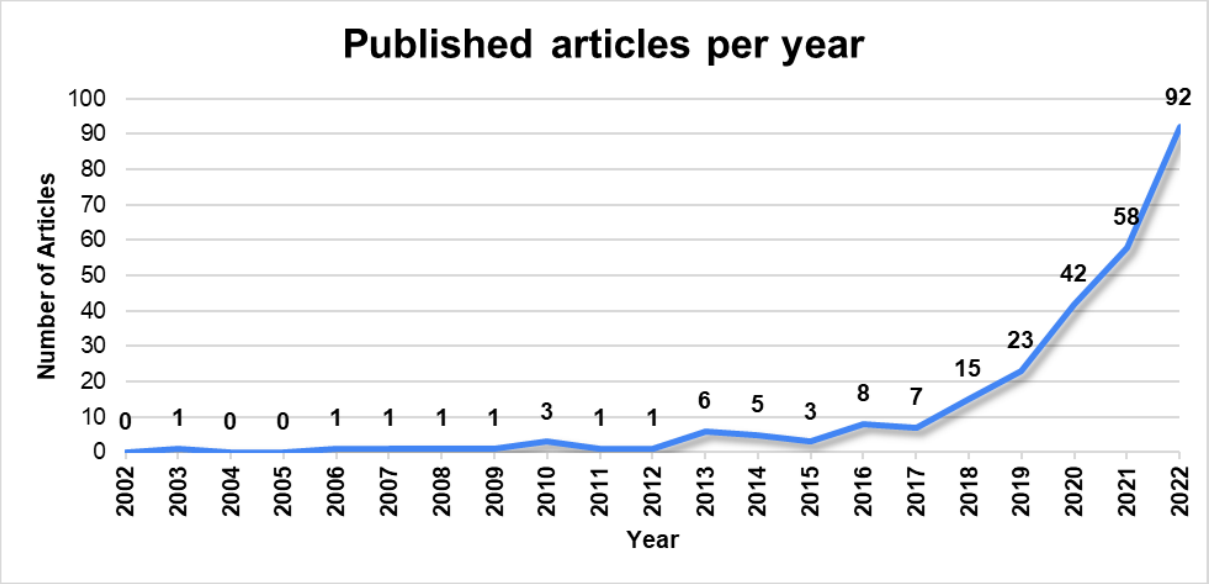

Figure 31. Number of publications per year throughout the period 2002 to 2022.

The higher number of articles in the last years can be explained by a confluence of factors such as technological advancements in ICT, augmented research funding, and an expanding understanding of remote sensing applications.

3.1.1 Key contributor countries and crops

This systematic review also provided insights into the geographical distribution of research and the key contributors in the field. The studies spanned across 55 countries, with China emerging as the most prevalent location, succeeded by the USA, India, Australia, and Brazil (Figure 32). While experiments in developing countries exist, they often focus on a single crop and are less abundant. In Europe, research efforts are geographically diverse, correlating somewhat with country size and production share, yet Eastern Europe exhibits a scarcity of studies. Notably, these findings pertain to the study areas within the articles, not necessarily the countries of authorship.

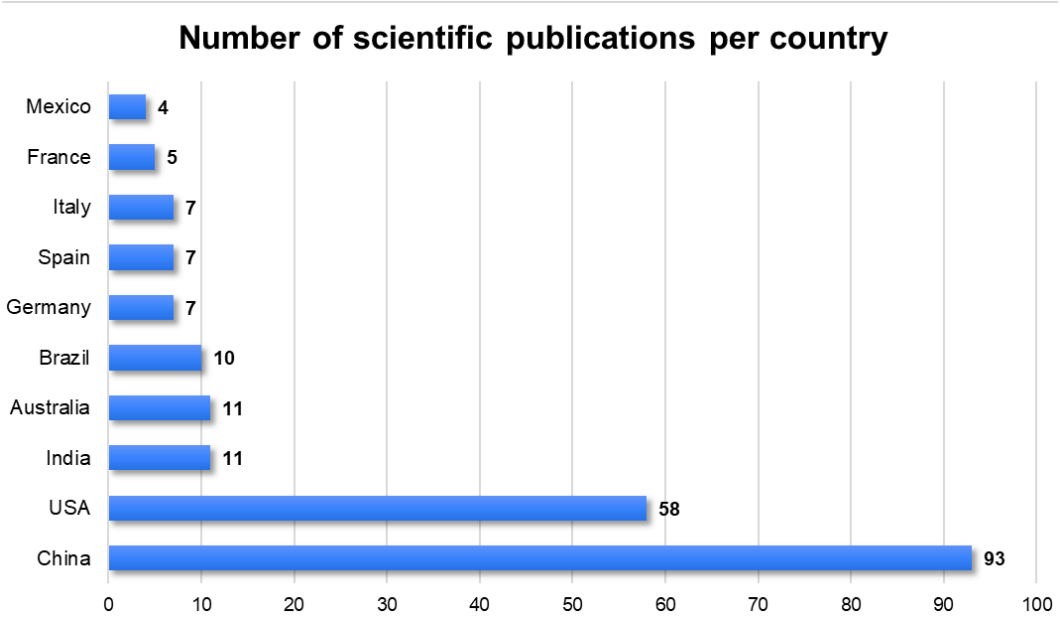

Figure 32. Top 10 countries in terms of publications 2002–2022.

The selection of crops for yield estimation plays a pivotal role in remote sensing-based agriculture research. Through a comprehensive analysis of the available literature, this study has identified the most commonly investigated crops when using remote sensing techniques for yield estimation. The research covered a wide range of crops, encompassing 48 different types, further categorized into nine groups based on the classification provided by the Food and Agriculture Organization (FAO) [383] . Figure 33 provides an overview of the number of studies that encompass crops from each category, highlighting the prominent crops that have received extensive attention in the field of remote sensing-based yield estimation. It's important to note that several studies addressed multiple crops, which is why the total number of crops mentioned exceeds the number of studies analyzed.

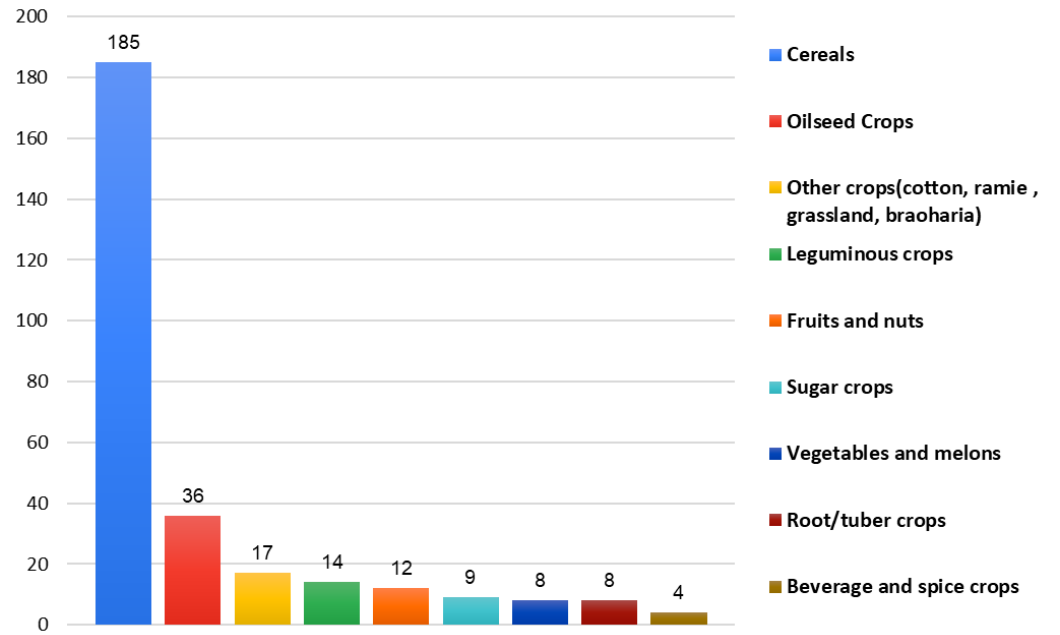

Figure 33 Categories of crops included in literature between 2002 and 2022.

Figure 34 offers a more detailed breakdown of the number of studies corresponding to various crops. It's important to highlight that several studies investigated multiple crops, which accounts for the total number of crops being greater than the number of studies analyzed.

Figure 34. Number of studies per crop category and crop.

Among these crops, wheat (including durum wheat), maize, and rice stand out as highly studied, not only within the cereal category but across all categories. Additionally, oilseed crops, with soybeans taking the lead, also garner significant attention in scientific publications. On the other hand, the categories of fruits and nuts, as well as vegetables and melons, appear to be the least explored in terms of research publications. It's worth noting that the "Grass crops" category encompasses various crops, including Bachiaria pastures, grassland, miscanthus, perennial bioenergy grass, and ryegrass. Similarly, the "tomato" category includes research related to processing tomato crops.

3.1.2 Trends in platforms and sensors used.

The literature on remote sensing platforms for crop yield forecasting encompasses a wide range of options with unique strengths and drawbacks. These platforms vary in spatial and temporal resolution, spectral and radiometric capabilities, coverage area, revisit frequency, data availability, cost, and processing demand. Consequently, choosing the ideal remote sensing platform for a specific crop yield forecasting scenario relies on multiple factors such as crop type, analysis scale, forecasting objectives, available resources, and user preferences.

The study's findings reveal that a wide range of remote sensing platforms were commonly employed for crop yield estimation, with many studies using multiple platforms concurrently. Notably, the majority of the reviewed studies (62%) relied on satellite-derived data to generate yield forecasts throughout the growing season. However, for small-scale investigations conducted on experimental plots, ground-based sensors (27%) or airborne/UAS sensors (30%) were more frequently utilized (as depicted in Figure 35). Despite the utilization of multiple platforms, satellites remained the predominant choice for crop yield estimation. This diverse utilization of remote sensing platforms highlights their versatility and their advantages in collecting crucial data for crop yield forecasting.

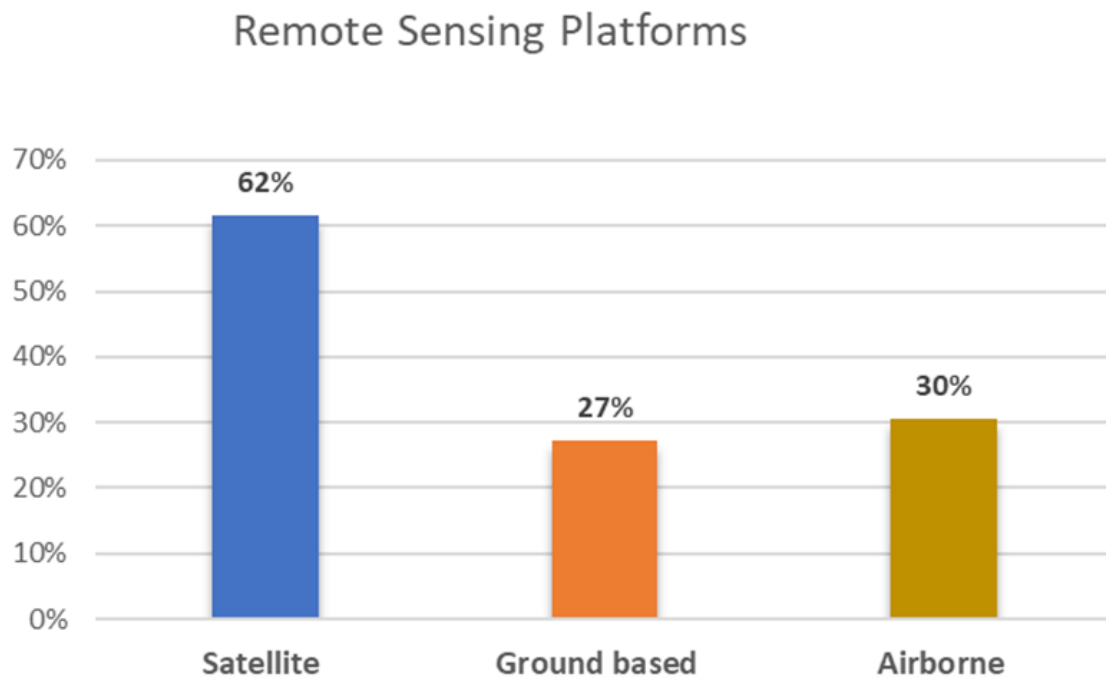

Figure 35. Remote sensing platforms for yield forecasting used in the literature [381].

Figure 36 provides a visual representation of the satellite systems that are most commonly utilized for crop yield prediction. The most prevalent satellite system employed for this purpose is the Moderate Resolution Imaging Spectroradiometer (MODIS), followed by Sentinel-2, Landsat, and Satellite pour l'Observation de la Terre (SPOT). Additionally, Synthetic Aperture Radar (SAR) sensors, primarily Sentinel-1, have been extensively utilized. Moreover, airborne/UAS platforms have contributed significantly to yield predictions. Out of the 269 reviewed studies, 84 utilized airborne/UAS data for crop yield prediction, involving both manned and unmanned flights. These studies utilized multispectral cameras (45), RGB cameras (30), and hyperspectral data (15). Thermal and SAR sensors were less frequently employed. Notably, many studies employed more than one sensor, indicating the integration of multiple data sources to enhance the accuracy and comprehensiveness of crop yield prediction models.

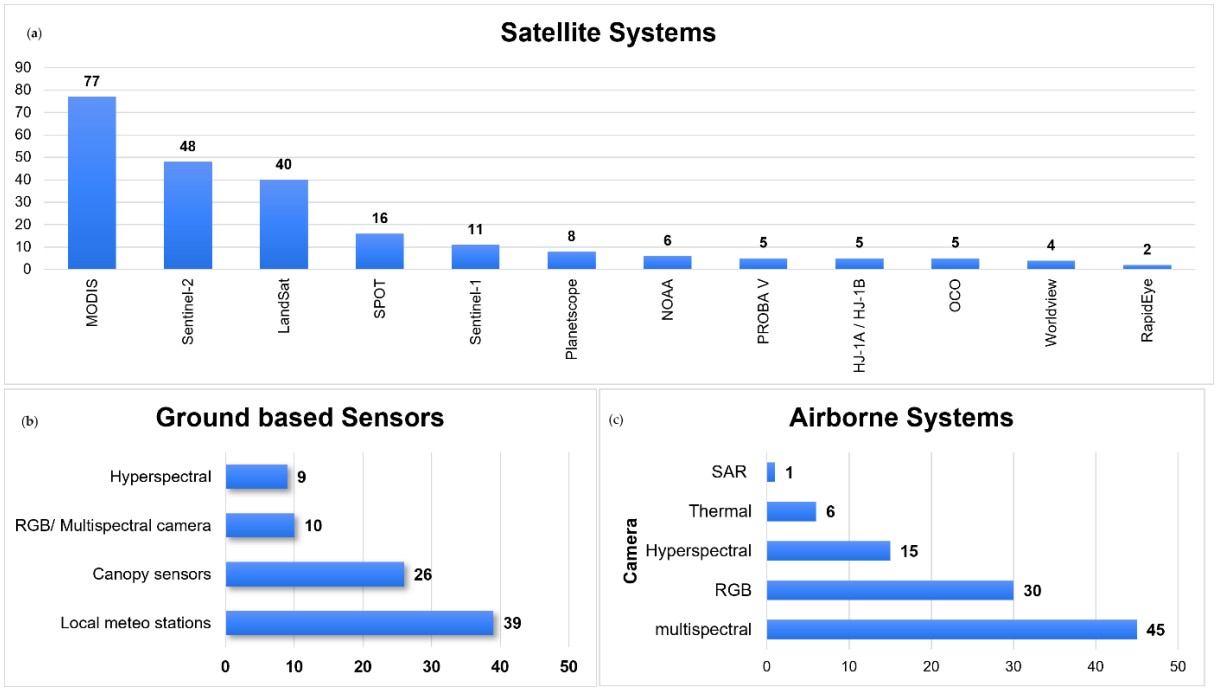

Figure 36. i) Satellite platforms for yield forecasting used in the literature; ii) ground-based platforms for yield forecasting used in the literature; iii) airborne/ UAS platforms for yield forecasting used in the literature. Source.[381].

Ground-based sensors were classified based on their functionalities and applications. Canopy sensors and analyzers constituted instruments for Chlorophyll Measurement (SPAD), Crop Health, and Nutrient Management (such as GreenSeeker, NTech Industries, Ukiah, CA, USA, and CropCircle, Holland Scientific Inc., Lincoln, NA, USA), in addition to Spectral Analysis and Canopy Analysis sensors (like Spectroradiometer, spectrometers, Li-Cor 2000 Plant Canopy Analyzer from Li-Cor, Lincoln, NE, USA). Among these sensors, local meteorological stations emerged as the most prevalent, being featured in 39 studies. Canopy sensors also saw frequent utilization. Conversely, thermal sensors and LiDAR/Laser scanner data were the least employed within the spectrum of ground-based sensor categories.

3.1.3 Trends in VIs and methods used

As indicated by the study's results (Figure 37), the NDVI emerges as the most prevalent vegetation index. This prominence is justified by its strong correlation with vital yield variables like above-ground biomass, crop height, and LAI [9,384]. NDVI's extensive documentation in literature contributes to its reliability in estimating crop health and productivity, pivotal for accurate yield predictions [385]. Following NDVI is the Enhanced Vegetation Index (EVI), an enhanced version addressing some limitations of NDVI, especially in regions with dense vegetation or atmospheric interferences. Additionally, LAI and GNDVI find substantial application in studies. Each index offers distinct advantages and serves specific research or monitoring objectives. Researchers, agronomists, and environmental scientists rely on these indices to scrutinize vegetation dynamics, evaluate crop health, monitor alterations in land cover, and make informed management decisions.

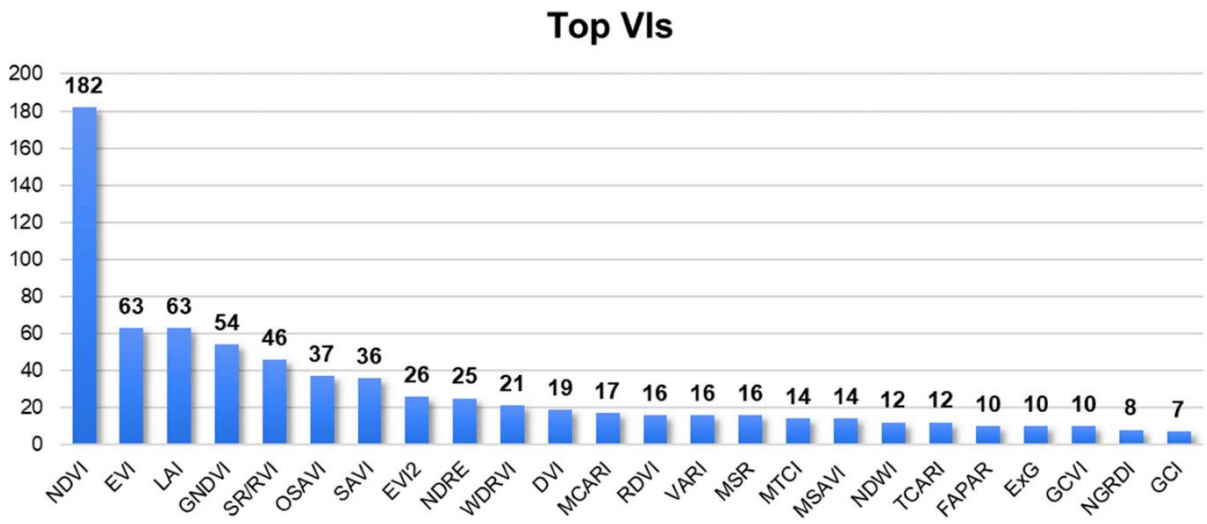

Figure 37. Most widely used VIs for crop yield prediction [381].

Analyzing remote sensing products for yield prediction involves various methodologies encompassing ML, DL, statistical, and model-based approaches. These methods leverage remote sensing data's power to estimate and accurately predict crop yields.

Based on the findings of this study (Figure 38), statistical analysis is the most prevalent method employed in the reviewed studies for crop yield prediction. ML and DL techniques are also widely utilized for yield estimation. In contrast, model-based approaches are less frequently used in these studies. Statistical analysis techniques often offer clear and interpretable relationships between variables, making them a popular choice for analyzing and understanding the impact of different factors on crop yields. On the other hand, machine learning and deep learning methods excel at capturing intricate patterns and relationships in large and high-dimensional datasets, which is particularly advantageous when dealing with remote sensing data. While model-based approaches are less common in this context, they provide valuable insights and predictions by simulating the entire crop growth process and its complex interactions with the environment from an ecological physiology perspective.

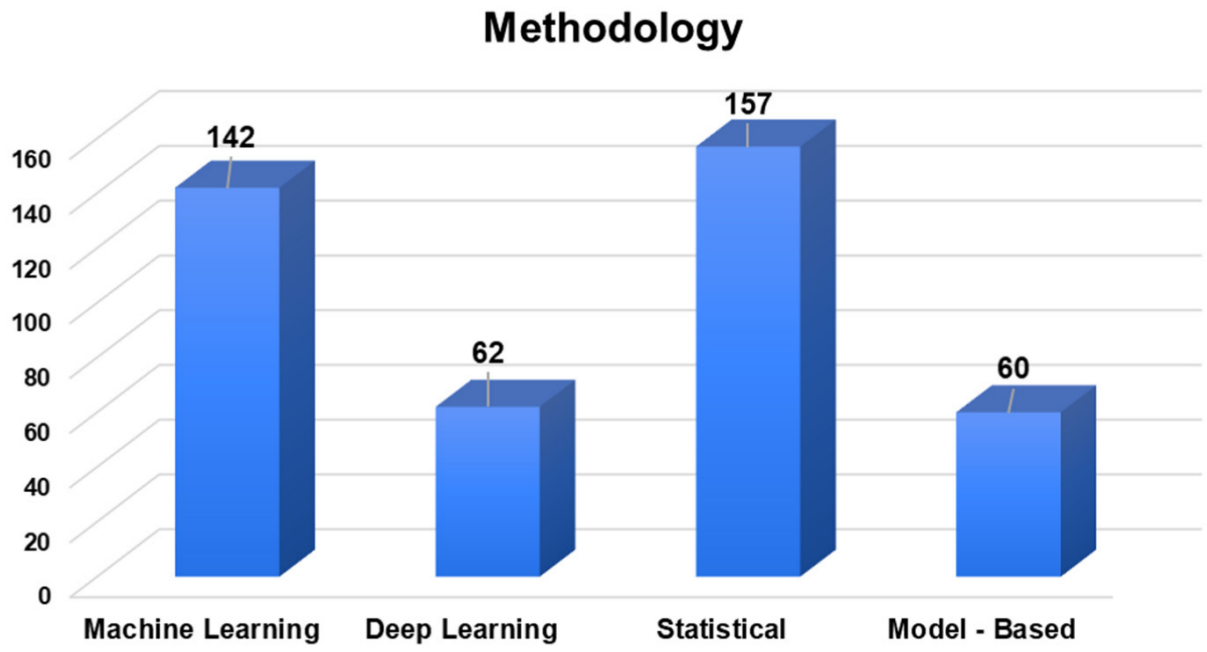

Figure 38. Overview of the methodological approach in the studies considered [381].

In essence, Statistical Analysis and Machine Learning methods stand out in crop yield estimation due to their adeptness in managing intricate nonlinear relationships within expansive datasets, encompassing known parametric structures and unobserved cross-sectional variations [386]. Additionally, the performance of Deep Learning methods may be inadequate due to the fact that they heavily rely on the quality of the extracted features [387]. Lastly, the limited adoption of model-based methods in crop yield prediction could be attributed to their substantial demands for data and computational resources, coupled with their comparatively lower flexibility when juxtaposed with other methodologies [388].

3.1.4 Accuracy Performance Per Crop Category

Assessing accuracy performance per crop category is crucial for understanding the effectiveness of different methods and platforms in estimating yields for specific crops, aiding in informed decision-making and optimizing agricultural practices. Consequently, the highest performance measures (R^2) obtained for each study were extracted and organized into tables based on crop categories. The following tables summarize crop-specific studies along with the methods and platforms used for yield prediction, as well as the corresponding R^2 values.

Table 12 summarizes the methods, platforms, and associated R^2 values for the sugar, beverage, and spice crop category. The results show that a combination of statistical and machine learning methods has been used for yield prediction. For sugarcane, these methods, coupled with satellite data, have provided R^2 values ranging from 0.53 to 0.94. For coriander and tea, statistical methods using satellite data yielded R^2 values between 0.68 and 0.87. In the case of coffee tree crops, statistical and model-based techniques with satellite data achieved R^2 values in the range of 0.64 to 0.93. R^2

Table 12. Reported method, platform, and R^2, for sugar, beverage, and spice crop category.

Crop	References	Method	Platform	R^2
Sugarcane	[389]	Statistical	Satellite × Proximal	0.53
	[390–393]	Statistical	Satellite	0.55 to 0.8
	[394], [395]	ML, Statistical	Satellite	0.87 to 0.94
	[396]	ML	Satellite	0.70
	[397]	Model based	Satellite	0.86
Coriander	[398]	Statistical	Satellite	0.81 to 0.87
Tea	[399]	ML	Satellite	0.68 to 0.71
Coffee Tree	[400]	Statistical, Model based	Satellite	0.64 to 0.69
	[401]	ML, Statistical	Satellite	0.88 to 0.93

In Table 13, the reported methods, platforms, and corresponding R^2 values for the Vegetables and Melons crop category are presented. These findings reveal a variety of methods applied for yield prediction in different vegetable crops. For Chinese cabbage and white radish, statistical methods using UAS platforms demonstrated R^2 values between 0.66 and 0.90. In the case of carrots, statistical methods with satellite data resulted in R^2 values ranging from 0.29 to 0.78. African eggplant, when studied with statistical methods in conjunction with UAS and proximal sensing, achieved R^2 values between 0.54 and 0.87. For table beet, a statistical approach using UAS data provided an R^2 of 0.89. For tomatoes, both processing and fresh fruits, a combination of statistical and machine learning methods with satellite and UAS platforms yielded R^2 values in the range of 0.69 to 0.90.

Table 13. Reported method, platform, and R^2 for the Vegetables and Melons crop category.

Crop	Reference	Method	Platform	R^2
Chinese Cabbage White Radish	[402]	Statistical	UAS	0.66 to 0.90
Carrot	[403]	Statistical	Satellite	0.29 to 0.78
African Eggplant	[404]	Statistical	UAS × Proximal	0.54 to 0.87
Table Beet	[405]	Statistical	UAS	0.89
Tomato	[350] *	Statistical	Satellite	0.69 to 0.81
	[406]*, [407], [408]	ML, Statistical	UAS	0.70 to 0.90

*** Processing Tomato**.

Table 14 summarizes the methods, platforms, and R^2 values for various oilseed crops. Notably, groundnut achieved an R^2 of 0.96 using a combination of machine learning and statistical methods with satellite and proximal data. Sunflower performed well with an R^2 of 0.90 using machine learning on satellite data. Olive tree and palm oil had high R^2 values of 0.97 and 0.82, respectively, using statistical and machine learning methods on UAS and satellite platforms. Canola yielded good results with R^2 values of 0.82 (UAS) and 0.86 (satellite) with statistical methods. Rapeseed showed promise with an R^2 of 0.86 using a combination of model-based and statistical approaches with satellite and proximal data. Soybean demonstrated a wide range of R^2 values from 0.49 to 0.98, depending on the method and platform chosen.

Table 14. Reported methods, platforms, and R^2 for the Oilseed Crop category.

Crop	References	Method	Platform	R^2
Groundnut	[351]	ML, Statistical	Satellite × Proximal	0.96
	[409]	ML/DL, Model based	Satellite × Proximal	0.68
Sunflower	[410]	ML	Satellite	0.90
	[398]	Statistical	Satellite	0.56
	[411]	ML/DL, Statistical	UAS	0.43
	[412]	Statistical	Satellite	0.91
Olive Tree	[413]	Statistical	UAS	0.97
Palm Oil	[414]	ML/DL	Satellite	0.82
Canola	[415]	Statistical	UAS	0.82
	[416]	Statistical	Satellite	0.86
Rapeseed	[417]	Statistical	UAS × Proximal	0.81
	[418]	Model based, Statistical	Satellite × Proximal	0.86
	[419]	Model based	Satellite × Proximal	0.82
	[412]	Statistical	Satellite	0.97
Soybean	[420], [421], [422]	ML/DL, Statistical	Satellite	0.87 to 0.90
	[412,423–429]	Statistical	Satellite	0.49 to 0.98
	[430], [431]	ML/DL	Satellite	0.85
	[432]	ML	Satellite	0.61
	[433], [434]	ML, Statistical	Satellite	0.86 to 0.90

	[435], [436]	ML/DL	UAS	0.72 to 0.66
	[352]	ML	UAS	0.89
	[437]	Statistical	UAS	0.74
	[438]	ML/DL	Satellite × Proximal	0.85
	[439]	ML, Statistical	Satellite × Proximal	0.82
	[440]	ML	UAS × Proximal	0.97
	[441]	ML/DL, Statistical	Satellite × Proximal	0.67

In the Fruits and Nuts category (

Table **15**), orchard yield estimation has predominantly been conducted using proximal sensing and UAS sensing, or a combination of both along with satellite data. Notably, multiple methods and platforms have been applied for vineyard yield prediction, with ML and DL approaches, demonstrating high performance, with an R^2 of 0.91 when using proximal data. Satellite and proximal data combinations also achieve strong results, with R^2 values ranging from 0.42 to 0.87.

Table 15. Reported methods, platforms, and R^2 for the Fruits and Nuts crop category.

Crop	References	Method	Platform	R^2
Vineyards	[203,442]	Statistical	Satellite × Proximal	0.42–0.87
	[443]	ML	Satellite × Proximal	0.79
	[444]	ML/DL	Proximal	0.91
	[445]	ML, Statistical	Proximal	0.86
Almond	[446]	Statistical	UAS	0.84
	[447]	ML/DL, Statistical	Satellite × UAS	0.71
Apple	[448]	ML/DL	UAS	0.88
Jujube	[436,449]	Model based	Satellite	0.62 to 0.78
Mango	[450]	ML/DL, Statistical	Satellite	0.77
	[451]	ML, Statistical	UAS	0.77

Table 16 offers a comprehensive overview of yield prediction methods, platforms, and associated R^2 values for a range of root tuber and other crops. Notably, for potato crops, the adoption of ML approaches, either with satellite or UAS data, demonstrates high performance, achieving R^2 values of up to 0.89. Cotton yield prediction, on the other hand, involves a spectrum of methods, including statistical, ML, and model-based approaches, often combining satellite, UAS, or proximal data sources. This results in a wide range of R^2 values from 0.52 to 0.97, highlighting the versatility and effectiveness of different techniques. Other crops like sweet potato, cassava tuber, ramie, milk thistle, and various grasses also display varying levels of accuracy, depending on the methodology and data source used.

Table 16. Reported methods, platforms, and R^2 for the Root tuber and other crops category.

Crop	References	Method	Platform	R^2
Potato	[452]	Statistical	Satellite	0.65
	[453]	ML, Statistical	Satellite	0.89
	[454]	ML	Satellite × Proximal	0.86
	[384]	ML	UAS	0.83
	[455]	ML, Statistical	Proximal	0.72

	[418]	Model based, Statistical	Satellite × Proximal	0.86
Cotton	[141,142]	Statistical	UAS	0.52 to 0.94
	[457]	ML/DL	UAS	0.85
	[458]	ML/DL, Statistical	Satellite	0.67
	[459]	Model based	Satellite × Proximal	0.96
	[460]	Statistical	UAS × Proximal	0.84
	[461]	ML	UAS × Proximal	0.93
	[462]	ML/DL, Statistical	UAS	0.97
	[463], [464]	ML, Statistical	UAS	0.77 to 0.91
Sweet Potato	[429]	Statistical	Satellite	0.68
Cassava Tuber	[465]	Statistical	UAS	0.87
Ramie	[466]	Statistical	UAS	0.66
Milk Thistle	[418]	Model based, Statistical	Satellite ×Proximal	0.86
Grassland *	[467]	ML	UAS	0.87
	[468]	Statistical	UAS	0.75
Perennial Ryegrass *	[469]	ML	UAS	0.93
Perennial Bioenergy Grass *	[470]	Statistical	Satellite	0.88
Brachiaria Pastures *	[471]	ML	Satellite × UAS	0.75
Miscanthus *	[472]	ML, Statistical, Model based	UAS	0.79

*** Grasses and other fodder crops.**

In the case of Leguminous crop category (Table 17), Alfa Alfa yield prediction benefits from statistical, ML, and DL methods, coupled with either satellite or UAS platforms, yielding R^2 values ranging from 0.64 to 0.94. Red Clover exhibits impressive R^2 values of 0.90, achieved through ML and DL techniques with UAS data. Chickpea yields are accurately estimated using ML methods combined with satellite and proximal data sources, achieving an R^2 value of 0.92. Additionally, Snap Bean and Peas show high predictive accuracy, especially with ML and DL methods using UAS data, attaining R^2 values of 0.98 and 0.95, respectively. Beans demonstrate the adaptability of statistical and ML techniques, whether with satellite or satellite-proximal data, resulting in R^2 values ranging from 0.54 to 0.84. Finally, Faba Bean benefits from a combination of ML and statistical methods with UAS data, achieving an R^2 value of 0.72. These findings underscore the significance of tailored approaches for different leguminous crops to enhance yield prediction accuracy.

Table 17. Reported methods, platforms, and R^2 for the Leguminous crop category.

Crop	References	Method	Platform	R^2
Alfa Alfa	[473], [474]	Statistical	Satellite	0.72 to 0.94
	[475]	ML/DL	UAS	0.87
	[476]	ML	UAS	0.84
	[477]	Statistical	UAS	0.64
	[478]	ML, Statistical	Satellite	0.93

Red Clover	[479]	ML/DL	UAS	0.90
Chickpea	[480]	ML	Satellite × Proximal	0.92
Snap Bean *	[481]	ML/DL	UAS	0.98
Peas	[473]	Statistical	Satellite	0.95
Beans *	[482]	Statistical	UAS × Proximal	0.70
	[483]	ML	Satellite	0.54
	[484]	Statistical	Satellite × Proximal	0.84
Faba Bean	[485]	ML, Statistical	UAS	0.72

*** Included in beans.**

The category of cereals encompasses a wide range of methods and platforms, prompting its separation into two tables: cereals (Table 18), and maize and wheat (Table 19). Table 18 shows that statistical methods with satellite data yield R^2 values in the range of 0.25 to 0.97 for Sorghum and Rice, demonstrating the efficacy of this approach. Barley exhibits R^2 values ranging from 0.70 to 0.93 when employing statistical methods with satellite data and data from multiple platforms. For Oats, the use of statistical and machine learning techniques, along with data from various sources, results in R^2 values of 0.68 to 0.929. Millet and Rice are also estimated using statistical and machine learning methods with satellite data, achieving R^2 values between 0.40 and 0.95. The application of model-based techniques and a combination of statistical, machine learning, and model-based methods contributes to successful yield predictions.

Table 18 Reported methods, platforms, and R2 for the cereal crop category.

Crop	Reference	Method	Platform	R^2
Cereal	[486], [487]	Statistical	Satellite	0.71
Barley	[416],[488], [473]	Statistical	Satellite	0.86 to 0.93
	[489]	Statistical	Satellite × UAS × Proximal	0.70
	[490],	Model based, Statistical	Satellite	0.6 to 0.77
	[492]	ML/DL	UAS × Proximal	0.93
	[493]	ML x Statistical	Satellite × Proximal	0.88
	[494]	ML, Statistical, Model based	Satellite	0.47
Oats	[489]	Statistical	Satellite × UAS × Proximal	0.79
	[492]	ML/DL	UAS × Proximal	0.929
	[495]	Statistical	Proximal	0.90
Millet	[429]	Statistical	Satellite	0.68
	[483]	ML	Satellite	0.40
Sorghum	[496], [474], [429]	Statistical	Satellite	0.25 to 0.81
	[497]	ML/DL	Satellite × Proximal	0.35
	[483]	ML	Satellite	0.44
Rice	[429,498–502]	Statistical	Satellite	0.56 to 0.97
	[503], [504], [505], [432]	ML	Satellite	0.43 to 0.95
	[506], [507]	Model based	Satellite	0.89 to 0.96
	[508]	ML, Model based	UAS × Proximal	0.75

	[509], [510]	ML/DL, Statistical	UAS × Proximal	0.22 0.51
	[511], [512]	ML, Statistical	UAS	0.76 to 0.8
	[513], [409]	ML/DL, Model based	Satellite × Proximal	0.75 to 0.86
	[514]	Statistical, Model based	Satellite	0.80
	[515]	ML/DL	Satellite	0.81
	[516]	ML/DL	UAS	0.84
	[517]	Statistical	UAS × Proximal	0.64
	[518]	ML, Statistical	UAS × Proximal	0.83
	[519]	ML, Statistical	Proximal	0.86
	[520]	Statistical, Model based	UAS	0.94
	[521], [522]	Statistical	Satellite × Proximal	0.66 to 0.90
	[523], [524], [525], [526]	Statistical	UAS	0.74 to 0.83

In the table focusing on wheat and maize (Table 19), it becomes evident that these crops have received special attention in the literature. The number of research papers dedicated to studying wheat and maize yield prediction is higher compared to other cereals, indicating their prominence in agricultural research. Moreover, the utilization of diverse approaches in predicting the yields of wheat and maize is also noteworthy.

Table 19. Reported methods, platforms, and R^2 for wheat and maize.

Crop	References	Method	Platform	R^2
Maize	[527]	Statistical	Satellite × Proximal	0.87
	[528]	Statistical	UAS ×Proximal	0.83
	[529]	Statistical	UAS	0.74
	[425–427,429,473,474,483,530–537]	Statistical	Satellite	0.46 to 0.99
	[538], [539]	Model based, ML/DL	Satellite	0.85
	[540], [541], [542], [543]	Model based	Satellite	0.68 to 0.83
	[544]	Model based	UAS × Proximal	0.855
	[545]	Model based	Proximal	0.68
	[410], [546], [547], [548], [549], [550], [432]	ML	Satellite	0.43 to 0.92
	[551]	ML, Statistical, Model based	Satellite	0.59
	[433], [552], [553]	ML, Statistical	Satellite	0.48 to 0.91
	[554], [438]	ML/DL	Satellite × Proximal	0.75 to 0.85
	[422], [555], [441], [421], [420], [556], [557]	ML/DL, Statistical	Satellite	0.70 to 0.92
	[558], [559], [560], [561]	ML/DL	UAS	0.57 to 0.93
	[562], [563]	ML, Statistical	Satellite × Proximal	0.35 to 0.98
	[564]	ML	Proximal	0.7

	[565]	Model based, ML	Satellite × Proximal	0.58
	[566]	Statistical, Model based	UAS	0.81
	[409]	ML/DL, Model based	Satellite × Proximal	0.75
	[567]	Statistical, Model based	Satellite	0.73
	[568]	ML, Model based	Satellite	0.76
	[569]	ML x Statistical	UAS	0.80
Wheat	[474], [488], [570], [533], [571], [572], [573], [416], [574], [473], [575], [425], [576], [398], [577], [578], [427]	Statistical	Satellite	0.37 to 0.99
	[579]	ML/DL, Model based	Satellite	0.83
	[580]	ML/DL	Satellite	0.75
	[555], [581]	ML/DL, Statistical	Satellite	0.72 to 0.78
	[490], [582], [583], [584], [585]	Model based, Statistical	Satellite	0.48 to 0.86
	[586], [587], [494]	ML, Model based	Satellite	0.55 to 0.75
	[433], [588], [589]	ML, Statistical	Satellite	0.72 to 0.89
	[548], [590], [591], [432], [592], [593]	ML	Satellite	0.51 to 0.99
	[594], [595], [596], [597], [598], [599], [600], [491], [601], [602], [603]	Model based	Satellite	0.49 to 0.86
	[604], [605], [606], [607], [608], [609]	ML/DL	Satellite	0.79 to 0.93
	[610], [611]	Model based, Statistical	Proximal	0.698 to 0.77
	[612],[613]	Statistical	Proximal	0.46 to 0.48
	[614], [615]	ML/DL	Proximal	0.83 to 0.891
	[616]	Model based	Proximal	0.84
	[617]	ML, Statistical	UAS	0.81
	[618],[619], [620]	ML/DL	UAS	0.62 to 0.85
	[621]	Statistical	UAS	0.70
	[622], [623], [624], [625], [626]	ML	UAS	0.62 to 0.93
	[627], [628], [629]	ML/DL, Statistical	UAS	0.59 to 0.84
	[630], [631], [632]	ML/DL, Statistical	UAS × Proximal	0.83 to 0.93
	[633], [492], [634]	Statistical	UAS × Proximal	0.73 to 0.929
	[635]	ML, Statistical	UAS × Proximal	0.78
	[493], [636]	ML, Statistical	Satellite × Proximal	0.83 to 0.88
	[637], [638]	ML/DL, Statistical	Satellite × Proximal	0.68 to 0.91

	Model based		
[639]	ML/DL, Statistical	Satellite × Proximal	0.50
[640], [641], [418], [642], [643]	Statistical, Model based	Satellite × Proximal	0.61 to 0.93
[644]	ML	Satellite × Proximal	0.89
[645], [646]	ML/DL	Satellite × Proximal	0.63 to 0.86
[647]	ML/DL, Statistical, Model based	Satellite × Proximal	0.77
[648]	Model based	Satellite × Proximal	0.49
[649], [650]	Statistical	Satellite × Proximal	0.55 to 0.76
[489]	Statistical	Satellite × UAS × Proximal	0.79

Both wheat and maize show a diverse range of techniques used for yield prediction. Statistical methods in conjunction with satellite, UAS, and proximal data provide R^2 values ranging from 0.37 to 0.99 for wheat, with similar statistics for maize in the range of 0.25 to 0.99. Model-based methods, machine learning, and deep learning techniques are also prevalent, further showcasing the variety of approaches utilized for yield estimation. The combination of satellite, proximal, and UAS data in different ways contributes to the overall accuracy, with R^2 values reaching 0.86 for wheat and 0.98 for maize in various studies. This table illustrates the complexity and diversity of methods and platforms employed to predict wheat and maize crop yields accurately.

3.2 Intercomparison of Proximal, UAS and Satellite Remote Sensing Platforms

Over the initial two years of the study, an investigation was undertaken across ten distinct fields (eight in the first year and two in the second year) at field level scale. These designated areas functioned as reference fields, facilitating the comparison of NDVI datasets derived from proximal, UAS and Satellite imagery. The analysis conducted at the level of 10x10 meters.

3.2.1 Descriptive Statistics

The summary statistics derived from the UAS (Table 20) and Sentinel (Table 21) NDVI dataset provide valuable information about the overall condition and diversity of vegetation in a total of ten distinct fields during the 2020 and 2021 seasons.

The mean NDVI values serve as a measure of the average vegetation health within each field. According to the results of descriptive statistics for the NDVI derived from UAS dataset (Table 20), the fields F20_1, F20_6, F20_3, and F21_2 stand out with the highest mean NDVI values (0.76 and 0.81), signifying relatively healthy vegetation conditions. Conversely, fields F20_7 and F20_8 exhibit the lowest mean NDVI values, suggesting the presence of less healthy or sparse vegetation. The standard error for all fields is remarkably low (around 0.01), indicating a high level of accuracy and reliability in the mean NDVI estimations. The median values provide a measure of the central tendency, with F20_1 having the highest median NDVI (0.82) and F20_7 the lowest (0.70).

Standard deviation measures the spread or variability in NDVI values. Fields F20_4 and F20_5 show the highest standard deviations, indicating a broader range of NDVI values and greater

variability in vegetation health. This variability is further exemplified by the sample variance, which is higher in these fields. Positive kurtosis in F20_2 suggests a distribution with a peak, while negative kurtosis in F20_7 and F20_8 points to flatter distributions. Negative skewness in most fields signifies a left-skewed distribution with a longer tail on the left side, indicating an abundance of lower NDVI values. The range between minimum and maximum NDVI values ranging from 0.11 to 0.93, indicating a broad spectrum of vegetation health throughout each season. Notably, the Field F20_7 boasts the lowest minimum NDVI (0.11), possibly indicating regions with very sparse or stressed vegetation. In contrast, F20_1 presents the highest maximum NDVI (0.89), highlighting areas with exceptionally healthy vegetation.

Table 20. Descriptive statistics for the NDVI derived from UAS dataset for the 2020 and 2021 seasons.

Field	Mean	St. Error	Median	Stand. Dev.	Sample Var.	Kurt.	Skew.	Range	Min.	Max.	Count
					2020						
F20_1	0.76	0.00	0.82	0.14	0.02	1.85	-1.77	0.69	0.20	0.89	1643
F20_2	0.74	0.00	0.76	0.08	0.01	5.54	-1.84	0.57	0.28	0.86	676
F20_3	0.77	0.00	0.78	0.08	0.01	1.00	-1.28	0.38	0.50	0.88	1035
F20_4	0.67	0.01	0.79	0.22	0.05	-0.44	-1.06	0.69	0.17	0.86	1164
F20_5	0.67	0.00	0.73	0.16	0.03	0.92	-1.30	0.75	0.11	0.86	3120
F20_6	0.77	0.00	0.84	0.16	0.02	0.60	-1.39	0.72	0.20	0.91	1446
F20_7	0.59	0.01	0.70	0.20	0.04	-0.39	-0.99	0.71	0.11	0.82	1710
F20_8	0.62	0.01	0.70	0.19	0.03	-1.11	-0.62	0.67	0.21	0.89	775
					2021						
F21_1	0.62	0.00	0.72	0.18	0.03	-0.32	-1.08	0.68	0.15	0.83	1460
F21_2	0.81	0.00	0.89	0.15	0.02	0.94	-1.44	0.70	0.24	0.93	1312

The satellite NDVI dataset reveals insights into vegetation health and variability across ten fields. F21_2 stands out with remarkably healthy vegetation (mean NDVI 0.77), while F20_7 shows less healthy vegetation (mean NDVI 0.56). F20_4 and F20_5 exhibit diverse vegetation conditions with high standard deviations, while F20_2 and F20_3 demonstrate more consistent health. Field F20_2 has a peaked distribution, while F20_7 shows a skewed distribution toward higher NDVI values. The range of NDVI values varies, with F20_5 and F21_2 having the widest range (0.73). F21_2 features the highest maximum NDVI (0.93), and F20_5 exhibits the lowest minimum (0.14), suggesting sparse or stressed vegetation. Higher variance values in F20_5 and F21_2 indicate greater variability in vegetation health.

Table 21. Descriptive statistics for the NDVI derived from Sentinel dataset for the 2020 and 2021 seasons.

Sentinel	Mean	St. Error	Median	Stand. Dev.	Sample Var.	Kurt.	Skew.	Range	Min.	Max.	Count
2020											
F20_1	0.71	0.00	0.75	0.14	0.02	0.14	-1.16	0.58	0.28	0.86	1643
F20_2	0.71	0.01	0.77	0.13	0.02	2.63	-1.69	0.68	0.18	0.86	676
F20_3	0.75	0.00	0.78	0.11	0.01	-0.73	-0.64	0.51	0.38	0.89	1035
F20_4	0.67	0.01	0.81	0.23	0.05	-0.67	-0.96	0.68	0.20	0.89	1164
F20_5	0.61	0.00	0.67	0.20	0.04	-0.61	-0.79	0.73	0.14	0.87	3120
F20_6	0.77	0.00	0.83	0.15	0.02	0.57	-1.39	0.66	0.25	0.91	1446
F20_7	0.56	0.01	0.66	0.22	0.05	-1.19	-0.55	0.67	0.16	0.83	1710
F20_8	0.62	0.01	0.67	0.16	0.03	-1.15	-0.43	0.58	0.29	0.87	775
2021											
F21_1	0.65	0.00	0.72	0.14	0.02	0.02	-1.12	0.61	0.26	0.87	1460
F21_2	0.77	0.01	0.86	0.18	0.03	0.31	-1.31	0.73	0.20	0.93	1312

The results of the descriptive statistics noteworthy resemblance in average NDVI values when comparing these two remote sensing techniques—UAS and Sentinel-2. In the majority of cases, the UAS multispectral data produces higher mean NDVI values, probably due to superior spatial resolution.

3.2.1 Regression Analysis

Below the Figure 39 presents the relationship between the UAS and satellite datasets for all the fields encompassing all the associated measurements recorded on multiple dates. The spectrum of R^2 values spans from 0.98 to 0.99, signifying a robust and substantial correlation between the measurements. This high degree of correlation underscores the consistency and reliability of the relationship between the two datasets, affirming their close alignment across various data points and dates. The intercept is omitted, as both datasets are expected to have a natural zero baseline when there is no vegetation.

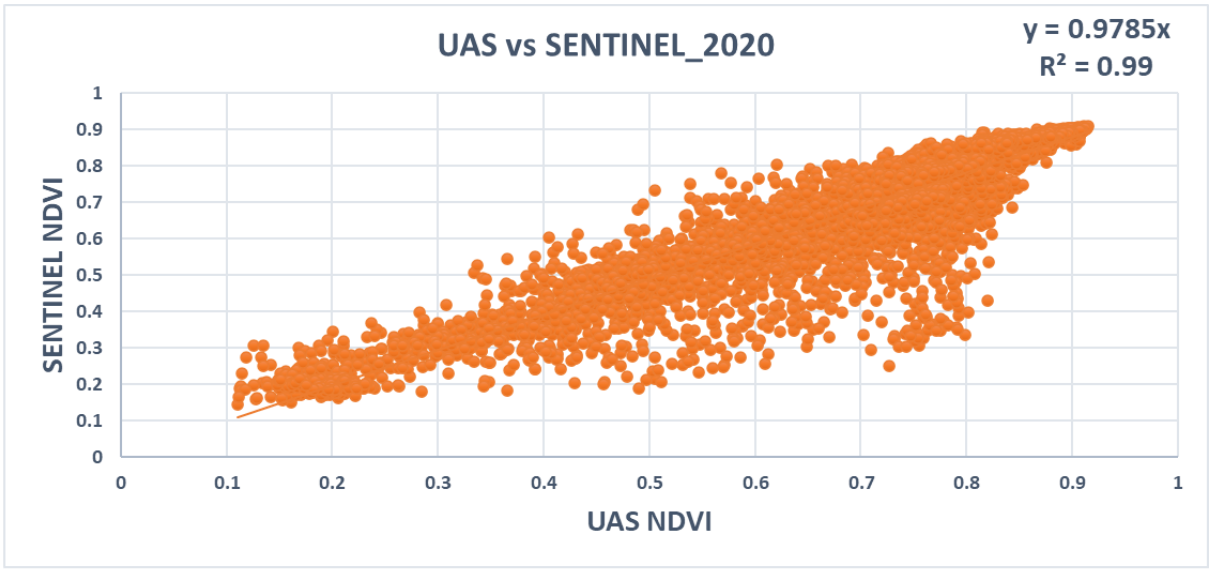

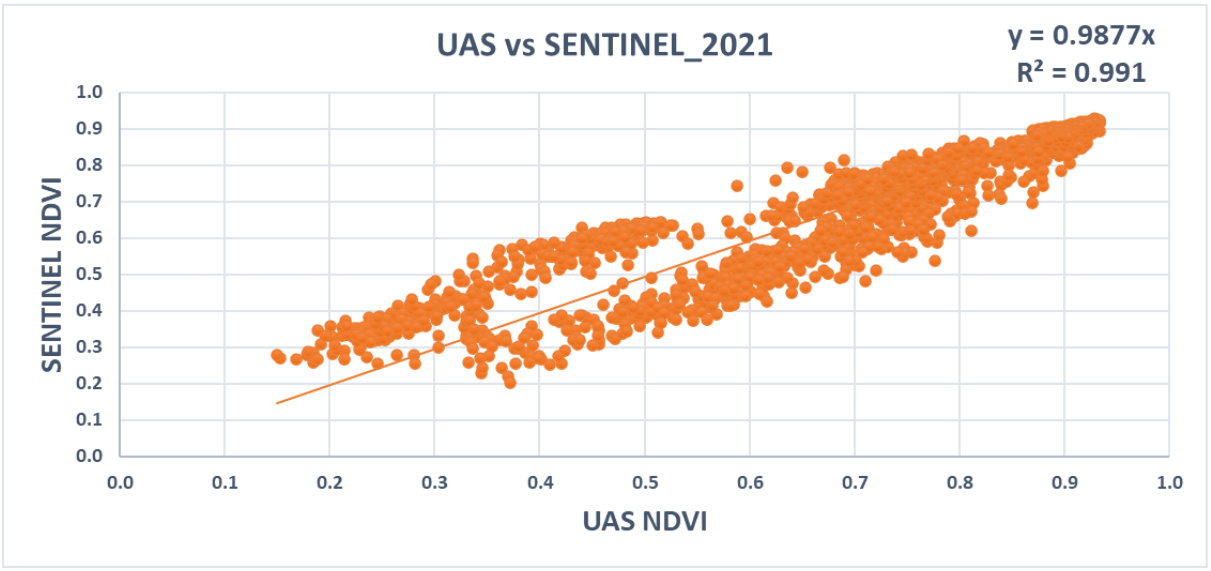

Figure 39. Regressive plots depicting the UAS and satellite NDVI datasets for the 2020 and 2021 seasons.

Below the

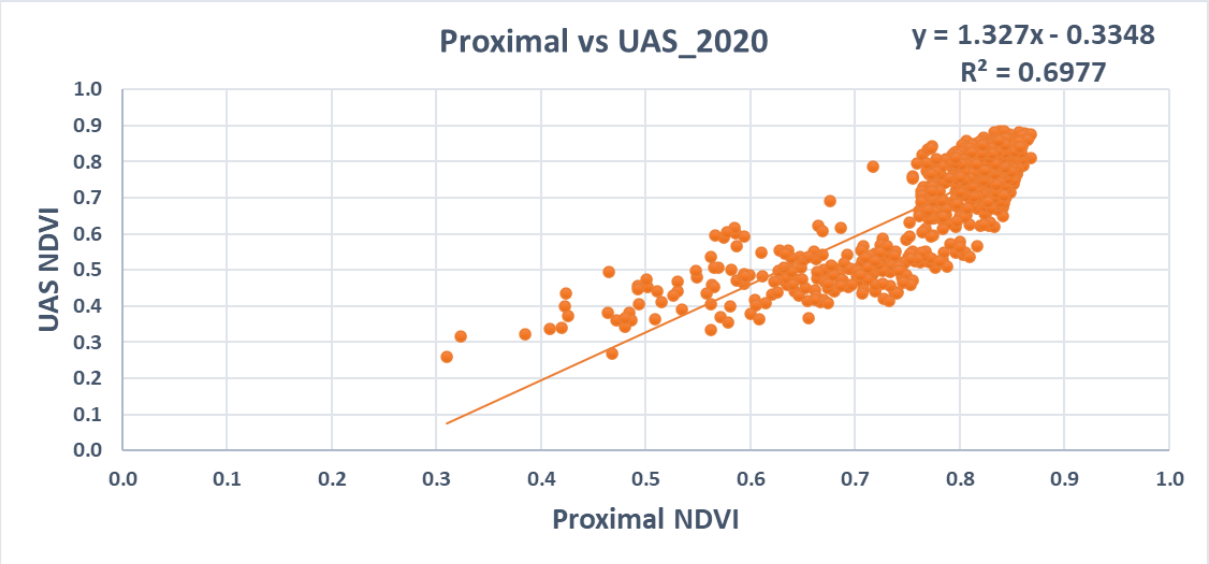

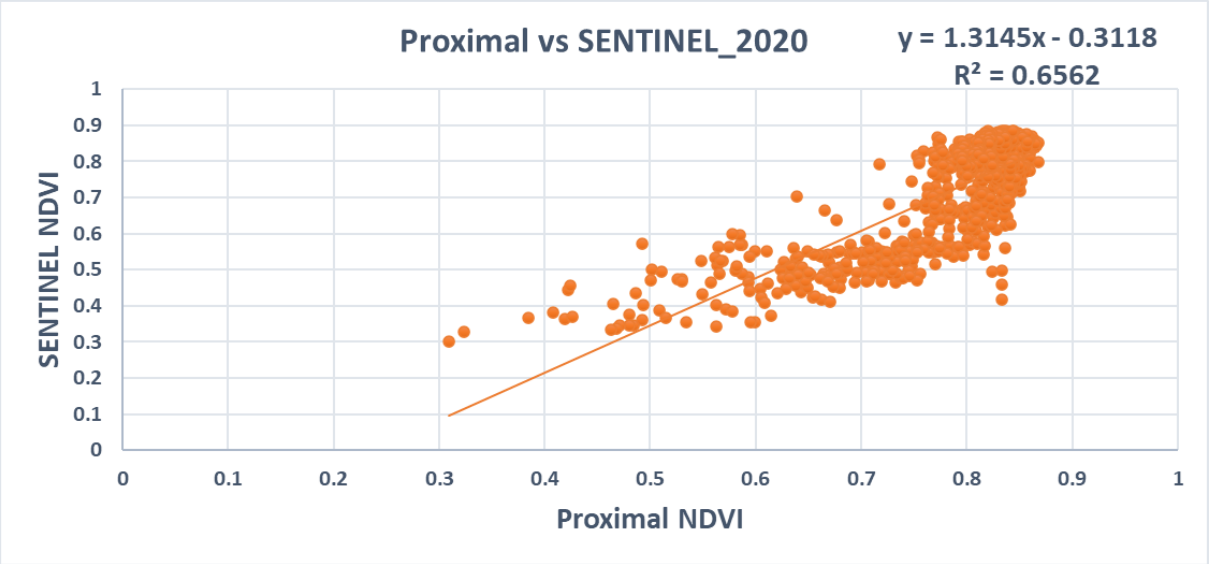

Figure 40 and Figure 41**Figure 39** present the relationship between the proximal, UAS and satellite datasets for all the fields encompassing all the associated measurements recorded on multiple dates. The spectrum of R^2 values spans from 0.66 to 0.70, signifying a moderate correlation between the measurements. This substantial correlation highlights the robust and dependable nature of the connection between the two datasets, confirming their close alignment across a diverse array of data points and temporal observations.

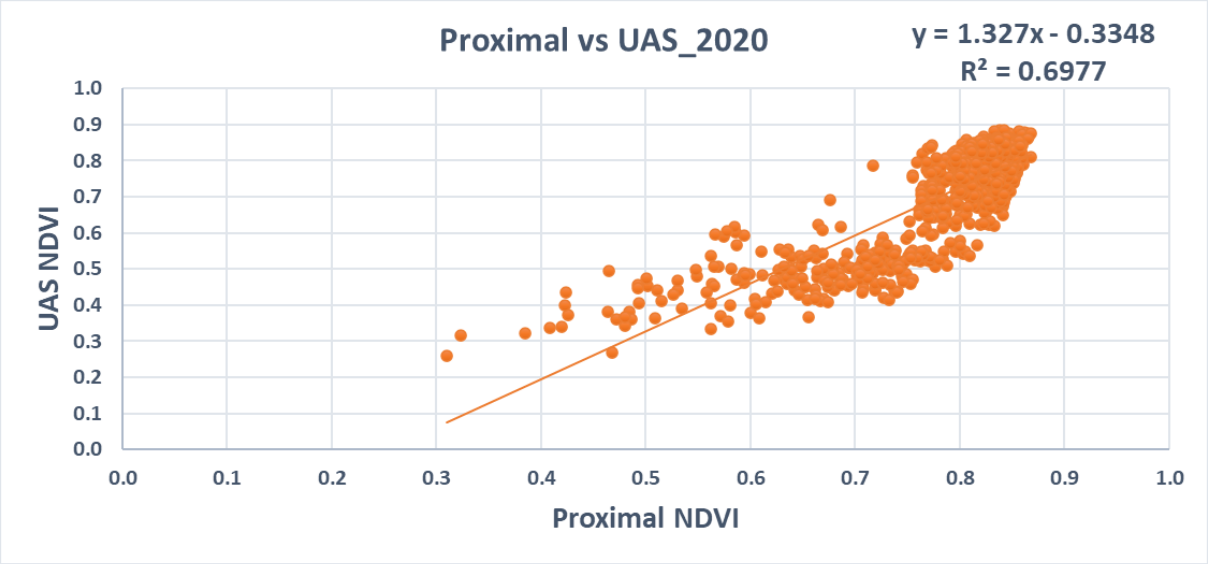

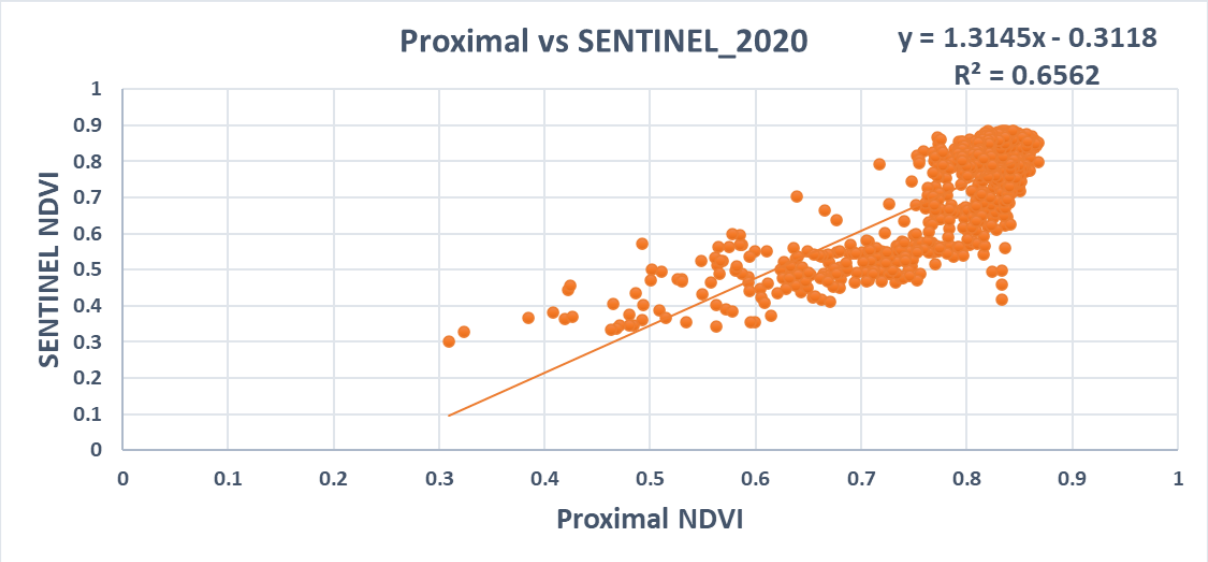

Figure 40 Regressive plots depicting the proximal, UAS, and Satellite NDVI datasets for the 2020 season.

Unlike the UAS and Sentinel datasets. the intercept was retained in the analysis, as it significantly deviated from zero. This outcome is expected, considering that the proximal sensor primarily concentrates on monitoring vegetation growth exclusively. In contrast, the UAS and Sentinel sensors encompass the influence of soil reflectance and atmospheric conditions in their measurements. Consequently, this discrepancy justifies the observation that proximal sensor values commence at approximately 0.3 and do not dip lower in comparison to the values of the UAS and Sentinel datasets.

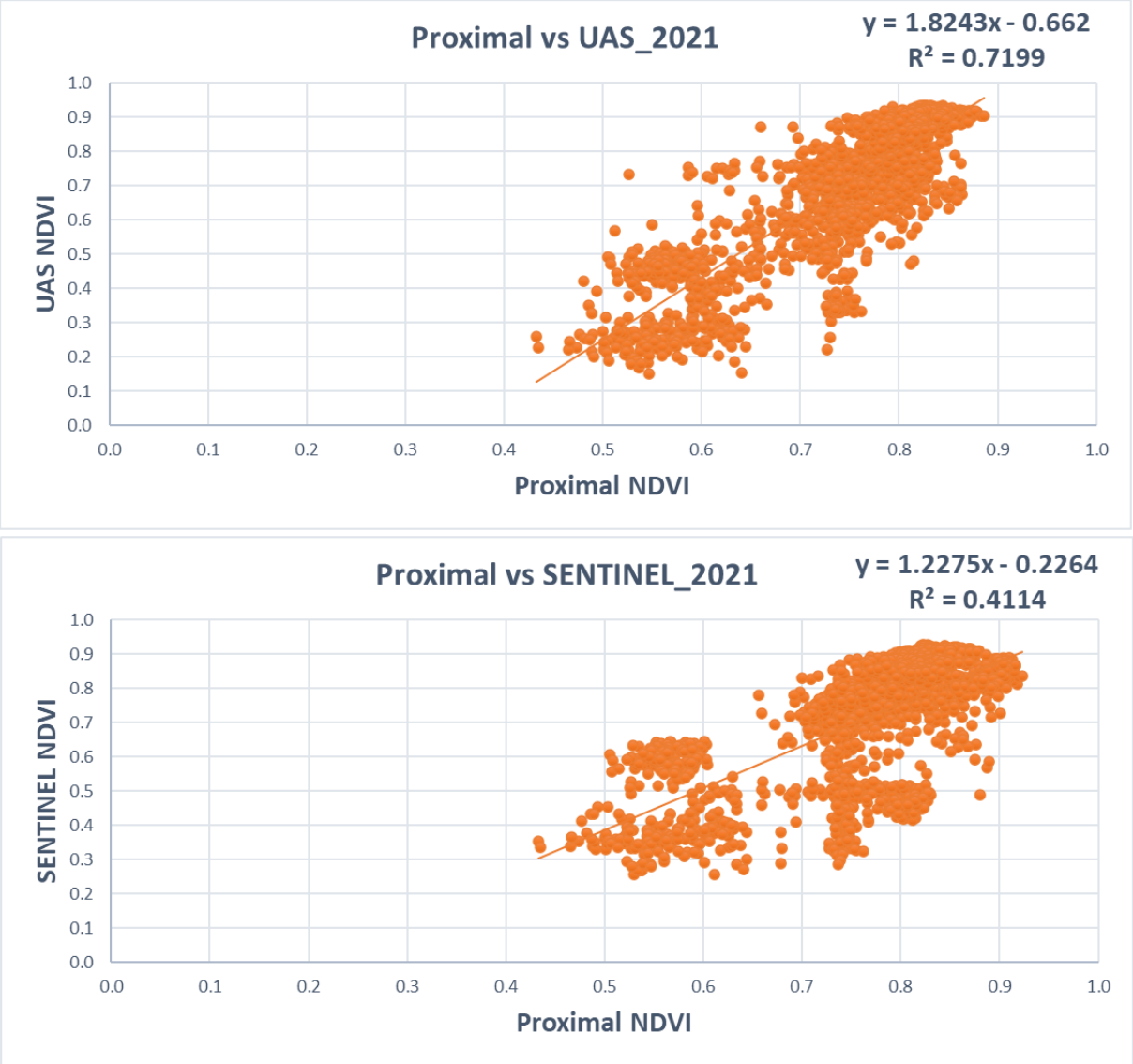

Figure 41. Regressive plots depicting the proximal, UAS, and satellite NDVI datasets for the 2021 season.

Given the robust correlation between UAS and Sentinel NDVI datasets, individual plots per field are presented below (Figure 42). These plots depict the regression relationships between UAS and Satellite NDVI datasets for each specific field in the year 2020.

Figure 42. Regression plots of UAS and Satellite NDVI datasets by field in 2020.

Figure 43 illustrate the relationship between the UAS and satellite datasets across the two fields for 2021 season.

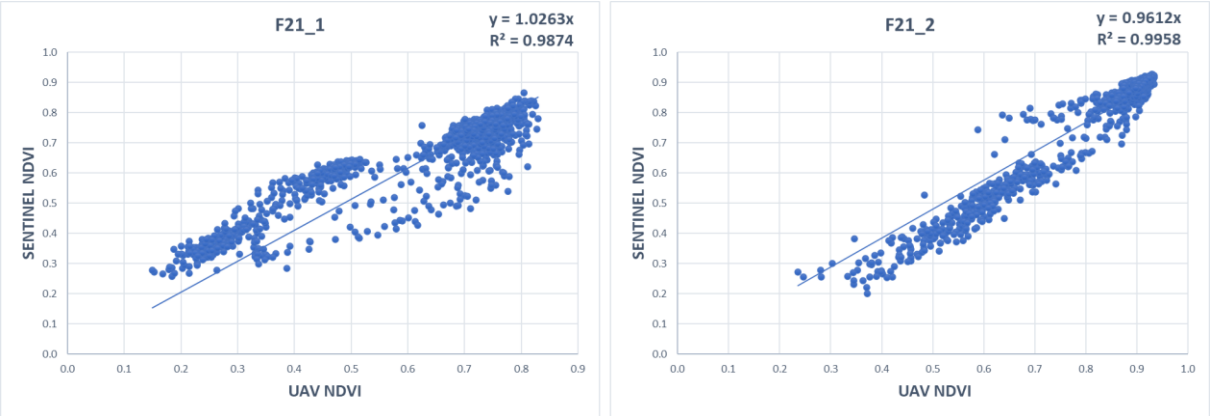

Figure 43. Regression plots of UAS and Satellite NDVI datasets by field in 2021.

The figure below (Figure 44)presents the correlation between the UAS and satellite datasets for one specific field per growth stage depicts the correlation between the UAS and satellite datasets for one specific field at each growth stage. Notably, the values show a linear progression from the canopy growth stage, with a steady increase observed until reaching maturity. This linear trend highlights the evolving relationship between the datasets as the crop grows and matures.

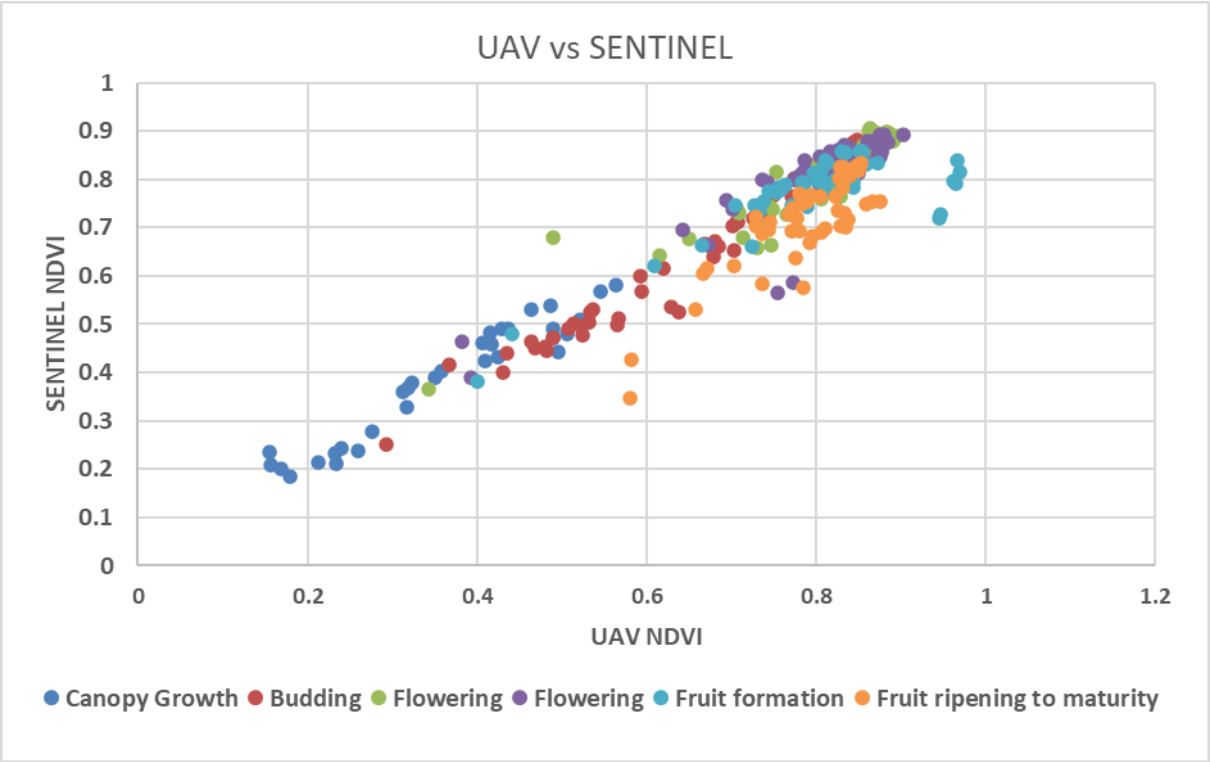

Figure 44 An example of correlation between the UAS and satellite datasets for one specific field per growth stage

Overall, the values of R^2 ranged from 0.97 to 0.99, providing robust confirmation of Sentinel-2's effectiveness in characterizing vegetation and evaluating plant health, with values similar to UAS data concerning the NDVI trends (R^2). This was apparent to the analysis conducted by field but also to the total datasets of each season. This consistency was evident not only in the field-specific analysis but also across the complete datasets for each season. Furthermore, both datasets exhibit a clear and linear increase in their values per growth stage.

3.3 Phenological stages of the processing tomato crop

A noteworthy byproduct of this study was the establishment of a connection between the phenological stages of the processing tomato crop and the corresponding VI values. This linkage offers valuable insights into the plant's growth and development throughout its various growth stages, enhancing our understanding of the crop's behavior in relation to remote sensing data.

3.3.1 Field level approach

In the second year, NDVI values were continuously recorded throughout the growing season for the two respective fields included in the study, relying on satellite time series data. Each of the fields under investigation was planted with three different varieties of processing tomatoes. The provided figures illustrate the yearly patterns of NDVI for these two fields. Even though all three tomato varieties were initially planted in the same field, Figure 45 reveals variations in the vigor curves of these varieties. Specifically, the Dexter variety exhibits rapid growth, and the decline in its curve after 100 days signifies the timing of its harvest. Conversely, the other varieties continue to grow, with a noticeable downward trend beyond 110 days.

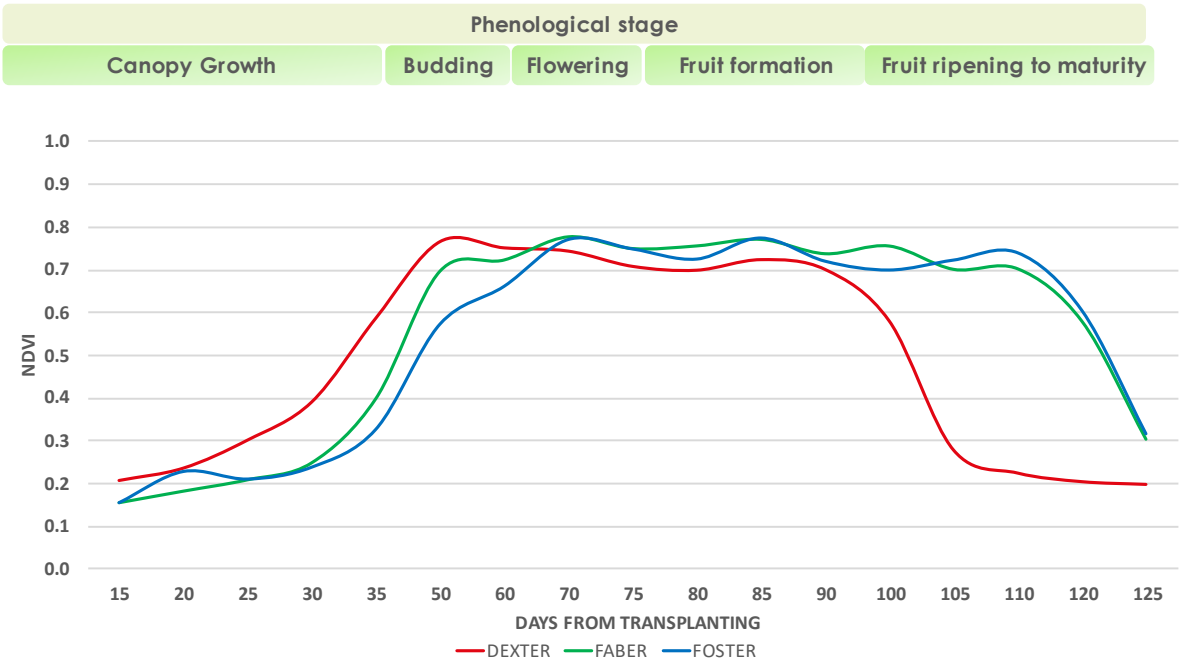

Figure 45: F21_1: NDVI dynamics curves for varieties i) Dexter (red), ii) Faber (green) and iii) Foster (blue),

In the context of Figure 46, depicting the second field, the robustness curves of the different varieties also show disparities within the initial 95 days. Notably, the Dexter variety displays a quicker growth rate, and the drop in its curve marks the culmination of the growing season.

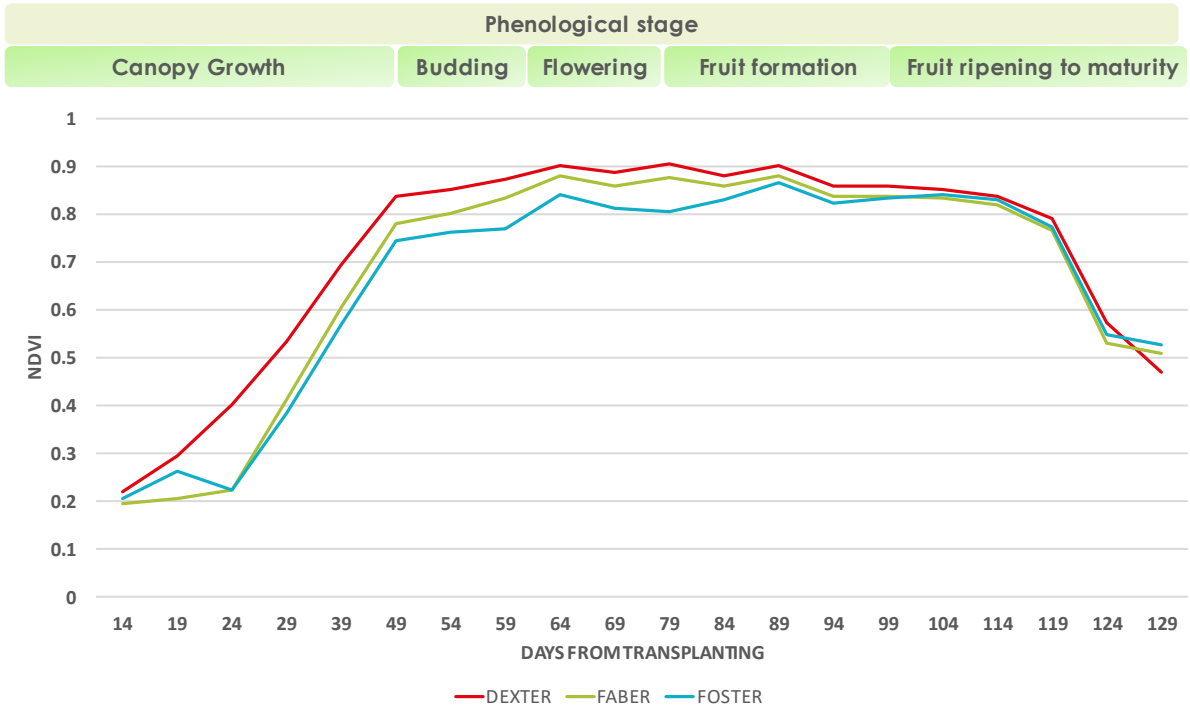

Figure 46: F21_2: NDVI curves for varieties i) Dexter (red), ii) Faber (green) and iii) Foster (blue),

Through an examination of NDVI values and mean values of multiple VIs, the study depicted the progressive growth of the crop, with peaks in VI values observed at specific growth stages. The examination of different tomato varieties also revealed variations in growth patterns, emphasizing the potential for tailored crop management.

3.3.2 Regional Approach

Based on the reported NDVI values, Figure 47 shows the NDVI dynamics and the corresponding phenological stages of the crop. During the second year of the study (2021), it was found that the highest NDVI values were recorded 75 to 80 days after transplanting. Early on, during the initial stages, the NDVI values were notably low, which aligns with expectations, especially in row crops where the remotely sensed images prominently displayed visible soil. The phase of full canopy cover and flowering was recorded in June, occurring approximately 60–75 days after transplanting, while the phase of tomato formation took place in July, contingent upon the transplanting date. These findings align with a previous study [412], which conducted phenological monitoring using NDVI values derived from Sentinel-2 imagery over the period spanning from 2016 to 2021.

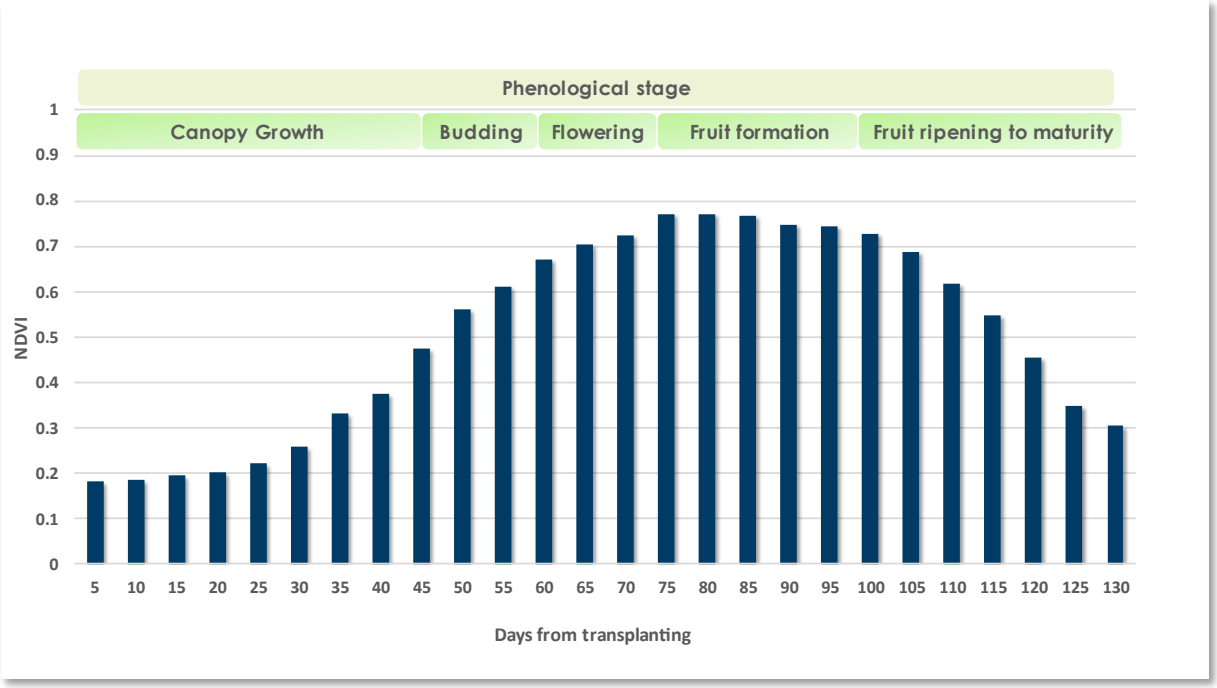

Figure 47. Annual NDVI dynamics and the respective phenological stages of the processing tomato crop.

Not surprisingly, based on the mean values of all five VIs (NDVI, PVI, WDVI, SAVI, and RVI), progressive canopy growth is observed (Figure 48).

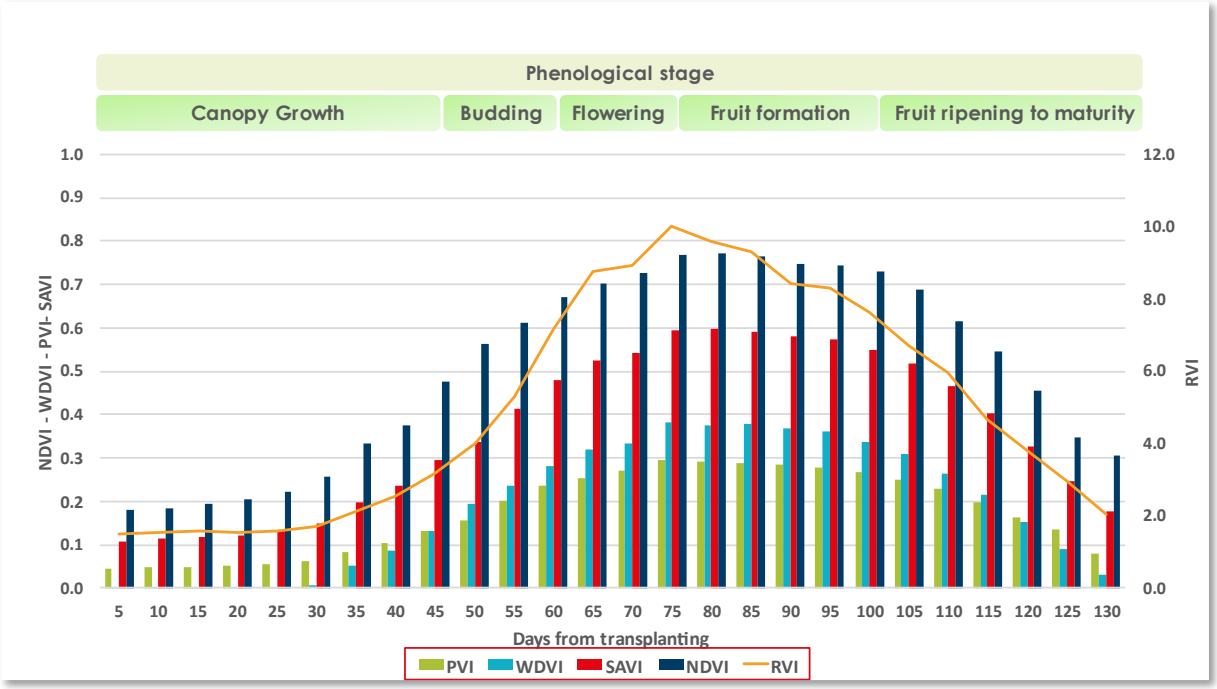

Figure 48. The mean values of the five VIs: (a) PVI (green); (b) WDVI (light blue); (c) SAVI (red); (d) NDVI (blue); (e) RVI (orange), which has different range of values and is incorporated in the secondary axes.

In the early stages, the influence of soil is strong due to the low canopy cover. There seems to be a positive trend that peaks at 80 days and is negative in the last stages of the crop.

3.4 Predicting yields

3.4.1 Field - Level yield predictions

During the first year, the following table (Table 22) demonstrates a positive and strengthening relationship between NDVI data from UAS and Sentinel platforms as plant growth progresses. The Pearson correlation coefficient (r) and R^2 values reveal the strength of the relationship between NDVI datasets and yield by plant growth stages. In the year 2020, the Pearson coefficient values for NDVI data from both UAS and Sentinel platforms ranged from 0.51 to 0.75, suggesting a moderately positive correlation with crop yield. The strongest correlation was observed during the flowering stage, with Pearson coefficient values of 0.67 for UAS and 0.75 for Sentinel. These results indicate that NDVI data from both platforms were positively associated with crop yield during this year, particularly during the flowering stage.

The R^2 values, which represent the goodness of fit, follow a similar pattern. The R^2 values ranged from 0.20 to 0.57, indicating that NDVI data explained a substantial portion of the variance in crop yield during various growth stages. The highest R-squared value was observed during the flowering stage for both UAS (0.45) and Sentinel (0.57). This suggests that NDVI data from both platforms had a considerable impact on explaining the variation in crop yield during this growth stage in 2020.

Table 22 Relationship between NDVI data from UAS and Sentinel platforms to yield samples.

Metrics	Canopy Growth	Budding	Flowering	Flowering	Fruit formation	Fruit ripening to maturity
NDVI UAS 2020						
Pearson (r)	0.54	0.59	0.67	0.72	0.65	0.65
R^2	0.29	0.35	0.45	0.52	0.42	0.43
NDVI Sentinel 2020						
Pearson (r)	0.51	0.62	0.75	0.74	0.73	0.44
R^2	0.26	0.38	0.57	0.54	0.53	0.20
NDVI Proximal 2020						
Pearson (r)	0.59	-	0.54	-	0.73	-
R^2	0.34	-	0.30	-	0.53	-

Overall, Table 22 illustrates that NDVI data from both UAS and Sentinel platforms were positively correlated with crop yield in 2020, with the strongest correlations occurring during the flowering stage. Additionally, these NDVI datasets explained a significant proportion of the variance in crop yield, particularly during the flowering stage.

To estimate the total yield of each field for 2021 the yield sample values were upscaled based on the average plant per hectare. The Figure 49 shows the results for the season 2021, indicating variations between the predicted (based on yield sampling) and the actual yield values. The accuracy of the predictions varies across different instances, with some close matches, slight underestimations, and a few overestimations.

Specifically, in the fields F20_2 and F20_5, the predicted yield fell notably short of the actual yield, with a difference of approximately 17 tons per hectare. In contrast, in the cases of F20_1 and F20_7, the predicted yield slightly surpassed the actual yield by roughly 7 tons per hectare, suggesting a minor overestimation. Further analysis and refinement of the predictive model may be necessary to improve its accuracy for these yield predictions.

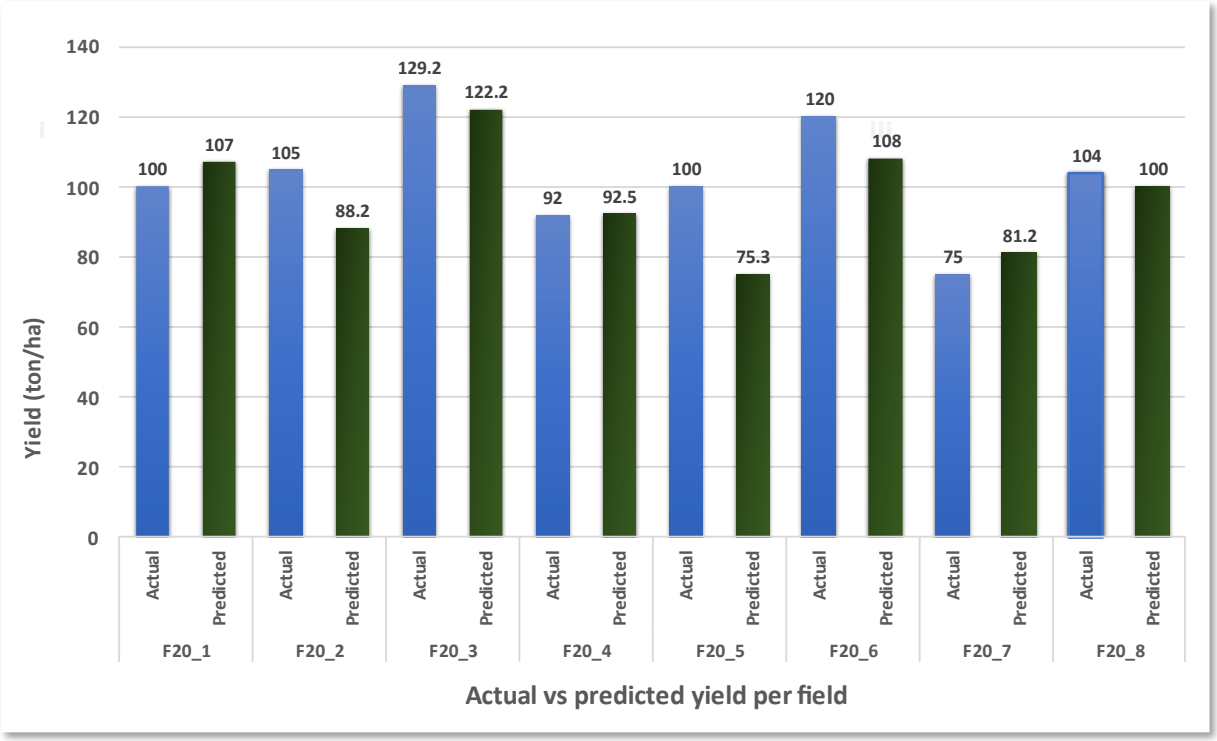

Figure 49. Comparison of Actual vs. Predicted Crop Yields for the 2020 growing season

In the following year (2021), the correlation between crop yield samples and NDVI datasets from both platforms exhibited a consistently weak relationship, and these correlations were not found to be statistically significant. The absence of statistical significance reinforces the notion that the observed correlations were not substantial enough to draw meaningful conclusions regarding the influence of NDVI on crop yield during that specific year.

To address the challenge posed by manual yield estimation, a process known for its time and cost intensity and susceptibility to human errors, this research recognized the need to create a comprehensive and farm-scale crop yield production dataset for the same year. Such a dataset could serve as a precise ground-truth reference for farm-scale yield predictions. This is particularly crucial, considering the existing scientific evidence [651–653], that highlights the value of satellite data in predicting regional-scale yield production. Additionally, the research capitalized on the knowledge of the robust correlation between UAS and satellite values, further enhancing the dataset's reliability. As part of this initiative, accurate field boundaries from 108 fields were deployed to retrieve actual yield values. These carefully curated ground-truth data were then used to conduct a rigorous analysis of satellite imagery, strengthening the overall accuracy of the study's findings.

3.4.1 Regional - Level yield predictions

An initial statistical analysis was conducted, estimating the Pearson coefficient (r) between yield and satellite derived NDVI mean values for 108 fields. This analysis involved the extraction of five VIs, collected at five-day intervals using satellite imagery (Table 23).

Table 23. The Pearson coefficient representing the relationships between the derived VIs and the yield for 2021 season.

VI	Pearson Coefficient			
	80 Days	85 Days	90 Days	95 Days
NDVI	0.68 *	**0.72** *	0.70 *	0.63 *
RVI	0.72 *	0.70 *	**0.75** *	0.56 *
SAVI	0.68 *	0.69 *	**0.74** *	0.65 *
PVI	0.67 *	0.64 *	**0.72** *	0.68 *
WDVI	0.58 *	0.65 *	**0.73** *	0.69 *

*** Correlation is significant at the 0.05 level.**

The analysis revealed that the highest values of Pearson coefficient, indicating stronger correlations, were observed towards the end of the growing season. This suggest that the relationship between the derived VIs and crop yield became more pronounced and significant as the crop matured. Notably, NDVI, RVI, SAVI, and PVI exhibited moderate to strong positive correlations with yield, with coefficients ranging from 0.63 to 0.75, making them potentially valuable for yield prediction. The NDVI peaked at 85 days post-transplanting, while the other vegetation indices reached their highest points at 90 days, with RVI taking the lead. While WDVI showed slightly lower correlations compared to the other indices, it remained positively related to yield, with coefficients ranging from 0.58 to 0.73. This implies that WDVI, although having slightly weaker correlations, may still provide meaningful insights into yield prediction.

Towards improving yield estimations, the next phase involved investigating the predictive capabilities of various VIs and growth stages through machine learning methods. Using AutoML, several combinations of sensors and growth stages per year were investigated to evaluate their performance in assessing processing tomato yield.

Figure 50 presents the progression of adjusted R^2 over the growing season. All indices show the best results in the 80–90-day period, aligning with the results reported in Table 23. Although NDVI demonstrated generally lower performance, it reached its predictive peak at 85 days post-transplanting. RVI displayed the most robust predictive performance especially at 90 post-transplanting; however, its effectiveness diminished more rapidly after reaching its peak compared to the other VIs. On the contrary, PVI and WDVI exhibited inferior performance when contrasted with SAVI and RVI.

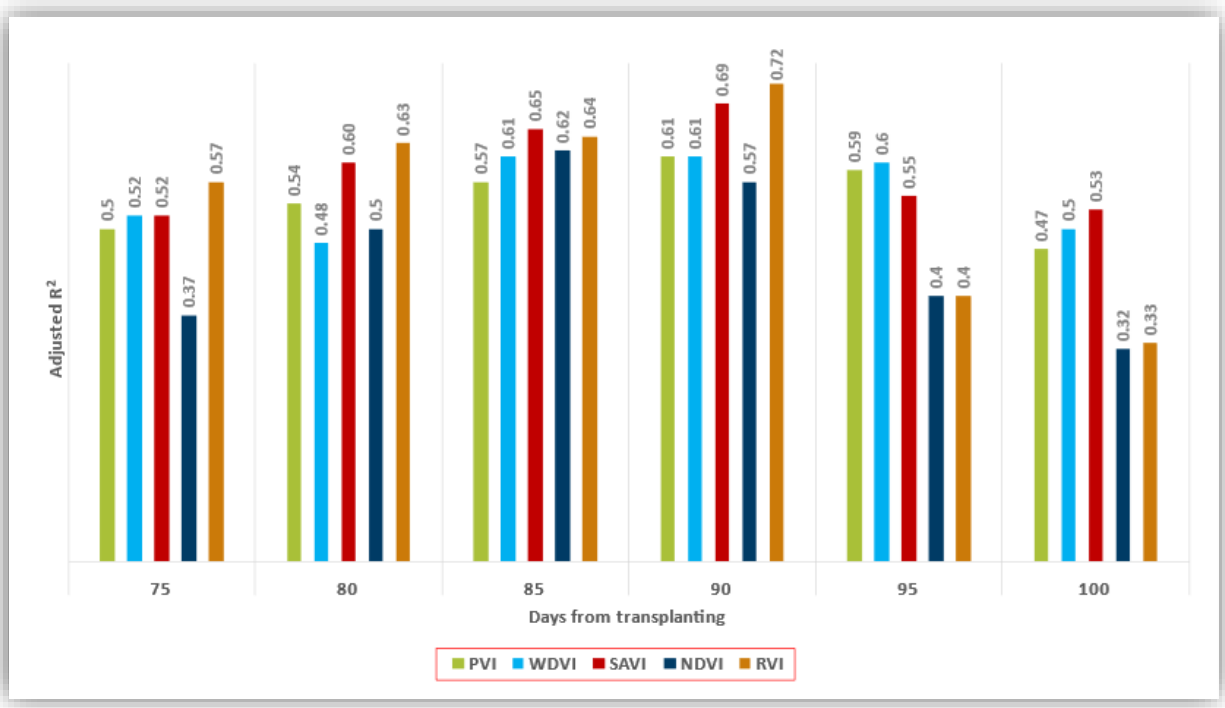

Figure 50 R² progress along the growth period for each of the VIs for the 2021 growing season.

For the AutoML experiment, the adjusted R² and RMSE were used to evaluate the predictive accuracy and determine the performance of the models for the best VI and period. In addition, a fivefold cross-validation was performed for each regression model to check its generalization ability and ensure its robustness. The experiments were also repeated 10 times to ensure that the final results were as accurate as possible. Table 24 shows that the best yield predictions were made by RVI and SAVI. Specifically, these two indices reached an average R² of 0.72 ± 0.02 and 0.69 ± 0.03, respectively, 90 days after transplanting. Moreover, their RMSEs were also the lowest (1.03 ± 0.03 and 1.06 ± 0.04, respectively). The remaining VIs (NDVI, WDVI, and PVI) are also among the regression models with the best performance. However, they all show a large difference relative to RVI and SAVI. Another observation from Table 24 is that the best result was achieved 90 and 85 days after transplanting.

Table 24 The 10 best-performing VIs and periods for the 2021 growing season.

VI	Period (Days)	Adjusted R²	RMSE
RVI	90	0.72 ± 0.02	1.03 ± 0.03
SAVI	90	0.69 ± 0.03	1.06 ± 0.04
SAVI	85	0.65 ± 0.03	1.09 ± 0.03
RVI	85	0.64 ± 0.02	1.12 ± 0.06
RVI	80	0.63 ± 0.02	1.13 ± 0.04
NDVI	85	0.62 ± 0.04	1.14 ± 0.06
WDVI	90	0.61 ± 0.02	1.15 ± 0.03
WDVI	85	0.61 ± 0.03	1.15 ± 0.04
PVI	90	0.61 ± 0.05	1.16 ± 0.05
SAVI	80	0.60 ± 0.04	1.15 ± 0.05
WDVI	90	0.61 ± 0.02	1.15 ± 0.03
WDVI	85	0.61 ± 0.03	1.15 ± 0.04

Figure 51 illustrates a scatter plot of RVI, comparing two high-performance dates (85 and 90 days after transplanting) with two dates showing lower performance (5 and 25 days after transplanting). The plot reveals that predictions closest to the actual yield values are found within the 85 to 95 days range. In contrast, the earlier dates with lower performance exhibit predictions that deviate from the actual yield values.

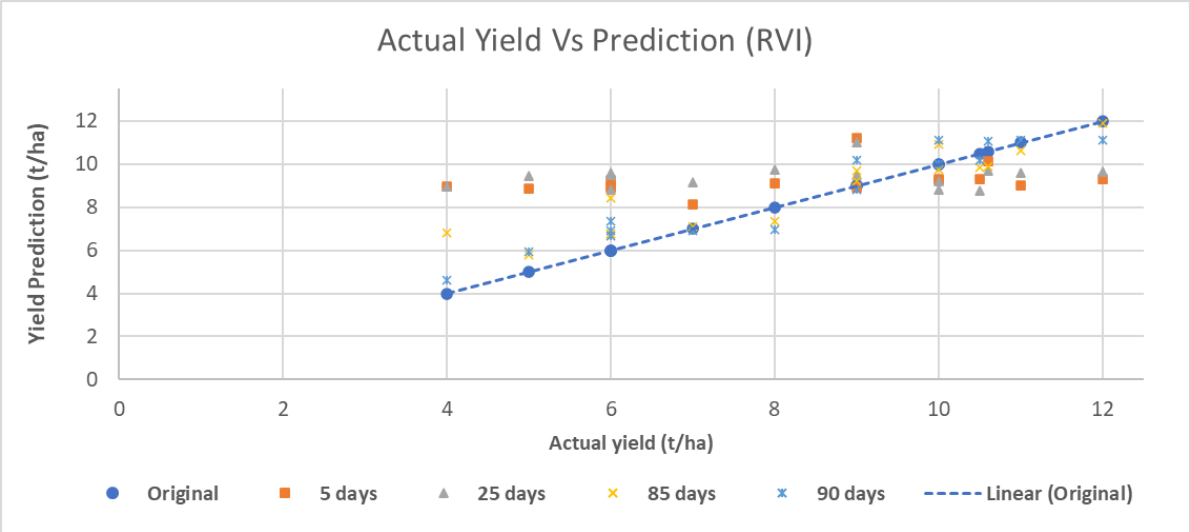

Figure 51 Scatter plot of actual yield vs. prediction of the four predictor dates for the 2021 growing season.

The plot (Figure 51) reveals a distinct pattern in the dataset, where the predictive models tend to behave differently under certain conditions. When actual yields are less than or equal to 9 t/ha, the regressors tend to overestimate yield. Conversely, when actual yields exceed 9 t/ha, the regressors tend to underestimate yield. This pattern suggests that the ensemble regressors may exhibit a central tendency or bias in their predictions, acting as a gravity point that affects the outcomes. In this case, the central tendency explains the behaviour of yields below and equal to 8 t/ha and those above 9 t/ha. For the specific case of 9 t/ha, the range of predicted values is not as broad as for lower yields, indicating a more balanced prediction around the actual value. However, further research is needed to refine the predictive models and reduce the tendency for overestimation.

In addition to selecting the VIs and growth stages with the highest predictive accuracy, it was also important to examine whether using ensembles of more than one regressor was a better choice than using only one regression model. Figure 52 shows the rate of ensemble size for each of the experiments that used the VIs and growth stages. This means that 500 were considered (number of rows × number of experiments × number of folds). An ensemble size of two was the preferred size (67.86%) to provide the predictions with the highest adjusted R^2 and lowest RMSEs. The option with the second highest performance was to use single regressors (21.43%); finally, the least promising option was to use ensembles with a size of three regressors (10.71%).

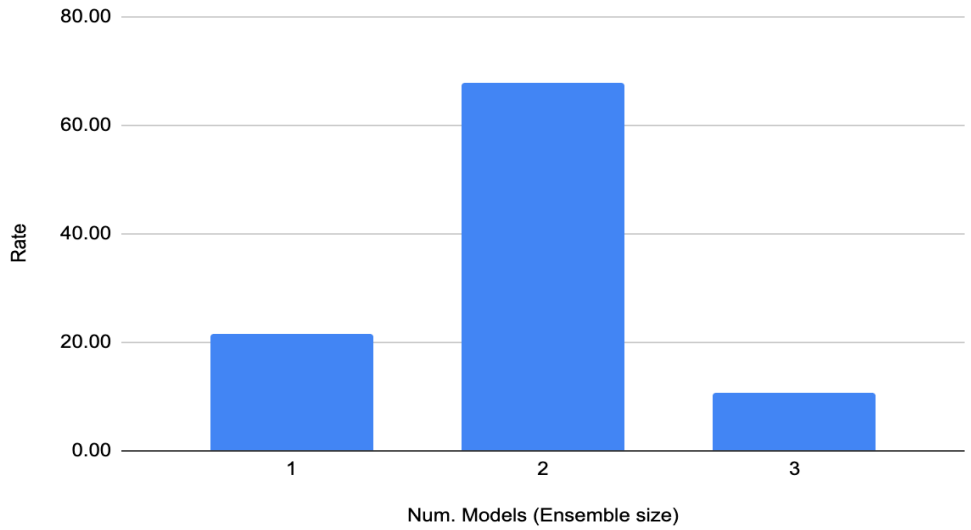

Figure 52. The optimal ensemble size (1, 2, 3) for the best regression models.

Table 25 expands on Figure 52 by showing which models and ensembles achieved the best performance and how often they occurred. The combination of ARD regression and SVR proved to be the most successful for constructing an ensemble, occurring frequently. SVR paired with Huber regression also demonstrated high performance in multiple instances. ARD and Huber regression models outperformed others several times when considering individual regressors. Interestingly, SVR excelled when used in combination with other regressors but didn't perform as effectively when used as a single regressor. It's worth noting that some of the evaluated regressors, such as OLS regression, AdaBoost, and extra trees, did not appear to be as successful. In cases where three models were utilized to form the ensemble, the combination of ARD, random forest, and SVR emerged as the highest-performing option.

Table 25. The 10 best-performing models (ensembles and single regressors) for the 2021 growing season.

Ensemble/Model	R^2	Number of appearances
ARD Regr. + SVR	0.67 ± 0.02	109
ARD Regr.	0.65 ± 0.03	87
Huber Regr. + SVR	0.65 ± 0.02	74
Huber Regr.	0.65 ± 0.04	63
ARD Regr. + Huber Regr.	0.66 ± 0.03	52
ARD Regr. + Random Forest + SVR	0.63 ± 0.03	41
ARD Regr. + Decision Tree	0.65 ± 0.02	30
Huber Regr. + Theil-Sen Regr.	0.64 ± 0.04	23
SVR + Theil-Sen Regr.	0.65 ± 0.03	12

ARD Regr. + Random Forest	0.63 ± 0.05	5

Overall, various combinations of sensors and growth stages were examined to assess their effectiveness in predicting processing tomato yield using AutoML. The analysis included a detailed evaluation of different VIs and their performance during the growing season. The results highlighted that all VIs performed best during the 85 to 90-day period after transplanting, with RVI outperforming the others. NDVI showed lower overall performance but reached its peak predictive power at 85 days after transplanting. Conversely, PVI and WDVI exhibited lower performance when compared to SAVI and RVI.

RVI and SAVI outperformed other VIs, achieving the most accurate yield predictions with average R^2 values of 0.72 ± 0.02 and 0.69 ± 0.03, respectively, at 90 days after transplanting. Additionally, they exhibited the lowest RMSEs of 1.03 ± 0.03 and 1.06 ± 0.04, respectively. Furthermore, the most precise yield predictions were concentrated within the 85 to 95-day range, while earlier date predictions exhibited more significant deviations.

Regarding model optimization, ensembles consisting of two regressors were the preferred choice (67.86%) for achieving higher adjusted R^2 and lower RMSE values. Single regressors were the second-best option (21.43%), whereas ensembles with three regressors showed less promising performance (10.71%).

Last but not least, the combination of ARD regression and SVR proved to be a frequently successful choice for creating ensembles. SVR paired with Huber regression also demonstrated strong performance in multiple instances. Among individual regressors, ARD and Huber regression models consistently outperformed others. Interestingly, SVR was most effective when used in combination with other regressors but showed weaker performance as a standalone regressor. It's worth noting that some regressors, like OLS regression, AdaBoost, and extra trees, did not perform as well. In cases where ensembles of three models were used, the combination of ARD, random forest, and SVR consistently achieved the highest performance.

3.4.2 Temporal – Level: Yield predictions across years

The AutoML pipeline underwent training using the 2021 Sentinel-2 dataset and was tested with the 2022 Sentinel-2 dataset to assess the relevance of each VI and band's reflectance in predicting crop yield. Aiming at developing a robust model, more 20 experiments were conducted on spectral data to obtain the average adjusted R^2 for each scenario. This enabled the selection of the most effective dates, spectral bands and models for yield prediction without manual intervention. Linear regression is also used for baseline against AutoML algorithms. Subsequently, tables were generated, showcasing the most effective VIs and combinations of bands for the years of 2021 and 2022, as well as their combined analysis at 5-day intervals post-transplanting.

The adjusted R^2 performances of spectral bands, derived from the dataset via the AutoML pipeline, are illustrated in Figure 53. The numerical values following the band channel denote the date post transplanting. Notably, the optimal timeframe for predicting yield appears to be from 80 to 90 days post transplanting, while spectral bands B4, B6, B7, B8, and B8A demonstrated the highest predictive performance for yield estimation. Across all cases, AutoML demonstrated superior performance when compared to linear models.

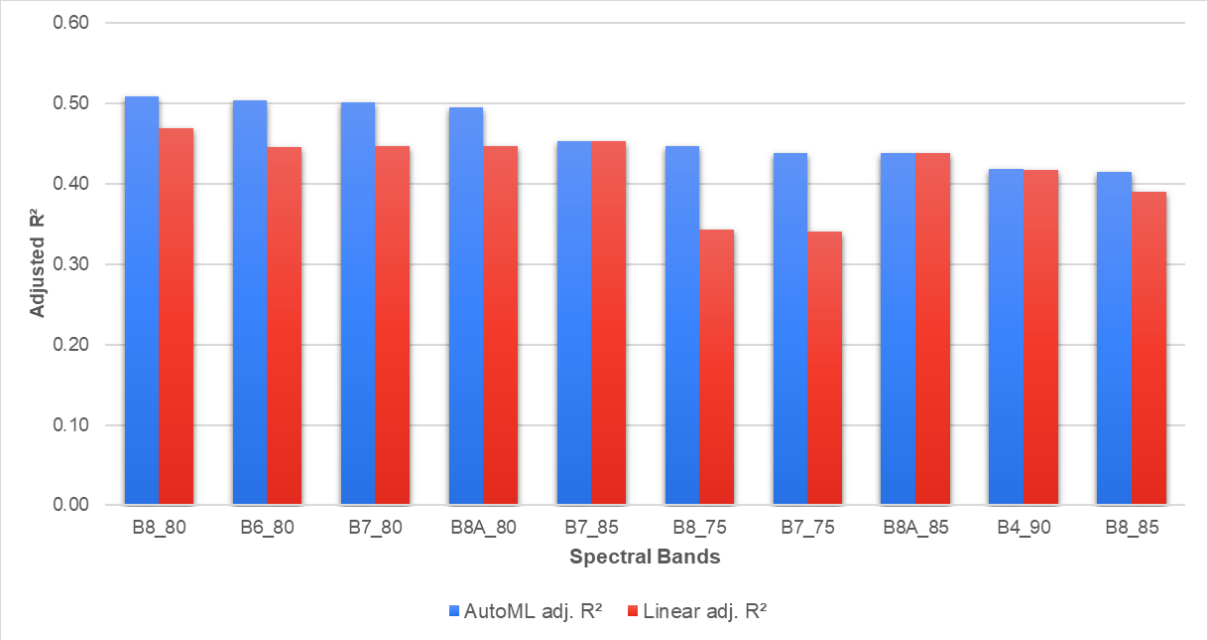

Figure 53. The 5 best-performing spectral bands for predicting the 2022 yield.

The subsequent table (Table 26), presents the overall efficacy of various VIs and spectral bands, gauged through adjusted R^2 values. When utilizing NDVI, the spectral band B8 corresponding to the NIR range demonstrates the highest performance, reaching an adjusted R2 of 0.56 at 80 days post transplanting. This performance is closely followed by B8A during the same period. Regarding RVI, lower performances were observed during 75 to 90 days after transplanting, with spectral bands B8, B9, B7, and B8A, achieving adjusted R^2 values ranging from 0.47 to 0.49. The AutoML models generally outperform linear regression models in the case of NDVI, while in the case of RVI similar results were retrieved. However, concerning RVI, both AutoML and linear regression yielded similar results in terms of predictive capability.

Table 26. The 10 best-performing VIs for predicting the 2022 yield.

	AutoML		Linear	
VIs	**Adj. R^2**	**RMSE**	**Adj. R^2**	**RMSE**
NDVI_B8_80	0.56	1.26	0.25	1.44
NDVI_B8A_80	0.55	1.26	0.23	1.45
RVI_B8_90	0.49	1.31	0.49	1.31
RVI_B9_85	0.49	1.31	0.49	1.31
RVI_B8A_90	0.49	1.31	0.49	1.31
RVI_B7_90	0.48	1.31	0.48	1.31
RVI_B8_85	0.47	1.32	0.47	1.32
RVI_B7_85	0.47	1.32	0.47	1.32

NDVI_B7_75	0.46	1.33	0.26	1.43
NDVI_B8_75	0.46	1.33	0.27	1.43

In the case of best performing spectral band combinations, the performances were notably increased reaching a R^2 of 0.64 (**Table 27Σφάλμα! Το αρχείο προέλευσης της αναφοράς δεν βρέθηκε.**). The combination [B4_70, B4_90, B6_65, B12_65'] stands out, demonstrating a remarkable adjusted R^2 of 0.65 and an RMSE of 1.19.

Table 27 The 5 best-performing combinations of spectral bands for predicting the 2022 yield.

	AutoML		Linear	
Combinations of spectral bands	**Adj. R^2**	**RMSE**	**Adj. R^2**	**RMSE**
B4_70, B4_90, B6_65, B12_65	0.65	1.19	0.64	1.20
B4_90, B8_65, B12_90, B12_95	0.64	1.20	0.63	1.21
B8_90, B8A_90, B4_90, B7_80	0.60	1.23	0.52	1.23
B4_90, B8_65, B12_90, B12_95	0.59	1.24	0.59	1.24
B4_70, B4_90, B6_65, B7_65'	0.60	1.23	0.57	1.25
B4_90, B8_65, B7_65, B6_65	0.58	1.24	0.56	1.29
B8_90, B8A_75, B4_90, B8_65	0.54	1.27	0.54	1.27
B12_65, B7_85, B8A_90, B8_80'	0.53	1.28	0.52	1.28
B4_90, B8_65, B7_65, B6_65	0.51	1.30	0.48	1.30
B4_90, B12_65, B9_95, B8A_85'	0.51	1.29	0.38	1.29

In all the cases, the spectral band B4 (that corresponds to the red wavelength) at 90 days post transplanting is appearing, while B12 (SWIR 2) and B6 (RE) are also featured in several cases. The period between 65 to 95 days post-transplanting, the Red Edge/NIR (B7 to B8A) bands were repeatedly appearing, indicating their importance for yield prediction the highest performance among all bands. Particularly, the NIR bands are widely acknowledged for characterizing vegetation status due to their vegetation-specific reflectance patterns attributed to internal scattering and minimal leaf absorption [654].

Additionally, several other combinations employing different models such as Random Forest, ARD Regression, and SVR combined spectral bands to achieve strong predictive capabilities, indicating their effectiveness in predicting crop yield during the 2021 season. ARD Regression was the most promising single model and the combination of ARD Regression and SVR was the best ensemble. Ensemble of two models demonstrated better performances than ensembles of three and one.

These findings emphasize how various combinations of bands and model selections can influence the accuracy of yield prediction, offering a comparative understanding of their effectiveness.

Part 4. Discussion

4.1 Yield estimation using Precision Agriculture – Systematic Review

The earliest efforts to estimate crop yield can be traced back to the pioneering work of Pinter et al. in 1981 [655] and Wiegand et al. 1991 [656], who employed remote sensing techniques. Prior to these studies, Al-Abbas et al. (1974) conducted laboratory investigations into the spectral characteristics of corn leaves under different nutrient stress levels [657]. In a separate study, Robert (1982) used color infrared aerial photography in Minnesota for diagnosis of "problems related to drainage, erosion, germination, grass and weed control, crop stand and damage, and machinery malfunction[139]. Since then, many studies and review papers were published focusing on yield prediction, offering valuable insights into the challenges and opportunities associated with employing remote sensing technologies [658–660]. Some reviews narrow their scope to concentrate on predicting the yields of specific crops, including widely cultivated ones such as maize, rice, sugarcane, sugar beet, and vines [53,661–664]. Others take a broader approach by providing an overview of remote sensing technologies in the context of various application domains like crop management, crop monitoring, phenology, and other ecophysiological processes [665–668]. An intriguing study conducted by Schauberger et al. conducted a systematic review spanning the years 2004 to 2019, to explore crop yield forecasting methods across three commonly utilized data domains: weather, remote sensing, and crop mask data. Their thorough investigation, spanning an extensive dataset of more than 350 articles, unveiled the prevalence of several widely embraced models, including statistical, process-based, and machine-learning models [343].

In this context, a systematic review [381] was conducted covering the years 2002 to 2022, investigating the most commonly used platforms and methods in precision agriculture for predicting crop yields. The initial finding of this study reveals a relatively low publication rate between 2002 and 2012, averaging approximately one paper per year. Nevertheless, from 2013 to 2019, a substantial surge in publications became apparent, signifying a heightened interest among researchers. This increase in the number of published articles can be traced back to several factors, including advancements in information and communication technology (ICT), progress in remote sensing technology, and the expanding availability of data. These developments have spurred a growing interest for utilizing these tools to create more efficient and precise crop yield prediction models.

4.1.1 Key contributor countries and crops

In terms of the most active countries conducting experiments within the scope of this study, China stands out prominently with more than 93 publications, leading the field. Following closely, the United States holds the second position with 58 publications, while India and Australia rank third each contributing 11 research studies, followed by Brazil. USA and China have displayed a substantial presence, marked by a significant number of research articles dedicated to crop yield estimation, through remote sensing applications. The notable impact of their research can be attributed to their status as the largest economies and their substantial investments in research and development. Consequently, they employ a substantial number of researchers who contribute to the production of research publications [669].

According to the findings of this study, the prevalent choice of crops for yield prediction primarily revolves around cereals and oilseed crops. These selections are influenced by several key factors, including their nutritional and economic significance, comprehensive data availability, and relevance to global food security [670,671]. An additional pivotal factor contributing to their widespread use is the accessibility of extensive datasets encompassing historical yield records, agronomic practices, and weather data. This data availability greatly simplifies the task of

conducting in-depth yield prediction studies for researchers. Furthermore, these crops lack the intricate structures found in vineyards and orchards, which can potentially impact remote sensing results [672]. The application of agricultural practices such as irrigation and pruning, commonly employed in vineyards and orchards, can introduce complexities in the interpretation of remote sensing data [673]. Subsequently, researchers may encounter more technical challenges and data processing requirements when dealing with these types of crops. Conversely, cereals and oilseed crops tend to encounter fewer disruptions from such factors, leading to more dependable and consistent outcomes in remote sensing.

4.1.2 Trends in platforms and methods used

Proximal, UAS and satellite platforms serve as significant tools for acquiring valuable insights into Earth's vegetation cover, making them integral components of precision agriculture practices. In the systematic review within this research, most studies leaned towards satellite platforms as their primary data source, followed by UAS and proximal sensors. Given the widespread adoption of these platforms, each with its distinct advantages and disadvantages. A comprehensive study conducted by Benos et al. [674], indicated that UASs are gaining prominence in comparison to satellites due to their flexibility and high-resolution imaging capabilities under various weather conditions. In contrast, satellites excel in providing time-series data over large areas.

In relation to the methods used, statistical analysis emerges as the predominant method utilized for predicting crop yield across the reviewed studies, according to this study's findings. Subsequently, ML and DL methods also feature prominently in yield estimation. Furthermore, the study highlighted that the majority of studies encompassing ML and DL approaches emerged between 2017 and 2022, signifying a growing interest and recognition of these advanced methods for predicting crop yields using remote sensing data. A notable finding is the prevalence of the Random Forest algorithm, followed by Support Vector Machine (SVM) and Linear regression. XGBoost and Partial Least Square Regression (PLSR) have also proven effective and versatile in yield prediction. Additionally, ANN and CNN lead among Neural Network approaches.

Among the identified model-based approaches, the Decision Support System for Agrotechnology Transfer (DSSAT) model [675] stands out, offering insights into agricultural management practices and crop responses to environmental conditions. Other common models used for yield estimations include the Simple Algorithm For Yield model (SAFY) and WOrld FOod STudies (WOFOST) model [676–678], AQUACROP,[679–681], Agricultural Production Systems Simulator (APSIM) model [682–684], considering various aspects of crop growth and management. These models cover various aspects of crop growth and management, each operating on distinct driving factors. For instance, WOFOST focuses on the influence of carbon dioxide (CO_2), water, and temperature on yield. In contrast, AQUACROP emphasizes the impact of water stress on crop growth, making it suitable for simulating irrigation scenarios. APSIM, functioning as a process-based model, considers a wide array of soil processes alongside water balance and nutrient transformations. Researchers have also explored coupled models, merging different principles from two or more models, aiming to enhance simulation accuracy, system stability, and reduce operational costs. These advancements in model-based approaches contribute significantly to understanding crop-environment interactions, facilitating informed decisions for sustainable agriculture.

Each approach presented distinct advantages and catered to specific research objectives, enabling the extraction of meaningful insights from remote sensing data for crop yield estimations. Notably, Statistical Analysis and Machine Learning methods are frequently employed in crop yield estimation owing to their capability to manage intricate nonlinear relationships within vast datasets, along with their proficiency in dealing with known parametric structures and unobserved cross-sectional differences [386]. Furthermore, the efficacy of Deep Learning methods might be limited as they heavily hinge on the quality of the extracted features [387]. Lastly, the limited utilization of model-based methods in crop yield prediction could be attributed to their substantial

demands for data and computational resources, as well as their lower adaptability compared to other methods [388].

4.1.3 Accuracy Performance Per Crop Category

When comparing different methods in the case of sugar, beverage, and spice crops, the predominance of statistical and machine learning methods coupled with satellite data is apparent. For sugarcane & coffee tree, these methods, have provided high R^2 values reaching 0.94, while in the cases of coriander and tea cropd, statistical methods using satellite data yielded R^2 values between 0.68 and 0.87. ML techniques exhibit high performance and specifically the Random Forest method stands out with an impressive RMSE of 1.51 t/ha and an R^2 value of 0.94, surpassing other methods like Classification and Regression Tree, Support Vector Regression, and K-Nearest Neighbor [396], These results align with Canata et al.'s findings, where RF regression outperformed Multiple Linear Regression (MLR) in sugarcane yield prediction, as well as Martello et al.'s discovery of RF regression's superiority in predicting coffee tree yields [401]. Moreover, satellite systems were the most commonly used platform, showing promising prediction accuracies with an R^2 of 0.87 and an RMSE of 11.33 (t·ha– 1) compared to actual harvested yields [395]. SAR-based yield prediction models have also proven useful in refining yield estimates for sugar crops [391]. However, Duveiller et al.'s study highlighted that sugarcane yield estimation is influenced by various factors, including the consideration of time (thermal or calendar), signal purity, data extraction methods from time series, and the timing of information availability, which can explain the range of R^2 values observed in satellite-based yield prediction[393]. Moral et al. [392] propose that the empirical NDVI model emerges as the most fitting approach for estimating sugarcane yield at the field level, owing to its simplicity and consistently high accuracy across the entire crop cycle. Conversely, a separate study [390] highlights that among linear, logarithmic, power, and exponential models, the polynomial model exhibits significantly enhanced performance. Regarding model-based yield prediction, the findings suggest a medium to high performance, with R^2 values ranging from 0.64 to 0.86. This variability can be attributed to the specific model employed. In a study conducted in the US, three statistical models integrating remote sensing and weather data were compared, revealing that the SiPAR model outperformed the Cumulated DNVI (CNDVI) and Kumar and Monteith (K–M) models in terms of yield prediction[397].

In the category of Vegetables and Melons, there is predominance of statistical methods coupled with satellite and UAS measurements, while ML techniques have exhibited high performance, achieving an impressive R^2 value of 0.90. The choice of VIs plays a pivotal role in achieving optimal performance. According to Suarez et al.'s study [403], the best results were obtained when using predictor variables such as Renormalized Vegetation Index (RDVI), SAVI, and OSAVI (R^2= 0.77), with the lowest standard deviation (σ) of 10.75 t/ha achieved with RDVI. EVI2 also outperformed GNDVI (R^2 = 0.55) in a separate study[406] that focused on processing tomato crops. This study identified plant height and VIs during the early to mid-fruit formation period as significant variables for predicting shoot masses. Additionally, NDVI and WDVI were notably important for predicting tomato weight, while VIs obtained one month before harvest played a crucial role in predicting fruit quantity. Recent research findings[350] suggest a strong correlation between the developmental stages of the primary canopy in processing tomatoes and their final yield. This correlation may indicate a critical stage during which noticeable changes occur in the crops, detectable using satellite-derived data. Furthermore, studies have demonstrated the possibility of predicting average tomato biomass and yield up to eight weeks before harvest and at the individual plant level up to four weeks before harvest, using time-series phenotypic features derived from UAS. Linear Regression models have shown strong correlations (R^2 > 0.7) in this context [408].

For oilseed crops, numerous studies involved soybeans in their research, as soybean is a widely cultivated and economically important crop. There is predominance of ML/DL and statistical approaches, often combining satellite, UAS, or proximal data sources, while high performances (R^2 > 0.90) have been achieved in all crops except from palm oil and canola. A promising approach

for estimating sunflower yields involves using satellite NDVI series captured 50 days before harvest [88]. Furthermore, the effectiveness of Evolutionary Product-Unit Neural Network (EPUNN) models has been demonstrated, showing superior accuracy compared to linear SMLR models in both training and generalization sets [411]. When it comes to estimating rapeseed yields, a strong correlation has been observed between plot-level VIs and leaf-related abundance, resulting in an R^2 value exceeding 0.75. Among the tested VIs, the most accurate yield estimation in rapeseed was achieved by multiplying NDVI, Chlorophyll Index Red Edge (CIred edge), Transformed Vegetation Index (TVI), and SAVI by short-stalk-leaf abundance [417]. Regarding model-based methods [418], comparing the WOFOST model and the coupled CASA-WOFOST model revealed that the CASA-WOFOST model has faster simulation speed while maintaining similar accuracy. This makes the proposed CASA-WOFOST model suitable for large-scale assessments using high-spatial-resolution images to obtain accurate yield simulations. A study examining the monitoring of winter rapeseed crops through the utilization of multisensor optical and multiorbital SAR data alongside the SAFY agrometeorological model revealed that integrating both SAR-derived dry matter (DM) and optically derived Green Area Index (GAI) enhanced model control. This assimilation proved to be more effective compared to solely relying on SAR or optical data in isolation [419]. Another critical factor influencing satellite-based crop yield estimation is the spatial and temporal resolution of the deployed satellites. As noted by Chen et al. [416], challenges arise from the sparse time series of satellite remote sensing, characterized by low temporal frequency and cloud interference. These challenges hinder accurate crop yield estimation at regional and national scales. To overcome this limitation, Chen et al. proposed a solution involving the fusion of high-spatial-resolution yet low-temporal-frequency images with low-spatial-resolution yet high-temporal-frequency images. This strategy aims to bolster the temporal resolution while retaining crucial spatial details, potentially elevating the precision of crop yield estimations.

It is not surprising to encounter numerous studies focusing on soybeans in their research, given its widespread cultivation and economic significance. A study [425] that compares various spatial resolutions provides convincing support for higher-resolution imagery over lower-resolution alternatives. The authors suggest opting for an NDVI resolution that equals or exceeds the current cropland mask resolution, while also taking into account factors like computational costs. Notably, another research study [439] reveals an interesting finding: county-scale models exhibit relatively poor performance in field-scale validation ($R^2 = 0.32$), especially in high-yielding fields. However, these county-scale models demonstrate similar performance to field-scale models when evaluated at the county level ($R^2 = 0.82$).

In the Fruits and Nuts category, there is increased number of studies in vineyards, with high performances ($R^2 > 0.90$) achieved through ML/ DL methods. The primary methods have involved proximal sensing, UAS sensing, or a combination of both, often complemented by satellite data. High-resolution satellite imagery has also been effectively used independently, showcasing a commendable performance with an R^2 value of 0.87 [203,450]. The effectiveness of these methods stems from their reliance on visual counting and the utilization of high-resolution data, enabling accurate and efficient estimations of orchard production. However, the application of above-ground remote sensing for tree production estimation remains limited, requiring specific calibration for individual orchards and yearly variations, accounting for climatic and site-specific effects [451].

In relation to root tuber and other crops, all methods and all sensors were used, and high performances ($R^2 > 0.90$) have been achieved through all methods in Cotton, Sweet Potato, Perennial Ryegrass. ML approaches are notably prevalent, demonstrating exceptional accuracy levels ($R^2 > 0.90$) compared to alternative methods. Particularly in cotton cultivation, the utilization of multispectral remote sensing systems mounted on UAS exhibits considerable promise. These systems offer rapid, precise, and cost-effective assessments of agricultural crop traits and yields. The correlation between crop growth indicators like LAI and chlorophyll content with canopy spectral reflectance enables the utilization of spectral indices collected during the growing season for estimating crop yields. This correlation between yield and the amount of photosynthetic tissue allows for wide-scale application, contrasting with traditional measurements of agronomic

parameters such as LAI and chlorophyll [460]. Furthermore, the feasibility of estimating cotton yield using low-altitude UAS imaging was confirmed in this study [462].

Researchers extensively utilized diverse data sources, including UAS, satellites and proximal sensors, to gather insights into leguminous crops. High performances ($R^2 > 0.90$) have been achieved in Alfa Alfa, Red Clover, Chickpea, Snap Bean, Peas. Some studies solely focused on employing ML or DL algorithms, while others combined these approaches or integrated statistical methods to boost accuracy and interpretability. In a study by Minch et al. [476], the exploration of efficient flight parameters aimed to establish successful models for determining canopy heights, particularly in alfalfa yield estimation. The researchers strongly advocate using a flight parameter within the range of 50–75°, as it is likely to yield optimal data for precise canopy height estimation in alfalfa fields.

In the domain of cereals, an array of methods and platforms was employed, leading to the subdivision of this category into two segments: cereals and maize and wheat. Notably, research dedicated to predicting wheat and maize yields surpasses that for other cereals, underscoring their pivotal role in agricultural research. Furthermore, researchers explored a spectrum of approaches for predicting wheat and maize yields, lacking a clear and consistent trend in the methodologies employed for yield prediction. Nevertheless, maize and, to a lesser extent, wheat, rice have been extensively studied using machine learning techniques. The variety of approaches used is consistent with a previous study [343] that also noted the use of diverse methods for predicting yields of staple crops, emphasizing the importance of appropriate validation for each specific context.

Overall, the results emphasize the importance of tailoring methodologies to specific crop categories to enhance yield estimation techniques. The compilation of the highest R^2 performance measures from various studies is categorized by crop type. ML techniques, especially Random Forest, demonstrate excellence in the prediction of sugar, beverage, and spice crops. Satellite systems, such as SAR, exhibit effectiveness in sugarcane yield forecasting. ML approaches yield promising results in the context of vegetables, with a focus on essential VIs. Orchards benefit from the utilization of proximal and UAS sensing technologies, while leguminous crops are examined through a combination of ML, DL, and statistical methods. Wheat and maize receive substantial attention and are explored using a wide array of methods, encompassing ML, DL, statistical techniques, and model-based approaches.

4.2 Proximal vs UAS vs. Satellite NDVI: Are They Truly in Sync?

The alignment of proximal, UAS, and satellite data often varies due to factors like sensor spectral and spatial resolution, proximity and the timing of data capture. While these technologies measure vegetation health, their outputs might differ due to their distinct data acquisition methods and instruments. Achieving complete alignment among them is challenging, but careful data interpretation can provide complementary insights into vegetation status and yield assessments.

In this study, the average NDVI values demonstrated remarkable similarity between the two remote sensing technologies—UAS and Sentinel-2—highlighting a robust correlation in NDVI values, particularly during the later stages of the crop's phenological cycle. This suggests a more pronounced agreement or similarity between data collected from Sentinel and UAS sources as the crop matures. The mean NDVI values from UAS multispectral data were generally higher, reflecting the superior spatial resolution of the UAS's sensor, while Sentinel-2 presented higher standard deviation. This conforms with previous studies [685–693], acknowledging challenges faced by Sentinel-2 imagery in capturing localized conditions, especially in regions marked by pronounced heterogeneity due to abiotic or biotic stress factors. In such scenarios, the use of UAS becomes imperative for obtaining more precise and detailed data [694]. It is also reported that UASs can be optimal for finely characterizing fields in terms of resolution and pinpointing intra-crop variability [692]

Despite the excellent spatial ground resolution and flexible real-time monitoring offered by UAS, deploying them on a commercial scale incurs significant expenses, encompassing equipment, data processing, and software costs, which can be a considerable investment, particularly for small-scale farmers [216,217]. Additionally UAS surveys involve the storage and management of substantial data and require preprocessing, and the resulting datasets are limited to what the user collects [218]. Consequently, relying solely on UAS for weekly monitoring can be financially burdensome and impractical, especially when managing multiple fields that may not be extensive or are widely dispersed. In such cases, leveraging satellite imagery to assess the overall field conditions is more practical.

Satellite remote sensing excels in mapping field variability with a higher temporal continuity that remains consistent across seasons and multiple years. This allows for monitoring various vegetation stages throughout the growing season and facilitates historical analysis of past seasons. Satellite platforms also offer the advantages of extensive coverage, high temporal resolution, and cost-effectiveness [706], allowing the integration of data from multiple sources, including optical and SAR remote sensing [707]. An additional noteworthy factor is the substantial volume of data they generate, making them conducive to applying data consuming methods such as machine learning. These benefits help explain why the majority of the studies chose to incorporate satellite remote sensing methods.

To overcome the limitations associated with the described platforms, the synergistic use of both remote sensing techniques is considered to be the optimum solution in precision agriculture [695]. High-resolution UAS images can be selectively deployed during critical phases of the crop cycle to provide detailed insights. Additionally, it is desirable to combine UAS images, (preferably with a resolution exceeding 4 cm), with high-resolution satellite imagery to enhance the quality of the data obtained. This comprehensive approach offers a balanced and cost-effective solution for precision agriculture while adapting to the specific needs of different fields and crops.

On the other side of the spectrum, proximal sensors offer real-time or near-real-time NDVI data, contributing to a fast and targeted diagnosis of nutritional and physiological states, stress incidence, and potential crop yield. Unlike aerial and satellite imagery, this system provides information obtained locally and quickly by terrestrial determinations. Most of these sensors are active, making them less affected by weather conditions. Their proximity to the target reduces atmospheric interference, resulting in more accurate data and high spatial resolution [249]. In addition, they can contribute to lower production costs, because it would allow applying the exact amount of fertilizers and water and mitigating stress at the appropriate time and in the right place [696]. Therefore, the importance of these remote sensing systems lies in the ease of obtaining reliable results, as stated in other studies about other type of crops (cereals, rice paddies, vineyards, forest stands, etc.)[697–699]. Multiple studies have consistently demonstrated that the developmental growth trends of NDVI derived from UASs and GreenSeeker sensors are highly comparable, irrespective of the measurement approach [700–703]. However, they do come with limitations related to area coverage, data interpretation, maintenance requirements, and initial costs. Therefore, it is essential to evaluate specific needs and available resources when considering the adoption of remote sensor technology.

In this research, a comprehensive examination of the relationship between proximal sensor data in comparison to UAS and satellite datasets revealed a moderate level of correlation, as discerned from R^2 values spanning from 0.41 to 0.72. The moderate correlation observed can be primarily attributed to the specific focus of proximal sensors, which are designed primarily for monitoring vegetation growth and do not account for reflective effects originating from the soil. Therefore, the retention of the intercept in the analysis deviates significantly from zero, which differs from the cases of UAS and Sentinel datasets. This outcome is expected, as the proximal sensor values commence at higher NDVI values compared to the NDVI values retrieved from the UAS and Sentinel datasets. Additionally, a crucial contributing factor is the variation in electromagnetic spectrum wavelengths used for measurements among the different platforms. Specifically, the Sentinel-2 satellite employs the Near Infrared band (NIR, Band 8) with a mean wavelength of 832.8 nm, while the GreenSeeker™ NIR band measures at 774 nm, and UAS-based sensors operate

at 790 nm. This can be the reason for the stronger correlations between UAS and proximal datasets compared to the Sentinel and proximal datasets.

While proximal platforms offer real-time or near-real-time data, it is evident that they are most suitable for small to medium-sized fields and may not be practical for continuous monitoring of larger areas. Given that these sensors provide point measurements, conducting comprehensive assessments of extensive agricultural fields is impractical [704,705]. The accuracy of proximal platforms is heavily dependent on local factors such as soil type, weather conditions, and agricultural activities like pruning, limiting their applicability in diverse contexts. A notable drawback of proximal sensing is that terrestrial sensors require regular maintenance and need to be reattached each time, making them more susceptible to operator error. Furthermore, interpreting the high-resolution data collected by these sensors can be complex, necessitating expertise in data analysis. These limitations can impact the accuracy of estimating vegetation characteristics. For instance a study [706] reported that NDVI obtained from Sentinel-2 satellite observations outperformed NDVI obtained from the handheld GreenSeeker™ platform in estimating fAPAR (Fraction of Absorbed Photosynthetically Active Radiation).

In conclusion, the integration of proximal, UAS, and satellite platforms represents a promising approach in precision agriculture. This study highlights the importance of strategically blending these technologies to maximize the quality and scope of data while being mindful of practical and financial considerations. The key takeaway is the imperative need to carefully select the appropriate sensor type based on the specific scale and objectives of the assessment. Proximal sensors excel in fine-scale, localized monitoring, but should be deployed judiciously, taking into account specific needs and constraints of the application. UASs and satellites found to generate very similar results and provide a broader, more comprehensive perspective over larger geographical regions. The synergy of these technologies enables more precise and efficient agricultural operations, helping farmers and researchers address critical issues related to resource allocation, crop health, and sustainability. This approach not only contributes to enhanced agricultural productivity but also supports the long-term goal of sustainable and environmentally responsible farming practices.

4.3 Processing Tomato Crop: Phenological Stages Revealed

Accurate assessment of plant growth and development is essential for agronomic management particularly for the decisions that are time-critical and growth stage-dependent in order to maximize efficiency of crop inputs and increase crop yields [667]. Identifying crop phenological stages at both subfield and field scales provides essential information for producers to make timely adjustments in input strategies, such as nitrogen application, herbicide and fungicide use. Remote sensing platforms, which observe crops' morphological and physiological traits based on spectral, structural, biophysical, or agronomic characteristics, are commonly employed in agriculture. However, these systems require continuous, cloud-free data to accurately capture all phenological stages and transitions between periods. Reduced spatial and temporal resolutions can limit their ability to distinguish subtle phenological differences between similar crops.

Satellites offer extensive coverage and historical data, making them suitable for large-scale crop-type classification and growth monitoring. The high spatial resolution of Sentinel-2 imagery enables monitoring of species-specific phenology, whereas its high temporal resolution increases the possibility to acquire dense time series. Thus far, Sentinel-2 time series have been used in monitoring forest phenology in several studies [707]. However, their drawbacks include low spatial resolution and vulnerability to cloud interference. UAS platforms, equipped with multi-/hyperspectral, RGB, or thermal sensors, provide high resolutions and real-time data collection, addressing a wide range of crop attributes. Nevertheless, they come with high costs, weather dependence, and limited availability. Ground-based, cost-effective and IoT-enabled systems deliver high resolution close to objects but require labor-intensive surveys. Each platform presents a unique

set of advantages and drawbacks, highlighting the need for careful consideration based on specific application needs and constraints in precision agriculture.

This research has unveiled a distinctive pattern of annual growth dynamics in tomato plants, and this pattern is effectively captured and elucidated by vegetation index values. Specifically, the UAS and proximal NDVI measurements exhibited elevated values as the crop canopy progressed. However, their limitations were evident in capturing dynamic canopy changes due to infrequent revisiting intervals. In contrast, satellite datasets proved more effective in offering indicative results regarding the phenology of the crop. The analysis of VIs dynamics from Sentinel-2 images revealed a narrative of seasonal progression and phenological stages in processing tomato crops. Notably, the study observed that the lowest mean values for all VIs occurred in the period following transplanting, when the canopy cover was limited, and substantial gaps between rows were occupied by exposed soil. As the season progressed, there was a gradual increase in the percentage of canopy cover, particularly during the middle of the season when tomato plants reached their peak vigor just before they began reallocating sugars to their fruits. Respectively, as the tomato canopy expanded throughout the season, VI values showed a discernible increase. Specifically, the highest mean VI levels were observed in July, corresponding to the flowering and fruit tomato emergence stage, which occurs between 75 to 95 days after planting. Subsequently, there was a gradual decline in VI values. As tomato plants progress through their growth stages, particularly transitioning from the fruit emergence stage to later growth phases, their vegetation characteristics change. The rate of growth may slow down, causing a decline in VI values. Plants naturally undergo physiological changes such as processes like leaf aging, senescence (aging of plant parts), or fruit development that affect the VI values, resulting in a decline.

This trend aligns with the research conducted by Lykhovyd et al. [708], revealing that different phenological phases in processing tomato crop are associated with distinct ranges of NDVI values. Similarly, Veloso et al. [709] , utilized bands similar to Sentinel-2 in other optical sensors, demonstrating a high correlation between VI values and fresh biomass as well as the green area index (GAI). Veloso et al.'s findings enabled the precise monitoring of short-lived phenological stages, contributing to a nuanced understanding of crop development. Such findings emphasize the capacity of remote sensing techniques in capturing the intricacies of plant growth and phenological development, offering valuable insights for crop monitoring and management.

4.4 Bridging the Gap: Accurate Crop Yield Predictions

This research evaluated the effectiveness of individual UAS, proximal sensors, and satellite-derived VIs in forecasting the yield of three distinct varieties of processing tomato. VIs derived from spectral bands found in multispectral imagery have a longstanding history in estimating crop canopy and yield. The application of remote sensing technologies for assessing field and yield variability is increasingly prevalent in precision agriculture, largely owing to their comparatively reduced expenses and. non-invasive approach [710]. The study adopts a dual approach, exploring both field-level and regional perspectives to yield results applicable to varying scales.

4.4.1 Yield Predictions: The Field- Level Approach

Three different platforms were utilised to assess their performance in predicting the yield across ten fields. The GreenSeeker proximal sensor, UAS, and Sentinel-2 satellite imagery were utilized to assess crop vigor from distinct altitudes. Each sensor's performance is influenced by various data acquisition parameters, including proximity to the plants and the unique technical characteristics of the equipment used. NDVI was deployed, being the most widely VI used and can be generated from all the different sensors deployed in this study.

The study's results reveal distinctive patterns in the performance of different sensing platforms across various growth stages of the crop. During the early phase of canopy growth, the proximal sensor demonstrates a higher explanatory power ($R^2 = 0.34$) in predicting yield variance compared

to the UAS (R^2 = 0.29) and satellite (R^2 = 0.26) platform. This outcome is anticipated as the canopy, at this point, is not fully covering the lines, and the measurements from UAS and satellite platforms incorporate the soil effect, limiting their ability to represent canopy growth accurately compared to the proximal sensor. As the crop progresses to the budding stage, where canopy coverage increases, there is a notable uptick in the R-squared values for NDVI derived from UAS (R^2 =0.35) and satellite (R^2 =0.38) platforms. This suggests an improved capacity of these platforms to capture and explain yield variability as the canopy progresses. During the critical flowering stage, the satellite platform outperforms others with the highest R-squared value (R^2 =0.57), indicating its exceptional effectiveness in elucidating yield variability. Both the UAS (R^2 =0.45) and proximal sensor (R^2 =0.30) also contribute significantly at this stage, emphasizing their relevance in assessing crop dynamics. Moving into the Fruit Formation stage, both UAS (R^2 =0.52) and satellite (R^2 =0.54) platforms exhibit substantial R-squared values, highlighting their ability to explain a considerable portion of yield variability during this growth phase. In the final growth stage, the R-squared values underscore the persistent strength of the Sentinel platform (R2 =0.53) as a key explanatory factor for yield variability. The UAS (R^2 =0.42) and Proximal sensor (R^2 =0.53) also maintain significant contributions. These findings align with a similar study [706], corroborating the superior performance of the Sentinel satellite, particularly in its broader coverage that facilitates a more comprehensive understanding of vegetation even in suboptimal study areas.

In the final step, the yield sample values were extrapolated by leveraging the average number of plants per hectare. This comparison showcased variations between the predicted values, derived from the yield sampling, and the actual yield values. The accuracy of these predictions demonstrated variability across different instances, with some closely aligning with the actual values, others slightly underestimating, and a few overestimating. The deviations in predicted yield ranged from 5 to 10 percent. This outcome highlights the effectiveness of the yield sampling strategy in providing satisfactory outcomes for yield prediction. Despite some discrepancies, the general alignment between predicted and actual values within a relatively small margin of deviation suggests that the yield sampling approach holds promise for estimating crop yield with reasonable accuracy.

Overall, the temporal aspect emerged as a critical factor, with later growth phases presenting a strong foundation for data convergence and correlation. The observed positive and strengthening correlation, provides substantial support for the reliability and utility of NDVI data obtained from proximal. UAS and satellite platforms at different stages. The flowering stage is particularly noteworthy, where the correlation is most pronounced, with R-squared values reaching 0.52 for UAS and 0.57 for Sentinel. During the Fruit Ripening to Maturity stage, the proximal sensor exhibits a robust correlation with an R-squared value of 0.53. This robust correlation reaffirms the conclusion that NDVI data from both platforms positively influences crop yield, particularly during the critical flowering stage, offering valuable insights for precision agriculture. It also emphasizes the importance of selecting the appropriate sensing platform based on the specific growth stage, highlighting the Sentinel's consistent efficacy across various stages in the specific crop.

Conversely, the year 2021 analysis revealed a stark contrast, with the correlation between crop yield samples and NDVI datasets from all platforms declining significantly. Lacking a clear indication of the underlying cause, these correlations did not reach statistical significance, for that specific year. It's worth noting that the dataset for the year 2021 encompassed only two fields, a relatively low number, potentially contributing to the insufficient data available for generating a statistically significant model.

It's important to recognize that estimating crop production is a complex process influenced by a multitude of factors. These factors include microclimate conditions, weather patterns, soil characteristics, fertilizer usage, and the choice of seed varieties [711]. Considering the numerous methods and techniques have been developed and used for optimizing yield prediction and improving the effectiveness of the developed models [712,713], it became apparent that there was a need for a precise regional-scale crop yield dataset. This dataset would play a crucial role in integrating machine learning methods for more accurate predictions. Therefore, a dataset was

created, encompassing actual yield values and field boundaries from 108 fields in 2021 and 44 fields in 2022, serving as a ground-truth reference. The analysis of satellite imagery, guided by these ground-truth data, yielded promising results. Due to operational constraints, the analysis focused solely on satellite imagery, as deploying UAS and proximal surveys at such a scale was not feasible.

4.4.2 Yield predictions: The Regional-Level approach

Based on the systematic review, the statistical analysis is the most prevalent method employed for crop yield prediction in the reviewed studies, however, ML is also widely used for yield estimation providing high accuracy. A notable distinction lies in the approach: while statistical methods necessitate the selection of a model based on our understanding of the system, machine learning relies on the empirical capabilities of predictive algorithms. [714]. This study introduces an innovative approach to predicting tomato yield by integrating machine learning techniques with vegetation index (VI) data obtained from satellite platforms at different growth stages, commonly employed in precision agriculture. While prior research has explored various correlation and regression models between VIs and crop production, the utilization of machine learning techniques for estimating processing tomato yield has not been extensively investigated until now. The investigation involved the examination of different VIs over the growing season to assess their performance in predicting yield.

The initial phase of the analysis involved the application of basic statistics, primarily utilizing the Pearson correlation coefficient, which is widely common in the literature. This coefficient is a statistical measure adept at evaluating the strength and direction of a linear relationship between various VIs and crop yield. During the initial growth stages of the plants lower r values were recorded. Such observations are anticipated, given the minimal canopy cover during that stage and the fact that the 10-meter spatial resolution imposes constraints, particularly for row-cultivated crops. Considering also that a substantial portion of the field area is covered by bare soil introduces additional noise into the spectral data, contributing to these limitations.

Nonetheless, the findings revealed that all VIs demonstrated optimal performance during the 85 to 90-day period post transplanting, with RVI exhibiting superior predictive capabilities compared to others. Although NDVI displayed lower overall performance, it reached its peak predictive power at 85 days after transplanting. On the other hand, PVI and WDVI exhibited comparatively lower performance than SAVI and RVI. Each VI demonstrated strong and consistent performance, consistently exhibiting Pearson correlation (r) values exceeding 0.6 at 80 days. The most exceptional performance across all VIs assessed in this study was observed at 90 days ($r > 0.7$). Specifically, the heightened values of the RVI during this timeframe were deemed optimal for predicting yield. These findings suggest the potential utility of these indices in predicting crop yield, especially during the later stages of crop development. These results collectively imply that certain VIs exhibit promising relationships with yield, particularly in the later phases of the crop growth cycle. Variability among the different varieties and VIs is to be expected because canopy development is a complex process and not homogeneous in all fields. Although the results are aligned with the findings of Psiroukis et al. [715], who adopted a similar approach, the Pearson correlation values we acquired did not attain the elevated levels reported in their study. This disparity might stem from variations in the dates of the datasets used or differences in the agricultural practices implemented in the different regions.

Recognizing the potential of machine learning to enhance yield prediction accuracy, various ML algorithms were integrated, marking a strategic move towards optimizing the predictive capabilities of the model. This strategic move was aimed at optimizing the predictive capabilities of the model, with a specific emphasis on using AutoML to discover ensembles of regressors with high predictive power, which was one of the primary goals of this research.

Extensively used regression methods have been compared against more complex methods that deal better with outliers. Specifically, linear and nonlinear regression models were evaluated, including OLS, Theil-Sen and the Huber regression models, and Ensemble Methods based on Decision Trees. Regression analysis was performed using those highly correlated VI data, in order to evaluate their performance in assessing the crop yield. The analysis incorporated the use of adjusted coefficients of determination (R^2) and root mean square error (RMSE) to evaluate predictive accuracy.

According to the findings, the regression models between yield and VI data presented different degrees of accuracy, depending on the model fitted, the sensor used, and the growth stage assessed. The most effective VIs for predicting yield were RVI and SAVI, displaying average R^2 values of 0.72 and 0.69, respectively, at the 90-day mark post-transplanting. This timeframe potentially signifies a crucial stage in the development of processing tomato crops, distinctly detectable through Sentinel-2-derived data. Furthermore, these VIs demonstrated the lowest RMSEs of 1.03 and 1.06, respectively. Numerous researchers advocate for the utilization of the SAVI due to its reduced bias associated with soil properties present in remote sensing images, allowing for improved identification and differentiation of plants from the soil [685,708]. Conversely, NDVI performed less effectively compared to other VIs, exhibiting values below 0.62. The limited relationship between yield and NDVI and PVI may be influenced by non-weather-related factors dictating yield, such as atmospheric influences or NDVI's sensitivity to soil brightness and canopy shadow effects [203]. The most accurate predictions were concentrated within the 85 to 90-day range, while earlier date predictions exhibited more significant deviations.

In terms of model optimization, ensembles consisting of two regressors were found to achieve the highest adjusted R^2 in most cases (67.86%) and lower RMSE values. This signifies that combining the predictions of two precise regressors enhances accuracy. This finding aligns with Zhang's suggestion [716] advocating for the balanced utilization of diverse viewpoints from various models or regressors, leading to more resilient and consistent predictions. Single regressors were the second-best option (21.43%), whereas ensembles with three regressors showed less promising performance (10.71%).

The combination of ARD regression and SVR emerged as a frequently successful choice for creating ensembles. SVR paired with Huber regression also demonstrated strong performance in multiple instances. Among individual regressors, ARD and Huber regression models consistently outperformed others. Notably, SVR exhibited its highest effectiveness when used in combination with other regressors but showed weaker performance as a standalone regressor. Some regressors, such as OLS regression, AdaBoost, and extra trees, did not perform as well. Generally, tree-based regressors like extra trees or random forests did not yield successful outcomes. However, this doesn't imply that these methods will universally fail in other related regression problems. It adheres to the "no free lunch" theorem [717], , suggesting that no single algorithm universally outperforms others across all datasets. Consequently, even the most potent algorithm might not be optimal for all yield prediction challenges. Contrarily, leveraging consistently successful regressors within AutoML, while constraining the search space, could enhance the efficiency of the overall pipeline by identifying suitable solutions. In instances where ensembles of three models were employed, the amalgamation of ARD, random forest, and SVR consistently showcased the highest performance.

An important point is that satellite imagery proves valuable in estimating crop variables at a regional scale, yet high-resolution Earth observations often face disruptions due to cloud cover. In this study, cloud interference hindered VI computation in several instances, resulting in varying sample counts across different dates. Moreover, as is common in machine learning applications on real-world data, some variables did not conform to a Gaussian distribution. However, those adhering to this distribution displayed superior performance. Specifically, the VIs exhibited Gaussian distribution from 55 to 115 days after transplanting.

In summary, the results confirm that the Sentinel-2 platform is highly effective in predicting yield at a regional scale. This study proved that indeed advanced sensing techniques may have many applications, especially with the help of the increasing computing power, allowing for more complex

machine learning techniques to be used to find patterns and correlations between canopy reflectance data and specific crop quality characteristics. Overall, the outcomes provide evidence on the diverse platform's accuracy and reliability when it comes to forecasting crop yield across local and broader geographical areas.

4.4.1 Temporal – Level: Yield predictions across years

In yield estimation based on multispectral remote sensing data, the red and NIR bands hold critical significance due to their distinct reflectance properties. This significance arises because the NIR band exhibits high reflectance for green vegetation due to substantial internal leaf scattering, while the red band shows low reflectance owing to chlorophyll absorption as vegetation cover increases. Consequently, there exists a distinct and pronounced reflectance slope between these bands, commonly known as the red-edge (RE) spectral region, residing within the 680 nm to 750 nm range [718]. This region captures the sharp alteration in canopy reflectance. Reflectance within the RE band is highly correlated with various crucial physiological vegetation parameters such as nitrogen and chlorophyll content, portraying an essential indicator of plant pigment status and overall health [719,720]. The presence of a shift in RE within vegetation reflectance signifies alterations in the biological state of plants [721]. For example, Ramoelo et al. used WorldView-2 satellite's RE band reflectances to estimate leaf nitrogen content and above-ground biomass, and concluded that RE bands had the ability to improve leaf nitrogen content and biomass estimation accuracy [722]. Furthermore, the red-edge inflection point (REIP), identifying the wavelength of maximum slope in the RE region, exhibits lower sensitivity to spectral noise induced by soil or atmospheric conditions when estimating chlorophyll content. [723,724]. Current earth resource satellites like RapidEye, WorldView-2, WorldView-3, and Sentinel-2 are equipped with RE bands, amplifying their significance in vegetation assessment.

Notably, the blue band exhibits minimal reflectance over vegetation due to chlorophyll absorption, yet it plays a crucial role in vegetation monitoring through remote sensing data. Various VIs, like the EVI [725] capitalize on the blue band's reflectance to characterize vegetation status. However, the shorter wavelength of the blue band renders it more susceptible to atmospheric influence [726]. On the other hand, the Shortwave Infrared (SWIR) band's sensitivity to foliar water content, attributable to water absorption [727] makes it valuable for biomass estimation, despite not being present in certain operational satellite instruments such as SPOT, Chinese GF-1, and GF-2.

Although various VIs leverage selected spectral bands, their impact on yield estimation accuracy remains understudied. Therefore, it's crucial to explore the potential of spectral bands in enhancing biomass and yield estimation precision.

The Sentinel-2 satellites (comprising S2A and S2B) equipped with Multi-Spectral Instruments (MSI) provide extensive spectral coverage across 13 bands, spanning from visible and near-infrared to shortwave infrared (SWIR) bands. These bands are pivotal for vegetation monitoring and yield prediction. However, not all bands hold equal significance in yield estimation. Some bands might carry more pertinent information, exerting a stronger influence on the accuracy of yield estimation, while others may contain less relevant data for this purpose. As data dimensions expand, there's a consequential rise in computational and storage costs. Furthermore, redundant, noisy, or unreliable data within less important bands can impede the accuracy of yield estimation processes, potentially decreasing overall prediction accuracy.

Previous studies have introduced various methodologies to enhance yield estimation accuracy, including empirical approaches, pixel unmixing models, and physically based models. Despite this, a limited number of studies have underscored the pivotal role of spectral band information specifically in yield estimation. Notably, machine learning regression methods have showcased enhanced accuracy in predicting yields for crops like corn [728] and soybean[439] by leveraging spectral bands. Crusiol et al. suggest that Sentinel-2 Vis/NIR/SWIR images, associated with partial least squares regression and support vector regression, can be used as a fast and reliable proxy for yield monitoring, contributing to better site-specific management of agronomic practices,

economic policies and strategic planning of governmental and corporative decision making over technical issues[729].

To reduce data redundancy, increase computational efficiency and improve yield estimation accuracy, all bands were extracted for the seasons 2021 and 2022 respectively. The AutoML pipeline trained on the 2021 dataset and tested on the 2022 dataset resulted in twenty experiments showcasing various combinations of bands and models for predicting crop yield. Ensemble Machine learning methods enable the development of prediction models using several spectral bands or VIs acquired from the target area, or even their combination (spectral bands and VIs, contributing to the better characterization of the crop development condition across different wavelengths.

The findings suggested that the period between 75 to 90 days was the optimal for accurate yield predictions, based on vegetation indices. This aligns with the reproductive growth phase, commencing approximately 55 days post-transplanting with flowering and extending until about 88 days [311]. Within this phase, crucial developmental events like flower initiation, pollination, fertilization, and fruit set occur, spanning roughly 20 to 40 days depending on environmental factors and cultivar types [730]. Notably, combining bands like 'B4_70' 'B4_90' 'B6_65' 'B12_65 reached an R^2 of 0.65, highlighting their predictive strength. Red Edge/NIR bands (B7 to B8A) between 65 to 95 days post-transplanting showcased significant importance for yield prediction. Surprisingly B12 (R_{2190}) was appeared in this approach, indicating that important information can be retrieved when using it in combination with other bands. It is used in vegetation indices such as Normalized difference water index, NDWI and Normalized multiband drought index, NMDI due to its efficiency in depicting the water potential fluctuations SWIR band's (B12) sensitivity to foliar water content due to water absorption [727] makes it valuable for biomass estimation. In other studies SWIR bands (SWIR-1 and SWIR-2) were highly correlated with canopy cover [731]. and yield estimation [732]. Various combinations utilizing models like Random Forest, ARD Regression, and SVR demonstrated strong predictive capabilities, with ARD Regression standing out as the most promising single model, and its ensemble with SVR as the best-performing combination.

Part 5. Conclusions

One of the key objectives of the study was to provide valuable insights into the trends, patterns, and contributions of precision agriculture methodologies and technologies in the field of crop yield prediction. To this end a systematic literature review was conducted in the Scopus and WoS platforms.

Understanding the geographical distribution of research efforts and the significant academic institutions, in this domain is crucial for comprehending the research landscape. The research revealed that using remote sensing techniques, China and the USA are key contributors to the field of crop yield prediction, while cereal crops (185 papers) emerged as the most extensively researched for yield estimation, with a particular emphasis on wheat. Among the remote sensing platforms utilized, satellites were predominant, followed by UAS platforms and proximal sensors. The systematic review identified NDVI as the most frequently used VI in the studies reviewed. Methodologically, machine learning featured in 142 articles, while deep learning was employed in 62 articles specifically for yield prediction. Statistical methods were prevalent in 157 articles, whereas model-based approaches were present in 60 articles for predicting crop yields.

Notably, machine learning and deep learning techniques exhibited high accuracy in crop yield prediction, although other methodologies also showcased success, contingent upon the crop and approach used. Specifically, in the case of Vegetables and Melons category, statistical methods paired with satellite and UAS measurements dominate, while ML techniques shine with an impressive R^2 value of 0.90. For oilseed crops, exceptional performances ($R^2 > 0.90$) were common, except for palm oil and canola crop. In Fruits and Nuts, vineyards see a surge in studies achieving high performances ($R^2 > 0.90$) through ML/DL methods using proximal or UAS sensing, sometimes alongside satellite data. In the category of Root tuber and other crops, various methods were deployed, with outstanding performances ($R^2 > 0.90$) in Cotton, Sweet Potato, and Perennial Ryegrass, notably driven by ML approaches. Leguminous crop studies extensively leverage diverse data sources (UAS, satellites, proximal sensors), achieving high accuracies ($R^2 > 0.90$) in Alfa Alfa, Red Clover, Chickpea, Snap Bean, and Peas. Cereals employ a wide range of methods and platforms not indicating a clear trend. These findings contributed to a comprehensive understanding of the research domain, offering valuable insights for guiding future steps in crop yield estimation studies.

The study's second objective was to compare satellite, UAS, and proximal technologies thoroughly, emphasizing their unique strengths and limitations when applied in precision agriculture. Focusing on the NDVI as a common metric, data obtained from different proximal and remote sensing methods in a processing tomato crop and evaluate the differences between the NDVI datasets from these different sensing systems in a production context. The results confirmed the substantial similarity between UAS and satellite data, particularly in the later stages of the crop's phenological cycle, suggesting increased agreement as the crop matures. The higher spatial resolution of the UAS is reflected in generally higher NDVI values compared to Sentinel-2, which faces challenges in capturing localized conditions. The research reveals a moderate correlation between proximal sensor data and UAS/satellite datasets, with variations attributed to differences in measurement wavelengths and specific focuses of each platform. While UASs offer excellent spatial resolution and real-time monitoring, their commercial-scale deployment involves significant expenses, making them less practical for small-scale farmers managing multiple fields. Proximal sensors, providing real-time or near-real-time NDVI data, contribute to fast and targeted diagnoses of crop conditions. Their proximity to the target reduces atmospheric interference, ensuring high spatial resolution and accurate data. However, their limitations include area coverage, data interpretation challenges, maintenance requirements, and initial costs. The study recommends a synergistic approach, combining high-resolution UAS images selectively deployed during critical crop phases with satellite imagery for overall field assessment, offering a balanced and cost-effective solution.

Within the study's framework, the examination of VIs dynamics derived from Sentinel-2 images uncovered a narrative detailing the seasonal progression and phenological stages of processing

tomato crops. Notably, the study noted that the lowest mean values for all VIs occurred in the period following transplanting, characterized by limited canopy cover and exposed soil between rows. As the season advanced, there was a gradual increase in canopy cover percentage, particularly during the middle of the season when tomato plants attained peak vigor just before reallocating sugars to their fruits. Specifically, the highest mean VI levels were observed in July, corresponding to the tomato emergence stage, occurring between 75 to 95 days after planting, revealing a distinctive pattern in the annual growth dynamics of tomato plants, effectively captured and elucidated by vegetation index values.

The main objective of this study investigates the efficacy of various sensing platforms, including UAS, proximal, and satellite-derived VIs, in predicting the yield of processing tomato varieties. Adopting a dual approach, the research examines both field-level and regional perspectives to offer insights applicable to different scales.

At the field level approach, the study utilized the GreenSeeker proximal sensor, UAS, and Sentinel-2 satellite imagery to assess crop vigor across ten fields. Results highlight distinctive performance patterns of sensing platforms during different growth stages. The proximal sensor exhibits higher explanatory power in the early canopy growth phase, while UAS and Sentinel platforms improve as canopy coverage increases. The Sentinel platform outperforms others during the critical flowering stage, emphasizing its effectiveness in elucidating yield variability. Yield predictions, extrapolated using the average number of plants per hectare, show variations but overall demonstrate the promise of the yield sampling strategy for estimating crop yield with reasonable accuracy, despite some discrepancies. The temporal aspect emerges as critical, with later growth phases providing a solid foundation for data convergence and correlation. The study highlights the importance of selecting the appropriate sensing platform based on the specific growth stage, with Sentinel consistently effective across various stages. However, in the year 2021, the correlation between crop yield and NDVI datasets at field level approach declines significantly across all platforms, with the limited dataset size potentially contributing to this observed decline and the diminished statistical significance.

Acknowledging the complexity of estimating crop production and addressing the need for a precise farm yield dataset the study shifted to a regional scale integrating machine learning techniques with VI data retrieved from satellite platform. While prior research has explored correlations between VIs and crop production, the extensive use of machine learning for estimating processing tomato yield has not been thoroughly investigated until now. Previous studies have extensively investigated correlation and regression models linking VIs with crop production, alongside employing machine learning methods for crop yield estimation. However, the widespread exploration of AutoML, as detailed earlier, remains limited in this context. Within agriculture, AutoML techniques have been documented primarily for time series processing and analysis of proximal and satellite imagery [733,734], weed identification [735], and forecasting quality attributes in grapes [736]. An analysis of five different VIs over the growing season reveals their optimal performance during the 85 to 90-day period after transplanting, with RVI exhibiting superior predictive capabilities. Despite early growth stages showing poor correlation between VIs and yield, the study identifies promising relationships, particularly in the later stages of crop development. The investigation incorporates basic statistics using the Pearson correlation coefficient, emphasizing the optimal performance of VIs during specific growth stages. Machine learning algorithms, integrated to enhance yield prediction accuracy, identified RVI and SAVI as the best-performing VIs for yield predictions, achieving high R^2 values and low RMSEs, especially at 90 days after transplanting. Ensembles consisting of two regressors emerge as the optimal choice for enhanced predictive accuracy. The combination of ARD regression and SVR proves frequently successful in creating ensembles, emphasizing the effectiveness of combining different regressors. The study recognizes challenges such as cloud cover in satellite imagery but highlights the potential of machine learning in leveraging such data for precise crop yield predictions on a regional scale.

Aiming at improving yield estimation accuracy, all bands were extracted for the seasons 2021 and 2022 respectively. In this study, the various ensemble models were trained using the Sentinel-2

reflectance's, which provided an indication for each band reflectance to represent the importance degree for yield estimation. Prominent spectral bands, such as those involving B4, B6, B7, B8, and B8A, demonstrated exceptional predictive power within the 80 to 90 days post-transplanting window. Effective VIs, notably RVI and NDVI with spectral bands B8, B7 and B8A showcased strong predictive capabilities. Similarly, RVI_B8_90, RVI_B7_90, and RVI_B8A_90 showed equivalent performance. Combining bands [B4_70, B4_90, B6_65, B12_65] stands out with an adjusted R^2 of 0.65 and an RMSE of 1.19., highlighting their predictive strength. This research will be extended, evaluating different machine learning algorithms/pipelines, thus increasing predictive power, and providing a more reliable and sustainable solution that can be used in the long term. Bagging, boosting or stacking as ensemble frameworks that reuse the best performing pipelines will be implemented to investigate whether they could lead to better performance.

Part 6. Future work

As the global population continues to grow, the role of PA becomes increasingly pivotal in bolstering productivity, conserving resources, and curbing environmental impact [555]. Yield prediction stands out as a crucial strategy within PA, empowering farmers and the agricultural sector to make informed decisions, effectively manage resources, and optimize various production stages, from harvesting to logistics. This predictive capability yields increased productivity and substantial cost savings. It enables farmers to identify and address areas with lower yield potential due to factors like inadequate irrigation or poor soil fertility, leading to targeted interventions that enhance overall farm yields. The long-term viability of small and medium-sized farms, critical to the agriculture industry's growth, can be sustained by the profitability improvements facilitated by precision agriculture. Consequently, there is an urgent need for accessible and affordable precision agriculture technologies and techniques through further research and development.

Based on this research some specific areas that need further research are:

1)Integration to crop modelling: Integrating annual VI dynamics into models for tomato crops can streamline crop identification, mapping, and monitoring of crop growth phases. This integration can be complemented by leveraging weather data, particularly in gauging parameters like thermal days, which are instrumental in estimating tomato maturity accurately.

2) The development of more accurate sensors and monitoring systems: The findings presented in this research are encouraging for the development of a large-scale monitoring system, especially based on the strategic use of remote sensor platforms. Identifying the factors contributing to yield variability enables farmers to develop strategies that ensure consistent and reliable harvests. Additionally, timely yield forecasts serve as a valuable risk management tool, enabling farmers to proactively plan for potential threats, such as severe weather events or pest outbreaks, allowing them to take swift actions to mitigate their impact on crop yield [137].

3) Enhancing the accuracy of forecasting models remains a key focus. Exploring the potential of spectral band reflectance coupled with advanced machine learning algorithms is a crucial step toward refining crop yield prediction accuracy. These advancements are imperative, especially given the impact of climate change on tomato production. Precision agriculture techniques can mitigate these effects and also facilitate better pest and disease management, reducing dependence on harmful chemicals.

The ongoing evolution of precision agriculture technologies and methodologies underscores the potential to significantly enhance agricultural efficiency, sustainability, and profitability. The use of these techniques can help farmers better manage pests and diseases and reduce the need for harmful chemicals. Overall, the potential benefits of precision agriculture are significant and there is a strong demand for research and development in this area. If researchers and practitioners continue to advance precision agriculture technologies and techniques, they can help improve the efficiency, sustainability and profitability of crop production.

Part 7. References

1. Precision Ag Definition | International Society of Precision Agriculture Available online: https://www.ispag.org/about/definition (accessed on 26 October 2023).
2. Thayer, A.W.; Vargas, A.; Castellanos, A.A.; Lafon, C.W.; McCarl, B.A.; Roelke, D.L.; Winemiller, K.O.; Lacher, T.E. Integrating Agriculture and Ecosystems to Find Suitable Adaptations to Climate Change. *Climate* **2020**, *8*, 10, doi:10.3390/cli8010010.
3. Nassani, A.A.; Awan, U.; Zaman, K.; Hyder, S.; Aldakhil, A.M.; Abro, M.M.Q. Management of Natural Resources and Material Pricing: Global Evidence. *Resources Policy* **2019**, *64*, 101500, doi:10.1016/j.resourpol.2019.101500.
4. Conrad, Z.; Niles, M.T.; Neher, D.A.; Roy, E.D.; Tichenor, N.E.; Jahns, L. Relationship between Food Waste, Diet Quality, and Environmental Sustainability. *PLOS ONE* **2018**, *13*, e0195405, doi:10.1371/journal.pone.0195405.
5. Benos, L.; Bechar, A.; Bochtis, D. Safety and Ergonomics in Human-Robot Interactive Agricultural Operations. *Biosystems Engineering* **2020**, *200*, 55–72, doi:10.1016/j.biosystemseng.2020.09.009.
6. WHO World Hunger Is Still Not Going down after Three Years and Obesity Is Still Growing – UN Report Available online: https://www.who.int/news/item/15-07-2019-world-hunger-is-still-not-going-down-after-three-years-and-obesity-is-still-growing-un-report (accessed on 17 May 2023).
7. The-Sustainable-Development-Goals-Report-2022.Pdf.
8. Tey, Y.S.; Brindal, M. Factors Influencing the Adoption of Precision Agricultural Technologies: A Review for Policy Implications. *Precision Agriculture* **2012**, *13*, doi:10.1007/s11119-012-9273-6.
9. Sishodia, R.P.; Shukla, S.; Graham, W.D.; Wani, S.P.; Jones, J.W.; Heaney, J. Current and Future Groundwater Withdrawals: Effects, Management and Energy Policy Options for a Semi-Arid Indian Watershed. *Advances in Water Resources* **2017**, *110*, 459–475, doi:10.1016/j.advwatres.2017.05.014.
10. Konikow, L.F.; Kendy, E. Groundwater Depletion: A Global Problem. *Hydrogeol J* **2005**, *13*, 317–320, doi:10.1007/s10040-004-0411-8.
11. Wen, F.; Chen, X. Evaluation of the Impact of Groundwater Irrigation on Streamflow in Nebraska. *Journal of Hydrology* **2006**, *327*, 603–617, doi:10.1016/j.jhydrol.2005.12.016.
12. Kleinman, P.J.A.; Sharpley, A.N.; McDowell, R.W.; Flaten, D.N.; Buda, A.R.; Tao, L.; Bergstrom, L.; Zhu, Q. Managing Agricultural Phosphorus for Water Quality Protection: Principles for Progress. *Plant Soil* **2011**, *349*, 169–182, doi:10.1007/s11104-011-0832-9.
13. Konikow, L.F. Long-Term Groundwater Depletion in the United States. *Groundwater* **2015**, *53*, 2–9, doi:10.1111/gwat.12306.
14. Stoate, C.; Báldi, A.; Beja, P.; Boatman, N.D.; Herzon, I.; van Doorn, A.; de Snoo, G.R.; Rakosy, L.; Ramwell, C. Ecological Impacts of Early 21st Century Agricultural Change in Europe – A Review. *Journal of Environmental Management* **2009**, *91*, 22–46, doi:10.1016/j.jenvman.2009.07.005.
15. Vitousek, P.M.; Naylor, R.; Crews, T.; David, M.B.; Drinkwater, L.E.; Holland, E.; Johnes, P.J.; Katzenberger, J.; Martinelli, L.A.; Matson, P.A.; et al. Nutrient Imbalances in Agricultural Development. *Science* **2009**, *324*, 1519–1520, doi:10.1126/science.1170261.
16. Nitrogen in Agriculture: Balancing the Cost of an Essential Resource | Annual Review of Environment and Resources Available online: https://www.annualreviews.org/doi/abs/10.1146/annurev.environ.032108.105046 (accessed on 9 September 2023).
17. Quinton, J.N.; Govers, G.; Van Oost, K.; Bardgett, R.D. The Impact of Agricultural Soil Erosion on Biogeochemical Cycling. *Nature Geosci* **2010**, *3*, 311–314, doi:10.1038/ngeo838.
18. Lal, R. Enhancing Eco-Efficiency in Agro-Ecosystems through Soil Carbon Sequestration. *Crop Science* **2010**, *50*, S-120-S-131, doi:10.2135/cropsci2010.01.0012.

19. Montgomery, D.R. Soil Erosion and Agricultural Sustainability. *Proceedings of the National Academy of Sciences* **2007**, *104*, 13268–13272, doi:10.1073/pnas.0611508104.
20. Lal, R. Soil Carbon Sequestration Impacts on Global Climate Change and Food Security. *Science* **2004**, *304*, 1623–1627, doi:10.1126/science.1097396.
21. Hendricks, G.S.; Shukla, S.; Roka, F.M.; Sishodia, R.P.; Obreza, T.A.; Hochmuth, G.J.; Colee, J. Economic and Environmental Consequences of Overfertilization under Extreme Weather Conditions. *Journal of Soil and Water Conservation* **2019**, *74*, 160–171, doi:10.2489/jswc.74.2.160.
22. Delgado, J.A.; Short, N.M.; Roberts, D.P.; Vandenberg, B. Big Data Analysis for Sustainable Agriculture on a Geospatial Cloud Framework. *Frontiers in Sustainable Food Systems* **2019**, *3*.
23. Fountas, S.; Blackmore, S.; Ess, D.; Hawkins, S.; Blumhoff, G.; Lowenberg-Deboer, J.; Sorensen, C.G. Farmer Experience with Precision Agriculture in Denmark and the US Eastern Corn Belt. *Precision Agric* **2005**, *6*, 121–141, doi:10.1007/s11119-004-1030-z.
24. Socioeconomic Profiles of Early Adopters of Precision Agriculture Technologies. *Journal of Agribusiness* **1998**, doi:10.22004/ag.econ.90442.
25. Precision Agriculture Definitions Available online: https://www.grap.udl.cat/en/presentacio/que-fem/definicions-agricultura-de-precisio/index.html (accessed on 3 September 2023).
26. Trivelli, L.; Apicella, A.; Chiarello, F.; Rana, R.; Fantoni, G.; Tarabella, A. From Precision Agriculture to Industry 4.0: Unveiling Technological Connections in the Agrifood Sector. *British Food Journal* **2019**, *121*, 1730–1743, doi:10.1108/BFJ-11-2018-0747.
27. Pierce, F.J.; Nowak, P. Aspects of Precision Agriculture. In *Advances in Agronomy*; Sparks, D.L., Ed.; Academic Press, 1999; Vol. 67, pp. 1–85.
28. Kirchmann, H.; Thorvaldsson, G. Challenging Targets for Future Agriculture. *European Journal of Agronomy* **2000**, *12*, 145–161, doi:10.1016/S1161-0301(99)00053-2.
29. Stafford, J.V. Implementing Precision Agriculture in the 21st Century. *Journal of Agricultural Engineering Research* **2000**, *76*, 267–275, doi:10.1006/jaer.2000.0577.
30. Zhang, N.; Wang, M.; Wang, N. Precision Agriculture—a Worldwide Overview. *Computers and Electronics in Agriculture* **2002**, *36*, 113–132, doi:10.1016/S0168-1699(02)00096-0.
31. Blackmore, S.; Godwin, R.J.; Fountas, S. The Analysis of Spatial and Temporal Trends in Yield Map Data over Six Years. *Biosystems Engineering* **2003**, *84*, 455–466, doi:10.1016/S1537-5110(03)00038-2.
32. Bongiovanni, R.; Lowenberg-Deboer, J. Precision Agriculture and Sustainability. *Precision Agriculture* **2004**, *5*, 359–387, doi:10.1023/B:PRAG.0000040806.39604.aa.
33. McBratney, A.; Whelan, B.; Ancev, T.; Bouma, J. Future Directions of Precision Agriculture. *Precision Agric* **2005**, *6*, 7–23, doi:10.1007/s11119-005-0681-8.
34. Fountas, S.; Aggelopoulou, K.; Gemtos, T.A. Precision Agriculture. In *Supply Chain Management for Sustainable Food Networks*; John Wiley & Sons, Ltd, 2015; pp. 41–65 ISBN 978-1-118-93749-5.
35. Haneklaus, S. An Agronomic, Ecological and Economic Assessment of Site-Specific Fertilisation. *Landbauforschung Völkenrode*.
36. Mulla, D.; Khosla, R. Historical Evolution and Recent Advances in Precision Farming.
37. Lowenberg-DeBoer, J.; Erickson, B. Setting the Record Straight on Precision Agriculture Adoption. *Agronomy Journal* **2019**, *111*, 1552–1569, doi:10.2134/agronj2018.12.0779.
38. Fountas, S.; Pedersen, S.M.; Blackmore, S. ICT in Precision Agriculture – Diffusion of Technology.
39. Pathak, H.S.; Brown, P.; Best, T. A Systematic Literature Review of the Factors Affecting the Precision Agriculture Adoption Process. *Precision Agric* **2019**, *20*, 1292–1316, doi:10.1007/s11119-019-09653-x.
40. Subeesh, A.; Mehta, C.R. Automation and Digitization of Agriculture Using Artificial Intelligence and Internet of Things. *Artificial Intelligence in Agriculture* **2021**, *5*, 278–291, doi:10.1016/j.aiia.2021.11.004.

41. Brustein, J. GPS as We Know It Happened Because of Ronald Reagan. *Bloomberg. com* **2014**.
42. Rip, M.R.; Hasik, J.M. *The Precision Revolution: GPS and the Future of Aerial Warfare*; Naval Institute Press, 2002; ISBN 978-1-55750-973-4.
43. Civilian Applications | Time and Navigation Available online: https://timeandnavigation.si.edu/satellite-navigation/who-uses-satellite-navigation/civilian-applications (accessed on 8 September 2023).
44. Khosla 10th ICPA History.Pdf.
45. About Us - Ag Leader - Farming Products & Solutions.
46. Vellidis: Simultaneous Assessment of Cotton Yield Monitors - Google Scholar Available online: https://scholar.google.com/scholar_lookup?oi=gsb80&publisher=American%20Society%20of%20Agricultural%20and%20Biological%20Engineers&language=English&title=SIMULTANEOUS%20ASSESSMENT%20OF%20COTTON%20YIELD%20MONITOR&doi=10.13031%2F2013.13658&author=G.%20Vellidis&author=C.%20D.%20Perry&author=G.C.%20Rains&author=D.%20L.%20Thomas&author=N.%20Wells&firstpage=259&volume=19&issue=3&journal_title=Applied%20Engineering%20in%20Agriculture&publication_year=2003&lookup=0&hl=en (accessed on 8 September 2023).
47. *Precision Agriculture*; A, W., J, S., Eds.; Wageningen Academic Publishers, 2003; ISBN 978-90-76998-21-3.
48. Coalition to Save Our GPS Available online: https://rasky.com/success-stories/coalition-to-save-our-gps/ (accessed on 8 September 2023).
49. Rutto, E.; Arnall, D.B. The History of the GreenSeeker TM Sensor. *Oklahoma Cooperative Extension Fact Sheets. Oklahoma State University, Stillwater, Oklahoma* **2017**.
50. Soil pH Sensor Commercialized Available online: https://ag.purdue.edu/ssmc/frames/dec2003_purdue_nl1.htm (accessed on 8 September 2023).
51. Trimble Combines GPS Guidance and Rate Control to Automate Agricultural Spraying Operations | Trimble, Inc. Available online: https://investor.trimble.com/news-releases/news-release-details/trimble-combines-gps-guidance-and-rate-control-automate (accessed on 8 September 2023).
52. Timeline - Hands Free Hectare Available online: https://www.handsfreehectare.co.uk/timeline.html (accessed on 8 September 2023).
53. Giovos, R.; Tassopoulos, D.; Kalivas, D.; Lougkos, N.; Priovolou, A. Remote Sensing Vegetation Indices in Viticulture: A Critical Review. *Agriculture* **2021**, *11*, 457, doi:10.3390/agriculture11050457.
54. Bramley, R.G.V.; Proffitt, A.P.B. Managing Variability in Viticultural Production. *Grapegrower and Winemaker* **1999**, *427*, 11–16.
55. Pena-Yewtukhiw, E.M.; Grove, J.H.; Beck, E.G. Nonparametric Geostatistics/Probabilistic Sourcing of Nitrate to a Contaminated Well. *Proceedings of the 5th International Conference on Precision Agriculture, Bloomington, Minnesota, USA, 16-19 July, 2000* **2000**, 1–12.
56. Werner, A.; Dölling, S.; Jarfe, A.; Kühn, J.; Pauly, J.; Roth, R. Deriving Maps of Yield-Potentials with Crop Models, Site Information and Remote Sensing. *Proceedings of the 5th International Conference on Precision Agriculture, Bloomington, Minnesota, USA, 16-19 July, 2000* **2000**, 1–20.
57. Lowenberg-BeBoer, J. Economics of Precision Farming: Payoff in the Future. *Soil Science News and Views* **1997**, *18*.
58. Robertson, M.; Carberry, P.; Brennan, L. The Economic Benefits of Precision Agriculture: Case Studies from Australian Grain Farms. *Crop and Pasture Science* **2007**, *60*.
59. Griffin, T.; Lowenberg-DeBoer, J. Worldwide Adoption and Profitability of Precision Agriculture. *Revista de Politica Agricola* **2005**, *14*, 20–38.
60. *Farm Profits and Adoption of Precision Agriculture*; Schimmelpfennig, D., Ed.; Economic Research Report; 2016;

61. Timmermann, C.; Gerhards, R.; Kühbauch, W. The Economic Impact of Site-Specific Weed Control. *Precision Agriculture* **2003**, *4*, 249–260, doi:10.1023/A:1024988022674.
62. Heisel: Weed Managing Model for Patch Spraying in Cereal - Μελετητής Google Available online: https://scholar.google.com/scholar_lookup?title=Weed%20managing%20model%20for%20patch%20spraying%20in%20cereal&pages=999-1007&publication_year=1996&author=Heisel%2CT&author=Christensen%2CS&author=Walter%2CA (accessed on 8 September 2023).
63. Biermachera: The Economic Potential of Precision... - Μελετητής Google Available online: https://scholar.google.com/scholar_lookup?title=The%20economic%20potential%20of%20precision%20nitrogen%20application%20with%20wheat%20based%20on%20plant%20sensing&journal=Agricultural%20Economics&doi=10.1111%2Fj.1574-0862.2009.00387.x&volume=40&pages=397-407&publication_year=2009&author=Biermachera%2CJT&author=Brorsenb%2CBW&author=Epplinb%2CFM&author=Soliec%2CJB&author=Raun%2CWR (accessed on 8 September 2023).
64. Farming Soils, Not Fields: A Strategy for Increasing Fertilizer Profitability - Carr - 1991 - Journal of Production Agriculture - Wiley Online Library Available online: https://acsess.onlinelibrary.wiley.com/doi/abs/10.2134/jpa1991.0057?casa_token=MPazF1iKF_IAAAAA:pDwo72u2AcLLOq3AENQPAGS8wOeVFhtNxx3o8Mjdg_w3vqth5CTCrrpWHalSGS41mv8TyVu2vR4y0oaU (accessed on 8 September 2023).
65. Swinton, S.M.; Lowenberg-DeBoer, J. Evaluating the Profitability of Site-Specific Farming. *Journal of Production Agriculture* **1998**, *11*, 439–446, doi:10.2134/jpa1998.0439.
66. Average Returns and Risk Characteristics of Site Specific P and K Management: Eastern Corn Belt On-Farm Trial Results - Lowenberg-DeBoer - 1999 - Journal of Production Agriculture - Wiley Online Library Available online: https://acsess.onlinelibrary.wiley.com/doi/abs/10.2134/jpa1999.0276?casa_token=vcqGnPYQsUMAAAAA:6q1MnGyFiEinmI_AntjG9yiEFPNEjfqes3tx4s8u81MmbApBnu9DfC8DsZgYAzg-xja1pf3csETErtYp (accessed on 8 September 2023).
67. APPLICATIONS OF A FIELD–LEVEL GEOGRAPHIC INFORMATION SYSTEM (FIS) IN PRECISION AGRICULTURE Available online: https://doi.org/10.13031/2013.6829 (accessed on 28 October 2023).
68. Runquist, S.; Zhang, N.; Taylor, R.K. Development of a Field-Level Geographic Information System. *Computers and Electronics in Agriculture* **2001**, *31*, 201–209, doi:10.1016/S0168-1699(00)00155-1.
69. Burlacu, G.; Costa, R.; Sarraipa, J.; Jardim-Golcalves, R.; Popescu, D. A Conceptual Model of Farm Management Information System for Decision Support. In Proceedings of the Technological Innovation for Collective Awareness Systems; Camarinha-Matos, L.M., Barrento, N.S., Mendonça, R., Eds.; Springer: Berlin, Heidelberg, 2014; pp. 47–54.
70. Saiz-Rubio, V.; Rovira-Más, F. From Smart Farming towards Agriculture 5.0: A Review on Crop Data Management. *Agronomy* **2020**, *10*, 207, doi:10.3390/agronomy10020207.
71. Tzounis, A.; Katsoulas, N.; Bartzanas, T.; Kittas, C. Internet of Things in Agriculture, Recent Advances and Future Challenges. *Biosystems Engineering* **2017**, *164*, 31–48, doi:10.1016/j.biosystemseng.2017.09.007.
72. Gralla, P. Precision Agriculture Yields Higher Profits, Lower Risks. *Hewlett Packard Enterprise* **2018**.
73. Post, S. What Is IoT in Agriculture? Farmers Aren't Quite Sure Despite $4bn US Opportunity - Report Available online: https://agfundernews.com/iot-agriculture-farmers-arent-quite-sure-despite-4bn-us-opportunity (accessed on 9 September 2023).
74. From Dirt to Data: The Second Green Revolution and the Internet of Things Available online: https://www2.deloitte.com/content/www/us/en/insights/deloitte-review/issue-18/second-green-revolution-and-internet-of-things.html (accessed on 9 September 2023).

75. Mykleby, M.; Doherty, P.; Makower, J. *The New Grand Strategy: Restoring America's Prosperity, Security, and Sustainability in the 21st Century*; St. Martin's Publishing Group, 2016; ISBN 978-1-4668-8389-5.
76. Kunisch, M. Big Data in Der Landwirtschaft – Perspektiven Eines Datendienstleisters. *LANDTECHNIK* **2016**, 1-3 Seiten, doi:10.15150/LT.2016.3117.
77. Kamilaris, A.; Kartakoullis, A.; Prenafeta-Boldú, F.X. A Review on the Practice of Big Data Analysis in Agriculture. *Computers and Electronics in Agriculture* **2017**, *143*, 23–37, doi:10.1016/j.compag.2017.09.037.
78. Wolfert, S.; Ge, L.; Verdouw, C.; Bogaardt, M.-J. Big Data in Smart Farming – A Review. *Agricultural Systems* **2017**, *153*, 69–80, doi:10.1016/j.agsy.2017.01.023.
79. Agriculture, I.C. for T.; Institute, I.F.P.R.; Agriculture, C.P. for B.D. in CGIAR Big Data Coordination Platform Full Proposal. **2016**.
80. Navarro-Hellín, H.; Martínez-del-Rincon, J.; Domingo-Miguel, R.; Soto-Valles, F.; Torres-Sánchez, R. A Decision Support System for Managing Irrigation in Agriculture. *Computers and Electronics in Agriculture* **2016**, *124*, 121–131, doi:10.1016/j.compag.2016.04.003.
81. FieldNET Resources | Lindsay Irrigation Available online: https://www.lindsay.com/mea/en/irrigation/brands/fieldnet/resources/ (accessed on 9 September 2023).
82. Lindsay's FieldNET® Technology Receives National Recognition for Innovative Design Available online: https://www.lindsay.com/lam/es/resource/lindsays-fieldnet-technology-receives-national-recognition-for-innovative-design/ (accessed on 9 September 2023).
83. Richards, Q.D.; Bange, M.P.; Johnston, S.B. HydroLOGIC: An Irrigation Management System for Australian Cotton. *Agricultural Systems* **2008**, *98*, 40–49, doi:10.1016/j.agsy.2008.03.009.
84. Damos, P.; Karabatakis, S. Real Time Pest Modeling through the World Wide Web: Decision Making from Theory to Praxis.
85. He, J.; Wang, J.; He, D.; Dong, J.; Wang, Y. The Design and Implementation of an Integrated Optimal Fertilization Decision Support System. *Mathematical and Computer Modelling* **2011**, *54*, 1167–1174, doi:10.1016/j.mcm.2010.11.050.
86. Walker, T.; Friday, J.; Casimero, M.; Dollentas, R.; Mataia, A.; Acda, R.; Yost, R. The Early Economic Impact of a Nutrient Management Decision Support System (NuMaSS) on Small Farm Households Cultivating Maize on Acidic, Upland Soils in the Philippines. *Agricultural Systems* **2009**, *101*, 162–172, doi:10.1016/j.agsy.2009.05.004.
87. Recio, B.; Rubio, F.; Criado, J.A. A Decision Support System for Farm Planning Using AgriSupport II. *Decision Support Systems* **2003**, *36*, 189–203, doi:10.1016/S0167-9236(02)00134-3.
88. Welch, S.M.; Jones, J.W.; Brennan, M.W.; Reeder, G.; Jacobson, B.M. PCYield: Model-Based Decision Support for Soybean Production. *Agricultural Systems* **2002**, *74*, 79–98, doi:10.1016/S0308-521X(02)00022-7.
89. CIGR Handbook of Agricultural Engineering | CIGR Available online: https://cigr.org/node/640 (accessed on 9 September 2023).
90. Zambon, I.; Cecchini, M.; Egidi, G.; Saporito, M.G.; Colantoni, A. Revolution 4.0: Industry vs. Agriculture in a Future Development for SMEs. *Processes* **2019**, *7*, 36, doi:10.3390/pr7010036.
91. Choi, K.H.; Han, S.K.; Han, S.H.; Park, K.-H.; Kim, K.-S.; Kim, S. Morphology-Based Guidance Line Extraction for an Autonomous Weeding Robot in Paddy Fields. *Computers and Electronics in Agriculture* **2015**, *113*, 266–274, doi:10.1016/j.compag.2015.02.014.
92. Intelligence: Global Agricultural Robots: Market... - Μελετητής Google Available online: https://scholar.google.com/scholar_lookup?title=Global+Agriculture+Robots.+Market+Size,+Status+and+Forecast+to+2025&author=Verified+Market+Intelligence&publication_year=2018 (accessed on 9 September 2023).
93. Walch, K. How AI Is Transforming Agriculture Available online: https://www.forbes.com/sites/cognitiveworld/2019/07/05/how-ai-is-transforming-agriculture/ (accessed on 9 September 2023).

94. Bechar, A.; Vigneault, C. Agricultural Robots for Field Operations: Concepts and Components. *Biosystems Engineering* **2016**, *149*, 94–111, doi:10.1016/j.biosystemseng.2016.06.014.
95. Bechar, A.; Vigneault, C. Agricultural Robots for Field Operations. Part 2: Operations and Systems. *Biosystems Engineering* **2017**, *153*, 110–128, doi:10.1016/j.biosystemseng.2016.11.004.
96. Bergerman, M.; Billingsley, J.; Reid, J.; van Henten, E. Robotics in Agriculture and Forestry. In *Springer Handbook of Robotics*; Siciliano, B., Khatib, O., Eds.; Springer Handbooks; Springer International Publishing: Cham, 2016; pp. 1463–1492 ISBN 978-3-319-32552-1.
97. Reddy, N.; Vishnu, A.; Reddy, A.; Pranavadithya, S.; Kumar, J.J. A Critical Review on Agricultural Robots. *International Association of Engineering and Management Education* **2016**, *7*, 183–188.
98. Shamshiri: Research and Development in Agricultural... - Μελετητής Google Available online: https://scholar.google.com/scholar_lookup?title=Research+and+development+in+agricultural+robotics:+A+perspective+of+digital+farming&author=Shamshiri,+R.R.&author=Weltzien,+C.&author=Hameed,+I.A.&author=Yule,+I.J.&author=Grift,+T.E.&author=Balasundram,+S.K.&author=Pitonakova,+L.&author=Ahmad,+D.&author=Chowdhary,+G.&publication_year=2018&journal=Int.+J.+Agric.+Biol.+Eng.&volume=11&pages=1%E2%80%9314&doi=10.25165/j.ijabe.20181104.4278 (accessed on 9 September 2023).
99. AI, Robotics, And The Future Of Precision Agriculture - CB Insights Research Available online: https://www.cbinsights.com/research/ai-robotics-agriculture-tech-startups-future/ (accessed on 9 September 2023).
100. Murugesan: Artificial Intelligence and Agriculture 5. 0 - Μελετητής Google Available online: https://scholar.google.com/scholar_lookup?title=Artificial+Intelligence+and+Agriculture+5.+0&author=Murugesan,+R.&author=Sudarsanam,+S.K.&author=Malathi,+G.&author=Vijayakumar,+V.&author=Neelanarayanan,+V.&author=Venugopal,+R.&author=Rekha,+D.&author=Summit,+S.&author=Rahul,+B.&author=Atishi,+M.&publication_year=2019&journal=Int.+J.+Recent+Technol.+Eng.+(IJRTE)&volume=8&pages=8 (accessed on 9 September 2023).
101. Lamborelle, A.; Álvarez, L.F. Farming 4.0: The Future of Agriculture? Available online: https://www.euractiv.com/section/agriculture-food/infographic/farming-4-0-the-future-of-agriculture/ (accessed on 9 September 2023).
102. Big Data and the Ag Sector: More than Lots of Numbers. *International Food and Agribusiness Management Review* **2014**, doi:10.22004/ag.econ.163351.
103. Ag Tech Deal Activity More Than Triples Available online: https://www.cbinsights.com/research/agriculture-farm-tech-startup-funding-trends/ (accessed on 9 September 2023).
104. Grand View Research: Precision Farming Market Analysis.... - Μελετητής Google Available online: https://scholar.google.com/scholar_lookup?title=Precision+Farming+Market+Analysis.+Estimates+and+Trend+Analysis&author=Grand+View+Research&publication_year=2019 (accessed on 9 September 2023).
105. Montzka, S.A.; Dlugokencky, E.J.; Butler, J.H. Non-CO2 Greenhouse Gases and Climate Change. *Nature* **2011**, *476*, 43–50, doi:10.1038/nature10322.
106. Mulla, D.J.; Perillo, C.A.; Cogger, C.G. A Site-Specific Farm-Scale GIS Approach for Reducing Groundwater Contamination by Pesticides. *Journal of Environmental Quality* **1996**, *25*, 419–425, doi:10.2134/jeq1996.00472425002500030006x.
107. Khanna, M.; Zilberman, D. Incentives, Precision Technology and Environmental Protection. *Ecological Economics* **1997**, *23*, 25–43, doi:10.1016/S0921-8009(96)00553-8.
108. Oriade, C.A.; King, R.P.; Forcella, F.; Gunsolus, J.L. A Bioeconomic Analysis of Site-Specific Management for Weed Control. *Review of Agricultural Economics* **1996**, *18*, 523–535, doi:10.2307/1349587.
109. Schnitkey: Precision Agriculture Technologies: Do... - Μελετητής Google Available online: https://scholar.google.com/scholar_lookup?title=Precision%20agriculture%20technologies%3

A%20do%20they%20have%20environmental%20benefits%3F&journal=Ohio%E2%80%99s%20Challenge&volume=10&pages=16-19&publication_year=1997&author=Schnitkey%2CG&author=Hopkins%2CJ (accessed on 9 September 2023).

110. Hudson, D.; Hite, D. Producer Willingness to Pay for Precision Application Technology: Implications for Government and the Technology Industry. *Canadian Journal of Agricultural Economics/Revue canadienne d'agroeconomie* **2003**, *51*, 39–53, doi:10.1111/j.1744-7976.2003.tb00163.x.
111. Reichardt, M.; Jürgens, C. Adoption and Perspective of Precision Farming (PF) in Germany: Results of Several Surveys among the Different Agricultural Target Groups. *Precision Agriculture* **2009**, *10*, 73–94, doi:10.1007/s11119-008-9101-1.
112. Balafoutis, A.T.; Evert, F.K.V.; Fountas, S. Smart Farming Technology Trends: Economic and Environmental Effects, Labor Impact, and Adoption Readiness. *Agronomy* **2020**, *10*, 743, doi:10.3390/agronomy10050743.
113. Maloku, D.; Balogh, P.; Bai, A.; Gabnai, Z.; Lengyel, P. Trends in Scientific Research on Precision Farming in Agriculture Using Science Mapping Method. *International Review of Applied Sciences and Engineering* **2020**, *11*, 232–242, doi:10.1556/1848.2020.00086.
114. Say, S.M.; Keskin, M.; Sehri, M.; Sekerli, Y.E. Adoption of Precision Agriculture Technologies in Developed and Developing Countries. *The Online Journal of Science and Technology-January* **2018**, *8*, 7–15.
115. Lambert, D.M.; Paudel, K.P.; Larson, J.A. Bundled Adoption of Precision Agriculture Technologies by Cotton Producers. *Journal of Agricultural and Resource Economics* **2015**, *40*, 325–345.
116. Robertson, M.J.; Llewellyn, R.S.; Mandel, R.; Lawes, R.; Bramley, R.G.V.; Swift, L.; Metz, N.; O'Callaghan, C. Adoption of Variable Rate Fertiliser Application in the Australian Grains Industry: Status, Issues and Prospects. *Precision Agric* **2012**, *13*, 181–199, doi:10.1007/s11119-011-9236-3.
117. Batte, M.T.; Jones, E.; Schnitkey, G.D. Computer Use by Ohio Commercial Farmers. *American Journal of Agricultural Economics* **1990**, *72*, 935–945, doi:10.2307/1242625.
118. Roberts, R.; English, B.; Larson, J.; Cochran, R.; Goodman, W.; Larkin, S.; Marra, M.; Martin, S.; Shurley, W.; Reeves, J. Adoption of Site-Specific Information and Variable Rate Technologies in Cotton Precision Farming. *Journal of Agricultural & Applied Economics* **2004**, *36*, 143–158, doi:10.1017/S107407080002191X.
119. Larson, J.; Roberts, R.; English, B.; Larkin, S.; Marra, M.; Martin, S.; Paxton, K.; Reeves, J. Factors Affecting Farmer Adoption of Remotely Sensed Imagery for Precision Management in Cotton Production. *Precis. Agric.* **2008**, *9*, 195–208, doi:10.1007/s11119-008-9065-1.
120. Khanna, M. Sequential Adoption of Site-Specific Technologies and Its Implications for Nitrogen Productivity: A Double Selectivity Model. *American Journal of Agricultural Economics* **2001**, *83*, doi:10.1111/0002-9092.00135.
121. Adhikari, A.; Mishra, A.K.; Chintawar, S. Adoption of Technology and Its Impact on Profitability of Young and Beginning Farmers: A Quantile Regression Approach. *2009 Annual Meeting, January 31-February 3, 2009, Atlanta, Georgia* **2009**.
122. Isgin, T.; Bilgic, A.; Forster, D.; Batte, M. Using Count Data Models to Determine the Factors Affecting Farmers' Quantity Decisions of Precision Farming Technology Adoption. *Computers and Electronics in Agriculture - COMPUT ELECTRON AGRIC* **2008**, *62*, 231–242, doi:10.1016/j.compag.2008.01.004.
123. Daberkow, S.G.; McBride, W.D. Farm and Operator Characteristics Affecting the Awareness and Adoption of Precision Agriculture Technologies in the US. *Precision Agriculture* **2003**, *4*, 163–177, doi:10.1023/A:1024557205871.
124. Fernandez-Cornejo, J.; Daberkow, S.; McBride, W.D. Decomposing the Size Effect on the Adoption of Innovations: Agrobiotechnology and Precision Agriculture. *AgBioForum* **2001**, *4*.

125. Kendall, H.; Naughton, P.; Clark, B.; Taylor, J.; Li, Z.; Zhao, C.; Guijun, Y.; Chen, J.; Frewer, L. Precision Agriculture in China: Exploring Awareness, Understanding, Attitudes and Perceptions of Agricultural Experts and End-Users in China. *Advances in Animal Biosciences* **2017**, *8*, 703–707, doi:10.1017/S2040470017001066.
126. Pierpaoli, E.; Carli, G.; Pignatti, E.; Canavari, M. Drivers of Precision Agriculture Technologies Adoption: A Literature Review. *Procedia Technology* **2013**, *8*, 61–69, doi:10.1016/j.protcy.2013.11.010.
127. Paustian, M.; Theuvsen, L. Adoption of Precision Agriculture Technologies by German Crop Farmers. *Precision Agric* **2017**, *18*, 701–716, doi:10.1007/s11119-016-9482-5.
128. Tamirat, T.W.; Pedersen, S.M.; Lind, K.M. Farm and Operator Characteristics Affecting Adoption of Precision Agriculture in Denmark and Germany. *Acta Agriculturae Scandinavica, Section B — Soil & Plant Science* **2018**, *68*, 349–357, doi:10.1080/09064710.2017.1402949.
129. Antolini, L.; Scare, R.F. ADOPTION OF PRECISION AGRICULTURE TECHNOLOGIES BY FARMERS : A SYSTEMATIC LITERATURE REVIEW AND PROPOSITION OF AN INTEGRATED CONCEPTUAL FRAMEWORK.; 2015.
130. Torbett, J.; Roberts, R.; Larson, J.; English, B. Perceived Importance of Precision Farming Technologies in Improving Phosphorus and Potassium Efficiency in Cotton Production. *Precision Agriculture* **2007**, *8*, 127–137, doi:10.1007/s11119-007-9033-1.
131. Walton, J.C.; Lambert, D.; Roberts, R.; Larson, J.; English, B.; Larkin, S.; Martin, S.W.; Marra, M.; Paxton, K.W.; Reeves, J.M. Adoption and Abandonment of Precision Soil Sampling in Cotton Production. *Journal of Agricultural and Resource Economics* **2008**, *33*.
132. Keskin, M.; Sekerli, Y. Awareness and Adoption of Precision Agriculture in the Cukurova Region of Turkey (Full Text) (Çukurova Bölgesinde Hassas Tarım Teknolojilerinin Bilinirlik ve Kullanım Durumu). *Agronomy Research* **2016**, *14*, 1307–1320.
133. Jacobs, A.J.; van Tol, J.J.; Du Preez, C.C. Farmers Perceptions of Precision Agriculture and the Role of Agricultural Extension: A Case Study of Crop Farming in the Schweizer-Reneke Region, South Africa. *South African Journal of Agricultural Extension* **2018**, *46*, 107–118, doi:10.17159/2413-3221/2018/v46n2a484.
134. D'Antoni, J.M.; Mishra, A.K.; Joo, H. Farmers' Perception of Precision Technology: The Case of Autosteer Adoption by Cotton Farmers. *Computers and Electronics in Agriculture* **2012**, *87*, 121–128, doi:10.1016/j.compag.2012.05.017.
135. Thompson, N.M.; Bir, C.; Widmar, D.A.; Mintert, J.R. FARMER PERCEPTIONS OF PRECISION AGRICULTURE TECHNOLOGY BENEFITS. *Journal of Agricultural and Applied Economics* **2019**, *51*, 142–163, doi:10.1017/aae.2018.27.
136. Mondal, P.; Basu, M. Adoption of Precision Agriculture Technologies in India and in Some Developing Countries: Scope, Present Status and Strategies. *Progress in Natural Science* **2009**, *19*, 659–666, doi:10.1016/j.pnsc.2008.07.020.
137. Mase, A.S.; Prokopy, L.S. Unrealized Potential: A Review of Perceptions and Use of Weather and Climate Information in Agricultural Decision Making. *Weather, Climate, and Society* **2014**, *6*, 47–61, doi:10.1175/WCAS-D-12-00062.1.
138. Kadhim, N.; Mourshed, M.; Bray, M. Advances in Remote Sensing Applications for Urban Sustainability. *Euro-Mediterr J Environ Integr* **2016**, *1*, 7, doi:10.1007/s41207-016-0007-4.
139. Robert, P.C. Evaluation of Some Remote Sensing Techniques for Soil and Crop Management (Minnesota). **1983**, 1.
140. Bhatti, A.U.; Mulla, D.J.; Frazier, B.E. Estimation of Soil Properties and Wheat Yields on Complex Eroded Hills Using Geostatistics and Thematic Mapper Images. *Remote Sensing of Environment* **1991**, *37*, 181–191, doi:10.1016/0034-4257(91)90080-P.
141. Zheng, F.; Schreier, H. Quantification of Soil Patterns and Field Soil Fertility Using Spectral Reflection and Digital Processing of Aerial Photographs. *Fertilizer Research* **1988**, *16*, 15.
142. Graphics Library | Landsat Science Available online: https://landsat.gsfc.nasa.gov/multimedia/graphics-library/ (accessed on 28 October 2023).

143. Mulla, D.J. Twenty Five Years of Remote Sensing in Precision Agriculture: Key Advances and Remaining Knowledge Gaps. *Biosystems Engineering* **2013**, *114*, 358–371, doi:10.1016/j.biosystemseng.2012.08.009.
144. Yang, G.; Pu, R.; Zhao, C.; Xue, X. Estimating High Spatiotemporal Resolution Evapotranspiration over a Winter Wheat Field Using an IKONOS Image Based Complementary Relationship and Lysimeter Observations. *Agricultural Water Management* **2014**, *133*, 34–43, doi:10.1016/j.agwat.2013.10.018.
145. IKONOS Imagery to Estimate Surface Soil Property Variability in Two Alabama Physiographies - Sullivan - 2005 - Soil Science Society of America Journal - Wiley Online Library Available online: https://acsess.onlinelibrary.wiley.com/doi/abs/10.2136/sssaj2005.0071?casa_token=eNg9XcOwWqcAAAAA:TKurK9LKREkUNztaQ0M8yySsaIoHxfDJfSbQKFEMlBl8SJNqJlkEh5bUQPd4F7nAL42AYdeGxt0zDOVI (accessed on 2 September 2023).
146. Seelan, S.K.; Laguette, S.; Casady, G.M.; Seielstad, G.A. Remote Sensing Applications for Precision Agriculture: A Learning Community Approach. *Remote Sensing of Environment* **2003**, *88*, 157–169, doi:10.1016/j.rse.2003.04.007.
147. Sentinel-1 - Missions - Sentinel Online Available online: https://copernicus.eu/missions/sentinel-1 (accessed on 2 September 2023).
148. Sentinel-2 - Missions - Sentinel Online Available online: https://copernicus.eu/missions/sentinel-2 (accessed on 2 September 2023).
149. Hall, A.; Lamb, D. w.; Holzapfel, B.; Louis, J. Optical Remote Sensing Applications in Viticulture - a Review. *Australian Journal of Grape and Wine Research* **2002**, *8*, 36–47, doi:10.1111/j.1755-0238.2002.tb00209.x.
150. Satellite Sensors and Specifications | Satellite Imaging Corp Available online: https://www.satimagingcorp.com/satellite-sensors/ (accessed on 28 October 2023).
151. Salgadoe, A.S.A.; Robson, A.J.; Lamb, D.W.; Dann, E.K.; Searle, C. Quantifying the Severity of Phytophthora Root Rot Disease in Avocado Trees Using Image Analysis. *Remote Sensing* **2018**, *10*, 226, doi:10.3390/rs10020226.
152. Bannari, A.; Mohamed, A.M.A.; El-Battay, A. Water Stress Detection as an Indicator of Red Palm Weevil Attack Using Worldview-3 Data. In Proceedings of the 2017 IEEE International Geoscience and Remote Sensing Symposium (IGARSS); July 2017; pp. 4000–4003.
153. Navrozidis, I.; Alexandridis, T.K.; Dimitrakos, A.; Lagopodi, A.L.; Moshou, D.; Zalidis, G. Identification of Purple Spot Disease on Asparagus Crops across Spatial and Spectral Scales. *Computers and Electronics in Agriculture* **2018**, *148*, 322–329, doi:10.1016/j.compag.2018.03.035.
154. Sishodia, R.P.; Ray, R.L.; Singh, S.K. Applications of Remote Sensing in Precision Agriculture: A Review. *Remote Sensing* **2020**, *12*, 3136, doi:10.3390/rs12193136.
155. Leslie, C.R.; Serbina, L.O.; Miller, H.M. *Landsat and Agriculture—Case Studies on the Uses and Benefits of Landsat Imagery in Agricultural Monitoring and Production*; U.S. Geological Survey, 2017;
156. Scudiero, E.; Corwin, D.L.; Wienhold, B.J.; Bosley, B.; Shanahan, J.F.; Johnson, C.K. Downscaling Landsat 7 Canopy Reflectance Employing a Multi-Soil Sensor Platform. *Precision Agric* **2016**, *17*, 53–73, doi:10.1007/s11119-015-9406-9.
157. Venancio, L.P.; Mantovani, E.C.; do Amaral, C.H.; Usher Neale, C.M.; Gonçalves, I.Z.; Filgueiras, R.; Campos, I. Forecasting Corn Yield at the Farm Level in Brazil Based on the FAO-66 Approach and Soil-Adjusted Vegetation Index (SAVI). *Agricultural Water Management* **2019**, *225*, 105779, doi:10.1016/j.agwat.2019.105779.
158. Dong, T.; Liu, J.; Qian, B.; Zhao, T.; Jing, Q.; Geng, X.; Wang, J.; Huffman, T.; Shang, J. Estimating Winter Wheat Biomass by Assimilating Leaf Area Index Derived from Fusion of Landsat-8 and MODIS Data. *International Journal of Applied Earth Observation and Geoinformation* **2016**, *49*, 63–74, doi:10.1016/j.jag.2016.02.001.

159. The Regional Institute - Assessing Flood Damage Using SPOT and NOAA AVHRR Data Available online: http://www.regional.org.au/au/gia/12/397worsley.htm#TopOfPage (accessed on 10 September 2023).
160. Koenig, K.; Höfle, B.; Hämmerle, M.; Jarmer, T.; Siegmann, B.; Lilienthal, H. Comparative Classification Analysis of Post-Harvest Growth Detection from Terrestrial LiDAR Point Clouds in Precision Agriculture. *ISPRS Journal of Photogrammetry and Remote Sensing* **2015**, *104*, 112–125, doi:10.1016/j.isprsjprs.2015.03.003.
161. McNairn, H.; Ellis, J.; Van Der Sanden, J.J.; Hirose, T.; Brown, R.J. Providing Crop Information Using RADARSAT-1 and Satellite Optical Imagery. *International Journal of Remote Sensing* **2002**, *23*, 851–870, doi:10.1080/01431160110070753.
162. Enclona, E.A.; Thenkabail, P.S.; Celis, D.; Diekmann, J. Within-Field Wheat Yield Prediction from IKONOS Data: A New Matrix Approach. *International Journal of Remote Sensing* **2004**, *25*, 377–388, doi:10.1080/0143116031000102485.
163. Sullivan, D.G.; Shaw, J.N.; Rickman, D. IKONOS Imagery to Estimate Surface Soil Property Variability in Two Alabama Physiographies. *Soil Science Society of America Journal* **2005**, *69*, 1789–1798, doi:10.2136/sssaj2005.0071.
164. Omran, E.-S.E. Remote Estimation of Vegetation Parameters Using Narrowband Sensor for Precision Agriculture in Arid Environment. *Egyptian Journal of Soil Science* **2018**, *58*, 73–92, doi:10.21608/ejss.2018.5614.
165. Apan, A.; Held, A.; Phinn, S.; Markley, J. Detecting Sugarcane 'Orange Rust' Disease Using EO-1 Hyperion Hyperspectral Imagery. *International Journal of Remote Sensing* **2004**, *25*, 489–498, doi:10.1080/01431160310001618031.
166. Filippi, P.; Jones, E.J.; Wimalathunge, N.S.; Somarathna, P.D.S.N.; Pozza, L.E.; Ugbaje, S.U.; Jephcott, T.G.; Paterson, S.E.; Whelan, B.M.; Bishop, T.F.A. An Approach to Forecast Grain Crop Yield Using Multi-Layered, Multi-Farm Data Sets and Machine Learning. *Precision Agric* **2019**, *20*, 1015–1029, doi:10.1007/s11119-018-09628-4.
167. Houborg, R.; McCabe, M.F. High-Resolution NDVI from Planet's Constellation of Earth Observing Nano-Satellites: A New Data Source for Precision Agriculture. *Remote Sensing* **2016**, *8*, 768, doi:10.3390/rs8090768.
168. Mobasheri: On the Methods of Sugarcane Water Stress... - Μελετητής Google Available online: https://scholar.google.com/scholar_lookup?title=On+the+methods+of+sugarcane+water+stress+detection+using+Terra/ASTER+images&author=Mobasheri,+M.R.&author=Jokar,+J.&author=Ziaeian,+P.&author=Chahardoli,+M.&publication_year=2007&journal=Am.+Eurasian+J.+Agric.+Environ.+Sci.&volume=2&pages=619%E2%80%93627 (accessed on 10 September 2023).
169. Santoso, H.; Gunawan, T.; Jatmiko, R.H.; Darmosarkoro, W.; Minasny, B. Mapping and Identifying Basal Stem Rot Disease in Oil Palms in North Sumatra with QuickBird Imagery. *Precision Agric* **2011**, *12*, 233–248, doi:10.1007/s11119-010-9172-7.
170. Jackson, T.J.; Bindlish, R.; Klein, M.; Gasiewski, A.J.; Njoku, E.G. Soil Moisture Retrieval and AMSR-E Validation Using an Airborne Microwave Radiometer in SMEX02. In Proceedings of the IGARSS 2003. 2003 IEEE International Geoscience and Remote Sensing Symposium. Proceedings (IEEE Cat. No.03CH37477); July 2003; Vol. 1, pp. 401–403 vol.1.
171. Yang, C.; Everitt, J.H.; Bradford, J.M. Evaluating High Resolution SPOT 5 Satellite Imagery to Estimate Crop Yield. *Precision Agric* **2009**, *10*, 292–303, doi:10.1007/s11119-009-9120-6.
172. Sesha Sai, M.V.R.; Narasimha Rao, P.V. Utilization of Resourcesat-1 Data for Improved Crop Discrimination. *International Journal of Applied Earth Observation and Geoinformation* **2008**, *10*, 206–210, doi:10.1016/j.jag.2008.02.009.
173. Lee: Analysis of Relationship between Vegetation... - Μελετητής Google Available online: https://scholar.google.com/scholar_lookup?title=Analysis+of+relationship+between+vegetation+indices+and+crop+yield+using+KOMPSAT+(KoreaMulti-Purpose+SATellite)-2+imagery+and+field+investigation+data&author=Lee,+J.W.&author=Park,+G.&author=Joh,+H.K.&author=Lee,+K.H.&author=Na,+S.I.&author=Park,+J.H.&author=Kim,+S.J.&publication_year

=2011&journal=JKSAE&volume=53&pages=75%E2%80%9382 (accessed on 10 September 2023).
174. Gao, S.; Niu, Z.; Huang, N.; Hou, X. Estimating the Leaf Area Index, Height and Biomass of Maize Using HJ-1 and RADARSAT-2. *International Journal of Applied Earth Observation and Geoinformation* **2013**, *24*, 1–8, doi:10.1016/j.jag.2013.02.002.
175. Siegfried, J.; Longchamps, L.; Khosla, R. Multispectral Satellite Imagery to Quantify In-Field Soil Moisture Variability. *Journal of Soil and Water Conservation* **2019**, *74*, 33–40, doi:10.2489/jswc.74.1.33.
176. de Lara, A.; Longchamps, L.; Khosla, R. Soil Water Content and High-Resolution Imagery for Precision Irrigation: Maize Yield. *Agronomy* **2019**, *9*, 174, doi:10.3390/agronomy9040174.
177. Shang, J.; Liu, J.; Ma, B.; Zhao, T.; Jiao, X.; Geng, X.; Huffman, T.; Kovacs, J.M.; Walters, D. Mapping Spatial Variability of Crop Growth Conditions Using RapidEye Data in Northern Ontario, Canada. *Remote Sensing of Environment* **2015**, *168*, 113–125, doi:10.1016/j.rse.2015.06.024.
178. Caturegli, L.; Casucci, M.; Lulli, F.; Grossi, N.; Gaetani, M.; Magni, S.; Bonari, E.; Volterrani, M. GeoEye-1 Satellite versus Ground-Based Multispectral Data for Estimating Nitrogen Status of Turfgrasses. *International Journal of Remote Sensing* **2015**, *36*, 2238–2251, doi:10.1080/01431161.2015.1035409.
179. Tian, J.; Wang, L.; Li, X.; Gong, H.; Shi, C.; Zhong, R.; Liu, X. Comparison of UAV and WorldView-2 Imagery for Mapping Leaf Area Index of Mangrove Forest. *International Journal of Applied Earth Observation and Geoinformation* **2017**, *61*, 22–31, doi:10.1016/j.jag.2017.05.002.
180. Kokhan, S.; Vostokov, A. Using Vegetative Indices to Quantify Agricultural Crop Characteristics. *Journal of Ecological Engineering* **2020**, *Vol. 21*, doi:10.12911/22998993/119808.
181. OhioLINK ETD: Romanko, Matthew Available online: https://etd.ohiolink.edu/acprod/odb_etd/etd/r/1501/10?clear=10&p10_accession_num=bgsu1490964339514842 (accessed on 10 September 2023).
182. Skakun, S.; Justice, C.O.; Vermote, E.; Roger, J.-C. Transitioning from MODIS to VIIRS: An Analysis of Inter-Consistency of NDVI Data Sets for Agricultural Monitoring. *International Journal of Remote Sensing* **2018**, *39*, 971–992, doi:10.1080/01431161.2017.1395970.
183. Kim, S.; Lee, M.-S.; Kim, S.-H.; Park, G.-A. Potential Application Topics of KOMPSAT-3 Image in the Field of Precision Agriculture. *Journal of The Korean Society of Agricultural Engineers* **2006**, *48*, doi:10.5389/KSAE.2006.48.7.017.
184. Yuan, L.; Pu, R.; Zhang, J.; Wang, J.; Yang, H. Using High Spatial Resolution Satellite Imagery for Mapping Powdery Mildew at a Regional Scale. *Precision Agric* **2016**, *17*, 332–348, doi:10.1007/s11119-015-9421-x.
185. Ferguson, R.; Rundquist, D. Remote Sensing for Site-Specific Crop Management. In *Precision Agriculture Basics*; John Wiley & Sons, Ltd, 2018; pp. 103–117 ISBN 978-0-89118-367-9.
186. Sidike, P.; Sagan, V.; Maimaitijiang, M.; Maimaitiyiming, M.; Shakoor, N.; Burken, J.; Mockler, T.; Fritschi, F.B. dPEN: Deep Progressively Expanded Network for Mapping Heterogeneous Agricultural Landscape Using WorldView-3 Satellite Imagery. *Remote Sensing of Environment* **2019**, *221*, 756–772, doi:10.1016/j.rse.2018.11.031.
187. Mandal, D.; Kumar, V.; Ratha, D.; Dey, S.; Bhattacharya, A.; Lopez-Sanchez, J.M.; McNairn, H.; Rao, Y.S. Dual Polarimetric Radar Vegetation Index for Crop Growth Monitoring Using Sentinel-1 SAR Data. *Remote Sensing of Environment* **2020**, *247*, 111954, doi:10.1016/j.rse.2020.111954.
188. Martínez-Casasnovas, J. a.; Uribeetxebarría, A.; Escolà, A.; Arnó, J. Sentinel-2 Vegetation Indices and Apparent Electrical Conductivity to Predict Barley (Hordeum Vulgare L.) Yield. In *Precision agriculture ?19*; Wageningen Academic Publishers, 2019; pp. 307–313 ISBN 978-90-8686-337-2.
189. Wolters, S.; Söderström, M.; Piikki, K.; Stenberg, M. Near-Real Time Winter Wheat N Uptake from a Combination of Proximal and Remote Optical Measurements: How to Refine Sentinel-2 Satellite Images for Use in a Precision Agriculture Decision Support System. In *Precision agriculture ?19*; Wageningen Academic Publishers, 2019; pp. 1001–1007 ISBN 978-90-8686-337-2.

190. Bajwa, S.G.; Rupe, J.C.; Mason, J. Soybean Disease Monitoring with Leaf Reflectance. *Remote Sensing* **2017**, *9*, 127, doi:10.3390/rs9020127.
191. Sharif, H.E.; Wang, J.; Georgakakos, A.P. Modeling Regional Crop Yield and Irrigation Demand Using SMAP Type of Soil Moisture Data. *Journal of Hydrometeorology* **2015**, *16*, 904–916, doi:10.1175/JHM-D-14-0034.1.
192. Hao, Z.; Zhao, H.; Zhang, C.; Wang, H.; Jiang, Y. Detecting Winter Wheat Irrigation Signals Using SMAP Gridded Soil Moisture Data. *Remote Sensing* **2019**, *11*, 2390, doi:10.3390/rs11202390.
193. Saygın, F.; Aksoy, H.; Alaboz, P.; Dengiz, O. Different Approaches to Estimating Soil Properties for Digital Soil Map Integrated with Machine Learning and Remote Sensing Techniques in a Sub-Humid Ecosystem. *Environ Monit Assess* **2023**, *195*, 1061, doi:10.1007/s10661-023-11681-0.
194. Fisher, J.B.; Lee, B.; Purdy, A.J.; Halverson, G.H.; Dohlen, M.B.; Cawse-Nicholson, K.; Wang, A.; Anderson, R.G.; Aragon, B.; Arain, M.A.; et al. ECOSTRESS: NASA's Next Generation Mission to Measure Evapotranspiration From the International Space Station. *Water Resources Research* **2020**, *56*, e2019WR026058, doi:10.1029/2019WR026058.
195. Moran, M.S.; Inoue, Y.; Barnes, E.M. Opportunities and Limitations for Image-Based Remote Sensing in Precision Crop Management. *Remote Sensing of Environment* **1997**, *61*, 319–346, doi:10.1016/S0034-4257(97)00045-X.
196. Yao, Y.; Sun, Y.; Han, Y.; Yan, C. Preparation of Resorcinarene-Functionalized Gold Nanoparticles and Their Catalytic Activities for Reduction of Aromatic Nitro Compounds. *Chinese Journal of Chemistry* **2010**, *28*, 705–712, doi:10.1002/cjoc.201090135.
197. Wang, Q.; Tang, Y.; Ge, Y.; Xie, H.; Tong, X.; Atkinson, P.M. A Comprehensive Review of Spatial-Temporal-Spectral Information Reconstruction Techniques. *Science of Remote Sensing* **2023**, *8*, 100102, doi:10.1016/j.srs.2023.100102.
198. Unmanned Aerial Systems in Agriculture - 1st Edition Available online: https://shop.elsevier.com/books/unmanned-aerial-systems-in-agriculture/bochtis/978-0-323-91940-1 (accessed on 10 September 2023).
199. Sugeno, M.; Hirano, I.; Nakamura, S.; Kotsu, S. Development of an Intelligent Unmanned Helicopter. In Proceedings of the Proceedings of 1995 IEEE International Conference on Fuzzy Systems.; March 1995; Vol. 5, pp. 33–34 vol.5.
200. Commercial Drone Market Size, 2019-2025 | Industry Growth Report Available online: https://www.millioninsights.com (accessed on 10 September 2023).
201. Commercial Drone Market Size, Share & Trends Report 2030 Available online: https://www.grandviewresearch.com/industry-analysis/global-commercial-drones-market (accessed on 10 September 2023).
202. del Cerro, J.; Cruz Ulloa, C.; Barrientos, A.; de León Rivas, J. Unmanned Aerial Vehicles in Agriculture: A Survey. *Agronomy* **2021**, *11*, 203, doi:10.3390/agronomy11020203.
203. Darra, N.; Psomiadis, E.; Kasimati, A.; Anastasiou, A.; Anastasiou, E.; Fountas, S. Remote and Proximal Sensing-Derived Spectral Indices and Biophysical Variables for Spatial Variation Determination in Vineyards. *Agronomy* **2021**, *11*, 741.
204. Islam, N.; Rashid, M.M.; Wibowo, S.; Xu, C.-Y.; Morshed, A.; Wasimi, S.A.; Moore, S.; Rahman, S.M. Early Weed Detection Using Image Processing and Machine Learning Techniques in an Australian Chilli Farm. *Agriculture* **2021**, *11*, 387, doi:10.3390/agriculture11050387.
205. Hasan, A.S.M.M.; Sohel, F.; Diepeveen, D.; Laga, H.; Jones, M.G.K. A Survey of Deep Learning Techniques for Weed Detection from Images. *Computers and Electronics in Agriculture* **2021**, *184*, 106067, doi:10.1016/j.compag.2021.106067.
206. Louargant, M.; Villette, S.; Jones, G.; Vigneau, N.; Paoli, J.N.; Gée, C. Weed Detection by UAV: Simulation of the Impact of Spectral Mixing in Multispectral Images. *Precision Agric* **2017**, *18*, 932–951, doi:10.1007/s11119-017-9528-3.
207. Bah, M.D.; Hafiane, A.; Canals, R. Deep Learning with Unsupervised Data Labeling for Weed Detection in Line Crops in UAV Images. *Remote Sensing* **2018**, *10*, 1690, doi:10.3390/rs10111690.

208. Martinez-Guanter, J.; Agüera, P.; Agüera, J.; Pérez-Ruiz, M. Spray and Economics Assessment of a UAV-Based Ultra-Low-Volume Application in Olive and Citrus Orchards. *Precision Agric* **2020**, *21*, 226–243, doi:10.1007/s11119-019-09665-7.
209. Study on Assistant Pollination of Facility Tomato by UAV Available online: https://doi.org/10.13031/aim.201900055 (accessed on 24 September 2023).
210. Roldán, J.J.; Garcia-Aunon, P.; Garzón, M.; De León, J.; Del Cerro, J.; Barrientos, A. Heterogeneous Multi-Robot System for Mapping Environmental Variables of Greenhouses. *Sensors* **2016**, *16*, 1018, doi:10.3390/s16071018.
211. Roldán, J.J.; Joossen, G.; Sanz, D.; Del Cerro, J.; Barrientos, A. Mini-UAV Based Sensory System for Measuring Environmental Variables in Greenhouses. *Sensors* **2015**, *15*, 3334–3350, doi:10.3390/s150203334.
212. Simon, J.; Petkovic, I.; Petkovic, D.; Petkovics, Á. Navigation and Applicability of Hexa Rotor Drones in Greenhouse Environment. *Tehnički vjesnik* **2018**, *25*, 249–255, doi:10.17559/TV-20161109211133.
213. Aslan, M.F.; Durdu, A.; Sabanci, K.; Ropelewska, E.; Gültekin, S.S. A Comprehensive Survey of the Recent Studies with UAV for Precision Agriculture in Open Fields and Greenhouses. *Applied Sciences (Switzerland)* **2022**, *12*, doi:10.3390/app12031047.
214. Fountas, S.; Mylonas, N.; Malounas, I.; Rodias, E.; Hellmann Santos, C.; Pekkeriet, E. Agricultural Robotics for Field Operations. *Sensors* **2020**, *20*, 2672, doi:10.3390/s20092672.
215. Ampatzidis, Y.; Tan, L.; Haley, R.; Whiting, M.D. Cloud-Based Harvest Management Information System for Hand-Harvested Specialty Crops. *Computers and Electronics in Agriculture* **2016**, *122*, 161–167, doi:10.1016/j.compag.2016.01.032.
216. Honrado, J.L.E.; Solpico, D.B.; Favila, C.M.; Tongson, E.; Tangonan, G.L.; Libatique, N.J.C. UAV Imaging with Low-Cost Multispectral Imaging System for Precision Agriculture Applications. In Proceedings of the 2017 IEEE Global Humanitarian Technology Conference (GHTC); July 2017; pp. 1–7.
217. Abdullahi, H.S.; Mahieddine, F.; Sheriff, R.E. Technology Impact on Agricultural Productivity: A Review of Precision Agriculture Using Unmanned Aerial Vehicles. In Proceedings of the Wireless and Satellite Systems; Pillai, P., Hu, Y.F., Otung, I., Giambene, G., Eds.; Springer International Publishing: Cham, 2015; pp. 388–400.
218. Darra, N.; Kasimati, A.; Koutsiaras, M.; Psiroukis, V.; Fountas, S. Digital Transformation of SMEs in Agriculture. In *SMEs in the Digital Era*; Edward Elgar Publishing, 2023; pp. 65–83 ISBN 978-1-80392-164-8.
219. Zhang, S.; Zhao, G.; Lang, K.; Su, B.; Chen, X.; Xi, X.; Zhang, H. Integrated Satellite, Unmanned Aerial Vehicle (UAV) and Ground Inversion of the SPAD of Winter Wheat in the Reviving Stage. *Sensors* **2019**, *19*, 1485, doi:10.3390/s19071485.
220. Sundmaeker, H.; Verdouw, C.N.; Wolfert, J.; Freire, L.P. Internet of Food and Farm 2020. In *Digitising the Industry: Internet of Things Connecting the Physical, Digital and Virtual Worlds*; River Publishers, 2016; pp. 129–150.
221. Nativi, S.; Mazzetti, P.; Santoro, M.; Papeschi, F.; Craglia, M.; Ochiai, O. Big Data Challenges in Building the Global Earth Observation System of Systems. *Environ. Model. Softw.* **2015**, *68*, 1–26, doi:10.1016/j.envsoft.2015.01.017.
222. Schepers, J.S.; Francis, D.D.; Vigil, M.; Below, F.E. Comparison of Corn Leaf Nitrogen Concentration and Chlorophyll Meter Readings. *Communications in Soil Science and Plant Analysis* **1992**, *23*, 2173–2187, doi:10.1080/00103629209368733.
223. Blackmer, T. m.; Schepers, J. s. Use of a Chlorophyll Meter to Monitor Nitrogen Status and Schedule Fertigation for Corn. *Journal of Production Agriculture* **1995**, *8*, 56–60, doi:10.2134/jpa1995.0056.
224. Use of Spectral Radiance for Correcting In-Season Fertilizer Nitrogen Deficiencies in Winter Wheat Available online: https://doi.org/10.13031/2013.27678 (accessed on 14 September 2023).

225. Link, A.; Panitzki, M.; Reusch, S. Hydro N-Sensor: Tractor-Mounted Remote Sensing for Variable Nitrogen Fertilization. *Proceedings of the 6th International Conference on Precision Agriculture and Other Precision Resources Management, Minneapolis, MN, USA, 14-17 July, 2002* **2003**, 1012–1017.
226. Haboudane, D.; Miller, J.R.; Tremblay, N.; Zarco-Tejada, P.J.; Dextraze, L. Integrated Narrow-Band Vegetation Indices for Prediction of Crop Chlorophyll Content for Application to Precision Agriculture. *Remote Sensing of Environment* **2002**, *81*, 416–426, doi:10.1016/S0034-4257(02)00018-4.
227. Haboudane, D.; Miller, J.R.; Pattey, E.; Zarco-Tejada, P.J.; Strachan, I.B. Hyperspectral Vegetation Indices and Novel Algorithms for Predicting Green LAI of Crop Canopies: Modeling and Validation in the Context of Precision Agriculture. *Remote Sensing of Environment* **2004**, *90*, 337–352, doi:10.1016/j.rse.2003.12.013.
228. Herwitz, S.R.; Johnson, L.F.; Dunagan, S.E.; Higgins, R.G.; Sullivan, D.V.; Zheng, J.; Lobitz, B.M.; Leung, J.G.; Gallmeyer, B.A.; Aoyagi, M.; et al. Imaging from an Unmanned Aerial Vehicle: Agricultural Surveillance and Decision Support. *Computers and Electronics in Agriculture* **2004**, *44*, 49–61, doi:10.1016/j.compag.2004.02.006.
229. Apostol, S.; Viau, A.A.; Tremblay, N.; Briantais, J.-M.; Prasher, S.; Parent, L.-E.; Moya, I. Laser-Induced Fluorescence Signatures as a Tool for Remote Monitoring of Water and Nitrogen Stresses in Plants. *Canadian Journal of Remote Sensing* **2003**, *29*, 57–65, doi:10.5589/m02-076.
230. Holland, K.H.; Schepers, J.S.; Shanahan, J.F.; Horst, G.L. Plant Canopy Sensor with Modulated Polychromatic Light Source. *Proceedings of the 7th International Conference on Precision Agriculture and Other Precision Resources Management, Hyatt Regency, Minneapolis, MN, USA, 25-28 July, 2004* **2004**, 148–160.
231. Varvel, G.E.; Schepers, J.S.; Francis, D.D. Ability for In-Season Correction of Nitrogen Deficiency in Corn Using Chlorophyll Meters. *Soil Science Society of America Journal* **1997**, *61*, 1233–1239, doi:10.2136/sssaj1997.03615995006100040032x.
232. Bausch, W.C.; Duke, H.R. Remote Sensing of Plant Nitrogen Status in Corn. *Transactions of the American Society of Agricultural Engineers* **1996**, *39*, 1869–1875.
233. Ritchie, S.W.; Hanway, J.J.; Benson, G.O. How a Corn Plant Develops. Iowa State Univ. *Coop. Ext. Serv. Spec. Rep* **1993**, *48*, 21.
234. Solie, J.B.; Raun, W.R.; Whitney, R.W.; Stone, M.L.; Ringer, J.D. Optical Sensor Based Field Element Size and Sensing Strategy for Nitrogen Application. *Transactions of the American Society of Agricultural Engineers* **1996**, *39*, 1983–1992.
235. Raun, W.R.; Solie, J.B.; Johnson, G.V.; Stone, M.L.; Mutten, R.W.; Freeman, K.W.; Thomason, W.E.; Lukina, E.V. Improving Nitrogen Use Efficiency in Cereal Grain Production with Optical Sensing and Variable Rate Application. *Agronomy Journal* **2002**, *94*, 815–820, doi:10.2134/agronj2002.8150.
236. Shanahan, J.F.; Kitchen, N.R.; Raun, W.R.; Schepers, J.S. Responsive In-Season Nitrogen Management for Cereals. *Computers and Electronics in Agriculture* **2008**, *61*, 51–62, doi:10.1016/j.compag.2007.06.006.
237. Reusch, S.; Link, A.; Lammel, J. Tractor-Mounted Multispectral Scanner for Remote Field Investigation. *Proceedings of the 6th International Conference on Precision Agriculture and Other Precision Resources Management, Minneapolis, MN, USA, 14-17 July, 2002* **2003**, 1465–1473.
238. Link, G. Asymptotic Geometry and Growth of Conjugacy Classes of Nonpositively Curved Manifolds. *Ann Glob Anal Geom* **2007**, *31*, 37–57, doi:10.1007/s10455-006-9016-x.
239. Gitelson, A.A.; Kaufman, Y.J.; Merzlyak, M.N. Use of a Green Channel in Remote Sensing of Global Vegetation from EOS- MODIS. *Remote Sensing of Environment* **1996**, *58*, 289–298, doi:10.1016/S0034-4257(96)00072-7.
240. Shanahan, J.F.; Schepers, J.S.; Francis, D.D.; Varvel, G.E.; Wilhelm, W.W.; Tringe, J.M.; Schlemmer, M.R.; Major, D.J. Use of Remote-Sensing Imagery to Estimate Corn Grain Yield. *Agronomy Journal* **2001**, *93*, 583–589, doi:10.2134/agronj2001.933583x.

241. Sripada, R.P.; Heiniger, R.W.; White, J.G.; Meijer, A.D. Aerial Color Infrared Photography for Determining Early In-Season Nitrogen Requirements in Corn. *Agronomy Journal* **2006**, *98*, 968–977, doi:10.2134/agronj2005.0200.
242. Solari, F.; Shanahan, J.; Ferguson, R.; Schepers, J.; Gitelson, A. Active Sensor Reflectance Measurements of Corn Nitrogen Status and Yield Potential. *Agronomy Journal* **2008**, *100*, 571–579, doi:10.2134/agronj2007.0244.
243. Sripada, R.P.; Schmidt, J.P.; Dellinger, A.E.; Beegle, D.B. Evaluating Multiple Indices from a Canopy Reflectance Sensor to Estimate Corn N Requirements. *Agronomy Journal* **2008**, *100*, 1553–1561, doi:10.2134/agronj2008.0017.
244. Kitchen, N.R.; Sudduth, K.A.; Drummond, S.T.; Scharf, P.C.; Palm, H.L.; Roberts, D.F.; Vories, E.D. Ground-Based Canopy Reflectance Sensing for Variable-Rate Nitrogen Corn Fertilization. *Agronomy Journal* **2010**, *102*, 71–84, doi:10.2134/agronj2009.0114.
245. Scharf, P.C.; Shannon, D.K.; Palm, H.L.; Sudduth, K.A.; Drummond, S.T.; Kitchen, N.R.; Mueller, L.J.; Hubbard, V.C.; Oliveira, L.F. Sensor-Based Nitrogen Applications out-Performed Producer-Chosen Rates for Corn in on-Farm Demonstrations. *Agronomy Journal* **2011**, *103*, 1683–1691, doi:10.2134/agronj2011.0164.
246. Samborski, S.M.; Tremblay, N.; Fallon, E. Strategies to Make Use of Plant Sensors-Based Diagnostic Information for Nitrogen Recommendations. *Agronomy Journal* **2009**, *101*, 800–816, doi:10.2134/agronj2008.0162Rx.
247. Mamo, M.; Malzer, G.L.; Mulla, D.J.; Huggins, D.R.; Strock, J. Spatial and Temporal Variation in Economically Optimum Nitrogen Rate for Corn. *Agronomy Journal* **2003**, *95*, 958–964, doi:10.2134/agronj2003.9580.
248. Carter: Mechanization of Soil Salinity Assessment... - Μελετητής Google Available online: https://scholar.google.com/scholar_lookup?title=Mechanization%20of%20soil%20salinity%20assessment%20for%20mapping&publication_year=1993&author=L.M.%20Carter&author=J.D.%20Rhoades&author=J.H.%20Chesson (accessed on 24 September 2023).
249. Shaver, T.M.; Khosla, R.; Westfall, D.G. Evaluation of Two Ground-Based Active Crop Canopy Sensors in Maize: Growth Stage, Row Spacing, and Sensor Movement Speed. *Soil Science Society of America Journal* **2010**, *74*, 2101–2108, doi:10.2136/sssaj2009.0421.
250. Xue, J.; Su, B. Significant Remote Sensing Vegetation Indices: A Review of Developments and Applications. *Journal of Sensors* **2017**, *2017*, e1353691, doi:10.1155/2017/1353691.
251. Hu, C. Remote Detection of Marine Debris Using Satellite Observations in the Visible and near Infrared Spectral Range: Challenges and Potentials. *Remote Sensing of Environment* **2021**, *259*, 112414, doi:10.1016/j.rse.2021.112414.
252. Montero, D.; Aybar, C.; Mahecha, M.D.; Martinuzzi, F.; Söchting, M.; Wieneke, S. A Standardized Catalogue of Spectral Indices to Advance the Use of Remote Sensing in Earth System Research. *Sci Data* **2023**, *10*, 197, doi:10.1038/s41597-023-02096-0.
253. Rouse, J.W.; Haas, R.H.; Schell, J.A.; Deering, D.W. Monitoring Vegetation Systems in the Great Plains with ERTS: Proceedings of the Third Earth Resources Technology Satellite-1 Symposium. *NASA SP-351* **1974**, 301–317.
254. Thenkabail, P.S.; Smith, R.B.; De Pauw, E. Hyperspectral Vegetation Indices and Their Relationships with Agricultural Crop Characteristics. *Remote Sensing of Environment* **2000**, *71*, 158–182, doi:10.1016/S0034-4257(99)00067-X.
255. Thenkabail, P. Biophysical and Yield Information for Precision Farming from Near-Real-Time and Historical Landsat TM Images. *International Journal of Remote Sensing* **2003**, *24*, 2879–2904, doi:10.1080/01431160710155974.
256. Miao, Y.; Mulla, D.J.; Randall, G.W.; Vetsch, J.A.; Vintila, R. Combining Chlorophyll Meter Readings and High Spatial Resolution Remote Sensing Images for In-Season Site-Specific Nitrogen Management of Corn. *Precision Agric* **2009**, *10*, 45–62, doi:10.1007/s11119-008-9091-z.

257. Sripada, R.P.; Heiniger, R.W.; White, J.G.; Weisz, R. Aerial Color Infrared Photography for Determining Late-Season Nitrogen Requirements in Corn. *Agronomy Journal* **2005**, *97*, 1443–1451, doi:10.2134/agronj2004.0314.
258. Jordan, C.F. Derivation of Leaf-Area Index from Quality of Light on the Forest Floor. *Ecology* **1969**, *50*, 663–666, doi:10.2307/1936256.
259. Tucker, C.J. Red and Photographic Infrared Linear Combinations for Monitoring Vegetation. *Remote Sensing of Environment* **1979**, *8*, 127–150, doi:10.1016/0034-4257(79)90013-0.
260. Rouse, J.W.; Haas, R.H.; Schell, J.A.; Deering, D.W. Monitoring Vegetation Systems in the Great Plains with ERTS Proceeding. *In Third Earth Reserves Technology Satellite Symposium, Greenbelt: NASA SP-351* **1974**, *30103017*.
261. Huete, A.R. A Soil-Adjusted Vegetation Index (SAVI). *Remote Sensing of Environment* **1988**, *25*, 295–309, doi:10.1016/0034-4257(88)90106-X.
262. Rondeaux, G.; Steven, M.; Frederic, B. Optimization of Soil-Adjusted Vegetation Indices. *Remote Sensing of Environment* **1996**, *55*, 95–107, doi:10.1016/0034-4257(95)00186-7.
263. Nix v. Hedden, 149 U.S. 304 (1893) Available online: https://supreme.justia.com/cases/federal/us/149/304/ (accessed on 25 September 2023).
264. Jeguirim, M.; Zorpas, A.A. *Tomato Processing By-Products: Sustainable Applications*; Academic Press, 2021; ISBN 978-0-12-822867-8.
265. Gould, W.A. *Tomato Production, Processing and Technology*; Elsevier, 2013; ISBN 978-1-84569-614-6.
266. Our History – Tomato Industrial Museum "D. Nomikos."
267. Foolad, M.R. Genome Mapping and Molecular Breeding of Tomato. *International Journal of Plant Genomics* **2007**, *2007*, doi:10.1155/2007/64358.
268. Razdan, M.K.; Mattoo, A.K. *Genetic Improvement of Solanaceous Crops: Tomato*; CRC Press, 2006; ISBN 978-1-57808-179-0.
269. Bauchet: Genetic Diversity in Tomato and Its Wild... - Μελετητής Google Available online: https://scholar.google.com/scholar_lookup?title=Genetic%20diversity%20in%20tomato%20%20and%20its%20wild%20relatives&publication_year=2012&author=G.%20Bauchet&author=M.%20Causse (accessed on 27 October 2023).
270. Bai, Y.; Lindhout, P. Domestication and Breeding of Tomatoes: What Have We Gained and What Can We Gain in the Future? *Annals of Botany* **2007**, *100*, 1085–1094, doi:10.1093/aob/mcm150.
271. Bergougnoux, V. The History of Tomato: From Domestication to Biopharming. *Biotechnology Advances* **2014**, *32*, 170–189, doi:10.1016/j.biotechadv.2013.11.003.
272. Stevens, M.A.; Rick, C.M. Genetics and Breeding. In *The Tomato Crop: A scientific basis for improvement*; Atherton, J.G., Rudich, J., Eds.; The Tomato Crop; Springer Netherlands: Dordrecht, 1986; pp. 35–109 ISBN 978-94-009-3137-4.
273. C, T.E. Tomato Breeding. *Breeding vegetable crops* **1986**.
274. Barrios-Masias, F.H.; Jackson, L.E. California Processing Tomatoes: Morphological, Physiological and Phenological Traits Associated with Crop Improvement during the Last 80 Years. *European Journal of Agronomy* **2014**, *53*, 45–55, doi:10.1016/j.eja.2013.11.007.
275. Hanna: Breeding Tomatoes for Mechanical Harvesting... - Μελετητής Google Available online: https://scholar.google.com/scholar_lookup?title=Breeding%20tomatoes%20for%20mechanical%20harvesting%20in%20California&publication_year=1971&author=G.C.%20Hanna (accessed on 27 October 2023).
276. A. N. Lukyanenko, "Disease Resistance in Tomato," In G. Kalloo, Ed., Monographs on Theoretical and Applied Genetics 14, Genetic Improvement of Tomato, SpringerVerlag, Berlin, Heidelberg, New York, 1991, Pp. 99-119. - References - Scientific Research Publishing Available online: https://www.scirp.org/(S(vtj3fa45qm1ean45vvffcz55))/reference/referencespapers.aspx?referenceid=1001228 (accessed on 25 September 2023).
277. Crop Guide: Tomato Plant Nutrition Available online: https://www.haifa-group.com/crop-guide/vegetables/tomato/crop-guide-tomato-plant-nutrition (accessed on 4 November 2023).

278. Bar-Yosef, B. Fertilization Under Drip Irrigation. In *Fluid Fertilizer Science and Technology*; CRC Press, 1991 ISBN 978-1-00-306574-6.
279. De C. Carmello, Q.A.; Anti, G.R. ACCUMULATION OF NUTRIENTS AND GROWTH OF PROCESSING TOMATO. *Acta Hortic.* **2006**, 85–90, doi:10.17660/ActaHortic.2006.724.9.
280. Huett, D.O.; Dettmann, E.B. Effect of Nitrogen on Growth, Fruit Quality and Nutrient Uptake of Tomatoes Grown in Sand Culture. *Aust. J. Exp. Agric.* **1988**, *28*, 391–399, doi:10.1071/ea9880391.
281. *The Tomato Crop: A Scientific Basis for Improvement*; Atherton, J.G., Rudich, J., Eds.; Springer Netherlands: Dordrecht, 1986; ISBN 978-94-010-7910-5.
282. Farneselli, M.; Benincasa, P.; Tosti, G.; Simonne, E.; Guiducci, M.; Tei, F. High Fertigation Frequency Improves Nitrogen Uptake and Crop Performance in Processing Tomato Grown with High Nitrogen and Water Supply. *Agricultural Water Management* **2015**, *154*, 52–58, doi:10.1016/j.agwat.2015.03.002.
283. Conversa, G.; Lazzizera, C.; Bonasia, A.; Elia, A. Yield and Phosphorus Uptake of a Processing Tomato Crop Grown at Different Phosphorus Levels in a Calcareous Soil as Affected by Mycorrhizal Inoculation under Field Conditions. *Biol Fertil Soils* **2013**, *49*, 691–703, doi:10.1007/s00374-012-0757-3.
284. Hartz, T.K.; Bottoms, T.G. Humic Substances Generally Ineffective in Improving Vegetable Crop Nutrient Uptake or Productivity. *HortScience* **2010**, *45*, 906–910, doi:10.21273/HORTSCI.45.6.906.
285. Deficit Irrigation as a Strategy to Save Water: Physiology and Potential Application to Horticulture - Costa - 2007 - Journal of Integrative Plant Biology - Wiley Online Library Available online: https://onlinelibrary.wiley.com/doi/abs/10.1111/j.1672-9072.2007.00556.x?casa_token=B0o330XzOaUAAAAA:PAk4tTPFa9vM5tW5vAovoukdu1DdMizrDNA6paO8l8CUVggjL3aFoRv8fDloQnCAVgnfWfaRJJKi1A (accessed on 2 November 2023).
286. Kuşçu, H.; Turhan, A.; Demir, A.O. The Response of Processing Tomato to Deficit Irrigation at Various Phenological Stages in a Sub-Humid Environment. *Agricultural Water Management* **2014**, *133*, 92–103, doi:10.1016/j.agwat.2013.11.008.
287. Geisenberg, C.; Stewart, K. Field Crop Management. In *The Tomato Crop: A scientific basis for improvement*; Atherton, J.G., Rudich, J., Eds.; The Tomato Crop; Springer Netherlands: Dordrecht, 1986; pp. 511–557 ISBN 978-94-009-3137-4.
288. Rudich, J.; Zamski, E.; Regev, Y. Genotypic Variation for Sensitivity to High Temperature in the Tomato: Pollination and Fruit Set. *Botanical Gazette* **1977**, *138*, 448–452, doi:10.1086/336947.
289. Rendon-Poblete E. Effect of Soil Water Status on Yield, Quality and Root Development of Several Tomato Genotypes. **1981**, 1.
290. HELYES, L.; LUGASI, A.; PÉK, Z. Effect of Irrigation on Processing Tomato Yield and Antioxidant Components. *Turkish Journal of Agriculture and Forestry* **2012**, *36*, 702–709, doi:10.3906/tar-1107-9.
291. Liu, K.; Zhang, T.Q.; Tan, C.S.; Astatkie, T. Responses of Fruit Yield and Quality of Processing Tomato to Drip-Irrigation and Fertilizers Phosphorus and Potassium. *Agronomy Journal* **2011**, *103*, 1339–1345, doi:10.2134/agronj2011.0111.
292. Kuscu, H.; Turhan, A.; Ozmen, N.; Aydinol, P.; Demir, A.O. Optimizing Levels of Water and Nitrogen Applied through Drip Irrigation for Yield, Quality, and Water Productivity of Processing Tomato (Lycopersicon Esculentum Mill.). *Hortic. Environ. Biotechnol.* **2014**, *55*, 103–114, doi:10.1007/s13580-014-0180-9.
293. Physiological Responses of Drought Stress in Tomato: A Review - ProQuest Available online: https://www.proquest.com/openview/74b9f3c01cf8d18366ea0611d31e2434/1?pq-origsite=gscholar&cbl=2032162 (accessed on 4 November 2023).
294. Muntean, N.; Chawdhery, R.A.; Potopová, V.; Tűrkott, L. The Ability of CROPGRO-Tomato Model to Simulate the Growth Characteristics of Thomas F1 Tomato Cultivar Grown under Open Field

Conditions. *The Journal of Agricultural Science* **2021**, *159*, 473–487, doi:10.1017/S0021859621000770.

295. van de Vooren, J.; Welles, G.W.H.; Hayman, G. Glasshouse Crop Production. In *The Tomato Crop: A scientific basis for improvement*; Atherton, J.G., Rudich, J., Eds.; The Tomato Crop; Springer Netherlands: Dordrecht, 1986; pp. 581–623 ISBN 978-94-009-3137-4.
296. Heuvelink, E. Developmental Processes. In *Tomatoes*; CABI, 2005; pp. 53–83.
297. Reyes-Pérez, J.J.; Enríquez-Acosta, E.A.; Murillo-Amador, B.; Ramírez-Arrebato, M.A.; Rodríguez-Pedroso, A.T.; Lara-Capistrán, L.; Hernández-Montiel, L.G. Physiological, Phenological and Productive Responses of Tomato (Solanum Licopersicum L.) Plants Treated with QuitoMax. *Ciencia e investigación agraria* **2018**, *45*, 120–127, doi:10.7764/rcia.v45i2.1943.
298. Picken, A.J.F.; Stewart, K.; Klapwijk, D. Germination and Vegetative Development. In *The Tomato Crop: A scientific basis for improvement*; Atherton, J.G., Rudich, J., Eds.; The Tomato Crop; Springer Netherlands: Dordrecht, 1986; pp. 111–166 ISBN 978-94-009-3137-4.
299. Van Ploeg, D.; Heuvelink, E. Influence of Sub-Optimal Temperature on Tomato Growth and Yield: A Review. *The Journal of Horticultural Science and Biotechnology* **2005**, *80*, 652–659, doi:10.1080/14620316.2005.11511994.
300. De Koning, A.N.M. GROWTH OF A TOMATO CROP. *Acta Hortic.* **1993**, 141–146, doi:10.17660/ActaHortic.1993.328.11.
301. Koning, A.N.M. de Development and Dry Matter Distribution in Glasshouse Tomato : A Quantitative Approach. **1994**.
302. Adams, S.R.; Cockshull, K.E.; Cave, C.R.J. Effect of Temperature on the Growth and Development of Tomato Fruits. *Annals of Botany* **2001**, *88*, 869–877, doi:10.1006/anbo.2001.1524.
303. Lambers, H.; Chapin, F.S.; Pons, T.L. *Plant Physiological Ecology*; Springer New York: New York, NY, 2008; ISBN 978-0-387-78340-6.
304. Heuvelink, E.; Dorais, M. Crop Growth and Yield. In *Tomatoes*; CABI, 2005; pp. 85–144.
305. Ogweno, J.-O.; Song, X.-S.; Hu, W.-H.; Shi, K.; Zhou, Y.-H.; Yu, J.-Q. Detached Leaves of Tomato Differ in Their Photosynthetic Physiological Response to Moderate High and Low Temperature Stress. *Scientia Horticulturae* **2009**, *123*, 17–22, doi:10.1016/j.scienta.2009.07.011.
306. Xu: Tomato Leaf Photosynthetic Responses to Humidity... - Μελετητής Google Available online: https://scholar.google.com/scholar_lookup?title=Tomato+leaf+photosynthetic+responses+to+humidity+and+temperature+under+salinity+and+water+deficit&author=H.L.+R.+L.+A.+Xu%2C+Wang%2C+Gauthier%2C+Gosselin%2C&publication_year=1999&journal=Pedosphere&volume=9&pages=105-112 (accessed on 2 November 2023).
307. Hu, W.H.; Zhou, Y.H.; Du, Y.S.; Xia, X.J.; Yu, J.Q. Differential Response of Photosynthesis in Greenhouse- and Field-Ecotypes of Tomato to Long-Term Chilling under Low Light. *Journal of Plant Physiology* **2006**, *163*, 1238–1246, doi:10.1016/j.jplph.2005.10.006.
308. Byrd, G.T.; Ort, D.R.; Ogren, W.L. The Effects of Chilling in the Light on Ribulose-1,5-Bisphosphate Carboxylase/Oxygenase Activation in Tomato (Lycopersicon Esculentum Mill.). *Plant Physiology* **1995**, *107*, 585–591, doi:10.1104/pp.107.2.585.
309. Martin, B.; Ort, D.R.; Boyer, J.S. Impairment of Photosynthesis by Chilling-Temperatures in Tomato 1. *Plant Physiology* **1981**, *68*, 329–334, doi:10.1104/pp.68.2.329.
310. PREDICTING PHENOLOGICAL EVENTS OF CALIFORNIA PROCESSING TOMATOES | International Society for Horticultural Science Available online: http://www.actahort.org/books/487/487_2.htm (accessed on 2 November 2023).
311. Patanè, C.; Tringali, S.; Sortino, O. Effects of Deficit Irrigation on Biomass, Yield, Water Productivity and Fruit Quality of Processing Tomato under Semi-Arid Mediterranean Climate Conditions. *Scientia Horticulturae* **2011**, *129*, 590–596, doi:10.1016/j.scienta.2011.04.030.
312. Hurd, R.G.; Cooper, A.J. Increasing Flower Number in Single-Truss Tomatoes. *Journal of Horticultural Science* **1967**, *42*, 181–188, doi:10.1080/00221589.1967.11514206.
313. Fisher, K.J. Competition Effects between Fruit Trusses of the Tomato Plant. *Scientia Horticulturae* **1977**, *7*, 37–42, doi:10.1016/0304-4238(77)90041-3.

314. Slack, G.; Calvert, A. The Effect of Truss Removal on the Yield of Early Sown Tomatoes. *Journal of Horticultural Science* **1977**, *52*, 309–315, doi:10.1080/00221589.1977.11514759.
315. Verkerk, K. 1955 Temperature, Light and the Tomato. Mededelingen van de Landbouwhogeschool, Wageningen, The Netherlands. 55:175–224 - Αναζήτηση Google Available online: https://www.google.com/search?q=Verkerk%2C+K.+1955+Temperature%2C+light+and+the+tomato.+Mededelingen+van+de+Landbouwhogeschool%2C+Wageningen%2C+The+Netherlands.+55%3A175%E2%80%93224&oq=Verkerk%2C+K.+1955+Temperature%2C+light+and+the+tomato.+Mededelingen+van+de+Landbouwhogeschool%2C+Wageningen%2C+The+Netherlands.+55%3A175%E2%80%93224&gs_lcrp=EgZjaHJvbWUyBggAEEUYOTIHCAEQIRiPAtIBCDE2NTVqMGo3qAIAsAIA&sourceid=chrome&ie=UTF-8 (accessed on 2 November 2023).
316. Abreu, P.; Meneses, J.F.; Gary, C. TOMPOUSSE, A MODEL OF YIELD PREDICTION FOR TOMATO CROPS: CALIBRATION STUDY FOR UNHEATED PLASTIC GREENHOUSES. *Acta Hortic.* **2000**, 141–150, doi:10.17660/ActaHortic.2000.519.14.
317. TAKAHASHI: Studies on the Flower Formation in Tomatoes... - Google Scholar Available online: https://scholar.google.com/scholar_lookup?oi=gsb80&journal_title=Journal%20of%20the%20Japanese%20Society%20for%20Horticultural%20Science&journal_abbrev=J.%20Japan.%20Soc.%20Hort.%20Sci.&journal_abbrev=%E5%9C%92%E5%AD%A6%E9%9B%91%EF%BC%8E&publisher=THE%20JAPANESE%20SOCIETY%20FOR%20HORTICULTURAL%20SCIENCE&author=Bunjiro%20TAKAHASHI&author=Tuneo%20EGUCHI&author=Kazuo%20YONEDA&title=Studies%20on%20the%20Flower%20Formation%20in%20Tomatoes%20and%20Egg-plants%20I.%20Effect%20of%20Temperature%20Regimes%20and%20Fertilizer%20Levels%20on%20the%20Flower%20Bud%20Differentiation%20in%20Tomatoes&publication_year=1973&online_date=2007%2F07%2F05&volume=42&issue=2&firstpage=147&lastpage=154&doi=10.2503%2Fjjshs.42.147&issn=0013-7626&issn=1880-358X&language=en&lookup=0&hl=en (accessed on 3 November 2023).
318. Benedictos Jr, P.; Yavari, N. OPTIMUM SOWING DATE IN RELATION TO FLOWER DROP REDUCTION IN TOMATO. *Acta Hortic.* **2000**, 351–360, doi:10.17660/ActaHortic.2000.533.43.
319. Some Effects of Shading and Para-Chlo-Rophenoxyacetic Acid on Fruitfulness of Tomato | CiNii Research Available online: https://cir.nii.ac.jp/crid/1572261549558128256 (accessed on 2 November 2023).
320. Boote, K.J.; Rybak, M.R.; Scholberg, J.M.S.; Jones, J.W. Improving the CROPGRO-Tomato Model for Predicting Growth and Yield Response to Temperature. *HortScience* **2012**, *47*, 1038–1049, doi:10.21273/HORTSCI.47.8.1038.
321. De Koning, A.N.M. THE EFFECT OF TEMPERATURE, FRUIT LOAD AND SALINITY ON DEVELOPMENT RATE OF TOMATO FRUIT. *Acta Hortic.* **2000**, 85–94, doi:10.17660/ActaHortic.2000.519.7.
322. Rylski, I. Fruit Set and Development of Seeded and Seedless Tomato Fruits under Diverse Regimes of Temperature and Pollination1. *Journal of the American Society for Horticultural Science* **1979**, *104*, 835–838, doi:10.21273/JASHS.104.6.835.
323. Adams, S.R.; Valdeés, V.M. The Effect of Periods of High Temperature and Manipulating Fruit Load on the Pattern of Tomato Yields. *The Journal of Horticultural Science and Biotechnology* **2002**, *77*, 461–466, doi:10.1080/14620316.2002.11511522.
324. Aikman, D.P. A Procedure for Optimizing Carbon Dioxide Enrichment of a Glasshouse Tomato Crop. *Journal of Agricultural Engineering Research* **1996**, *63*, 171–183, doi:10.1006/jaer.1996.0019.
325. Scholberg, J.M.S.; McNeal, B.L.; Jones, J.; Locascio, S.; Olsen, S.R.; Stanley, C. Adaptation of the CROPGRO Model to Simulate Yield of Fresh-Market Tomato. *HortScience* **1996**, *31*, 572f–5572, doi:10.21273/HORTSCI.31.4.572f.
326. Rudich, J.; Luchinsky, U. Water Economy. In *The Tomato Crop: A scientific basis for improvement*; Atherton, J.G., Rudich, J., Eds.; The Tomato Crop; Springer Netherlands: Dordrecht, 1986; pp. 335–367 ISBN 978-94-009-3137-4.

327. Orzolek, M.D.; Angell, F.F. Seasonal Trends of Four Quality Factors in Processing Tomatoes (Lycopersicon Esculentum Mill.)1. *Journal of the American Society for Horticultural Science* **1975**, *100*, 554–557, doi:10.21273/JASHS.100.5.554.
328. Pill, W.G.; Lambeth, V.N. Effects of Soil Water Regime and Nitrogen Form on Blossom-End Rot, Yield, Water Relations, and Elemental Composition of Tomato1. *Journal of the American Society for Horticultural Science* **1980**, *105*, 730–734, doi:10.21273/JASHS.105.5.730.
329. Valcárcel, M.; Lahoz, I.; Campillo, C.; Martí, R.; Leiva-Brondo, M.; Roselló, S.; Cebolla-Cornejo, J. Controlled Deficit Irrigation as a Water-Saving Strategy for Processing Tomato. *Scientia Horticulturae* **2020**, *261*, 108972, doi:10.1016/j.scienta.2019.108972.
330. Giuliani, M.M.; Nardella, E.; Gagliardi, A.; Gatta, G. Deficit Irrigation and Partial Root-Zone Drying Techniques in Processing Tomato Cultivated under Mediterranean Climate Conditions. *Sustainability* **2017**, *9*, 2197, doi:10.3390/su9122197.
331. Bergougnoux, V. The History of Tomato: From Domestication to Biopharming. *Biotechnology Advances* **2014**, *32*, 170–189, doi:10.1016/j.biotechadv.2013.11.003.
332. Ronga, D.; Francia, E.; Rizza, F.; Badeck, F.-W.; Caradonia, F.; Montevecchi, G.; Pecchioni, N. Changes in Yield Components, Morphological, Physiological and Fruit Quality Traits in Processing Tomato Cultivated in Italy since the 1930's. *Scientia Horticulturae* **2019**, *257*, 108726, doi:10.1016/j.scienta.2019.108726.
333. Grandillo, S.; Zamir, D.; Tanksley, S.D. Genetic Improvement of Processing Tomatoes: A 20 Years Perspective. *Euphytica* **1999**, *110*, 85–97, doi:10.1023/A:1003760015485.
334. Ruiz Celma, A.; Cuadros, F.; López-Rodríguez, F. Characterisation of Industrial Tomato By-Products from Infrared Drying Process. *Food and Bioproducts Processing* **2009**, *87*, 282–291, doi:10.1016/j.fbp.2008.12.003.
335. Pathak, T.B.; Stoddard, C.S. Climate Change Effects on the Processing Tomato Growing Season in California Using Growing Degree Day Model. *Model. Earth Syst. Environ.* **2018**, *4*, 765–775, doi:10.1007/s40808-018-0460-y.
336. Gao, Y.-F.; Liu, J.-K.; Yang, F.-M.; Zhang, G.-Y.; Wang, D.; Zhang, L.; Ou, Y.-B.; Yao, Y.-A. The WRKY Transcription Factor WRKY8 Promotes Resistance to Pathogen Infection and Mediates Drought and Salt Stress Tolerance in Solanum Lycopersicum. *Physiologia Plantarum* **2020**, *168*, 98–117, doi:10.1111/ppl.12978.
337. Ide, R.; Ichiki, A.; Suzuki, T.; Jitsuyama, Y. Analysis of Yield Reduction Factors in Processing Tomatoes under Waterlogging Conditions. *Scientia Horticulturae* **2022**, *295*, doi:10.1016/j.scienta.2021.110840.
338. Wu, W.; Lin, Z.; Zhu, X.; Li, G.; Zhang, W.; Chen, Y.; Ren, L.; Luo, S.; Lin, H.; Zhou, H.; et al. Improved Tomato Yield and Quality by Altering Soil Physicochemical Properties and Nitrification Processes in the Combined Use of Organic-Inorganic Fertilizers. *European Journal of Soil Biology* **2022**, *109*, doi:10.1016/j.ejsobi.2022.103384.
339. Li, X.; Wei, Y.; Xu, J.; Feng, X.; Wu, F.; Zhou, R.; Jin, J.; Xu, K.; Yu, X.; He, Y. SSC and pH for Sweet Assessment and Maturity Classification of Harvested Cherry Fruit Based on NIR Hyperspectral Imaging Technology. *Postharvest Biology and Technology* **2018**, *143*, 112–118, doi:10.1016/j.postharvbio.2018.05.003.
340. Greece: Revamped Exports - Tomato News Available online: https://www.tomatonews.com/en/greece-revamped-exports_2_354.html (accessed on 5 November 2023).
341. Greece: Exports Are on the Rise - Tomato News Available online: https://www.tomatonews.com/en/greece-exports-are-on-the-rise_2_1983.html (accessed on 5 November 2023).
342. Moher, D.; Liberati, A.; Tetzlaff, J.; Altman, D.G. Preferred Reporting Items for Systematic Reviews and Meta-Analyses: The PRISMA Statement. *International Journal of Surgery* **2010**, *8*, 336–341, doi:10.1016/j.ijsu.2010.02.007.

343. Schauberger, B.; Jägermeyr, J.; Gornott, C. A Systematic Review of Local to Regional Yield Forecasting Approaches and Frequently Used Data Resources. *European Journal of Agronomy* **2020**, *120*, 126153, doi:10.1016/j.eja.2020.126153.
344. van Klompenburg, T.; Kassahun, A.; Catal, C. Crop Yield Prediction Using Machine Learning: A Systematic Literature Review. *Computers and Electronics in Agriculture* **2020**, *177*, 105709, doi:10.1016/j.compag.2020.105709.
345. Barriguinha, A.; de Castro Neto, M.; Gil, A. Vineyard Yield Estimation, Prediction, and Forecasting: A Systematic Literature Review. *Agronomy* **2021**, *11*, 1789, doi:10.3390/agronomy11091789.
346. Taylor, J.A.; McBratney, A.B.; Whelan, B.M. Establishing Management Classes for Broadacre Agricultural Production. *Agronomy Journal* **2007**, *99*, 1366–1376, doi:10.2134/agronj2007.0070.
347. Whelan, B.M.; McBratney, A.B.; Minasny, B. Vesper 1.5–Spatial Prediction Software for Precision Agriculture. In Proceedings of the Precision Agriculture, Proc. 6th Int. Conf. on Precision Agriculture, ASA/CSSA/SSSA, Madison, WI, USA; 2002; Vol. 179.
348. Casanova, D.; Epema, G.F.; Goudriaan, J. Monitoring Rice Reflectance at Field Level for Estimating Biomass and LAI. *Field Crops Research* **1998**, *55*, 83–92, doi:10.1016/S0378-4290(97)00064-6.
349. Basso, B.; Cammarano, D.; De Vita, P. Remotely Sensed Vegetation Indices: Theory and Application for Crop Management. *Rivista Italiana di Agrometeorologia* **2004**, *1*, 36–53.
350. Psiroukis, V.; Darra, N.; Kasimati, A.; Trojacek, P.; Hasanli, G.; Fountas, S. Development of a Multi-Scale Tomato Yield Prediction Model in Azerbaijan Using Spectral Indices from Sentinel-2 Imagery. *Remote Sensing* **2022**, *14*, 4202.
351. Kpienbaareh, D.; Mohammed, K.; Luginaah, I.; Wang, J.; Bezner Kerr, R.; Lupafya, E.; Dakishoni, L. Estimating Groundnut Yield in Smallholder Agriculture Systems Using PlanetScope Data. *Land* **2022**, *11*, 1752, doi:10.3390/land11101752.
352. Alabi, T.R.; Abebe, A.T.; Chigeza, G.; Fowobaje, K.R. Estimation of Soybean Grain Yield from Multispectral High-Resolution UAV Data with Machine Learning Models in West Africa. *Remote Sensing Applications: Society and Environment* **2022**, *27*, 100782, doi:10.1016/j.rsase.2022.100782.
353. Clevers, J. Application of a Weighted Infrared-Red Vegetation Index for Estimating Leaf Area Index by Correcting for Soil Moisture. *Remote Sensing of Environment* **1989**, *29*, 25–37.
354. Clevers, J.; Verhoef, W. LAI Estimation by Means of the WDVI: A Sensitivity Analysis with a Combined PROSPECT-SAIL Model. *Remote Sensing Reviews* **1993**, *7*, 43–64.
355. Richardson, A.J.; Wiegand, C.L. Distinguishing Vegetation from Soil Background Information. In *Photogrammetric engineering and remote sensing*; 1977; pp. 1541–1552.
356. Pearson, R.L.; Miller, L.D. *Remote Mapping of Standing Crop Biomass for Estimation of the Productivity of the Shortgrass Prairie*; 1972; p. 1355;.
357. Chatziantoniou, A.; Petropoulos, G.P.; Psomiadis, E. Co-Orbital Sentinel 1 and 2 for LULC Mapping with Emphasis on Wetlands in a Mediterranean Setting Based on Machine Learning. *Remote Sensing* **2017**, *9*, 1259.
358. Efthimiou, N.; Psomiadis, E.; Panagos, P. Fire Severity and Soil Erosion Susceptibility Mapping Using Multi-Temporal Earth Observation Data: The Case of Mati Fatal Wildfire in Eastern Attica, Greece. *Catena* **2020**, *187*, 104320.
359. Fortes Gallego, R.; Prieto Losada, M. del H.; García Martín, A.; Córdoba Pérez, A.; Martínez, L.; Campillo Torres, C. Using NDVI and Guided Sampling to Develop Yield Prediction Maps of Processing Tomato Crop. **2015**.
360. Zhengwei Yang; Hu Zhao; Liping Di; Yu, G. A Comparison of Vegetation Indices for Corn and Soybean Vegetation Condition Monitoring. In Proceedings of the 2009 IEEE International Geoscience and Remote Sensing Symposium; IEEE: Cape Town, July 2009; p. IV-801-IV–804.
361. Bannari, A.; Morin, D.; Bonn, F.; Huete, A. A Review of Vegetation Indices. *Remote sensing reviews* **1995**, *13*, 95–120.

362. Major, D.J.; Baret, F.; Guyot, G. A Ratio Vegetation Index Adjusted for Soil Brightness. *International Journal of Remote Sensing* **1990**, *11*, 727–740, doi:10.1080/01431169008955053.
363. Qi, J.; Chehbouni, A.; Huete, A.R.; Kerr, Y.H.; Sorooshian, S. A Modified Soil Adjusted Vegetation Index. *Remote Sensing of Environment* **1994**, *48*, 119–126, doi:10.1016/0034-4257(94)90134-1.
364. Pałaś, K.W.; Zawadzki, J. Sentinel-2 Imagery Processing for Tree Logging Observations on the Białowieża Forest World Heritage Site. *Forests* **2020**, *11*, 857, doi:10.3390/f11080857.
365. Naji, T.A.H. Study of Vegetation Cover Distribution Using DVI, PVI, WDVI Indices with 2D-Space Plot. *J. Phys.: Conf. Ser.* **2018**, *1003*, 012083, doi:10.1088/1742-6596/1003/1/012083.
366. He, X.; Zhao, K.; Chu, X. AutoML: A Survey of the State-of-the-Art. *Knowledge-Based Systems* **2021**, *212*, 106622, doi:10.1016/j.knosys.2020.106622.
367. Zheng, Z.; Yang, L.; Wang, L.; Li, F. AD-DARTS: Adaptive Dropout for Differentiable Architecture Search. In Proceedings of the Artificial Intelligence: First CAAI International Conference, CICAI 2021, Hangzhou, China, June 5–6, 2021, Proceedings, Part II; Springer-Verlag: Berlin, Heidelberg, March 5 2021; pp. 115–126.
368. Shende, M.K.; Feijóo-Lorenzo, A.E.; Bokde, N.D. cleanTS: Automated (AutoML) Tool to Clean Univariate Time Series at Microscales. *Neurocomputing* **2022**, *500*, 155–176, doi:10.1016/j.neucom.2022.05.057.
369. Siriborvornratanakul, T. Human Behavior in Image-Based Road Health Inspection Systems despite the Emerging AutoML. *Journal of Big Data* **2022**, *9*, 96, doi:10.1186/s40537-022-00646-8.
370. Dietterich, T.G. Ensemble Methods in Machine Learning. In Proceedings of the International workshop on multiple classifier systems; Springer, 2000; pp. 1–15.
371. Prasetyo, Y.; Sukmono, A.; Aziz, K.W.; Prakosta Santu Aji, B.J. Rice Productivity Prediction Model Design Based On Linear Regression of Spectral Value Using NDVI and LSWI Combination On Landsat-8 Imagery. *IOP Conf. Ser.: Earth Environ. Sci.* **2018**, *165*, 012002, doi:10.1088/1755-1315/165/1/012002.
372. Van Gestel, T.; Suykens, J.A.; De Moor, B.; Vandewalle, J. Automatic Relevance Determination for Least Squares Support Vector Machines Classifiers. In Proceedings of the ESANN; 2001; pp. 13–18.
373. Sen, P.K. Estimates of the Regression Coefficient Based on Kendall's Tau. *Journal of the American Statistical Association* **1968**, *63*, 1379–1389, doi:10.1080/01621459.1968.10480934.
374. Huber, P.J. Robust Regression: Asymptotics, Conjectures and Monte Carlo. *The annals of statistics* **1973**, 799–821.
375. Freund, Y.; Schapire, R.E. A Decision-Theoretic Generalization of On-Line Learning and an Application to Boosting. *Journal of Computer and System Sciences* **1997**, *55*, 119–139, doi:10.1006/jcss.1997.1504.
376. Breiman, L. Random Forests. *Machine learning* **2001**, *45*, 5–32.
377. Geurts, P.; Ernst, D.; Wehenkel, L. Extremely Randomized Trees. *Mach Learn* **2006**, *63*, 3–42, doi:10.1007/s10994-006-6226-1.
378. Feurer, M.; Klein, A.; Eggensperger, K.; Springenberg, J.; Blum, M.; Hutter, F. Efficient and Robust Automated Machine Learning. *Advances in neural information processing systems* **2015**, *28*.
379. Brochu, E.; Cora, V.M.; de Freitas, N. A Tutorial on Bayesian Optimization of Expensive Cost Functions, with Application to Active User Modeling and Hierarchical Reinforcement Learning 2010.
380. Vanschoren, J.; van Rijn, J.N.; Bischl, B.; Torgo, L. OpenML: Networked Science in Machine Learning. *SIGKDD Explor. Newsl.* **2014**, *15*, 49–60, doi:10.1145/2641190.2641198.
381. Darra, N.; Anastasiou, E.; Kriezi, O.; Lazarou, E.; Kalivas, D.; Fountas, S. Can Yield Prediction Be Fully Digitilized? A Systematic Review. *Agronomy* **2023**, *13*, 2441, doi:10.3390/agronomy13092441.

382. Muruganantham, P.; Wibowo, S.; Grandhi, S.; Samrat, N.H.; Islam, N. A Systematic Literature Review on Crop Yield Prediction with Deep Learning and Remote Sensing. *Remote Sensing* **2022**, *14*, 1990, doi:10.3390/rs14091990.
383. CLASSIFICATION OF CROPS.
384. Luo, S.; He, Y.; Li, Q.; Jiao, W.; Zhu, Y.; Zhao, X. Nondestructive Estimation of Potato Yield Using Relative Variables Derived from Multi-Period LAI and Hyperspectral Data Based on Weighted Growth Stage. *Plant Methods* **2020**, *16*, 150, doi:10.1186/s13007-020-00693-3.
385. Huang, S.; Tang, L.; Hupy, J.P.; Wang, Y.; Shao, G. A Commentary Review on the Use of Normalized Difference Vegetation Index (NDVI) in the Era of Popular Remote Sensing. *J. For. Res.* **2021**, *32*, 1–6, doi:10.1007/s11676-020-01155-1.
386. Crane-Droesch, A. Machine Learning Methods for Crop Yield Prediction and Climate Change Impact Assessment in Agriculture. *Environ. Res. Lett.* **2018**, *13*, 114003, doi:10.1088/1748-9326/aae159.
387. Elavarasan, D.; Vincent, P.M.D. Crop Yield Prediction Using Deep Reinforcement Learning Model for Sustainable Agrarian Applications. *IEEE Access* **2020**, *8*, 86886–86901, doi:10.1109/ACCESS.2020.2992480.
388. Wang, X.; Huang, J.; Feng, Q.; Yin, D. Winter Wheat Yield Prediction at County Level and Uncertainty Analysis in Main Wheat-Producing Regions of China with Deep Learning Approaches. *Remote Sensing* **2020**, *12*, 1744, doi:10.3390/rs12111744.
389. Mulianga, B.; Bégué, A.; Simoes, M.; Todoroff, P. Forecasting Regional Sugarcane Yield Based on Time Integral and Spatial Aggregation of MODIS NDVI. *Remote Sensing* **2013**, *5*, 2184–2199, doi:10.3390/rs5052184.
390. Singla, S.K.; Garg, R.D.; Dubey, O.P. Spatiotemporal Analysis of LANDSAT Data for Crop Yield Prediction. *Journal of Engineering Science and Technology Review* **2018**, *11*, 9–17, doi:10.25103/jestr.113.02.
391. Picoli, M.C.A.; Lamparelli, R.A.C.; Sano, E.E.; Rocha, J.V. The Use of ALOS/PALSAR Data for Estimating Sugarcane Productivity. *Eng. Agríc.* **2014**, *34*, 1245–1255, doi:10.1590/S0100-69162014000600019.
392. Morel, J.; Todoroff, P.; Bégué, A.; Bury, A.; Martiné, J.-F.; Petit, M. Toward a Satellite-Based System of Sugarcane Yield Estimation and Forecasting in Smallholder Farming Conditions: A Case Study on Reunion Island. *Remote Sensing* **2014**, *6*, 6620–6635, doi:10.3390/rs6076620.
393. Duveiller, G.; López-Lozano, R.; Baruth, B. Enhanced Processing of 1-Km Spatial Resolution fAPAR Time Series for Sugarcane Yield Forecasting and Monitoring. *Remote Sensing* **2013**, *5*, 1091–1116, doi:10.3390/rs5031091.
394. Singla, S.; Garg, R.; Dubey, O. Ensemble Machine Learning Methods to Estimate the Sugarcane Yield Based on Remote Sensing Information. *Revue d'Intelligence Artificielle* **2020**, *34*, 731–743, doi:10.18280/ria.340607.
395. Rahman, M.M.; Robson, A. Integrating Landsat-8 and Sentinel-2 Time Series Data for Yield Prediction of Sugarcane Crops at the Block Level. *Remote Sensing* **2020**, *12*, 1313, doi:10.3390/rs12081313.
396. Canata, T.F.; Wei, M.C.F.; Maldaner, L.F.; Molin, J.P. Sugarcane Yield Mapping Using High-Resolution Imagery Data and Machine Learning Technique. *Remote Sensing* **2021**, *13*, 232, doi:10.3390/rs13020232.
397. Hu, S.; Shi, L.; Zha, Y.; Zeng, L. Regional Yield Estimation for Sugarcane Using MODIS and Weather Data: A Case Study in Florida and Louisiana, United States of America. *Remote Sensing* **2022**, *14*, 3870, doi:10.3390/rs14163870.
398. Ali, A.; Martelli, R.; Lupia, F.; Barbanti, L. Assessing Multiple Years' Spatial Variability of Crop Yields Using Satellite Vegetation Indices. *Remote Sensing* **2019**, *11*, 2384, doi:10.3390/rs11202384.

399. Phan, P.; Chen, N.; Xu, L.; Dao, D.M.; Dang, D. NDVI Variation and Yield Prediction in Growing Season: A Case Study with Tea in Tanuyen Vietnam. *Atmosphere* **2021**, *12*, 962, doi:10.3390/atmos12080962.
400. Thao, N.T.T.; Khoi, D.N.; Denis, A.; Viet, L.V.; Wellens, J.; Tychon, B. Early Prediction of Coffee Yield in the Central Highlands of Vietnam Using a Statistical Approach and Satellite Remote Sensing Vegetation Biophysical Variables. *Remote Sensing* **2022**, *14*, 2975, doi:10.3390/rs14132975.
401. Martello, M.; Molin, J.P.; Wei, M.C.F.; Canal Filho, R.; Nicoletti, J.V.M. Coffee-Yield Estimation Using High-Resolution Time-Series Satellite Images and Machine Learning. *AgriEngineering* **2022**, *4*, 888–902, doi:10.3390/agriengineering4040057.
402. Kim, D.-W.; Yun, H.S.; Jeong, S.-J.; Kwon, Y.-S.; Kim, S.-G.; Lee, W.S.; Kim, H.-J. Modeling and Testing of Growth Status for Chinese Cabbage and White Radish with UAV-Based RGB Imagery. *Remote Sensing* **2018**, *10*, 563, doi:10.3390/rs10040563.
403. Suarez, L.A.; Robson, A.; McPhee, J.; O'Halloran, J.; van Sprang, C. Accuracy of Carrot Yield Forecasting Using Proximal Hyperspectral and Satellite Multispectral Data. *Precision Agric* **2020**, *21*, 1304–1326, doi:10.1007/s11119-020-09722-6.
404. Mwinuka, P.R.; Mbilinyi, B.P.; Mbungu, W.B.; Mourice, S.K.; Mahoo, H.F.; Schmitter, P. The Feasibility of Hand-Held Thermal and UAV-Based Multispectral Imaging for Canopy Water Status Assessment and Yield Prediction of Irrigated African Eggplant (Solanum Aethopicum L). *Agricultural Water Management* **2021**, *245*, 106584, doi:10.1016/j.agwat.2020.106584.
405. Chancia, R.; van Aardt, J.; Pethybridge, S.; Cross, D.; Henderson, J. Predicting Table Beet Root Yield with Multispectral UAS Imagery. *Remote Sensing* **2021**, *13*, 2180, doi:10.3390/rs13112180.
406. Tatsumi, K.; Igarashi, N.; Mengxue, X. Prediction of Plant-Level Tomato Biomass and Yield Using Machine Learning with Unmanned Aerial Vehicle Imagery. *Plant Methods* **2021**, *17*, 77, doi:10.1186/s13007-021-00761-2.
407. Johansen, K.; Morton, M.J.L.; Malbeteau, Y.; Aragon, B.; Al-Mashharawi, S.; Ziliani, M.G.; Angel, Y.; Fiene, G.; Negrão, S.; Mousa, M.A.A.; et al. Predicting Biomass and Yield in a Tomato Phenotyping Experiment Using UAV Imagery and Random Forest. *Frontiers in Artificial Intelligence* **2020**, *3*.
408. Chang, A.; Jung, J.; Yeom, J.; Maeda, M.M.; Landivar, J.A.; Enciso, J.M.; Avila, C.A.; Anciso, J.R. Unmanned Aircraft System- (UAS-) Based High-Throughput Phenotyping (HTP) for Tomato Yield Estimation. *Journal of Sensors* **2021**, *2021*, e8875606, doi:10.1155/2021/8875606.
409. Gumma, M.K.; Kadiyala, M.D.M.; Panjala, P.; Ray, S.S.; Akuraju, V.R.; Dubey, S.; Smith, A.P.; Das, R.; Whitbread, A.M. Assimilation of Remote Sensing Data into Crop Growth Model for Yield Estimation: A Case Study from India. *J Indian Soc Remote Sens* **2022**, *50*, 257–270, doi:10.1007/s12524-021-01341-6.
410. Yu, B.; Shang, S. Multi-Year Mapping of Major Crop Yields in an Irrigation District from High Spatial and Temporal Resolution Vegetation Index. *Sensors* **2018**, *18*, 3787, doi:10.3390/s18113787.
411. Gutiérrez, P.A.; López-Granados, F.; Peña-Barragán, J.M.; Jurado-Expósito, M.; Gómez-Casero, M.T.; Hervás-Martínez, C. Mapping Sunflower Yield as Affected by Ridolfia Segetum Patches and Elevation by Applying Evolutionary Product Unit Neural Networks to Remote Sensed Data. *Computers and Electronics in Agriculture* **2008**, *60*, 122–132, doi:10.1016/j.compag.2007.07.011.
412. Lykhovyd, P.V. Forecasting Oil Crops Yields on the Regional Scale Using Normalized Difference Vegetation Index. *J. Ecol. Eng.* **2021**, *22*, 53–57, doi:10.12911/22998993/132436.
413. Ortenzi, L.; Violino, S.; Pallottino, F.; Figorilli, S.; Vasta, S.; Tocci, F.; Antonucci, F.; Imperi, G.; Costa, C. Early Estimation of Olive Production from Light Drone Orthophoto, through Canopy Radius. *Drones* **2021**, *5*, 118, doi:10.3390/drones5040118.
414. Watson-Hernández, F.; Gómez-Calderón, N.; da Silva, R.P. Oil Palm Yield Estimation Based on Vegetation and Humidity Indices Generated from Satellite Images and Machine Learning Techniques. *AgriEngineering* **2022**, *4*, 279–291, doi:10.3390/agriengineering4010019.

415. Fernando, H.; Ha, T.; Attanayake, A.; Benaragama, D.; Nketia, K.A.; Kanmi-Obembe, O.; Shirtliffe, S.J. High-Resolution Flowering Index for Canola Yield Modelling. *Remote Sensing* **2022**, *14*, 4464, doi:10.3390/rs14184464.
416. Chen, Y.; McVicar, T.R.; Donohue, R.J.; Garg, N.; Waldner, F.; Ota, N.; Li, L.; Lawes, R. To Blend or Not to Blend? A Framework for Nationwide Landsat–MODIS Data Selection for Crop Yield Prediction. *Remote Sensing* **2020**, *12*, 1653, doi:10.3390/rs12101653.
417. Gong, Y.; Duan, B.; Fang, S.; Zhu, R.; Wu, X.; Ma, Y.; Peng, Y. Remote Estimation of Rapeseed Yield with Unmanned Aerial Vehicle (UAV) Imaging and Spectral Mixture Analysis. *Plant Methods* **2018**, *14*, 70, doi:10.1186/s13007-018-0338-z.
418. Ji, F.; Meng, J.; Cheng, Z.; Fang, H.; Wang, Y. Crop Yield Estimation at Field Scales by Assimilating Time Series of Sentinel-2 Data Into a Modified CASA-WOFOST Coupled Model. *IEEE Transactions on Geoscience and Remote Sensing* **2022**, *60*, 1–14, doi:10.1109/TGRS.2020.3047102.
419. Allies, A.; Roumiguié, A.; Fieuzal, R.; Dejoux, J.-F.; Jacquin, A.; Veloso, A.; Champolivier, L.; Baup, F. Assimilation of Multisensor Optical and Multiorbital SAR Satellite Data in a Simplified Agrometeorological Model for Rapeseed Crops Monitoring. *IEEE Journal of Selected Topics in Applied Earth Observations and Remote Sensing* **2022**, *15*, 1123–1138, doi:10.1109/JSTARS.2021.3136289.
420. Li, A.; Liang, S.; Wang, A.; Qin, J. Estimating Crop Yield from Multi-Temporal Satellite Data Using Multivariate Regression and Neural Network Techniques. *Photogrammetric Engineering & Remote Sensing* **2007**, *73*, 1149–1157, doi:10.14358/PERS.73.10.1149.
421. Sayago, S.; Bocco, M. Crop Yield Estimation Using Satellite Images: Comparison of Linear and Non-Linear Models. *AgriScientia* **2018**, *35*, 1–9, doi:10.31047/1668.298x.v1.n35.20447.
422. Gao, Y.; Wang, S.; Guan, K.; Wolanin, A.; You, L.; Ju, W.; Zhang, Y. The Ability of Sun-Induced Chlorophyll Fluorescence From OCO-2 and MODIS-EVI to Monitor Spatial Variations of Soybean and Maize Yields in the Midwestern USA. *Remote Sensing* **2020**, *12*, 1111, doi:10.3390/rs12071111.
423. Soybean Yield Prediction Using Remote Sensing in Southwestern Piauí State, Brazil. - Portal Embrapa Available online: https://www.embrapa.br/en/busca-de-publicacoes/-/publicacao/1138334/soybean-yield-prediction-using-remote-sensing-in-southwestern-piaui-state-brazil (accessed on 7 July 2023).
424. Stepanov, A.; Dubrovin, K.; Sorokin, A.; Aseeva, T. Predicting Soybean Yield at the Regional Scale Using Remote Sensing and Climatic Data. *Remote Sensing* **2020**, *12*, 1936, doi:10.3390/rs12121936.
425. Roznik, M.; Boyd, M.; Porth, L. Improving Crop Yield Estimation by Applying Higher Resolution Satellite NDVI Imagery and High-Resolution Cropland Masks. *Remote Sensing Applications: Society and Environment* **2022**, *25*, 100693, doi:10.1016/j.rsase.2022.100693.
426. Gao, F.; Anderson, M.; Daughtry, C.; Johnson, D. Assessing the Variability of Corn and Soybean Yields in Central Iowa Using High Spatiotemporal Resolution Multi-Satellite Imagery. *Remote Sensing* **2018**, *10*, 1489, doi:10.3390/rs10091489.
427. Liu, J.; Shang, J.; Qian, B.; Huffman, T.; Zhang, Y.; Dong, T.; Jing, Q.; Martin, T. Crop Yield Estimation Using Time-Series MODIS Data and the Effects of Cropland Masks in Ontario, Canada. *Remote Sensing* **2019**, *11*, 2419, doi:10.3390/rs11202419.
428. Figueiredo, G.K.D.A.; Brunsell, N.A.; Higa, B.H.; Rocha, J.V.; Lamparelli, R.A.C. Correlation Maps to Assess Soybean Yield from EVI Data in Paraná State, Brazil. *Sci. agric. (Piracicaba, Braz.)* **2016**, *73*, 462–470, doi:10.1590/0103-9016-2015-0215.
429. Wei, J.; Tang, X.; Gu, Q.; Wang, M.; Ma, M.; Han, X. Using Solar-Induced Chlorophyll Fluorescence Observed by OCO-2 to Predict Autumn Crop Production in China. *Remote Sensing* **2019**, *11*, 1715, doi:10.3390/rs11141715.
430. Sun, J.; Di, L.; Sun, Z.; Shen, Y.; Lai, Z. County-Level Soybean Yield Prediction Using Deep CNN-LSTM Model. *Sensors* **2019**, *19*, 4363, doi:10.3390/s19204363.

431. Huber, F.; Yushchenko, A.; Stratmann, B.; Steinhage, V. Extreme Gradient Boosting for Yield Estimation Compared with Deep Learning Approaches. *Computers and Electronics in Agriculture* **2022**, *202*, 107346, doi:10.1016/j.compag.2022.107346.
432. Marshall, M.; Belgiu, M.; Boschetti, M.; Pepe, M.; Stein, A.; Nelson, A. Field-Level Crop Yield Estimation with PRISMA and Sentinel-2. *ISPRS Journal of Photogrammetry and Remote Sensing* **2022**, *187*, 191–210, doi:10.1016/j.isprsjprs.2022.03.008.
433. Mateo-Sanchis, A.; Piles, M.; Muñoz-Marí, J.; Adsuara, J.E.; Pérez-Suay, A.; Camps-Valls, G. Synergistic Integration of Optical and Microwave Satellite Data for Crop Yield Estimation. *Remote Sensing of Environment* **2019**, *234*, 111460, doi:10.1016/j.rse.2019.111460.
434. Pejak, B.; Lugonja, P.; Antić, A.; Panić, M.; Pandžić, M.; Alexakis, E.; Mavrepis, P.; Zhou, N.; Marko, O.; Crnojević, V. Soya Yield Prediction on a Within-Field Scale Using Machine Learning Models Trained on Sentinel-2 and Soil Data. *Remote Sensing* **2022**, *14*, 2256, doi:10.3390/rs14092256.
435. Maimaitijiang, M.; Sagan, V.; Sidike, P.; Hartling, S.; Esposito, F.; Fritschi, F.B. Soybean Yield Prediction from UAV Using Multimodal Data Fusion and Deep Learning. *Remote Sensing of Environment* **2020**, *237*, 111599, doi:10.1016/j.rse.2019.111599.
436. Bai, D.; Li, D.; Zhao, C.; Wang, Z.; Shao, M.; Guo, B.; Liu, Y.; Wang, Q.; Li, J.; Guo, S.; et al. Estimation of Soybean Yield Parameters under Lodging Conditions Using RGB Information from Unmanned Aerial Vehicles. *Frontiers in Plant Science* **2022**, *13*.
437. Zhang, X.; Zhao, J.; Yang, G.; Liu, J.; Cao, J.; Li, C.; Zhao, X.; Gai, J. Establishment of Plot-Yield Prediction Models in Soybean Breeding Programs Using UAV-Based Hyperspectral Remote Sensing. *Remote Sensing* **2019**, *11*, 2752, doi:10.3390/rs11232752.
438. Peng, B.; Guan, K.; Zhou, W.; Jiang, C.; Frankenberg, C.; Sun, Y.; He, L.; Köhler, P. Assessing the Benefit of Satellite-Based Solar-Induced Chlorophyll Fluorescence in Crop Yield Prediction. *International Journal of Applied Earth Observation and Geoinformation* **2020**, *90*, 102126, doi:10.1016/j.jag.2020.102126.
439. Dado, W.T.; Deines, J.M.; Patel, R.; Liang, S.-Z.; Lobell, D.B. High-Resolution Soybean Yield Mapping Across the US Midwest Using Subfield Harvester Data. *Remote Sensing* **2020**, *12*, 3471, doi:10.3390/rs12213471.
440. Herrero-Huerta, M.; Rodriguez-Gonzalvez, P.; Rainey, K.M. Yield Prediction by Machine Learning from UAS-Based Multi-Sensor Data Fusion in Soybean. *Plant Methods* **2020**, *16*, 78, doi:10.1186/s13007-020-00620-6.
441. Franz, T.E.; Pokal, S.; Gibson, J.P.; Zhou, Y.; Gholizadeh, H.; Tenorio, F.A.; Rudnick, D.; Heeren, D.; McCabe, M.; Ziliani, M.; et al. The Role of Topography, Soil, and Remotely Sensed Vegetation Condition towards Predicting Crop Yield. *Field Crops Research* **2020**, *252*, 107788, doi:10.1016/j.fcr.2020.107788.
442. Sun, L.; Gao, F.; Anderson, M.C.; Kustas, W.P.; Alsina, M.M.; Sanchez, L.; Sams, B.; McKee, L.; Dulaney, W.; White, W.A.; et al. Daily Mapping of 30 m LAI and NDVI for Grape Yield Prediction in California Vineyards. *Remote Sensing* **2017**, *9*, 317, doi:10.3390/rs9040317.
443. Hacking, C.; Poona, N.; Poblete-Echeverria, C. Vineyard Yield Estimation Using 2-D Proximal Sensing: A Multitemporal Approach. *OENO One* **2020**, *54*, 793–812, doi:10.20870/oeno-one.2020.54.4.3361.
444. Olenskyj, A.G.; Sams, B.S.; Fei, Z.; Singh, V.; Raja, P.V.; Bornhorst, G.M.; Earles, J.M. End-to-End Deep Learning for Directly Estimating Grape Yield from Ground-Based Imagery. *Computers and Electronics in Agriculture* **2022**, *198*, 107081, doi:10.1016/j.compag.2022.107081.
445. Victorino, G.; Braga, R.P.; Santos-Victor, J.; Lopes, C.M. Comparing a New Non-Invasive Vineyard Yield Estimation Approach Based on Image Analysis with Manual Sample-Based Methods. *Agronomy* **2022**, *12*, 1464, doi:10.3390/agronomy12061464.
446. Zhang, X.; Pourreza, A.; Cheung, K.H.; Zuniga-Ramirez, G.; Lampinen, B.D.; Shackel, K.A. Estimation of Fractional Photosynthetically Active Radiation From a Canopy 3D Model; Case Study: Almond Yield Prediction. *Frontiers in Plant Science* **2021**, *12*.

447. Zhang, Z.; Jin, Y.; Chen, B.; Brown, P. California Almond Yield Prediction at the Orchard Level With a Machine Learning Approach. *Frontiers in Plant Science* **2019**, *10*.
448. Sun, G.; Wang, X.; Yang, H.; Zhang, X. A Canopy Information Measurement Method for Modern Standardized Apple Orchards Based on UAV Multimodal Information. *Sensors* **2020**, *20*, 2985, doi:10.3390/s20102985.
449. Bai, T.; Wang, S.; Meng, W.; Zhang, N.; Wang, T.; Chen, Y.; Mercatoris, B. Assimilation of Remotely-Sensed LAI into WOFOST Model with the SUBPLEX Algorithm for Improving the Field-Scale Jujube Yield Forecasts. *Remote Sensing* **2019**, *11*, 1945, doi:10.3390/rs11161945.
450. Rahman, M.M.; Robson, A.; Bristow, M. Exploring the Potential of High Resolution WorldView-3 Imagery for Estimating Yield of Mango. *Remote Sensing* **2018**, *10*, 1866, doi:10.3390/rs10121866.
451. Sarron, J.; Malézieux, É.; Sané, C.A.B.; Faye, É. Mango Yield Mapping at the Orchard Scale Based on Tree Structure and Land Cover Assessed by UAV. *Remote Sensing* **2018**, *10*, 1900, doi:10.3390/rs10121900.
452. Al-Gaadi, K.A.; Hassaballa, A.A.; Tola, E.; Kayad, A.G.; Madugundu, R.; Alblewi, B.; Assiri, F. Prediction of Potato Crop Yield Using Precision Agriculture Techniques. *PLOS ONE* **2016**, *11*, e0162219, doi:10.1371/journal.pone.0162219.
453. Gómez, D.; Salvador, P.; Sanz, J.; Casanova, J.L. Potato Yield Prediction Using Machine Learning Techniques and Sentinel 2 Data. *Remote Sensing* **2019**, *11*, 1745, doi:10.3390/rs11151745.
454. Salvador, P.; Gómez, D.; Sanz, J.; Casanova, J.L. Estimation of Potato Yield Using Satellite Data at a Municipal Level: A Machine Learning Approach. *ISPRS International Journal of Geo-Information* **2020**, *9*, 343, doi:10.3390/ijgi9060343.
455. Abbas, F.; Afzaal, H.; Farooque, A.A.; Tang, S. Crop Yield Prediction through Proximal Sensing and Machine Learning Algorithms. *Agronomy* **2020**, *10*, 1046, doi:10.3390/agronomy10071046.
456. Chu, T.; Chen, R.; Landivar, J.A.; Maeda, M.M.; Yang, C.; Starek, M.J. Cotton Growth Modeling and Assessment Using Unmanned Aircraft System Visual-Band Imagery. *JARS* **2016**, *10*, 036018, doi:10.1117/1.JRS.10.036018.
457. Xu, W.; Chen, P.; Zhan, Y.; Chen, S.; Zhang, L.; Lan, Y. Cotton Yield Estimation Model Based on Machine Learning Using Time Series UAV Remote Sensing Data. *International Journal of Applied Earth Observation and Geoinformation* **2021**, *104*, 102511, doi:10.1016/j.jag.2021.102511.
458. Kang, X.; Huang, C.; Zhang, L.; Zhang, Z.; Lv, X. Downscaling Solar-Induced Chlorophyll Fluorescence for Field-Scale Cotton Yield Estimation by a Two-Step Convolutional Neural Network. *Computers and Electronics in Agriculture* **2022**, *201*, 107260, doi:10.1016/j.compag.2022.107260.
459. Jeong, S.; Shin, T.; Ban, J.-O.; Ko, J. Simulation of Spatiotemporal Variations in Cotton Lint Yield in the Texas High Plains. *Remote Sensing* **2022**, *14*, 1421, doi:10.3390/rs14061421.
460. Shanmugapriya, P.; Latha, K.R.; Pazhanivelan, S.; Kumaraperumal, R.; Karthikeyan, G.; Sudarmanian, N.S. Cotton Yield Prediction Using Drone Derived LAI and Chlorophyll Content. *Journal of Agrometeorology* **2022**, *24*, 348–352, doi:10.54386/jam.v24i4.1770.
461. Rodriguez-Sanchez, J.; Li, C.; Paterson, A.H. Cotton Yield Estimation From Aerial Imagery Using Machine Learning Approaches. *Frontiers in Plant Science* **2022**, *13*.
462. Li, F.; Bai, J.; Zhang, M.; Zhang, R. Yield Estimation of High-Density Cotton Fields Using Low-Altitude UAV Imaging and Deep Learning. *Plant Methods* **2022**, *18*, 55, doi:10.1186/s13007-022-00881-3.
463. Shi, G.; Du, X.; Du, M.; Li, Q.; Tian, X.; Ren, Y.; Zhang, Y.; Wang, H. Cotton Yield Estimation Using the Remotely Sensed Cotton Boll Index from UAV Images. *Drones* **2022**, *6*, 254, doi:10.3390/drones6090254.
464. Ma, Y.; Ma, L.; Zhang, Q.; Huang, C.; Yi, X.; Chen, X.; Hou, T.; Lv, X.; Zhang, Z. Cotton Yield Estimation Based on Vegetation Indices and Texture Features Derived From RGB Image. *Frontiers in Plant Science* **2022**, *13*.

465. Rattanasopa, K.; Saengprachatanarug, K.; Wongpichet, S.; Posom, J.; Saikaew, K.; Ungsathittavorn, K.; Pilawut, S.; Chinapas, A.; Taira, E. UAV-Based Multispectral Imagery for Estimating Cassava Tuber Yields. *Engineering in Agriculture, Environment and Food* **2022**, *15*, 1–12, doi:10.37221/eaef.15.1_1.
466. Fu, H.; Wang, C.; Cui, G.; She, W.; Zhao, L. Ramie Yield Estimation Based on UAV RGB Images. *Sensors* **2021**, *21*, 669, doi:10.3390/s21020669.
467. Wengert, M.; Wijesingha, J.; Schulze-Brüninghoff, D.; Wachendorf, M.; Astor, T. Multisite and Multitemporal Grassland Yield Estimation Using UAV-Borne Hyperspectral Data. *Remote Sensing* **2022**, *14*, 2068, doi:10.3390/rs14092068.
468. Grüner, E.; Astor, T.; Wachendorf, M. Biomass Prediction of Heterogeneous Temperate Grasslands Using an SfM Approach Based on UAV Imaging. *Agronomy* **2019**, *9*, 54, doi:10.3390/agronomy9020054.
469. Pranga, J.; Borra-Serrano, I.; Aper, J.; De Swaef, T.; Ghesquiere, A.; Quataert, P.; Roldán-Ruiz, I.; Janssens, I.A.; Ruysschaert, G.; Lootens, P. Improving Accuracy of Herbage Yield Predictions in Perennial Ryegrass with UAV-Based Structural and Spectral Data Fusion and Machine Learning. *Remote Sensing* **2021**, *13*, 3459, doi:10.3390/rs13173459.
470. Hamada, Y.; Zumpf, C.R.; Cacho, J.F.; Lee, D.; Lin, C.-H.; Boe, A.; Heaton, E.; Mitchell, R.; Negri, M.C. Remote Sensing-Based Estimation of Advanced Perennial Grass Biomass Yields for Bioenergy. *Land* **2021**, *10*, 1221, doi:10.3390/land10111221.
471. Alvarez-Mendoza, C.I.; Guzman, D.; Casas, J.; Bastidas, M.; Polanco, J.; Valencia-Ortiz, M.; Montenegro, F.; Arango, J.; Ishitani, M.; Selvaraj, M.G. Predictive Modeling of Above-Ground Biomass in Brachiaria Pastures from Satellite and UAV Imagery Using Machine Learning Approaches. *Remote Sensing* **2022**, *14*, 5870, doi:10.3390/rs14225870.
472. Impollonia, G.; Croci, M.; Ferrarini, A.; Brook, J.; Martani, E.; Blandinières, H.; Marcone, A.; Awty-Carroll, D.; Ashman, C.; Kam, J.; et al. UAV Remote Sensing for High-Throughput Phenotyping and for Yield Prediction of Miscanthus by Machine Learning Techniques. *Remote Sensing* **2022**, *14*, 2927, doi:10.3390/rs14122927.
473. He, M.; Kimball, J.S.; Maneta, M.P.; Maxwell, B.D.; Moreno, A.; Beguería, S.; Wu, X. Regional Crop Gross Primary Productivity and Yield Estimation Using Fused Landsat-MODIS Data. *Remote Sensing* **2018**, *10*, 372, doi:10.3390/rs10030372.
474. Yadav, K.; Geli, H.M.E. Prediction of Crop Yield for New Mexico Based on Climate and Remote Sensing Data for the 1920–2019 Period. *Land* **2021**, *10*, 1389, doi:10.3390/land10121389.
475. Feng, L.; Zhang, Z.; Ma, Y.; Du, Q.; Williams, P.; Drewry, J.; Luck, B. Alfalfa Yield Prediction Using UAV-Based Hyperspectral Imagery and Ensemble Learning. *Remote Sensing* **2020**, *12*, 2028, doi:10.3390/rs12122028.
476. Minch, C.; Dvorak, J.; Jackson, J.; Sheffield, S.T. Creating a Field-Wide Forage Canopy Model Using UAVs and Photogrammetry Processing. *Remote Sensing* **2021**, *13*, 2487, doi:10.3390/rs13132487.
477. Chandel, A.K.; Khot, L.R.; Yu, L.-X. Alfalfa (Medicago Sativa L.) Crop Vigor and Yield Characterization Using High-Resolution Aerial Multispectral and Thermal Infrared Imaging Technique. *Computers and Electronics in Agriculture* **2021**, *182*, 105999, doi:10.1016/j.compag.2021.105999.
478. Azadbakht, M.; Ashourloo, D.; Aghighi, H.; Homayouni, S.; Shahrabi, H.S.; Matkan, A.; Radiom, S. Alfalfa Yield Estimation Based on Time Series of Landsat 8 and PROBA-V Images: An Investigation of Machine Learning Techniques and Spectral-Temporal Features. *Remote Sensing Applications: Society and Environment* **2022**, *25*, 100657, doi:10.1016/j.rsase.2021.100657.
479. Li, K.-Y.; Burnside, N.G.; Sampaio de Lima, R.; Villoslada Peciña, M.; Sepp, K.; Yang, M.-D.; Raet, J.; Vain, A.; Selge, A.; Sepp, K. The Application of an Unmanned Aerial System and Machine Learning Techniques for Red Clover-Grass Mixture Yield Estimation under Variety Performance Trials. *Remote Sensing* **2021**, *13*, 1994, doi:10.3390/rs13101994.

480. Rezapour, S.; Jooyandeh, E.; Ramezanzade, M.; Mostafaeipour, A.; Jahangiri, M.; Issakhov, A.; Chowdhury, S.; Techato, K. Forecasting Rainfed Agricultural Production in Arid and Semi-Arid Lands Using Learning Machine Methods: A Case Study. *Sustainability* **2021**, *13*, 4607, doi:10.3390/su13094607.
481. Hassanzadeh, A.; Zhang, F.; van Aardt, J.; Murphy, S.P.; Pethybridge, S.J. Broadacre Crop Yield Estimation Using Imaging Spectroscopy from Unmanned Aerial Systems (UAS): A Field-Based Case Study with Snap Bean. *Remote Sensing* **2021**, *13*, 3241, doi:10.3390/rs13163241.
482. Lipovac, A.; Bezdan, A.; Moravčević, D.; Djurović, N.; Ćosić, M.; Benka, P.; Stričević, R. Correlation between Ground Measurements and UAV Sensed Vegetation Indices for Yield Prediction of Common Bean Grown under Different Irrigation Treatments and Sowing Periods. *Water* **2022**, *14*, 3786, doi:10.3390/w14223786.
483. Karst, I.G.; Mank, I.; Traoré, I.; Sorgho, R.; Stückemann, K.-J.; Simboro, S.; Sié, A.; Franke, J.; Sauerborn, R. Estimating Yields of Household Fields in Rural Subsistence Farming Systems to Study Food Security in Burkina Faso. *Remote Sensing* **2020**, *12*, 1717, doi:10.3390/rs12111717.
484. Gonzalez-Gonzalez, M.A.; Guertin, D.P. Seasonal Bean Yield Forecast for Non-Irrigated Croplands through Climate and Vegetation Index Data: Geospatial Effects. *International Journal of Applied Earth Observation and Geoinformation* **2021**, *105*, 102623, doi:10.1016/j.jag.2021.102623.
485. Ji, Y.; Chen, Z.; Cheng, Q.; Liu, R.; Li, M.; Yan, X.; Li, G.; Wang, D.; Fu, L.; Ma, Y.; et al. Estimation of Plant Height and Yield Based on UAV Imagery in Faba Bean (Vicia Faba L.). *Plant Methods* **2022**, *18*, 26, doi:10.1186/s13007-022-00861-7.
486. Laurila, H.; Karjalainen, M.; Kleemola, J.; Hyyppä, J. Cereal Yield Modeling in Finland Using Optical and Radar Remote Sensing. *Remote Sensing* **2010**, *2*, 2185–2239, doi:10.3390/rs2092185.
487. Panek, E.; Gozdowski, D. Relationship between MODIS Derived NDVI and Yield of Cereals for Selected European Countries. *Agronomy* **2021**, *11*, 340, doi:10.3390/agronomy11020340.
488. Vicente-Serrano, S.M.; Cuadrat-Prats, J.M.; Romo, A. Early Prediction of Crop Production Using Drought Indices at Different Time-scales and Remote Sensing Data: Application in the Ebro Valley (North-east Spain). *International Journal of Remote Sensing* **2006**, *27*, 511–518, doi:10.1080/01431160500296032.
489. Laurila, H.; Karjalainen, M.; Hyyppä, J.; Kleemola, J. Integrating Vegetation Indices Models and Phenological Classification with Composite SAR and Optical Data for Cereal Yield Estimation in Finland (Part I). *Remote Sensing* **2010**, *2*, 76–114, doi:10.3390/rs2010076.
490. Chahbi, A.; Zribi, M.; Lili-Chabaane, Z.; Duchemin, B.; Shabou, M.; Mougenot, B.; Boulet, G. Estimation of the Dynamics and Yields of Cereals in a Semi-Arid Area Using Remote Sensing and the SAFY Growth Model. *International Journal of Remote Sensing* **2014**, *35*, 1004–1028, doi:10.1080/01431161.2013.875629.
491. Chahbi Bellakanji, A.; Zribi, M.; Lili-Chabaane, Z.; Mougenot, B. Forecasting of Cereal Yields in a Semi-Arid Area Using the Simple Algorithm for Yield Estimation (SAFY) Agro-Meteorological Model Combined with Optical SPOT/HRV Images. *Sensors* **2018**, *18*, 2138, doi:10.3390/s18072138.
492. Nevavuori, P.; Narra, N.; Linna, P.; Lipping, T. Crop Yield Prediction Using Multitemporal UAV Data and Spatio-Temporal Deep Learning Models. *Remote Sensing* **2020**, *12*, 4000, doi:10.3390/rs12234000.
493. Bouras, E. houssaine; Jarlan, L.; Er-Raki, S.; Balaghi, R.; Amazirh, A.; Richard, B.; Khabba, S. Cereal Yield Forecasting with Satellite Drought-Based Indices, Weather Data and Regional Climate Indices Using Machine Learning in Morocco. *Remote Sensing* **2021**, *13*, 3101, doi:10.3390/rs13163101.
494. Meroni, M.; Waldner, F.; Seguini, L.; Kerdiles, H.; Rembold, F. Yield Forecasting with Machine Learning and Small Data: What Gains for Grains? *Agricultural and Forest Meteorology* **2021**, *308–309*, 108555, doi:10.1016/j.agrformet.2021.108555.

495. Coelho, A.P.; Faria, R.T. de; Leal, F.T.; Barbosa, J. de A.; Rosalen, D.L. Validation of White Oat Yield Estimation Models Using Vegetation Indices. *Bragantia* **2020**, *79*, 236–241, doi:10.1590/1678-4499.20190387.
496. Lobell, D.B.; Di Tommaso, S.; You, C.; Yacoubou Djima, I.; Burke, M.; Kilic, T. Sight for Sorghums: Comparisons of Satellite- and Ground-Based Sorghum Yield Estimates in Mali. *Remote Sensing* **2020**, *12*, 100, doi:10.3390/rs12010100.
497. Habyarimana, E.; Baloch, F.S. Machine Learning Models Based on Remote and Proximal Sensing as Potential Methods for In-Season Biomass Yields Prediction in Commercial Sorghum Fields. *PLOS ONE* **2021**, *16*, e0249136, doi:10.1371/journal.pone.0249136.
498. Rahman, A.; Roytman, L.; Krakauer, N.Y.; Nizamuddin, M.; Goldberg, M. Use of Vegetation Health Data for Estimation of Aus Rice Yield in Bangladesh. *Sensors* **2009**, *9*, 2968–2975, doi:10.3390/s90402968.
499. Aboelghar, M.; Arafat, S.; Abo Yousef, M.; El-Shirbeny, M.; Naeem, S.; Massoud, A.; Saleh, N. Using SPOT Data and Leaf Area Index for Rice Yield Estimation in Egyptian Nile Delta. *The Egyptian Journal of Remote Sensing and Space Science* **2011**, *14*, 81–89, doi:10.1016/j.ejrs.2011.09.002.
500. Noureldin, N.A.; Aboelghar, M.A.; Saudy, H.S.; Ali, A.M. Rice Yield Forecasting Models Using Satellite Imagery in Egypt. *The Egyptian Journal of Remote Sensing and Space Science* **2013**, *16*, 125–131, doi:10.1016/j.ejrs.2013.04.005.
501. Huang, J.; Wang, X.; Li, X.; Tian, H.; Pan, Z. Remotely Sensed Rice Yield Prediction Using Multi-Temporal NDVI Data Derived from NOAA's-AVHRR. *PLOS ONE* **2013**, *8*, e70816, doi:10.1371/journal.pone.0070816.
502. Wang, J.; Dai, Q.; Shang, J.; Jin, X.; Sun, Q.; Zhou, G.; Dai, Q. Field-Scale Rice Yield Estimation Using Sentinel-1A Synthetic Aperture Radar (SAR) Data in Coastal Saline Region of Jiangsu Province, China. *Remote Sensing* **2019**, *11*, 2274, doi:10.3390/rs11192274.
503. Clauss, K.; Ottinger, M.; Leinenkugel, P.; Kuenzer, C. Estimating Rice Production in the Mekong Delta, Vietnam, Utilizing Time Series of Sentinel-1 SAR Data. *International Journal of Applied Earth Observation and Geoinformation* **2018**, *73*, 574–585, doi:10.1016/j.jag.2018.07.022.
504. Alebele, Y.; Wang, W.; Yu, W.; Zhang, X.; Yao, X.; Tian, Y.; Zhu, Y.; Cao, W.; Cheng, T. Estimation of Crop Yield From Combined Optical and SAR Imagery Using Gaussian Kernel Regression. *IEEE Journal of Selected Topics in Applied Earth Observations and Remote Sensing* **2021**, *14*, 10520–10534, doi:10.1109/JSTARS.2021.3118707.
505. Ali, A.M.; Savin, I.; Poddubskiy, A.; Abouelghar, M.; Saleh, N.; Abutaleb, K.; El-Shirbeny, M.; Dokukin, P. Integrated Method for Rice Cultivation Monitoring Using Sentinel-2 Data and Leaf Area Index. *The Egyptian Journal of Remote Sensing and Space Science* **2021**, *24*, 431–441, doi:10.1016/j.ejrs.2020.06.007.
506. Pagani, V.; Guarneri, T.; Busetto, L.; Ranghetti, L.; Boschetti, M.; Movedi, E.; Campos-Taberner, M.; Garcia-Haro, F.J.; Katsantonis, D.; Stavrakoudis, D.; et al. A High-Resolution, Integrated System for Rice Yield Forecasting at District Level. *Agricultural Systems* **2019**, *168*, 181–190, doi:10.1016/j.agsy.2018.05.007.
507. Wang, F.; Wang, F.; Hu, J.; Xie, L.; Yao, X. Rice Yield Estimation Based on an NPP Model With a Changing Harvest Index. *IEEE Journal of Selected Topics in Applied Earth Observations and Remote Sensing* **2020**, *13*, 2953–2959, doi:10.1109/JSTARS.2020.2993905.
508. Ge, H.; Ma, F.; Li, Z.; Du, C. Grain Yield Estimation in Rice Breeding Using Phenological Data and Vegetation Indices Derived from UAV Images. *Agronomy* **2021**, *11*, 2439, doi:10.3390/agronomy11122439.
509. Bellis, E.S.; Hashem, A.A.; Causey, J.L.; Runkle, B.R.K.; Moreno-García, B.; Burns, B.W.; Green, V.S.; Burcham, T.N.; Reba, M.L.; Huang, X. Detecting Intra-Field Variation in Rice Yield With Unmanned Aerial Vehicle Imagery and Deep Learning. *Frontiers in Plant Science* **2022**, *13*.

510. Luo, S.; Jiang, X.; Yang, K.; Li, Y.; Fang, S. Multispectral Remote Sensing for Accurate Acquisition of Rice Phenotypes: Impacts of Radiometric Calibration and Unmanned Aerial Vehicle Flying Altitudes. *Frontiers in Plant Science* **2022**, *13*.
511. Wang, F.; Yi, Q.; Hu, J.; Xie, L.; Yao, X.; Xu, T.; Zheng, J. Combining Spectral and Textural Information in UAV Hyperspectral Images to Estimate Rice Grain Yield. *International Journal of Applied Earth Observation and Geoinformation* **2021**, *102*, 102397, doi:10.1016/j.jag.2021.102397.
512. Zheng, H.; Ji, W.; Wang, W.; Lu, J.; Li, D.; Guo, C.; Yao, X.; Tian, Y.; Cao, W.; Zhu, Y.; et al. Transferability of Models for Predicting Rice Grain Yield from Unmanned Aerial Vehicle (UAV) Multispectral Imagery across Years, Cultivars and Sensors. *Drones* **2022**, *6*, 423, doi:10.3390/drones6120423.
513. Jeong, S.; Ko, J.; Yeom, J.-M. Predicting Rice Yield at Pixel Scale through Synthetic Use of Crop and Deep Learning Models with Satellite Data in South and North Korea. *Science of The Total Environment* **2022**, *802*, 149726, doi:10.1016/j.scitotenv.2021.149726.
514. Pazhanivelan, S.; Geethalakshmi, V.; Tamilmounika, R.; Sudarmanian, N.S.; Kaliaperumal, R.; Ramalingam, K.; Sivamurugan, A.P.; Mrunalini, K.; Yadav, M.K.; Quicho, E.D. Spatial Rice Yield Estimation Using Multiple Linear Regression Analysis, Semi-Physical Approach and Assimilating SAR Satellite Derived Products with DSSAT Crop Simulation Model. *Agronomy* **2022**, *12*, 2008, doi:10.3390/agronomy12092008.
515. Liu, Y.; Wang, S.; Chen, J.; Chen, B.; Wang, X.; Hao, D.; Sun, L. Rice Yield Prediction and Model Interpretation Based on Satellite and Climatic Indicators Using a Transformer Method. *Remote Sensing* **2022**, *14*, 5045, doi:10.3390/rs14195045.
516. Wei, L.; Luo, Y.; Xu, L.; Zhang, Q.; Cai, Q.; Shen, M. Deep Convolutional Neural Network for Rice Density Prescription Map at Ripening Stage Using Unmanned Aerial Vehicle-Based Remotely Sensed Images. *Remote Sensing* **2022**, *14*, 46, doi:10.3390/rs14010046.
517. Luo, S.; Jiang, X.; Jiao, W.; Yang, K.; Li, Y.; Fang, S. Remotely Sensed Prediction of Rice Yield at Different Growth Durations Using UAV Multispectral Imagery. *Agriculture* **2022**, *12*, 1447, doi:10.3390/agriculture12091447.
518. Bascon, M.V.; Nakata, T.; Shibata, S.; Takata, I.; Kobayashi, N.; Kato, Y.; Inoue, S.; Doi, K.; Murase, J.; Nishiuchi, S. Estimating Yield-Related Traits Using UAV-Derived Multispectral Images to Improve Rice Grain Yield Prediction. *Agriculture* **2022**, *12*, 1141, doi:10.3390/agriculture12081141.
519. Gu, C.; Ji, S.; Xi, X.; Zhang, Z.; Hong, Q.; Huo, Z.; Li, W.; Mao, W.; Zhao, H.; Zhang, R.; et al. Rice Yield Estimation Based on Continuous Wavelet Transform With Multiple Growth Periods. *Frontiers in Plant Science* **2022**, *13*.
520. Wang, Z.; Wang, S.; Wang, H.; Liu, L.; Li, Z.; Zhu, Y.; Wang, K. Field-Scale Rice Yield Estimation Based on UAV-Based MiniSAR Data with Ku Band and Modified Water-Cloud Model of Panicle Layer at Panicle Stage. *Frontiers in Plant Science* **2022**, *13*.
521. Fu, X.; Zhao, G.; Wu, W.; Xu, B.; Li, J.; Zhou, X.; Ke, X.; Li, Y.; Li, W.; Zhou, C.; et al. Assessing the Impacts of Natural Disasters on Rice Production in Jiangxi, China. *International Journal of Remote Sensing* **2022**, *43*, 1919–1941, doi:10.1080/01431161.2022.2049914.
522. Chun, J.A.; Kim, S.; Lee, W.-S.; Oh, S.M.; Lee, H. Assessment of Multimodel Ensemble Seasonal Hindcasts for Satellite-Based Rice Yield Prediction. *Journal of Agricultural Meteorology* **2016**, *72*, 107–115, doi:10.2480/agrmet.D-15-00019.
523. Yang, K.; Gong, Y.; Fang, S.; Duan, B.; Yuan, N.; Peng, Y.; Wu, X.; Zhu, R. Combining Spectral and Texture Features of UAV Images for the Remote Estimation of Rice LAI throughout the Entire Growing Season. *Remote Sensing* **2021**, *13*, 3001, doi:10.3390/rs13153001.
524. Teoh, C.C.; Mohd Nadzim, N.; Mohd Shahmihaizan, M.J.; Mohd Khairil Izani, I.; Faizal, K.; Mohd Shukry, H.B. Rice Yield Estimation Using Below Cloud Remote Sensing Images Acquired by Unmanned Airborne Vehicle System. *International Journal on Advanced Science, Engineering and Information Technology* **2016**, *6*, 516–519.

525. Wang, F.; Wang, F.; Zhang, Y.; Hu, J.; Huang, J.; Xie, J. Rice Yield Estimation Using Parcel-Level Relative Spectral Variables From UAV-Based Hyperspectral Imagery. *Frontiers in Plant Science* **2019**, *10*.
526. Wang, F.; Yao, X.; Xie, L.; Zheng, J.; Xu, T. Rice Yield Estimation Based on Vegetation Index and Florescence Spectral Information from UAV Hyperspectral Remote Sensing. *Remote Sensing* **2021**, *13*, 3390, doi:10.3390/rs13173390.
527. Anil Kumar, D.; Neelima, T.L.; Srikanth, P.; Uma Devi, M.; Suresh, K.; Murthy, C.S. Maize Yield Prediction Using NDVI Derived from Sentinal 2 Data in Siddipet District of Telangana State. *Journal of Agrometeorology* **2022**, *24*, 165–168, doi:10.54386/jam.v24i2.1635.
528. Oglesby, C.; Fox, A.A.A.; Singh, G.; Dhillon, J. Predicting In-Season Corn Grain Yield Using Optical Sensors. *Agronomy* **2022**, *12*, 2402, doi:10.3390/agronomy12102402.
529. Geipel, J.; Link, J.; Claupein, W. Combined Spectral and Spatial Modeling of Corn Yield Based on Aerial Images and Crop Surface Models Acquired with an Unmanned Aircraft System. *Remote Sensing* **2014**, *6*, 10335–10355, doi:10.3390/rs61110335.
530. Ban, H.-Y.; Kim, K.S.; Park, N.-W.; Lee, B.-W. Using MODIS Data to Predict Regional Corn Yields. *Remote Sensing* **2017**, *9*, 16, doi:10.3390/rs9010016.
531. Holzman, M.E.; Rivas, R.E. Early Maize Yield Forecasting From Remotely Sensed Temperature/Vegetation Index Measurements. *IEEE Journal of Selected Topics in Applied Earth Observations and Remote Sensing* **2016**, *9*, 507–519, doi:10.1109/JSTARS.2015.2504262.
532. Wang, M.; Tao, F.; Shi, W. Corn Yield Forecasting in Northeast China Using Remotely Sensed Spectral Indices and Crop Phenology Metrics. *Journal of Integrative Agriculture* **2014**, *13*, 1538–1545, doi:10.1016/S2095-3119(14)60817-0.
533. Lobell, D.B.; Asner, G.P. Comparison of Earth Observing-1 ALI and Landsat ETM+ for Crop Identification and Yield Prediction in Mexico. *IEEE Transactions on Geoscience and Remote Sensing* **2003**, *41*, 1277–1282, doi:10.1109/TGRS.2003.812909.
534. Schwalbert, R.A.; Amado, T.J.C.; Nieto, L.; Varela, S.; Corassa, G.M.; Horbe, T.A.N.; Rice, C.W.; Peralta, N.R.; Ciampitti, I.A. Forecasting Maize Yield at Field Scale Based on High-Resolution Satellite Imagery. *Biosystems Engineering* **2018**, *171*, 179–192, doi:10.1016/j.biosystemseng.2018.04.020.
535. Jiang, L.; Yang, Y.; Shang, S. Remote Sensing—Based Assessment of the Water-Use Efficiency of Maize over a Large, Arid, Regional Irrigation District. *Remote Sensing* **2022**, *14*, 2035, doi:10.3390/rs14092035.
536. Ji, Z.; Pan, Y.; Zhu, X.; Zhang, D.; Wang, J. A Generalized Model to Predict Large-Scale Crop Yields Integrating Satellite-Based Vegetation Index Time Series and Phenology Metrics. *Ecological Indicators* **2022**, *137*, 108759, doi:10.1016/j.ecolind.2022.108759.
537. Li, C.; Chimimba, E.G.; Kambombe, O.; Brown, L.A.; Chibarabada, T.P.; Lu, Y.; Anghileri, D.; Ngongondo, C.; Sheffield, J.; Dash, J. Maize Yield Estimation in Intercropped Smallholder Fields Using Satellite Data in Southern Malawi. *Remote Sensing* **2022**, *14*, 2458, doi:10.3390/rs14102458.
538. Levitan, N.; Gross, B. Utilizing Collocated Crop Growth Model Simulations to Train Agronomic Satellite Retrieval Algorithms. *Remote Sensing* **2018**, *10*, 1968, doi:10.3390/rs10121968.
539. Dokoohaki, H.; Rai, T.; Kivi, M.; Lewis, P.; Gómez-Dans, J.L.; Yin, F. Linking Remote Sensing with APSIM through Emulation and Bayesian Optimization to Improve Yield Prediction. *Remote Sensing* **2022**, *14*, 5389, doi:10.3390/rs14215389.
540. Joshi, V.R.; Thorp, K.R.; Coulter, J.A.; Johnson, G.A.; Porter, P.M.; Strock, J.S.; Garcia y Garcia, A. Improving Site-Specific Maize Yield Estimation by Integrating Satellite Multispectral Data into a Crop Model. *Agronomy* **2019**, *9*, 719, doi:10.3390/agronomy9110719.
541. Ban, H.-Y.; Ahn, J.-B.; Lee, B.-W. Assimilating MODIS Data-Derived Minimum Input Data Set and Water Stress Factors into CERES-Maize Model Improves Regional Corn Yield Predictions. *PLOS ONE* **2019**, *14*, e0211874, doi:10.1371/journal.pone.0211874.

542. Deines, J.M.; Patel, R.; Liang, S.-Z.; Dado, W.; Lobell, D.B. A Million Kernels of Truth: Insights into Scalable Satellite Maize Yield Mapping and Yield Gap Analysis from an Extensive Ground Dataset in the US Corn Belt. *Remote Sensing of Environment* **2021**, *253*, 112174, doi:10.1016/j.rse.2020.112174.
543. Cheng, Z.; Meng, J.; Wang, Y. Improving Spring Maize Yield Estimation at Field Scale by Assimilating Time-Series HJ-1 CCD Data into the WOFOST Model Using a New Method with Fast Algorithms. *Remote Sensing* **2016**, *8*, 303, doi:10.3390/rs8040303.
544. Peng, X.; Han, W.; Ao, J.; Wang, Y. Assimilation of LAI Derived from UAV Multispectral Data into the SAFY Model to Estimate Maize Yield. *Remote Sensing* **2021**, *13*, 1094, doi:10.3390/rs13061094.
545. Mishra, V.; Cruise, J.F.; Mecikalski, J.R. Assimilation of Coupled Microwave/Thermal Infrared Soil Moisture Profiles into a Crop Model for Robust Maize Yield Estimates over Southeast United States. *European Journal of Agronomy* **2021**, *123*, 126208, doi:10.1016/j.eja.2020.126208.
546. Ji, Z.; Pan, Y.; Zhu, X.; Wang, J.; Li, Q. Prediction of Crop Yield Using Phenological Information Extracted from Remote Sensing Vegetation Index. *Sensors* **2021**, *21*, 1406, doi:10.3390/s21041406.
547. Khan, S.N.; Li, D.; Maimaitijiang, M. A Geographically Weighted Random Forest Approach to Predict Corn Yield in the US Corn Belt. *Remote Sensing* **2022**, *14*, 2843, doi:10.3390/rs14122843.
548. Cheng, M.; Jiao, X.; Shi, L.; Penuelas, J.; Kumar, L.; Nie, C.; Wu, T.; Liu, K.; Wu, W.; Jin, X. High-Resolution Crop Yield and Water Productivity Dataset Generated Using Random Forest and Remote Sensing. *Sci Data* **2022**, *9*, 641, doi:10.1038/s41597-022-01761-0.
549. Xu, C.; Ding, Y.; Zheng, X.; Wang, Y.; Zhang, R.; Zhang, H.; Dai, Z.; Xie, Q. A Comprehensive Comparison of Machine Learning and Feature Selection Methods for Maize Biomass Estimation Using Sentinel-1 SAR, Sentinel-2 Vegetation Indices, and Biophysical Variables. *Remote Sensing* **2022**, *14*, 4083, doi:10.3390/rs14164083.
550. Ngie, A.; Ahmed, F. Estimation of Maize Grain Yield Using Multispectral Satellite Data Sets (SPOT 5) and the Random Forest Algorithm. *South African Journal of Geomatics* **2018**, *7*, 11–30, doi:10.4314/sajg.v7i1.2.
551. Leroux, L.; Castets, M.; Baron, C.; Escorihuela, M.-J.; Bégué, A.; Lo Seen, D. Maize Yield Estimation in West Africa from Crop Process-Induced Combinations of Multi-Domain Remote Sensing Indices. *European Journal of Agronomy* **2019**, *108*, 11–26, doi:10.1016/j.eja.2019.04.007.
552. Li, F.; Miao, Y.; Chen, X.; Sun, Z.; Stueve, K.; Yuan, F. In-Season Prediction of Corn Grain Yield through PlanetScope and Sentinel-2 Images. *Agronomy* **2022**, *12*, 3176, doi:10.3390/agronomy12123176.
553. Tiedeman, K.; Chamberlin, J.; Kosmowski, F.; Ayalew, H.; Sida, T.; Hijmans, R.J. Field Data Collection Methods Strongly Affect Satellite-Based Crop Yield Estimation. *Remote Sensing* **2022**, *14*, 1995, doi:10.3390/rs14091995.
554. Sun, J.; Lai, Z.; Di, L.; Sun, Z.; Tao, J.; Shen, Y. Multilevel Deep Learning Network for County-Level Corn Yield Estimation in the U.S. Corn Belt. *IEEE Journal of Selected Topics in Applied Earth Observations and Remote Sensing* **2020**, *13*, 5048–5060, doi:10.1109/JSTARS.2020.3019046.
555. Qiao, M.; He, X.; Cheng, X.; Li, P.; Luo, H.; Zhang, L.; Tian, Z. Crop Yield Prediction from Multi-Spectral, Multi-Temporal Remotely Sensed Imagery Using Recurrent 3D Convolutional Neural Networks. *International Journal of Applied Earth Observation and Geoinformation* **2021**, *102*, 102436, doi:10.1016/j.jag.2021.102436.
556. Zhang, L.; Zhang, Z.; Luo, Y.; Cao, J.; Tao, F. Combining Optical, Fluorescence, Thermal Satellite, and Environmental Data to Predict County-Level Maize Yield in China Using Machine Learning Approaches. *Remote Sensing* **2020**, *12*, 21, doi:10.3390/rs12010021.
557. Geng, L.; Che, T.; Ma, M.; Tan, J.; Wang, H. Corn Biomass Estimation by Integrating Remote Sensing and Long-Term Observation Data Based on Machine Learning Techniques. *Remote Sensing* **2021**, *13*, 2352, doi:10.3390/rs13122352.

558. Guo, Y.; Wang, H.; Wu, Z.; Wang, S.; Sun, H.; Senthilnath, J.; Wang, J.; Robin Bryant, C.; Fu, Y. Modified Red Blue Vegetation Index for Chlorophyll Estimation and Yield Prediction of Maize from Visible Images Captured by UAV. *Sensors* **2020**, *20*, 5055, doi:10.3390/s20185055.
559. Danilevicz, M.F.; Bayer, P.E.; Boussaid, F.; Bennamoun, M.; Edwards, D. Maize Yield Prediction at an Early Developmental Stage Using Multispectral Images and Genotype Data for Preliminary Hybrid Selection. *Remote Sensing* **2021**, *13*, doi:10.3390/rs13193976.
560. Panda, S.S.; Ames, D.P.; Panigrahi, S. Application of Vegetation Indices for Agricultural Crop Yield Prediction Using Neural Network Techniques. *Remote Sensing* **2010**, *2*, 673–696, doi:10.3390/rs2030673.
561. Barzin, R.; Pathak, R.; Lotfi, H.; Varco, J.; Bora, G.C. Use of UAS Multispectral Imagery at Different Physiological Stages for Yield Prediction and Input Resource Optimization in Corn. *Remote Sensing* **2020**, *12*, 2392, doi:10.3390/rs12152392.
562. Zhu, B.; Chen, S.; Cao, Y.; Xu, Z.; Yu, Y.; Han, C. A Regional Maize Yield Hierarchical Linear Model Combining Landsat 8 Vegetative Indices and Meteorological Data: Case Study in Jilin Province. *Remote Sensing* **2021**, *13*, 356, doi:10.3390/rs13030356.
563. Meng, L.; Liu, H.; L. Ustin, S.; Zhang, X. Predicting Maize Yield at the Plot Scale of Different Fertilizer Systems by Multi-Source Data and Machine Learning Methods. *Remote Sensing* **2021**, *13*, 3760, doi:10.3390/rs13183760.
564. Zhu, X.; Guo, R.; Liu, T.; Xu, K. Crop Yield Prediction Based on Agrometeorological Indexes and Remote Sensing Data. *Remote Sensing* **2021**, *13*, 2016, doi:10.3390/rs13102016.
565. Cui, Y.; Liu, S.; Li, X.; Geng, H.; Xie, Y.; He, Y. Estimating Maize Yield in the Black Soil Region of Northeast China Using Land Surface Data Assimilation: Integrating a Crop Model and Remote Sensing. *Frontiers in Plant Science* **2022**, *13*.
566. Kayad, A.; Rodrigues, F.A.; Naranjo, S.; Sozzi, M.; Pirotti, F.; Marinello, F.; Schulthess, U.; Defourny, P.; Gerard, B.; Weiss, M. Radiative Transfer Model Inversion Using High-Resolution Hyperspectral Airborne Imagery – Retrieving Maize LAI to Access Biomass and Grain Yield. *Field Crops Research* **2022**, *282*, 108449, doi:10.1016/j.fcr.2022.108449.
567. Ziliani, M.G.; Altaf, M.U.; Aragon, B.; Houborg, R.; Franz, T.E.; Lu, Y.; Sheffield, J.; Hoteit, I.; McCabe, M.F. Early Season Prediction of Within-Field Crop Yield Variability by Assimilating CubeSat Data into a Crop Model. *Agricultural and Forest Meteorology* **2022**, *313*, 108736, doi:10.1016/j.agrformet.2021.108736.
568. Shuai, G.; Basso, B. Subfield Maize Yield Prediction Improves When In-Season Crop Water Deficit Is Included in Remote Sensing Imagery-Based Models. *Remote Sensing of Environment* **2022**, *272*, 112938, doi:10.1016/j.rse.2022.112938.
569. Adak, A.; Murray, S.C.; Božinović, S.; Lindsey, R.; Nakasagga, S.; Chatterjee, S.; Anderson, S.L.; Wilde, S. Temporal Vegetation Indices and Plant Height from Remotely Sensed Imagery Can Predict Grain Yield and Flowering Time Breeding Value in Maize via Machine Learning Regression. *Remote Sensing* **2021**, *13*, 2141, doi:10.3390/rs13112141.
570. Kouadio, L.; Duveiller, G.; Djaby, B.; El Jarroudi, M.; Defourny, P.; Tychon, B. Estimating Regional Wheat Yield from the Shape of Decreasing Curves of Green Area Index Temporal Profiles Retrieved from MODIS Data. *International Journal of Applied Earth Observation and Geoinformation* **2012**, *18*, 111–118, doi:10.1016/j.jag.2012.01.009.
571. Meroni, M.; Marinho, E.; Sghaier, N.; Verstrate, M.M.; Leo, O. Remote Sensing Based Yield Estimation in a Stochastic Framework - Case Study of Durum Wheat in Tunisia. *Remote Sensing* **2013**, *5*, 539–557, doi:10.3390/rs5020539.
572. Mumtaz, R.; Baig, S.; Fatima, I. Analysis of Meteorological Variations on Wheat Yield and Its Estimation Using Remotely Sensed Data. A Case Study of Selected Districts of Punjab Province, Pakistan (2001-14). *Italian Journal of Agronomy* **2017**, *12*, doi:10.4081/ija.2017.897.
573. Mashaba, Z.; Chirima, G.; Botai, J.O.; Combrinck, L.; Munghemezulu, C.; Dube, E. Forecasting Winter Wheat Yields Using MODIS NDVI Data for the Central Free State Region. *South African Journal of Science* **2017**, *113*, doi:10.17159/sajs.2017/20160201.

574. Zhang, P.-P.; Zhou, X.-X.; Wang, Z.-X.; Mao, W.; Li, W.-X.; Yun, F.; Guo, W.-S.; Tan, C.-W. Using HJ-CCD Image and PLS Algorithm to Estimate the Yield of Field-Grown Winter Wheat. *Sci Rep* **2020**, *10*, 5173, doi:10.1038/s41598-020-62125-5.
575. Durgun, Y.Ö.; Gobin, A.; Duveiller, G.; Tychon, B. A Study on Trade-Offs between Spatial Resolution and Temporal Sampling Density for Wheat Yield Estimation Using Both Thermal and Calendar Time. *International Journal of Applied Earth Observation and Geoinformation* **2020**, *86*, 101988, doi:10.1016/j.jag.2019.101988.
576. Barbouchi, M.; Lhissou, R.; Abdelfattah, R.; El Alem, A.; Chokmani, K.; Ben Aissa, N.; Cheikh M'hamed, H.; Annabi, M.; Bahri, H. The Potential of Using Radarsat-2 Satellite Image for Modeling and Mapping Wheat Yield in a Semiarid Environment. *Agriculture* **2022**, *12*, 315, doi:10.3390/agriculture12030315.
577. Gupta, A.K.; Soni, P. Wheat Crop Yield Estimation Using Geomatics Tools in Saharanpur District. *Indian Journal of Agricultural Research* **2021**.
578. Zhou, X.; Wang, P.; Tansey, K.; Zhang, S.; Li, H.; Tian, H. Reconstruction of Time Series Leaf Area Index for Improving Wheat Yield Estimates at Field Scales by Fusion of Sentinel-2, -3 and MODIS Imagery. *Computers and Electronics in Agriculture* **2020**, *177*, 105692, doi:10.1016/j.compag.2020.105692.
579. Zhao, Y.; Han, S.; Meng, Y.; Feng, H.; Li, Z.; Chen, J.; Song, X.; Zhu, Y.; Yang, G. Transfer-Learning-Based Approach for Yield Prediction of Winter Wheat from Planet Data and SAFY Model. *Remote Sensing* **2022**, *14*, 5474, doi:10.3390/rs14215474.
580. Han, J.; Zhang, Z.; Cao, J.; Luo, Y.; Zhang, L.; Li, Z.; Zhang, J. Prediction of Winter Wheat Yield Based on Multi-Source Data and Machine Learning in China. *Remote Sensing* **2020**, *12*, 236, doi:10.3390/rs12020236.
581. Tripathi, A.; Tiwari, R.K.; Tiwari, S.P. A Deep Learning Multi-Layer Perceptron and Remote Sensing Approach for Soil Health Based Crop Yield Estimation. *International Journal of Applied Earth Observation and Geoinformation* **2022**, *113*, 102959, doi:10.1016/j.jag.2022.102959.
582. Huang, J.; Tian, L.; Liang, S.; Ma, H.; Becker-Reshef, I.; Huang, Y.; Su, W.; Zhang, X.; Zhu, D.; Wu, W. Improving Winter Wheat Yield Estimation by Assimilation of the Leaf Area Index from Landsat TM and MODIS Data into the WOFOST Model. *Agricultural and Forest Meteorology* **2015**, *204*, 106–121, doi:10.1016/j.agrformet.2015.02.001.
583. Sui, J.; Qin, Q.; Ren, H.; Sun, Y.; Zhang, T.; Wang, J.; Gong, S. Winter Wheat Production Estimation Based on Environmental Stress Factors from Satellite Observations. *Remote Sensing* **2018**, *10*, 962, doi:10.3390/rs10060962.
584. Deng, Q.; Wu, M.; Zhang, H.; Cui, Y.; Li, M.; Zhang, Y. Winter Wheat Yield Estimation Based on Optimal Weighted Vegetation Index and BHT-ARIMA Model. *Remote Sensing* **2022**, *14*, 1994, doi:10.3390/rs14091994.
585. Liu, Z.; Wang, C.; Bi, R.; Zhu, H.; He, P.; Jing, Y.; Yang, W. Winter Wheat Yield Estimation Based on Assimilated Sentinel-2 Images with the CERES-Wheat Model. *Journal of Integrative Agriculture* **2021**, *20*, 1958–1968, doi:10.1016/S2095-3119(20)63483-9.
586. Lekakis, E.; Zaikos, A.; Polychronidis, A.; Efthimiou, C.; Pourikas, I.; Mamouka, T. Evaluation of Different Modelling Techniques with Fusion of Satellite, Soil and Agro-Meteorological Data for the Assessment of Durum Wheat Yield under a Large Scale Application. *Agriculture* **2022**, *12*, 1635, doi:10.3390/agriculture12101635.
587. Meraj, G.; Kanga, S.; Ambadkar, A.; Kumar, P.; Singh, S.K.; Farooq, M.; Johnson, B.A.; Rai, A.; Sahu, N. Assessing the Yield of Wheat Using Satellite Remote Sensing-Based Machine Learning Algorithms and Simulation Modeling. *Remote Sensing* **2022**, *14*, 3005, doi:10.3390/rs14133005.
588. Saad El Imanni, H.; El Harti, A.; El Iysaouy, L. Wheat Yield Estimation Using Remote Sensing Indices Derived from Sentinel-2 Time Series and Google Earth Engine in a Highly Fragmented and Heterogeneous Agricultural Region. *Agronomy* **2022**, *12*, 2853, doi:10.3390/agronomy12112853.

589. Hunt, M.L.; Blackburn, G.A.; Carrasco, L.; Redhead, J.W.; Rowland, C.S. High Resolution Wheat Yield Mapping Using Sentinel-2. *Remote Sensing of Environment* **2019**, *233*, 111410, doi:10.1016/j.rse.2019.111410.
590. Zhou, W.; Liu, Y.; Ata-Ul-Karim, S.T.; Ge, Q.; Li, X.; Xiao, J. Integrating Climate and Satellite Remote Sensing Data for Predicting County-Level Wheat Yield in China Using Machine Learning Methods. *International Journal of Applied Earth Observation and Geoinformation* **2022**, *111*, doi:10.1016/j.jag.2022.102861.
591. Cao, J.; Wang, H.; Li, J.; Tian, Q.; Niyogi, D. Improving the Forecasting of Winter Wheat Yields in Northern China with Machine Learning–Dynamical Hybrid Subseasonal-to-Seasonal Ensemble Prediction. *Remote Sensing* **2022**, *14*, 1707, doi:10.3390/rs14071707.
592. Ahmed, A.A.M.; Sharma, E.; Jui, S.J.J.; Deo, R.C.; Nguyen-Huy, T.; Ali, M. Kernel Ridge Regression Hybrid Method for Wheat Yield Prediction with Satellite-Derived Predictors. *Remote Sensing* **2022**, *14*, 1136, doi:10.3390/rs14051136.
593. Sun, Y.; Zhang, S.; Tao, F.; Aboelenein, R.; Amer, A. Improving Winter Wheat Yield Forecasting Based on Multi-Source Data and Machine Learning. *Agriculture* **2022**, *12*, 571, doi:10.3390/agriculture12050571.
594. Huang, J.; Ma, H.; Sedano, F.; Lewis, P.; Liang, S.; Wu, Q.; Su, W.; Zhang, X.; Zhu, D. Evaluation of Regional Estimates of Winter Wheat Yield by Assimilating Three Remotely Sensed Reflectance Datasets into the Coupled WOFOST–PROSAIL Model. *European Journal of Agronomy* **2019**, *102*, 1–13, doi:10.1016/j.eja.2018.10.008.
595. Fu, Y.; Huang, J.; Shen, Y.; Liu, S.; Huang, Y.; Dong, J.; Han, W.; Ye, T.; Zhao, W.; Yuan, W. A Satellite-Based Method for National Winter Wheat Yield Estimating in China. *Remote Sensing* **2021**, *13*, 4680, doi:10.3390/rs13224680.
596. Upreti, D.; Pignatti, S.; Pascucci, S.; Tolomio, M.; Huang, W.; Casa, R. Bayesian Calibration of the Aquacrop-OS Model for Durum Wheat by Assimilation of Canopy Cover Retrieved from VENµS Satellite Data. *Remote Sensing* **2020**, *12*, 2666, doi:10.3390/rs12162666.
597. Liu, Z.; Xu, Z.; Bi, R.; Wang, C.; He, P.; Jing, Y.; Yang, W. Estimation of Winter Wheat Yield in Arid and Semiarid Regions Based on Assimilated Multi-Source Sentinel Data and the CERES-Wheat Model. *Sensors* **2021**, *21*, 1247, doi:10.3390/s21041247.
598. Huang, H.; Huang, J.; Li, X.; Zhuo, W.; Wu, Y.; Niu, Q.; Su, W.; Yuan, W. A Dataset of Winter Wheat Aboveground Biomass in China during 2007–2015 Based on Data Assimilation. *Sci Data* **2022**, *9*, 200, doi:10.1038/s41597-022-01305-6.
599. Kirthiga, S.M.; Patel, N.R. In-Season Wheat Yield Forecasting at High Resolution Using Regional Climate Model and Crop Model. *AgriEngineering* **2022**, *4*, 1054–1075, doi:10.3390/agriengineering4040066.
600. Ma, H.; Huang, J.; Zhu, D.; Liu, J.; Su, W.; Zhang, C.; Fan, J. Estimating Regional Winter Wheat Yield by Assimilation of Time Series of HJ-1 CCD NDVI into WOFOST–ACRM Model with Ensemble Kalman Filter. *Mathematical and Computer Modelling* **2013**, *58*, 759–770, doi:10.1016/j.mcm.2012.12.028.
601. Pan, H.; Chen, Z.; de Wit, A.; Ren, J. Joint Assimilation of Leaf Area Index and Soil Moisture from Sentinel-1 and Sentinel-2 Data into the WOFOST Model for Winter Wheat Yield Estimation. *Sensors* **2019**, *19*, 3161, doi:10.3390/s19143161.
602. Zhuo, W.; Huang, J.; Li, L.; Zhang, X.; Ma, H.; Gao, X.; Huang, H.; Xu, B.; Xiao, X. Assimilating Soil Moisture Retrieved from Sentinel-1 and Sentinel-2 Data into WOFOST Model to Improve Winter Wheat Yield Estimation. *Remote Sensing* **2019**, *11*, 1618, doi:10.3390/rs11131618.
603. Franch, B.; Vermote, E.; Skakun, S.; Santamaria-Artigas, A.; Kalecinski, N.; Roger, J.-C.; Becker-Reshef, I.; Barker, B.; Justice, C.; Sobrino, J.A. The ARYA Crop Yield Forecasting Algorithm: Application to the Main Wheat Exporting Countries. *International Journal of Applied Earth Observation and Geoinformation* **2021**, *104*, 102552, doi:10.1016/j.jag.2021.102552.
604. Luo, Y.; Zhang, Z.; Cao, J.; Zhang, L.; Zhang, J.; Han, J.; Zhuang, H.; Cheng, F.; Tao, F. Accurately Mapping Global Wheat Production System Using Deep Learning Algorithms. *International*

Journal of Applied Earth Observation and Geoinformation **2022**, *110*, 102823, doi:10.1016/j.jag.2022.102823.

605. Huang, H.; Huang, J.; Feng, Q.; Liu, J.; Li, X.; Wang, X.; Niu, Q. Developing a Dual-Stream Deep-Learning Neural Network Model for Improving County-Level Winter Wheat Yield Estimates in China. *Remote Sensing* **2022**, *14*, 5280, doi:10.3390/rs14205280.
606. Di, Y.; Gao, M.; Feng, F.; Li, Q.; Zhang, H. A New Framework for Winter Wheat Yield Prediction Integrating Deep Learning and Bayesian Optimization. *Agronomy* **2022**, *12*, 3194, doi:10.3390/agronomy12123194.
607. Wang, J.; Si, H.; Gao, Z.; Shi, L. Winter Wheat Yield Prediction Using an LSTM Model from MODIS LAI Products. *Agriculture* **2022**, *12*, 1707, doi:10.3390/agriculture12101707.
608. Cheng, E.; Zhang, B.; Peng, D.; Zhong, L.; Yu, L.; Liu, Y.; Xiao, C.; Li, C.; Li, X.; Chen, Y.; et al. Wheat Yield Estimation Using Remote Sensing Data Based on Machine Learning Approaches. *Frontiers in Plant Science* **2022**, *13*.
609. Qiao, M.; He, X.; Cheng, X.; Li, P.; Luo, H.; Tian, Z.; Guo, H. Exploiting Hierarchical Features for Crop Yield Prediction Based on 3-D Convolutional Neural Networks and Multikernel Gaussian Process. *IEEE Journal of Selected Topics in Applied Earth Observations and Remote Sensing* **2021**, *14*, 4476–4489, doi:10.1109/JSTARS.2021.3073149.
610. Li, Z.; Wang, J.; Xu, X.; Zhao, C.; Jin, X.; Yang, G.; Feng, H. Assimilation of Two Variables Derived from Hyperspectral Data into the DSSAT-CERES Model for Grain Yield and Quality Estimation. *Remote Sensing* **2015**, *7*, 12400–12418, doi:10.3390/rs70912400.
611. Jin, X.; Kumar, L.; Li, Z.; Xu, X.; Yang, G.; Wang, J. Estimation of Winter Wheat Biomass and Yield by Combining the AquaCrop Model and Field Hyperspectral Data. *Remote Sensing* **2016**, *8*, 972, doi:10.3390/rs8120972.
612. Prey, L.; Schmidhalter, U. Deep Phenotyping of Yield-Related Traits in Wheat. *Agronomy* **2020**, *10*, 603, doi:10.3390/agronomy10040603.
613. Prey, L.; Hu, Y.; Schmidhalter, U. High-Throughput Field Phenotyping Traits of Grain Yield Formation and Nitrogen Use Efficiency: Optimizing the Selection of Vegetation Indices and Growth Stages. *Frontiers in Plant Science* **2020**, *10*.
614. Tian, H.; Wang, P.; Tansey, K.; Zhang, J.; Zhang, S.; Li, H. An LSTM Neural Network for Improving Wheat Yield Estimates by Integrating Remote Sensing Data and Meteorological Data in the Guanzhong Plain, PR China. *Agricultural and Forest Meteorology* **2021**, *310*, 108629, doi:10.1016/j.agrformet.2021.108629.
615. Li, Q.; Jin, S.; Zang, J.; Wang, X.; Sun, Z.; Li, Z.; Xu, S.; Ma, Q.; Su, Y.; Guo, Q.; et al. Deciphering the Contributions of Spectral and Structural Data to Wheat Yield Estimation from Proximal Sensing. *The Crop Journal* **2022**, *10*, 1334–1345, doi:10.1016/j.cj.2022.06.005.
616. Li, H.; Jiang, Z.; Chen, Z.; Ren, J.; Liu, B.; Hasituya Assimilation of Temporal-Spatial Leaf Area Index into the CERES-Wheat Model with Ensemble Kalman Filter and Uncertainty Assessment for Improving Winter Wheat Yield Estimation. *Journal of Integrative Agriculture* **2017**, *16*, 2283–2299, doi:10.1016/S2095-3119(16)61351-5.
617. Li, J.; Veeranampalayam-Sivakumar, A.-N.; Bhatta, M.; Garst, N.D.; Stoll, H.; Stephen Baenziger, P.; Belamkar, V.; Howard, R.; Ge, Y.; Shi, Y. Principal Variable Selection to Explain Grain Yield Variation in Winter Wheat from Features Extracted from UAV Imagery. *Plant Methods* **2019**, *15*, 123, doi:10.1186/s13007-019-0508-7.
618. Zhou, X.; Kono, Y.; Win, A.; Matsui, T.; Tanaka, T.S.T. Predicting Within-Field Variability in Grain Yield and Protein Content of Winter Wheat Using UAV-Based Multispectral Imagery and Machine Learning Approaches. *Plant Production Science* **2021**, *24*, 137–151, doi:10.1080/1343943X.2020.1819165.
619. Tian, Z.; Zhang, Y.; Liu, K.; Li, Z.; Li, M.; Zhang, H.; Wu, J. UAV Remote Sensing Prediction Method of Winter Wheat Yield Based on the Fused Features of Crop and Soil. *Remote Sensing* **2022**, *14*, 5054, doi:10.3390/rs14195054.

620. Shen, Y.; Mercatoris, B.; Cao, Z.; Kwan, P.; Guo, L.; Yao, H.; Cheng, Q. Improving Wheat Yield Prediction Accuracy Using LSTM-RF Framework Based on UAV Thermal Infrared and Multispectral Imagery. *Agriculture* **2022**, *12*, 892, doi:10.3390/agriculture12060892.
621. Panday, U.S.; Shrestha, N.; Maharjan, S.; Pratihast, A.K.; Shahnawaz; Shrestha, K.L.; Aryal, J. Correlating the Plant Height of Wheat with Above-Ground Biomass and Crop Yield Using Drone Imagery and Crop Surface Model, A Case Study from Nepal. *Drones* **2020**, *4*, 28, doi:10.3390/drones4030028.
622. Li, Z.; Chen, Z.; Cheng, Q.; Duan, F.; Sui, R.; Huang, X.; Xu, H. UAV-Based Hyperspectral and Ensemble Machine Learning for Predicting Yield in Winter Wheat. *Agronomy* **2022**, *12*, 202, doi:10.3390/agronomy12010202.
623. Fei, S.; Hassan, M.A.; He, Z.; Chen, Z.; Shu, M.; Wang, J.; Li, C.; Xiao, Y. Assessment of Ensemble Learning to Predict Wheat Grain Yield Based on UAV-Multispectral Reflectance. *Remote Sensing* **2021**, *13*, 2338, doi:10.3390/rs13122338.
624. Fei, S.; Hassan, M.A.; Xiao, Y.; Su, X.; Chen, Z.; Cheng, Q.; Duan, F.; Chen, R.; Ma, Y. UAV-Based Multi-Sensor Data Fusion and Machine Learning Algorithm for Yield Prediction in Wheat. *Precision Agric* **2023**, *24*, 187–212, doi:10.1007/s11119-022-09938-8.
625. Bian, C.; Shi, H.; Wu, S.; Zhang, K.; Wei, M.; Zhao, Y.; Sun, Y.; Zhuang, H.; Zhang, X.; Chen, S. Prediction of Field-Scale Wheat Yield Using Machine Learning Method and Multi-Spectral UAV Data. *Remote Sensing* **2022**, *14*, 1474, doi:10.3390/rs14061474.
626. Yang, B.; Zhu, W.; Rezaei, E.E.; Li, J.; Sun, Z.; Zhang, J. The Optimal Phenological Phase of Maize for Yield Prediction with High-Frequency UAV Remote Sensing. *Remote Sensing* **2022**, *14*, 1559, doi:10.3390/rs14071559.
627. Vatter, T.; Gracia-Romero, A.; Kefauver, S.C.; Nieto-Taladriz, M.T.; Aparicio, N.; Araus, J.L. Preharvest Phenotypic Prediction of Grain Quality and Yield of Durum Wheat Using Multispectral Imaging. *The Plant Journal* **2022**, *109*, 1507–1518, doi:10.1111/tpj.15648.
628. Tao, H.; Feng, H.; Xu, L.; Miao, M.; Yang, G.; Yang, X.; Fan, L. Estimation of the Yield and Plant Height of Winter Wheat Using UAV-Based Hyperspectral Images. *Sensors* **2020**, *20*, 1231, doi:10.3390/s20041231.
629. Moghimi, A.; Yang, C.; Anderson, J.A. Aerial Hyperspectral Imagery and Deep Neural Networks for High-Throughput Yield Phenotyping in Wheat. *Computers and Electronics in Agriculture* **2020**, *172*, 105299, doi:10.1016/j.compag.2020.105299.
630. Roy Choudhury, M.; Das, S.; Christopher, J.; Apan, A.; Chapman, S.; Menzies, N.W.; Dang, Y.P. Improving Biomass and Grain Yield Prediction of Wheat Genotypes on Sodic Soil Using Integrated High-Resolution Multispectral, Hyperspectral, 3D Point Cloud, and Machine Learning Techniques. *Remote Sensing* **2021**, *13*, 3482, doi:10.3390/rs13173482.
631. Feng, H.; Tao, H.; Fan, Y.; Liu, Y.; Li, Z.; Yang, G.; Zhao, C. Comparison of Winter Wheat Yield Estimation Based on Near-Surface Hyperspectral and UAV Hyperspectral Remote Sensing Data. *Remote Sensing* **2022**, *14*, 4158, doi:10.3390/rs14174158.
632. Zeng, L.; Peng, G.; Meng, R.; Man, J.; Li, W.; Xu, B.; Lv, Z.; Sun, R. Wheat Yield Prediction Based on Unmanned Aerial Vehicles-Collected Red–Green–Blue Imagery. *Remote Sensing* **2021**, *13*, 2937, doi:10.3390/rs13152937.
633. Rezzouk, F.Z.; Gracia-Romero, A.; Kefauver, S.C.; Gutiérrez, N.A.; Aranjuelo, I.; Serret, M.D.; Araus, J.L. Remote Sensing Techniques and Stable Isotopes as Phenotyping Tools to Assess Wheat Yield Performance: Effects of Growing Temperature and Vernalization. *Plant Science* **2020**, *295*, 110281, doi:10.1016/j.plantsci.2019.110281.
634. Fei, S.; Hassan, M.A.; Ma, Y.; Shu, M.; Cheng, Q.; Li, Z.; Chen, Z.; Xiao, Y. Entropy Weight Ensemble Framework for Yield Prediction of Winter Wheat Under Different Water Stress Treatments Using Unmanned Aerial Vehicle-Based Multispectral and Thermal Data. *Frontiers in Plant Science* **2021**, *12*.

635. Yue, J.; Yang, G.; Li, C.; Li, Z.; Wang, Y.; Feng, H.; Xu, B. Estimation of Winter Wheat Above-Ground Biomass Using Unmanned Aerial Vehicle-Based Snapshot Hyperspectral Sensor and Crop Height Improved Models. *Remote Sensing* **2017**, *9*, 708, doi:10.3390/rs9070708.
636. Segarra, J.; González-Torralba, J.; Aranjuelo, Í.; Araus, J.L.; Kefauver, S.C. Estimating Wheat Grain Yield Using Sentinel-2 Imagery and Exploring Topographic Features and Rainfall Effects on Wheat Performance in Navarre, Spain. *Remote Sensing* **2020**, *12*, 2278, doi:10.3390/rs12142278.
637. Evans, F.H.; Shen, J. Long-Term Hindcasts of Wheat Yield in Fields Using Remotely Sensed Phenology, Climate Data and Machine Learning. *Remote Sensing* **2021**, *13*, 2435, doi:10.3390/rs13132435.
638. Xie, Y.; Huang, J. Integration of a Crop Growth Model and Deep Learning Methods to Improve Satellite-Based Yield Estimation of Winter Wheat in Henan Province, China. *Remote Sensing* **2021**, *13*, 4372, doi:10.3390/rs13214372.
639. Zhang, J.; Tian, H.; Wang, P.; Tansey, K.; Zhang, S.; Li, H. Improving Wheat Yield Estimates Using Data Augmentation Models and Remotely Sensed Biophysical Indices within Deep Neural Networks in the Guanzhong Plain, PR China. *Computers and Electronics in Agriculture* **2022**, *192*, 106616, doi:10.1016/j.compag.2021.106616.
640. Beyene, A.N.; Zeng, H.; Wu, B.; Zhu, L.; Gebremicael, T.G.; Zhang, M.; Bezabh, T. Coupling Remote Sensing and Crop Growth Model to Estimate National Wheat Yield in Ethiopia. *Big Earth Data* **2022**, *6*, 18–35, doi:10.1080/20964471.2020.1837529.
641. Ma, C.; Liu, M.; Ding, F.; Li, C.; Cui, Y.; Chen, W.; Wang, Y. Wheat Growth Monitoring and Yield Estimation Based on Remote Sensing Data Assimilation into the SAFY Crop Growth Model. *Sci Rep* **2022**, *12*, 5473, doi:10.1038/s41598-022-09535-9.
642. Hank, T.B.; Bach, H.; Mauser, W. Using a Remote Sensing-Supported Hydro-Agroecological Model for Field-Scale Simulation of Heterogeneous Crop Growth and Yield: Application for Wheat in Central Europe. *Remote Sensing* **2015**, *7*, 3934–3965, doi:10.3390/rs70403934.
643. Li, H.; Chen, Z.; Liu, G.; Jiang, Z.; Huang, C. Improving Winter Wheat Yield Estimation from the CERES-Wheat Model to Assimilate Leaf Area Index with Different Assimilation Methods and Spatio-Temporal Scales. *Remote Sensing* **2017**, *9*, 190, doi:10.3390/rs9030190.
644. Pang, A.; Chang, M.W.L.; Chen, Y. Evaluation of Random Forests (RF) for Regional and Local-Scale Wheat Yield Prediction in Southeast Australia. *Sensors* **2022**, *22*, 717, doi:10.3390/s22030717.
645. Wang, Y.; Zhang, Z.; Feng, L.; Du, Q.; Runge, T. Combining Multi-Source Data and Machine Learning Approaches to Predict Winter Wheat Yield in the Conterminous United States. *Remote Sensing* **2020**, *12*, 1232, doi:10.3390/rs12081232.
646. Tian, H.; Wang, P.; Tansey, K.; Han, D.; Zhang, J.; Zhang, S.; Li, H. A Deep Learning Framework under Attention Mechanism for Wheat Yield Estimation Using Remotely Sensed Indices in the Guanzhong Plain, PR China. *International Journal of Applied Earth Observation and Geoinformation* **2021**, *102*, 102375, doi:10.1016/j.jag.2021.102375.
647. Feng, L.; Wang, Y.; Zhang, Z.; Du, Q. Geographically and Temporally Weighted Neural Network for Winter Wheat Yield Prediction. *Remote Sensing of Environment* **2021**, *262*, 112514, doi:10.1016/j.rse.2021.112514.
648. Han, D.; Wang, P.; Tansey, K.; Zhang, S.; Tian, H.; Zhang, Y.; Li, H. Improving Wheat Yield Estimates by Integrating a Remotely Sensed Drought Monitoring Index Into the Simple Algorithm for Yield Estimate Model. *IEEE Journal of Selected Topics in Applied Earth Observations and Remote Sensing* **2021**, *14*, 10383–10394, doi:10.1109/JSTARS.2021.3119398.
649. Zhao, Y.; Potgieter, A.B.; Zhang, M.; Wu, B.; Hammer, G.L. Predicting Wheat Yield at the Field Scale by Combining High-Resolution Sentinel-2 Satellite Imagery and Crop Modelling. *Remote Sensing* **2020**, *12*, 1024, doi:10.3390/rs12061024.
650. Tuvdendorj, B.; Wu, B.; Zeng, H.; Batdelger, G.; Nanzad, L. Determination of Appropriate Remote Sensing Indices for Spring Wheat Yield Estimation in Mongolia. *Remote Sensing* **2019**, *11*, 2568, doi:10.3390/rs11212568.

651. Lobell, D.B.; Thau, D.; Seifert, C.; Engle, E.; Little, B. A Scalable Satellite-Based Crop Yield Mapper. *Remote Sensing of Environment* **2015**, *164*, 324–333, doi:10.1016/j.rse.2015.04.021.
652. Wang, A.X.; Tran, C.; Desai, N.; Lobell, D.; Ermon, S. Deep Transfer Learning for Crop Yield Prediction with Remote Sensing Data. In Proceedings of the Proceedings of the 1st ACM SIGCAS Conference on Computing and Sustainable Societies; Association for Computing Machinery: New York, NY, USA, March 20 2018; pp. 1–5.
653. Shao: Multitemporal Remote Sensing Data Analysis... - Μελετητής Google Available online: https://scholar.google.com/scholar_lookup?title=Multitemporal+Remote+Sensing+Data+Analysis+for+Agricultural+Application&author=Shao,+Y.&author=Ren,+J.&author=Campbell,+J.B.&publication_year=2018&journal=Compr.+Remote+Sens.&volume=9&pages=29%E2%80%9338&doi=10.1016/B978-0-12-409548-9.10431-2 (accessed on 7 November 2023).
654. Knipling, E.B. Physical and Physiological Basis for the Reflectance of Visible and Near-Infrared Radiation from Vegetation. *Remote Sensing of Environment* **1970**, *1*, 155–159, doi:10.1016/S0034-4257(70)80021-9.
655. PINTER, P.J.; JACKSON, R.D.; IDSO, S.B.; REGINATO, R.J. Multidate Spectral Reflectance as Predictors of Yield in Water Stressed Wheat and Barley. *International Journal of Remote Sensing* **1981**, *2*, 43–48, doi:10.1080/01431168108948339.
656. Wiegand, C.L.; Richardson, A.J.; Escobar, D.E.; Gerbermann, A.H. Vegetation Indices in Crop Assessments. *Remote Sensing of Environment* **1991**, *35*, 105–119, doi:10.1016/0034-4257(91)90004-P.
657. Al-Abbas, A.H.; Barr, R.; Hall, J.D.; Crane, F.L.; Baumgardner, M.F. Spectra of Normal and Nutrient-Deficient Maize Leaves1. *Agronomy Journal* **1974**, *66*, 16–20, doi:10.2134/agronj1974.00021962006600010005x.
658. Ali, A.M.; Abouelghar, M.; Belal, A.A.; Saleh, N.; Yones, M.; Selim, A.I.; Amin, M.E.S.; Elwesemy, A.; Kucher, D.E.; Maginan, S.; et al. Crop Yield Prediction Using Multi Sensors Remote Sensing (Review Article). *Egyptian Journal of Remote Sensing and Space Science* **2022**, *25*, 711–716, doi:10.1016/j.ejrs.2022.04.006.
659. Atzberger, C. Advances in Remote Sensing of Agriculture: Context Description, Existing Operational Monitoring Systems and Major Information Needs. *Remote Sensing* **2013**, *5*, 949–981, doi:10.3390/rs5020949.
660. Huang, J.; Gómez-Dans, J.L.; Huang, H.; Ma, H.; Wu, Q.; Lewis, P.E.; Liang, S.; Chen, Z.; Xue, J.-H.; Wu, Y.; et al. Assimilation of Remote Sensing into Crop Growth Models: Current Status and Perspectives. *Agricultural and Forest Meteorology* **2019**, *276–277*, doi:10.1016/j.agrformet.2019.06.008.
661. Tandzi, L.N.; Mutengwa, C.S. Estimation of Maize (Zea Mays L.) Yield Per Harvest Area: Appropriate Methods. *Agronomy* **2020**, *10*, doi:10.3390/agronomy10010029.
662. Hongo, C.; Niwa, K. Yield prediction of sugar beet using agricultural spatial information. *Seimitsu Kogaku Kaishi/Journal of the Japan Society for Precision Engineering* **2013**, *79*, 991–994, doi:10.2493/jjspe.79.991.
663. dela Torre, D.M.G.; Gao, J.; Macinnis-Ng, C. Remote Sensing-Based Estimation of Rice Yields Using Various Models: A Critical Review. *Geo-Spatial Information Science* **2021**, *24*, 580–603, doi:10.1080/10095020.2021.1936656.
664. Som-Ard, J.; Atzberger, C.; Izquierdo-Verdiguier, E.; Vuolo, F.; Immitzer, M. Remote Sensing Applications in Sugarcane Cultivation: A Review. *Remote Sensing* **2021**, *13*, doi:10.3390/rs13204040.
665. Pinter Jr., P.J.; Hatfield, J.L.; Schepers, J.S.; Barnes, E.M.; Moran, M.S.; Daughtry, C.S.T.; Upchurch, D.R. Remote Sensing for Crop Management. *Photogrammetric Engineering and Remote Sensing* **2003**, *69*, 647–664, doi:10.14358/pers.69.6.647.
666. Dobrota, C.T.; Carpa, R.; Butiuc-Keul, A. Analysis of Designs Used in Monitoring Crop Growth Based on Remote Sensing Methods. *Turkish Journal of Agriculture and Forestry* **2021**, *45*, 730–742, doi:10.3906/tar-2012-79.

667. Potgieter, A.B.; Zhao, Y.; Zarco-Tejada, P.J.; Chenu, K.; Zhang, Y.; Porker, K.; Biddulph, B.; Dang, Y.P.; Neale, T.; Roosta, F.; et al. Evolution and Application of Digital Technologies to Predict Crop Type and Crop Phenology in Agriculture. *In Silico Plants* **2021**, *3*, doi:10.1093/insilicoplants/diab017.
668. Inoue, Y. Synergy of Remote Sensing and Modeling for Estimating Ecophysiological Processes in Plant Production. *Plant Production Science* **2003**, *6*, 3–16, doi:10.1626/pps.6.3.
669. Xie, Y.; Ji, L.; Zhang, B.; Huang, G. Evolution of the Scientific Literature on Input–Output Analysis: A Bibliometric Analysis of 1990–2017. *Sustainability* **2018**, *10*, 3135, doi:10.3390/su10093135.
670. Dutta, A.; Trivedi, A.; Nath, C.P.; Gupta, D.S.; Hazra, K.K. A Comprehensive Review on Grain Legumes as Climate-smart Crops: Challenges and Prospects. *Environmental Challenges* **2022**, *7*, 100479, doi:10.1016/j.envc.2022.100479.
671. Wang, J.; Vanga, S.K.; Saxena, R.; Orsat, V.; Raghavan, V. Effect of Climate Change on the Yield of Cereal Crops: A Review. *Climate* **2018**, *6*, 41, doi:10.3390/cli6020041.
672. Nieto, H.; Kustas, W.P.; Torres-Rúa, A.; Alfieri, J.G.; Gao, F.; Anderson, M.C.; White, W.A.; Song, L.; del Mar Alsina, M.; Prueger, J.H.; et al. Evaluation of TSEB Turbulent Fluxes Using Different Methods for the Retrieval of Soil and Canopy Component Temperatures from UAV Thermal and Multispectral Imagery. *Irrig Sci* **2019**, *37*, 389–406, doi:10.1007/s00271-018-0585-9.
673. Espinoza, C.Z.; Khot, L.R.; Sankaran, S.; Jacoby, P.W. High Resolution Multispectral and Thermal Remote Sensing-Based Water Stress Assessment in Subsurface Irrigated Grapevines. *Remote Sensing* **2017**, *9*, 961, doi:10.3390/rs9090961.
674. Benos, L.; Tagarakis, A.C.; Dolias, G.; Berruto, R.; Kateris, D.; Bochtis, D. Machine Learning in Agriculture: A Comprehensive Updated Review. *Sensors* **2021**, *21*, 3758, doi:10.3390/s21113758.
675. Jones, J.W.; Hoogenboom, G.; Porter, C.H.; Boote, K.J.; Batchelor, W.D.; Hunt, L.A.; Wilkens, P.W.; Singh, U.; Gijsman, A.J.; Ritchie, J.T. The DSSAT Cropping System Model. *European Journal of Agronomy* **2003**, *18*, 235–265, doi:10.1016/S1161-0301(02)00107-7.
676. Boogaard, H.; Wolf, J.; Supit, I.; Niemeyer, S.; van Ittersum, M. A Regional Implementation of WOFOST for Calculating Yield Gaps of Autumn-Sown Wheat across the European Union. *Field Crops Research* **2013**, *143*, 130–142, doi:10.1016/j.fcr.2012.11.005.
677. Curnel, Y.; de Wit, A.J.W.; Duveiller, G.; Defourny, P. Potential Performances of Remotely Sensed LAI Assimilation in WOFOST Model Based on an OSS Experiment. *Agricultural and Forest Meteorology* **2011**, *151*, 1843–1855, doi:10.1016/j.agrformet.2011.08.002.
678. van Ittersum, M.K.; Leffelaar, P.A.; van Keulen, H.; Kropff, M.J.; Bastiaans, L.; Goudriaan, J. On Approaches and Applications of the Wageningen Crop Models. *European Journal of Agronomy* **2003**, *18*, 201–234, doi:10.1016/S1161-0301(02)00106-5.
679. Raes, D.; Steduto, P.; Hsiao, T.C.; Fereres, E. AquaCrop—The FAO Crop Model to Simulate Yield Response to Water: II. Main Algorithms and Software Description. *Agronomy Journal* **2009**, *101*, 438–447, doi:10.2134/agronj2008.0140s.
680. Steduto, P.; Hsiao, T.C.; Raes, D.; Fereres, E. AquaCrop—The FAO Crop Model to Simulate Yield Response to Water: I. Concepts and Underlying Principles. *Agronomy Journal* **2009**, *101*, 426–437, doi:10.2134/agronj2008.0139s.
681. Hsiao, T.C.; Heng, L.; Steduto, P.; Rojas-Lara, B.; Raes, D.; Fereres, E. AquaCrop—The FAO Crop Model to Simulate Yield Response to Water: III. Parameterization and Testing for Maize. *Agronomy Journal* **2009**, *101*, 448–459, doi:10.2134/agronj2008.0218s.
682. Archontoulis, S.V.; Miguez, F.E.; Moore, K.J. A Methodology and an Optimization Tool to Calibrate Phenology of Short-Day Species Included in the APSIM PLANT Model: Application to Soybean. *Environmental Modelling & Software* **2014**, *62*, 465–477, doi:10.1016/j.envsoft.2014.04.009.
683. Keating, B.A.; Carberry, P.S.; Hammer, G.L.; Probert, M.E.; Robertson, M.J.; Holzworth, D.; Huth, N.I.; Hargreaves, J.N.G.; Meinke, H.; Hochman, Z.; et al. An Overview of APSIM, a Model Designed

for Farming Systems Simulation. *European Journal of Agronomy* **2003**, *18*, 267–288, doi:10.1016/S1161-0301(02)00108-9.

684. Wang, E.; Robertson, M.J.; Hammer, G.L.; Carberry, P.S.; Holzworth, D.; Meinke, H.; Chapman, S.C.; Hargreaves, J.N.G.; Huth, N.I.; McLean, G. Development of a Generic Crop Model Template in the Cropping System Model APSIM. *European Journal of Agronomy* **2002**, *18*, 121–140, doi:10.1016/S1161-0301(02)00100-4.
685. Messina, G.; Peña, J.M.; Vizzari, M.; Modica, G. A Comparison of UAV and Satellites Multispectral Imagery in Monitoring Onion Crop. An Application in the 'Cipolla Rossa Di Tropea' (Italy). *Remote Sensing* **2020**, *12*, 3424, doi:10.3390/rs12203424.
686. Pla, M.; Bota, G.; Duane, A.; Balagué, J.; Curcó, A.; Gutiérrez, R.; Brotons, L. Calibrating Sentinel-2 Imagery with Multispectral UAV Derived Information to Quantify Damages in Mediterranean Rice Crops Caused by Western Swamphen (Porphyrio Porphyrio). *Drones* **2019**, *3*, 45, doi:10.3390/drones3020045.
687. Khaliq, A.; Comba, L.; Biglia, A.; Ricauda Aimonino, D.; Chiaberge, M.; Gay, P. Comparison of Satellite and UAV-Based Multispectral Imagery for Vineyard Variability Assessment. *Remote Sensing* **2019**, *11*, 436, doi:10.3390/rs11040436.
688. Nonni, F.; Malacarne, D.; Pappalardo, S.E.; Codato, D.; Meggio, F.; De Marchi, M. Sentinel-2 Data Analysis and Comparison with UAV Multispectral Images for Precision Viticulture. *giforum* **2018**, *1*, 105–116, doi:10.1553/giscience2018_01_s105.
689. Borgogno-Mondino, E.; Lessio, A.; Tarricone, L.; Novello, V.; de Palma, L. A Comparison between Multispectral Aerial and Satellite Imagery in Precision Viticulture. *Precision Agric* **2018**, *19*, 195–217, doi:10.1007/s11119-017-9510-0.
690. Benincasa, P.; Antognelli, S.; Brunetti, L.; Fabbri, C.A.; Natale, A.; Sartoretti, V.; Modeo, G.; Guiducci, M.; Tei, F.; Vizzari, M. RELIABILITY OF NDVI DERIVED BY HIGH RESOLUTION SATELLITE AND UAV COMPARED TO IN-FIELD METHODS FOR THE EVALUATION OF EARLY CROP N STATUS AND GRAIN YIELD IN WHEAT. *Experimental Agriculture* **2018**, *54*, 604–622, doi:10.1017/S0014479717000278.
691. McCabe, M.F.; Houborg, R.; Lucieer, A. High-Resolution Sensing for Precision Agriculture: From Earth-Observing Satellites to Unmanned Aerial Vehicles. In Proceedings of the Remote Sensing for Agriculture, Ecosystems, and Hydrology XVIII; SPIE, October 25 2016; Vol. 9998, pp. 346–355.
692. Matese, A.; Toscano, P.; Di Gennaro, S.F.; Genesio, L.; Vaccari, F.P.; Primicerio, J.; Belli, C.; Zaldei, A.; Bianconi, R.; Gioli, B. Intercomparison of UAV, Aircraft and Satellite Remote Sensing Platforms for Precision Viticulture. *Remote Sensing* **2015**, *7*, 2971–2990, doi:10.3390/rs70302971.
693. Ünsalan, C.; Boyer, K.L. Remote Sensing Satellites and Airborne Sensors. In *Multispectral Satellite Image Understanding: From Land Classification to Building and Road Detection*; Ünsalan, C., Boyer, K.L., Eds.; Advances in Computer Vision and Pattern Recognition; Springer: London, 2011; pp. 7–15 ISBN 978-0-85729-667-2.
694. Messina, G.; Peña, J.M.; Vizzari, M.; Modica, G. A Comparison of UAV and Satellites Multispectral Imagery in Monitoring Onion Crop. An Application in the 'Cipolla Rossa Di Tropea' (Italy). *Remote Sensing* **2020**, *12*, 3424, doi:10.3390/rs12203424.
695. Bollas, N.; Kokinou, E.; Polychronos, V. Comparison of Sentinel-2 and UAV Multispectral Data for Use in Precision Agriculture: An Application from Northern Greece. *Drones* **2021**, *5*, 35, doi:10.3390/drones5020035.
696. Mostaza-Colado, D.; Ablanque, P.V.M.; Capuano, A. Assessing the Yield of a Multi-Varieties Crop of Camelina Sativa (L.) Crantz through NDVI Remote Sensing. In Proceedings of the 2019 Sixth International Conference on Internet of Things: Systems, Management and Security (IOTSMS); July 2019; pp. 596–602.
697. Liu, X.; Ferguson, R.B.; Zheng, H.; Cao, Q.; Tian, Y.; Cao, W.; Zhu, Y. Using an Active-Optical Sensor to Develop an Optimal NDVI Dynamic Model for High-Yield Rice Production (Yangtze, China). *Sensors* **2017**, *17*, 672, doi:10.3390/s17040672.

698. Moigne, M. *USING MULTIPLEX® AND GREENSEEKERTM TO MANAGE SPATIAL VARIATION OF VINE VIGOR IN CHAMPAGNE*; 2010;
699. Govaerts, B.; Verhulst, N. The Normalized Difference Vegetation Index (NDVI) Greenseeker (TM) Handheld Sensor: Toward the Integrated Evaluation of Crop Management Part A: Concepts and Case Studies 2010.
700. Balážová, K.; Chyba, J.; Kumhálová, J.; Mašek, J.; Petrásek, S. Monitoring of Khorasan (Triticum Turgidum Ssp. Turanicum) and Modern Kabot Spring Wheat (Triticum Aestivum) Varieties by UAV and Sensor Technologies under Different Soil Tillage. *Agronomy* **2021**, *11*, 1348, doi:10.3390/agronomy11071348.
701. Reynolds, A.G.; Lee, H.-S.; Dorin, B.; Brown, R.; Jollineau, M.; Shemrock, A.; Crombleholme, M.; Poirier, E.J.; Zheng, W.; Gasnier, M.; et al. Mapping Cabernet Franc Vineyards by Unmanned Aerial Vehicles (UAVs) for Variability in Vegetation Indices, Water Status, and Virus Titer. *E3S Web Conf.* **2018**, *50*, 02010, doi:10.1051/e3sconf/20185002010.
702. Wines & Vines - Viticultural Mapping by UAVs, Part 2 Available online: https://winebusinessanalytics.com/sections/printout_article.cfm?content=204455&article=feature (accessed on 5 November 2023).
703. Cardoso Arango, J.A.; Louhaichi, M. Case Study of Use of Different Source of Imageries and Data Fusion. **2019**.
704. Pellegrini, P.; Cossani, C.M.; Bella, C.M.D.; Piñeiro, G.; Sadras, V.O.; Oesterheld, M. Simple Regression Models to Estimate Light Interception in Wheat Crops with Sentinel-2 and a Handheld Sensor. *Crop Science* **2020**, *60*, 1607–1616, doi:10.1002/csc2.20129.
705. Kumhálová, J.; Matějková, Š. Yield Variability Prediction by Remote Sensing Sensors with Different Spatial Resolution. *International Agrophysics* **2017**, *31*, 195–202.
706. Della Nave, F.N.; Ojeda, J.J.; Irisarri, J.G.N.; Pembleton, K.; Oyarzabal, M.; Oesterheld, M. Calibrating APSIM for Forage Sorghum Using Remote Sensing and Field Data under Sub-Optimal Growth Conditions. *Agricultural Systems* **2022**, *201*, 103459, doi:10.1016/j.agsy.2022.103459.
707. Misra, G.; Cawkwell, F.; Wingler, A. Status of Phenological Research Using Sentinel-2 Data: A Review. *Remote Sensing* **2020**, *12*, 2760, doi:10.3390/rs12172760.
708. Lykhovyd, P.; Vozhehova, R.; Lavrenko, S. Annual NDVI Dynamics Observed in Industrial Tomato Grown in the South of Ukraine. *Modern Phytomorphology* **2022**, *16*, 164–169.
709. Veloso, A.; Mermoz, S.; Bouvet, A.; Le Toan, T.; Planells, M.; Dejoux, J.-F.; Ceschia, E. Understanding the Temporal Behavior of Crops Using Sentinel-1 and Sentinel-2-like Data for Agricultural Applications. *Remote Sensing of Environment* **2017**, *199*, 415–426, doi:10.1016/j.rse.2017.07.015.
710. Caruso, G.; Palai, G.; Gucci, R.; Priori, S. Remote and Proximal Sensing Techniques for Site-Specific Irrigation Management in the Olive Orchard. *Applied Sciences* **2022**, *12*, 1309.
711. Xu, X.; Gao, P.; Zhu, X.; Guo, W.; Ding, J.; Li, C.; Zhu, M.; Wu, X. Design of an Integrated Climatic Assessment Indicator (ICAI) for Wheat Production: A Case Study in Jiangsu Province, China. *Ecological Indicators* **2019**, *101*, 943–953, doi:10.1016/j.ecolind.2019.01.059.
712. Chlingaryan, A.; Sukkarieh, S.; Whelan, B. Machine Learning Approaches for Crop Yield Prediction and Nitrogen Status Estimation in Precision Agriculture: A Review. *Computers and Electronics in Agriculture* **2018**, *151*, 61–69, doi:10.1016/j.compag.2018.05.012.
713. Wu, B.; Zhang, M.; Zeng, H.; Tian, F.; Potgieter, A.B.; Qin, X.; Yan, N.; Chang, S.; Zhao, Y.; Dong, Q.; et al. Challenges and Opportunities in Remote Sensing-Based Crop Monitoring: A Review. *National Science Review* **2023**, *10*, nwac290, doi:10.1093/nsr/nwac290.
714. Bzdok, D.; Altman, N.; Krzywinski, M. Statistics versus Machine Learning. *Nat Methods* **2018**, *15*, 233–234.
715. Psiroukis, V.; Darra, N.; Kasimati, A.; Trojacek, P.; Hasanli, G.; Fountas, S. Development of a Multi-Scale Tomato Yield Prediction Model in Azerbaijan Using Spectral Indices from Sentinel-2 Imagery. *Remote Sensing* **2022**, *14*, 4202.

716. *Ensemble Machine Learning*; Zhang, C., Ma, Y., Eds.; Springer US: Boston, MA, 2012; ISBN 978-1-4419-9325-0.
717. Wolpert, D.H.; Macready, W.G. No Free Lunch Theorems for Optimization. *IEEE Trans. Evol. Computat.* **1997**, *1*, 67–82, doi:10.1109/4235.585893.
718. HORLER, D.N.H.; DOCKRAY, M.; BARBER, J. The Red Edge of Plant Leaf Reflectance. *International Journal of Remote Sensing* **1983**, *4*, 273–288, doi:10.1080/01431168308948546.
719. The Red Edge Position and Shape as Indicators of Plant Chlorophyll Content, Biomass and Hydric Status.: International Journal of Remote Sensing: Vol 15, No 7 Available online: https://www.tandfonline.com/doi/abs/10.1080/01431169408954177?casa_token=MUS6CwG6UC4AAAAA:zXJRidXtC-FIJSK-0645OqdQYj5kUNPRrg3rIxTNU5j1YnWILk31rN4Ga6aeXDeCuR23decwS3rTjw (accessed on 17 November 2023).
720. Leprieur, C.; Verstraete, M.M.; Pinty, B. Evaluation of the Performance of Various Vegetation Indices to Retrieve Vegetation Cover from AVHRR Data. *Remote Sensing Reviews* **1994**, *10*, 265–284, doi:10.1080/02757259409532250.
721. BOOCHS, F.; KUPFER, G.; DOCKTER, K.; KÜHBAUCH, W. Shape of the Red Edge as Vitality Indicator for Plants. *International Journal of Remote Sensing* **1990**, *11*, 1741–1753, doi:10.1080/01431169008955127.
722. Ramoelo, A.; Cho, M.A.; Mathieu, R.; Madonsela, S.; van de Kerchove, R.; Kaszta, Z.; Wolff, E. Monitoring Grass Nutrients and Biomass as Indicators of Rangeland Quality and Quantity Using Random Forest Modelling and WorldView-2 Data. *International Journal of Applied Earth Observation and Geoinformation* **2015**, *43*, 43–54, doi:10.1016/j.jag.2014.12.010.
723. Cho, M.A.; Skidmore, A.K.; Atzberger, C. Towards Red-edge Positions Less Sensitive to Canopy Biophysical Parameters for Leaf Chlorophyll Estimation Using Properties Optique Spectrales Des Feuilles (PROSPECT) and Scattering by Arbitrarily Inclined Leaves (SAILH) Simulated Data. *International Journal of Remote Sensing* **2008**, *29*, 2241–2255, doi:10.1080/01431160701395328.
724. Cho, M.A.; Skidmore, A.K. A New Technique for Extracting the Red Edge Position from Hyperspectral Data: The Linear Extrapolation Method. *Remote Sensing of Environment* **2006**, *101*, 181–193, doi:10.1016/j.rse.2005.12.011.
725. Matsushita, B.; Yang, W.; Chen, J.; Onda, Y.; Qiu, G. Sensitivity of the Enhanced Vegetation Index (EVI) and Normalized Difference Vegetation Index (NDVI) to Topographic Effects: A Case Study in High-Density Cypress Forest. *Sensors* **2007**, *7*, 2636–2651, doi:10.3390/s7112636.
726. Jiang, Z.; Huete, A.R.; Didan, K.; Miura, T. Development of a Two-Band Enhanced Vegetation Index without a Blue Band. *Remote Sensing of Environment* **2008**, *112*, 3833–3845, doi:10.1016/j.rse.2008.06.006.
727. Wang, C.; Chen, J.; Wu, J.; Tang, Y.; Shi, P.; Black, T.A.; Zhu, K. A Snow-Free Vegetation Index for Improved Monitoring of Vegetation Spring Green-up Date in Deciduous Ecosystems. *Remote Sensing of Environment* **2017**, *196*, 1–12, doi:10.1016/j.rse.2017.04.031.
728. Kayad, A.; Sozzi, M.; Gatto, S.; Marinello, F.; Pirotti, F. Monitoring Within-Field Variability of Corn Yield Using Sentinel-2 and Machine Learning Techniques. *Remote Sensing* **2019**, *11*, 2873, doi:10.3390/rs11232873.
729. Crusiol, L.G.T.; Sun, L.; Sibaldelli, R.N.R.; Junior, V.F.; Furlaneti, W.X.; Chen, R.; Sun, Z.; Wuyun, D.; Chen, Z.; Nanni, M.R.; et al. Strategies for Monitoring Within-Field Soybean Yield Using Sentinel-2 Vis-NIR-SWIR Spectral Bands and Machine Learning Regression Methods. *Precision Agric* **2022**, *23*, 1093–1123, doi:10.1007/s11119-022-09876-5.
730. Zalom, F.G.; Wilson, L.T. PREDICTING PHENOLOGICAL EVENTS OF CALIFORNIA PROCESSING TOMATOES. *Acta Hortic.* **1999**, 41–48, doi:10.17660/ActaHortic.1999.487.2.
731. Elders, A.; Carroll, M.L.; Neigh, C.S.R.; D'Agostino, A.L.; Ksoll, C.; Wooten, M.R.; Brown, M.E. Estimating Crop Type and Yield of Small Holder Fields in Burkina Faso Using Multi-Day Sentinel-

2. *Remote Sensing Applications: Society and Environment* **2022**, *27*, 100820, doi:10.1016/j.rsase.2022.100820.
732. Xiao, G.; Zhang, X.; Niu, Q.; Li, X.; Li, X.; Zhong, L.; Huang, J. Winter Wheat Yield Estimation at the Field Scale Using Sentinel-2 Data and Deep Learning. *Computers and Electronics in Agriculture* **2024**, *216*, 108555, doi:10.1016/j.compag.2023.108555.
733. Hayashi, M.; Tamai, K.; Owashi, Y.; Miura, K. Automated Machine Learning for Identification of Pest Aphid Species (Hemiptera: Aphididae). *Appl Entomol Zool* **2019**, *54*, 487–490, doi:10.1007/s13355-019-00642-0.
734. Koh, J.C.O.; Spangenberg, G.; Kant, S. Automated Machine Learning for High-Throughput Image-Based Plant Phenotyping. *Remote Sensing* **2021**, *13*, 858, doi:10.3390/rs13050858.
735. Espejo-Garcia, B.; Malounas, I.; Vali, E.; Fountas, S. Testing the Suitability of Automated Machine Learning for Weeds Identification. *AI* **2021**, *2*, 34–47, doi:10.3390/ai2010004.
736. Kasimati, A.; Espejo-García, B.; Darra, N.; Fountas, S. Predicting Grape Sugar Content under Quality Attributes Using Normalized Difference Vegetation Index Data and Automated Machine Learning. *Sensors* **2022**, *22*, 3249.